



University of Warwick institutional repository: <http://go.warwick.ac.uk/wrap>

A Thesis Submitted for the Degree of PhD at the University of Warwick

<http://go.warwick.ac.uk/wrap/56392>

This thesis is made available online and is protected by original copyright.

Please scroll down to view the document itself.

Please refer to the repository record for this item for information to help you to cite it. Our policy information is available from the repository home page.

**Biologically Active Kigamicin
Analogues by Sequential
Palladium Catalysed C–O and
C–C Bond Construction**

by

Penelope Alice Turner

A thesis submitted in partial fulfilment of the requirements
for the degree of Doctor of Philosophy in Chemistry

Department of Chemistry, University of Warwick

November 2012

Table of Contents

Acknowledgements	6
Declaration	7
Abstract	8
Abbreviations	9
Chapter 1: Introduction	12
1.1 Introduction.....	13
1.2 Pancreatic Cancer.....	14
1.2.1 Introduction.....	14
1.2.2 Current therapeutics.....	15
1.2.3 New anti-austerity approach.....	17
1.3 Kigamicins.....	19
1.3.1 Introduction.....	19
1.3.2 Discovery and isolation.....	20
1.3.3 Structure determination and absolute configuration.....	21
1.3.4 Biological activity.....	23
1.3.5 Mechanism of action.....	26
1.4 Structurally Related Natural Products.....	28
1.4.1 Secalonic acids.....	29
1.4.2 Actinoplanones.....	30
1.4.3 Simaomicin α and β	31
1.4.4 Sch 42137.....	33
1.4.5 Ascherxanthonones A and B.....	33

1.4.6 Kibdelones.....	35
1.4.7 Globosuxanthonnes A and B.....	39
1.4.8 Blennolides A, B and C.....	40
1.4.9 Dicerandrols A, B and C.....	42
1.5 Conclusions.....	43
Chapter 2: Synthesis of Tetrahydroxanthonnes.....	45
2.1 Initial Studies and Synthesis of Kigamicin Analogues.....	46
2.1.1 Introduction.....	46
2.1.2 Existing methodology for the synthesis of tetrahydroxanthonnes.....	47
2.1.3 Tetrahydroxanthone synthesis by acid catalysed dehydration.....	50
2.1.4 Suzuki-Miyaura couplings.....	52
2.1.5 Amide couplings.....	55
2.1.6 Initial library of natural product analogues.....	56
2.2 Attempted Synthesis of the Natural Product E ring.....	58
2.3 Metal Catalysed Route to Tetrahydroxanthonnes.....	64
2.3.1 Introduction.....	64
2.3.2 Synthesis of substrates for investigation of metal catalysed cyclisation...66	
2.3.3 Formation of heterocycles using metal catalysis.....	69
2.4 Tetrahydroxanthone Formation using Copper Catalysis.....	72
2.4.1 Optimisation studies.....	72
2.4.2 Scope of copper catalysed cyclisation.....	73
2.5 Tetrahydroxanthone Formation using Palladium Catalysis.....	75
2.5.1 Optimisation studies.....	76

2.5.2 Catalysed versus uncatalysed reaction.....	77
2.5.3 Scope of palladium catalysed cyclisation.....	83
2.6 Tandem Catalysis.....	86
2.6.1 Investigations into the reaction mechanism.....	87
2.6.2 Scope of tandem catalysis using Suzuki-Miyaura couplings.....	87
2.6.3 Tandem catalysis using Sonogashira and Heck cross couplings.....	89
2.7 Conclusions and Future Work.....	91
Chapter 3: Towards the Fused Rings of the Kigamicins.....	95
3.1 Introduction.....	96
3.2 Proposed Synthesis of the CDEF Rings of the Kigamicins.....	96
3.2.1 Synthesis of a model substrate for oxidative addition studies.....	106
3.3 Attempted Synthesis of Hexa-Substituted THX Precursor.....	116
3.4 Conclusions.....	119
3.5 Future Work.....	120
Chapter 4: Biological Assays and Development of Analogue SAR.....	123
4.1 Introduction.....	124
4.2 Attempted Isolation of Kigamicin D.....	124
4.3 Biological Assays.....	126
4.3.1 Introduction and assay development.....	126
4.3.2 Trypan blue assay.....	127
4.3.3 WST-1 colourimetric assay.....	130
4.3.4 Lactate dehydrogenase assay.....	133
4.4 Assay Results for Kigamicin Analogues.....	137

4.4.1 Introduction.....	137
4.4.2 Results for the first generation analogues.....	137
4.4.3 Results for the second generation analogues.....	142
4.5 Kibdelone C and analogues.....	145
4.6 Conclusions and Future Work.....	148
Chapter 5: Experimental.....	151
References.....	209
Appendix I.....	224
Appendix II.....	226

Acknowledgements

First and foremost, I wish to thank my supervisor Professor Mike Shipman, for not only allowing me this opportunity but for all his help and guidance throughout my PhD. For all the ideas, time and patience over the years, a huge thank you. I'd also like to thank my supervisor at the Peninsula Medical School in Exeter, Dr. Jackie Whatmore for her patience and help with understanding the biological aspects of this project. I am also grateful to Cancer Research UK for the funding for this project.

A big thank you goes to members of the Shipman group past and present for making the last four years enjoyable and for helping me in the lab: Alex (my walking encyclopaedia), Claire (for her patience and teaching in the lab when I first started), Mark, Pete, Greg, Karen, Matt, Emma, Mike, Sami, Amélie, Thuy, Fran, Ben, Nicola, Sam, Ricky and Jo. A thank you also to everyone in Exeter for making me feel welcome every year and for all their help in the lab: Alex, Brent, Gary, Jo, Letizia, Mohit, Miranda, Susan, Emma, Sam and Kate and a special thanks to Charles for teaching me everything I needed to know about tissue culture and for defrosting my cells. Thanks also to Bob for all his help and answering my endless questions. I would like to thank students who have worked with me during my PhD, for all their hard work and for keeping me on my toes: CK, Ellanna (for putting up with me for two summers, and for the green smudge!), Matt (for his help when things weren't working so well) and also Alex and Sam.

Thank you to all the technical staff past and present, for all their help over the last four years: Adam, Ivan and Edward for NMR, Lijiang and Phil for mass spec and Guy for x-ray crystallography. A special thanks goes to Rob for help with everything around the department. I wish to extend my gratitude to the Wills group (especially Tarn and Katie) for providing me with some of their catalyst and for their help with chiral HPLC. To Christophe for his help with the bacterial cultures, thank you, I learnt a lot. Thank you also to the Porco group in Boston for samples of the kibdelones.

Lastly but by no means least, thank you to mum, dad, Tracey and Mandy, for your unwavering encouragement and support. I couldn't have done it without you. I love you all very much.

Declaration

Except where clearly indicated, the work reported in this thesis is an account of my own independent research at the University of Warwick and the Peninsula Medical School in Exeter carried out between October 2008 and November 2012.

The research reported in this thesis has not been submitted, either wholly or in part, for a degree at another institution.

Abstract

This thesis describes the study of the synthesis and biological evaluation of analogues of the kigamicin natural products. Chapter One gives a background to pancreatic cancer and explains the anti-austerity strategy for new therapeutics. It then describes the kigamicins and their biological activity, focusing on why they are thought to be clinically applicable. Other structurally related, tetrahydroxanthone containing, natural products are also discussed.

Chapter Two focuses on the synthesis of the tetrahydroxanthone nucleus. Existing methodology is initially utilised, before exploring formation of the tetrahydroxanthone using milder, metal catalysed routes. Copper and palladium are both explored for this transformation and an underlying uncatalysed process is revealed and fully investigated. This methodology is extended to tandem catalysis for the synthesis of 7-arylated tetrahydroxanthenes through combination of this chemistry with Suzuki-Miyaura couplings. Examples of Sonogashira and Heck couplings as well as alternative substitution patterns, are also presented.

Chapter Three discusses the attempted synthesis of the fused rings of the kigamicins. Our efforts towards suitable substrates are detailed.

Chapter Four outlines the anti-austerity assays established to evaluate the potency and selectivity of analogues synthesised in Chapter Two. Kigamicin C is tested in this assay to compare with literature values and validate our assay. The potency and selectivity of our analogues are reported and compared to the natural product. The anti-austerity effect of kibdelone C and analogues, is investigated for the first time. Attempted isolation of the natural product is also described.

Chapter Five details the experimental procedures and characterisation data for the novel compounds produced.

Abbreviations

Ac	acetyl
Akt	protein kinase B
Ar	aryl
br	broad
calcd.	calculated
COSY	Correlation Spectroscopy
CNS	Central Nervous System
d	day
DABCO	1,4-diazabicyclo[2.2.2]octane
DEPT	Distortionless Enhancement by Polarisation Transfer
DIBAL	Di- <i>iso</i> -butylaluminium hydride
DMEDA	<i>N,N'</i> -Dimethylethylenediamine
DMEM	Dulbecco's modified Eagles medium
DMF	<i>N,N'</i> -Dimethylformamide
DMP	Dess-Martin periodinane
DMSO	Dimethyl sulphoxide
DPEphos	Bis[(2-diphenylphosphino)phenyl] ether
DPPB	Diphenylphosphino butane
ee	enantiomeric excess
ELISA	Enzyme-linked immunosorbent assay
ERK	Extracellular-signal regulated kinase
ES	Electrospray
equiv.	equivalent
FACS	Fluorescence activated cell sorting
GCMS	Gas chromatography mass spectroscopy
GI ₅₀	Half maximal growth inhibitory concentration
GYM	Glucose yeast and malt
h	hour
HIFU	High intensity focused ultrasound
HMBC	Heteronuclear Multiple Bond Coherence
HMDS	Hexamethyldisilazane
HMQC	Heteronuclear Multiple Quantum Coherence
HOBt	Hydroxybenzotriazole

HPLC	High performance liquid chromatography
HRMS	High resolution mass spectroscopy
IBX	2-Iodoxybenzoic acid
IC ₅₀	Inhibitory concentration
IR	Infra-red
<i>J</i>	Coupling constant
Johnphos	(2-Biphenyl)di- <i>tert</i> -butylphosphine
LCMS	Liquid chromatography-mass spectroscopy
LDA	Lithium diisopropylamide
LDH	Lactate dehydrogenase
MALDI-TOF	Matrix-assisted laser desorption/ionisation – time of flight
mCPBA	<i>meta</i> -chloroperbenzoic acid
MIC	Minimum inhibitory concentration
min	minute
m.p.	Melting point
MRSA	Methicillin resistant <i>Staphylococcus aureus</i>
MS	Mass spectrometry
MTT	3-(4,5-dimethylthiazol-2-yl)-2,5-diphenyltetrazolium bromide
MW	Molecular weight
NAD	Nicotinamide adenine dinucleotide
NBS	<i>N</i> -Bromosuccinimide
NDM	Nutrient deprived medium
NMI	<i>N</i> -Methylimidazole
NMR	Nuclear magnetic resonance
NOE	Nuclear overhauser effect
PBS	Phosphate buffered saline
PCC	Pyridinium chlorochromate
PDPK1	3-Phosphoinositide dependent protein kinase-1
PI	Propidium iodide
PI3K	Phosphatidylinositol 3' kinase
PIP ₂	Phosphatidylinositol 4,5-bisphosphate
PIP ₃	Phosphatidylinositol 3,4,5-bisphosphate
PPA	Polyphosphoric acid
ppm	parts per million

PTEN	Phosphatase and tensin homolog
PyBOP	Benzotriazol-1-yl-oxytripyrrolidinophosphonium hexafluorophosphate
<i>R_f</i>	Retention factor
rt	room temperature
SAR	Structure activity relationship
SPhos	2-(dicyclohexylphosphino)2',6'-dimethoxy 1, 1'-biphenyl
TFSA	Trifluoromethanesulfonic acid
THF	Tetrahydrofuran
THX	Tetrahydroxanthone
TLC	Thin layer chromatography
TMEDA	<i>N,N,N',N'</i> -Tetramethylethylenediamine
TMSCl	Trimethylsilylchloride
Ts-DPEN	<i>N</i> -tosylated 1,2-diphenyl-1,2-ethylenediamine
UV	Ultraviolet
v/v	volume per unit volume
w/v	weight per unit volume
WST	Water soluble tetrazolium salt
Xantphos	4,5-Bis(diphenylphosphino)-9,9-dimethylxanthene
Xphos	2-Dicyclohexylphosphino-2',4',6'-triisopropylbiphenyl

Chapter 1:

Introduction

1.1 Introduction

This thesis is focused on the kigamicin natural products (Figure 1.1) which have shown potent cytotoxicity against pancreatic cancer, and more specifically my work has focused on the synthesis and bioactivity of the tetrahydroxanthone core.

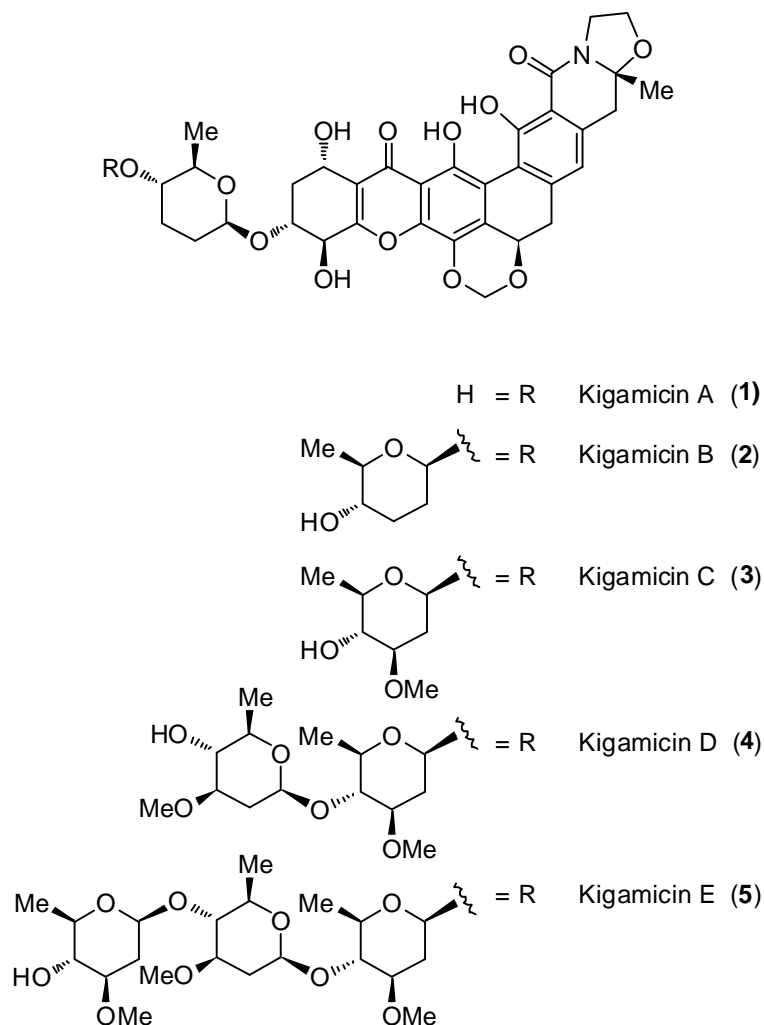


Figure 1.1: Kigamicins A-E

A significant focus of this project has been the synthesis of analogues of this natural product and the assessment of their biological activity. As such, it is important to begin with an introduction to pancreatic cancer and why the kigamicins provide such an exciting new avenue of research for treatment of this disease. This will be followed by a detailed description of the kigamicins and their biological activity before reviewing other structurally similar natural products.

1.2 Pancreatic Cancer

1.2.1 Introduction

Pancreatic cancer is the fourth deadliest cancer worldwide, claiming 30,000 lives in the US and 40,000 lives in Europe every year.¹⁻³ Complete remission from any form of pancreatic cancer is extremely rare and the prognosis for people with the disease is dismal with a survival rate of only 24% after one year and only 3-5% after five years,³ with the median survival being only 6 months.⁴ One of the key reasons for such a poor prognosis is the late diagnosis of this disease, which is predominantly due to lack of symptoms until very late stage in the cancer progression.⁵ These symptoms include weight loss, back pain and jaundice which is caused by the blockage of the bile ducts in the pancreas by the tumour.^{6,7} It is acknowledged that metastases occur in the early stages of the cancer^{5,8} with almost 100% of patients presenting with metastases during the course of the disease.¹ More significantly, 85% of patients have metastases at the time of diagnosis rendering medical intervention ineffective.⁹

Increasing age is a key risk factor in the development of pancreatic cancer with the majority of diagnoses made in people over the age of 65.^{5,7} Dietary factors have also been associated with the onset of pancreatic cancer. Larsson *et al*¹⁰ recently reported that an increased consumption of processed meats could be a risk factor for pancreatic cancer and an increased consumption of red meat could also be a risk factor in men. It has been suggested that there is no link between alcohol or coffee consumption and pancreatic cancer, whereas a decreased risk has been linked to an increase in vegetable consumption.¹¹⁻¹⁴ Smoking is a major associated risk factor of pancreatic cancer with a reported 25-29% of pancreatic cancer caused by smoking.^{1,11} It has been found that 80% of people with pancreatic cancer have

diabetes but there remains some controversy in the literature as to whether diabetes is actually a risk factor for pancreatic cancer or whether pancreatic cancer causes diabetes.¹⁵ Genetic factors are also thought to play a part. A family history of pancreatic cancer has been associated with onset of this disease with 10% of pancreatic cancer sufferers reporting at least one other family member with the disease.¹⁶

1.2.2 Current therapeutics

The only curative treatment is surgery, although in the vast majority of cases, at the time of diagnosis, the cancer has progressed too far for this to be a viable option. Only 9-15% of people diagnosed are eligible for this surgery.⁷ Even in those cases where surgery is undertaken, most patients subsequently relapse with metastases.⁵

Historically, 5-fluorouracil (Figure 1.2) was the main chemotherapy drug but it showed little selectivity, targeting DNA replication and therefore many side effects were suffered, including alopecia, nausea and severe fatigue.¹⁷ In 1996, gemcitabine (Figure 1.2) was launched¹⁸ and has subsequently replaced 5-fluorouracil in many cases. Despite providing only a modest improvement in median survival time (an additional month), it offers an improvement in quality of life for patients, reducing levels of pain experienced in the later stages of the disease.¹⁹

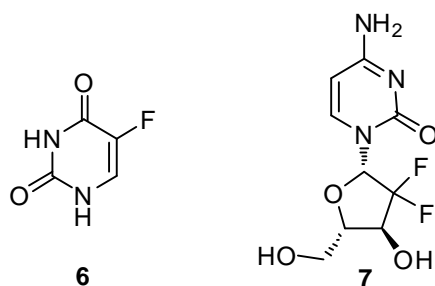


Figure 1.2: Structures of 5-fluorouracil²⁰ (6) and gemcitabine²¹ (7)

There has been very little progress in the development of new treatments for pancreatic cancer since the discovery of gemcitabine and consequently gemcitabine remains the main chemotherapy drug for the treatment of pancreatic cancer. A substantial number of investigations into the use of combination therapies have been carried out, including many phase III clinical trials. However, many of these did not provide a significant elongation of life expectancy or quality of life, and were therefore not approved for use.²²⁻²⁹ A combination of erlotinib with gemcitabine has been shown to provide a marginal improvement.³⁰ In 2011, Conroy *et al*³¹ reported studies comparing a new combination therapy FOLFIRINOX (a cocktail of 5-fluorouracil, oxaliplatin, leucovorin and irinotecan, Figure 1.3) to gemcitabine. They found that despite a higher incidence of adverse effects, there was a much higher median survival time (11.1 months compared with 6.8 months for gemcitabine) and the time before definitive degradation of quality of life was also extended.

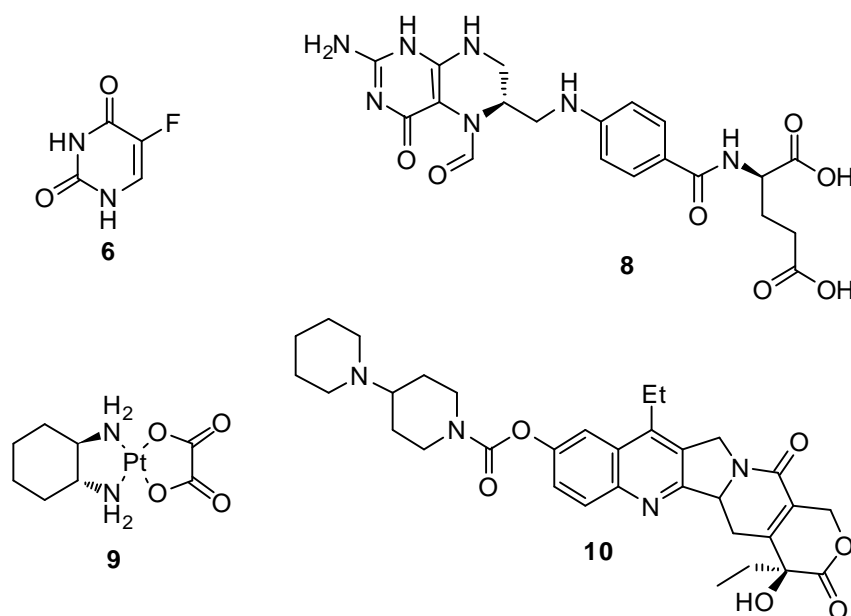


Figure 1.3: FOLFIRINOX; 5-fluorouracil²⁰ (6), leucovorin³² (8), oxaliplatin³³ (9) and irinotecan³⁴ (10)

Therapy which is gaining more clinical interest is that of high intensity focused ultrasound (HIFU). This is a non-invasive technique, where ultrasound is focused at a set depth and area, targeted at the site of the tumour and heated above the temperature of protein denaturation. This allows the target tumour tissue to be thermally destroyed, leaving the surrounding tissue intact.³⁵ This has shown promise for the treatment of a number of cancers, particularly prostate cancer. However, severe side effects have been reported in patients involved in studies for the use of HIFU on pancreatic cancer. In a study carried out by Han *et al* in 2011,³⁶ they reviewed the medical records for patients with pancreatic cancer, treated with HIFU between 2006 and 2008. They reported that 100% of patients suffered pain in the treated area and oedema. Major complications included fistula formation between the tumour and duodenum and third degree burns. A study by Hwang *et al* in 2009³⁷ showed fewer complications with only 3.4% of patients suffering second degree burns and 6.7% with subcutaneous sclerosis. Despite a lack of side effects, no patients had a complete response to therapy and only 14.6% had a partial response, with the remaining patients showing no change or cancer progression.

1.2.3 New anti-austerity approach

Despite small improvements being made in the prognosis for patients with pancreatic cancer, the overall prognosis and quality of life is still very poor. It is clear that new drugs and therapies are needed in order for significant advance.

Due to the rapid and uncontrolled growth of tumour cells, their microenvironment is often characterised as hypoxic and nutrient deficient with a lack of organised vasculature.³⁸ There are two main ways that these stressed cancer cells can survive; the first is by angiogenesis, the growth of new vasculature, and the second is by

acquiring a tolerance to these relatively austere conditions.³⁹ Anti-angiogenesis therapies have received a lot of attention⁴⁰⁻⁴³ however hypovascular tumours are particularly common in pancreatic cancer, as angiogenesis provides inadequate vasculature for tumour cells.^{44,45} In 2000, Esumi *et al*⁴⁶ carried out studies, whereby they exposed pancreatic cancer cell lines to nutrient deprived conditions (no serum, amino acids or glucose) and observed that there was greater than 50 % cell survival after 48 h. This suggests that many pancreatic cancer cells have a tolerance to such austere conditions. Removing a cancer cell's ability to tolerate these conditions, would have a dramatic effect on cell survival. If a drug could selectively kill cells under nutrient deprived conditions, then it would likely be selective to cancer as normal cells are seldom subjected to these conditions.⁴⁷ Such an approach to chemotherapy has been described as 'anti-austerity'.

Park *et al*⁴⁸ published research in 2009 carried out on *Ponciri Fructus*, an active component of a herbal medicine source. They tested the extracts using a lactate dehydrogenase assay against the PANC-1 cell line and observed selective cytotoxicity for cells under glucose deprived conditions.

Kadota *et al*³⁹ also used this strategy and screened the methanol extract of red propolis collected from Brazil against PANC-1 cells. This extract showed 100% selective cytotoxicity against cells under nutrient deprived conditions and their research describes the isolation of three new active component compounds (Figure 1.4).

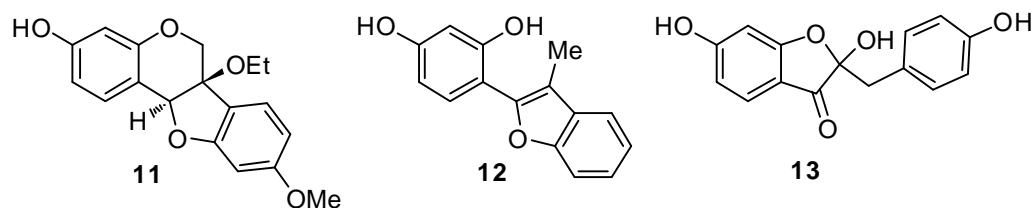


Figure 1.4: New active compounds isolated from red propolis

Interestingly two new flavones (**14** and **15**) isolated from extracts of Mexican propolis also exhibited similar selective cytotoxicity as described by Tezuka *et al* (Figure 1.5).⁴⁹

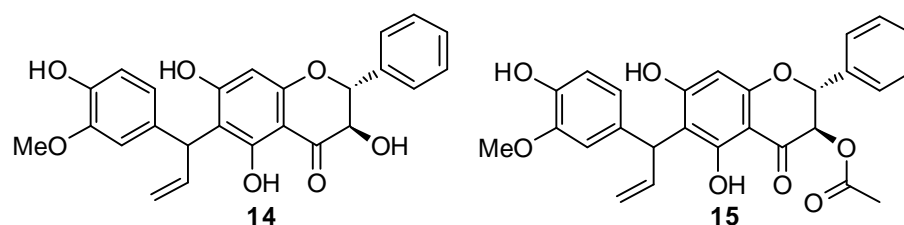


Figure 1.5: New active flavones

Other natural products exhibiting preferential cytotoxic effects include the kayeassamins,⁵⁰ kigamicins,⁵¹ panduratinins,⁵² and arctigenin.⁵³ The kigamicins have been the focus of this project and their significance is highlighted below.

1.3 Kigamicins

1.3.1 Introduction

The kigamicins are a group of five polycyclic natural products differing only in the length of the oligosaccharide attached to the aglycone (Figure 1.6).

Their discovery, isolation, structure determination and biological activity are described below. The rings of the natural products have been labelled A-H, and the

backbone numbered as indicated. This nomenclature and numbering convention will be used when describing portions of the natural product in later chapters.

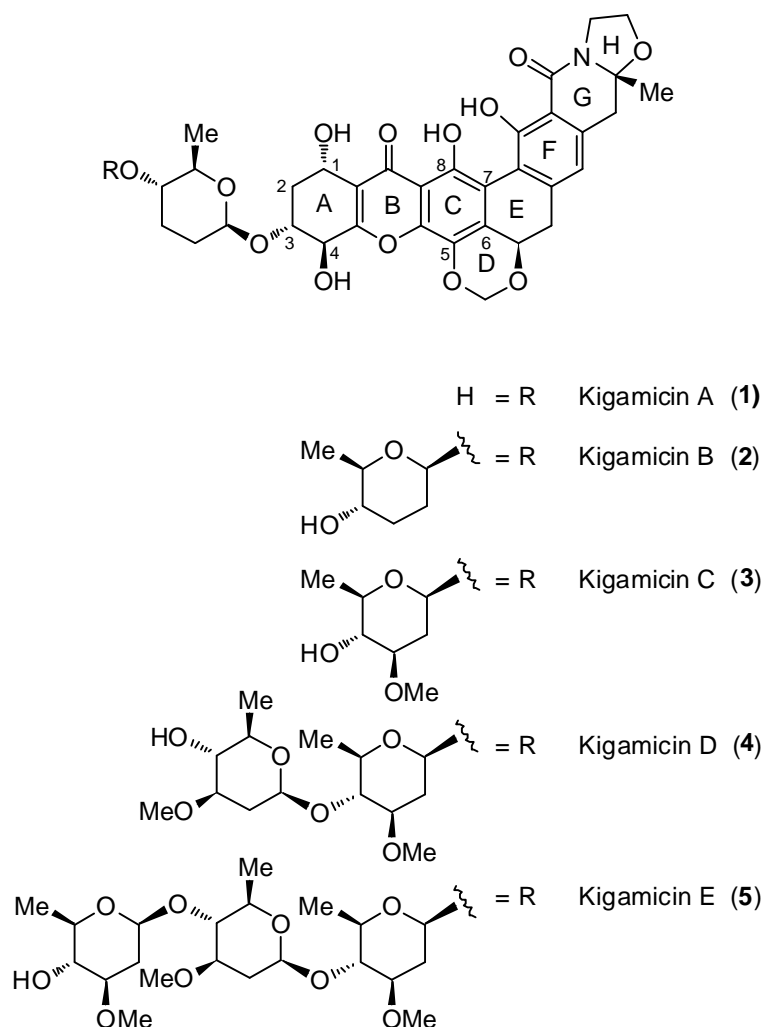


Figure 1.6: Structure of the kigamicins

1.3.2 Discovery and isolation

The kigamicins were discovered in 2003 by Kunimoto *et al*⁵¹ by the screening of over 2000 *actinomycete* culture media against pancreatic cancer cells. The culture media were screened in both Dulbecco's modified Eagles medium (DMEM) supplemented with foetal bovine serum and nutrient deprived medium (NDM). Those samples that exhibited potent and selective cytotoxicity in NDM were subject

to further investigation, as this indicated activity by an anti-austerity mechanism. One strain of active bacteria was identified as ML630-mF1.

ML630-mF1 was observed growing on various media and the physical properties probed in great detail. Partial DNA sequencing was also used in order to identify the bacteria as belonging to the genus *Amycolatopsis*. The organic phase isolated from production culture of this organism was purified using column chromatography. Further reverse phase chromatography and HPLC purification provided the five kigamicins. From a 12 L culture broth, kigamicin A (25.8 mg), kigamicin C (31.6 mg), kigamicin D (85.3 mg) and kigamicin E (19.4 mg) were isolated. Kigamicin B (4.1 mg) was isolated from a separate 3 L broth.

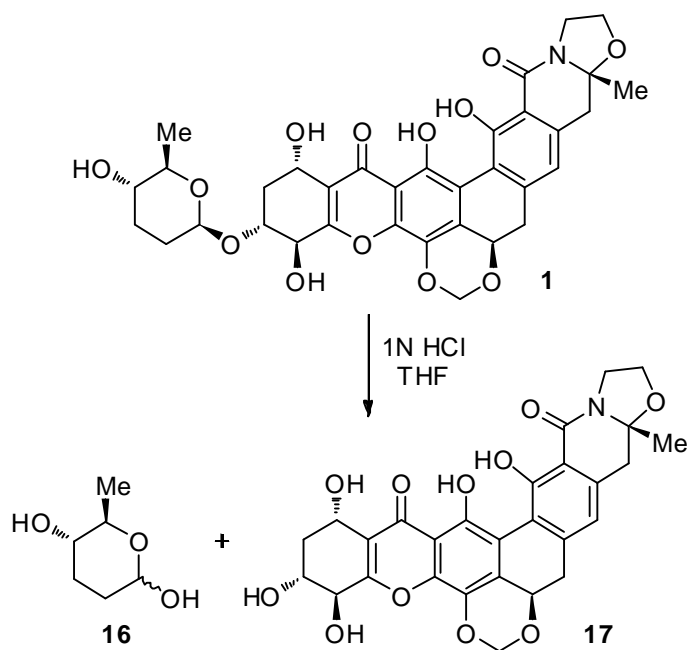
1.3.3 Structure determination and absolute configuration

Having isolated the natural products, Kunimoto and coworkers⁵⁴ set out to determine their structure. HRMS was used initially to establish the molecular formula of these compounds and were determined to be as follows: C₃₄H₃₅NO₁₃, MW 665 (kigamicin A), C₄₀H₄₅NO₁₅, MW 779 (kigamicin B), C₄₁H₄₇NO₁₆, MW 809 (kigamicin C), C₄₈H₅₉NO₁₉, MW 953 (kigamicin D) and C₅₅H₇₁NO₂₂, MW 1097 (kigamicin E). Their UV absorbances were all very similar and absorption bands at 227, 253, 306 and 384 nm indicated the presence of a polycyclic xanthone chromophore. Infra-red helped confirm the presence of hydroxyl, carbonyl and γ -pyrone moieties.

The ¹H NMR, ¹³C NMR, DEPT, HMQC, HMBC and COSY spectra of all five structures were the same in all but the oligosaccharide that they contained. The 48 signals in the ¹³C NMR and DEPT of kigamicin D included 6 methyl, 10

methylene, 16 methine and 16 quaternary carbons. The ^1H NMR showed 5 deuterium exchangeable protons (δ 2.45, 4.53, 5.22, 12.58 and 13.01 ppm) and based on their shifts, two of these were established as phenolic protons. The information obtained from the COSY and HMBC confirmed the structure of the aglycone with 7 spin systems observed in the COSY as well as some longer range couplings. Further evidence was provided for the structure of the H ring of the kigamicins by ^1H - ^{15}N NMR which revealed coupling from the ^{15}N signal to the methylene and methyl groups associated with that ring. Evidence from the HMQC indicated the location of the glycosidic linkage and further support for this was provided by NOE experiments.

The absolute configuration of the kigamicins was established by Someno *et al* in 2005.⁵⁵ The determination of absolute configuration was accomplished using a combination of x-ray crystallography and degradation studies. A single crystal x-ray of kigamicin A was achieved and from this the relative stereochemistry deduced. Hydrolysis of this material by treatment with 1N HCl in THF at room temperature for 18 h, provided aglycone **17** and amictose fragment **16** (Scheme 1.1). The optical rotation of the isolated amictose ($[\alpha]_{\text{D}}^{22} +42.5^\circ$ (c 0.7, Me_2CO)) agreed with literature values for D-amictose ($[\alpha]_{\text{D}}^{22} +43.6^\circ$ (c 1.0, Me_2CO)). From these studies both the relative and absolute configuration of kigamicin A could be unambiguously established.



Scheme 1.1: Hydrolysis of kigamicin A

Kigamicins C and D were also hydrolysed into their aglycone and oligosaccharide components. Crystal structures were obtained of the di and tri-saccharides and the aglycones were determined to be identical to **17** from hydrolysis of kigamicin A in all spectroscopic properties. From these studies, the structures of these natural products have been fully established.

1.3.4 Biological activity

Initial screening by Kunimoto *et al* in 2003⁵¹ when they first isolated the compounds, showed that the kigamicins exhibited both anti-cancer and anti-microbial properties. All five kigamicins inhibited Gram-positive bacteria including MRSA but showed no activity against Gram-negative bacteria. Perhaps more interestingly, the kigamicins all exhibited potent activity against pancreatic cancer (PANC-1) cells under nutrient deprived conditions; 100-fold more potent than under normal conditions.

Lu *et al*⁴⁷ reported kigamicin D to have an IC₅₀ of 85 ng/mL in NDM, demonstrating no activity at all in DMEM at any concentration tested (up to 10 µg/mL). These initial results were observed after 24 h incubation with kigamicin D. However, the authors also tested the cytotoxic effects of kigamicin over time and found that at 0.1 µg/mL there was total cell death after only 6 h. The authors examined which components of the nutrient rich media were responsible for the inactivity of kigamicin D. They discovered that when glucose was absent, kigamicin D had a strong cytotoxic effect, whereas in the presence of glucose, kigamicin D had little or no effect on cell viability.

In order to determine which mode of cell death the kigamicins were inducing, the authors treated the cells with kigamicin D under nutrient deprived conditions and then subjected the cells to Annexin V and propidium iodide (PI) staining. The cells were then analysed using FACS (fluorescence-activated cell sorting) analysis. They found that the cells had been stained with PI, clearly showing necrosis of the cells. Evidence for necrosis was also provided by studies carried out by Hata *et al*⁵⁶ also using flow cytometry. Further analysis of these cells showed degradation of the cytoplasm, whilst the nucleus remained viable, which is another indicator that the cells were undergoing necrosis.

Lu *et al*⁴⁷ carried out experiments in order to determine if kigamicin D displayed *in vivo* cytotoxic effects. They implanted a suspension of PANC-1 cells in DMEM, subcutaneously into the abdominal wall of five week old nude mice. After two weeks, mice with a tumour of approximately 5 mm in diameter were divided into a treatment group and a control group. Kigamicin D was dissolved in DMSO at 10 mg/mL and diluted with saline to a concentration of 15 µg/mL. This solution was

either force-fed intragastrically or injected into the tumour site six days a week. Tumour size and body weight were measured on a weekly basis. The results indicated a reduction of the tumour volume by 41% by subcutaneous administration of kigamicin D and a reduction by 20% by oral administration with no significant body weight loss. Other pancreatic cancer cell lines were tested (MIA Paca-2 and Capan-1) and results showed that kigamicin D also significantly inhibited these cell lines *in vivo*.

In order to determine whether kigamicin D had any detrimental effects on other normal cells, the oesophagus, stomach, lungs, liver and spleen were removed from the mice treated with kigamicin D. No toxic effects on these organs were observed. Further evidence was provided by Hata *et al*⁵⁶ who showed that lymphocytes were less susceptible to kigamicin than myeloma cells, supporting the hypothesis that these compounds could be clinically applicable.

In order to further demonstrate kigamicin D as unique from current therapeutics, the authors decided to test widely used drugs, in parallel to kigamicin D in both DMEM and NDM. All drugs tested (vincristine, 5-fluorouracil, taxol, doxorubicin, cisplatin and camptothecin) showed an inverse selectivity; they showed greater cytotoxic effects under normal conditions and a very weak effect under austere conditions. This may contribute to poor patient response using therapeutics for the treatment of pancreatic cancer.

Masuda *et al*⁵⁷ examined the effect of kigamicin D on a range of cancer cells and also on normal cells. They confirmed the potent activity of kigamicin D on pancreatic cancer cells with selectivity between NDM and DMEM. Normal cells such as lung fibroblast and prostrate stromal cells were tested alongside the

pancreatic cancer cells and a similar trend was found; the cells were relatively unaffected under normal conditions whereas under nutrient deprived conditions, toxicity was observed. They also carried out studies of human lung and colon cancer xenografts in nude mice. Surprisingly, contrary to results found *in vitro* by Lu *et al.*,⁴⁷ kigamicin D showed only a very weak effect on these cancers. Thus kigamicin D appears to have excellent anti-cancer properties but specifically to pancreatic cancers, perhaps due to the austere microenvironment surrounding the pancreatic cancer cells.⁵⁷

1.3.5 Mechanism of action

The PI3K-Akt pathway (Figure 1.7) has been implicated in the development and progression of human cancers.^{56,58,59} It has been shown that in cases of pancreatic cancer, there is a higher frequency of K-Ras and *p53* mutations⁶⁰ both of which are believed to upregulate the PI3K-Akt pathway. This could contribute to the diminished apoptosis of these cells resulting in drug resistance. When gemcitabine was used in combination with known PI3K inhibitors (Wortmannin and LY294002), there was an observed increase in the cytotoxic effects of gemcitabine.⁵⁹ This provides evidence of the involvement of this pathway in the progression of the cancer.

PI3K (phosphatidylinositol 3' kinase) is a lipid kinase and is involved in the phosphorylation of PIP₂ (phosphatidylinositol 4,5-bisphosphate) to provide the signalling messenger, PIP₃ (phosphatidylinositol 3,4,5-bisphosphate) which is responsible for a cascade of events. PIP₃ can bind to Akt thus altering the conformation of it and allowing it to be phosphorylated by PDK1 (3-phosphoinositide dependent protein kinase-1). Once activated, pAkt

(phosphorylated Akt) has a vast number of roles, perhaps its most pivotal being cell proliferation and motility.^{58,61} An increase in the activation of Akt also inhibits apoptosis and promotes survival of the cells.

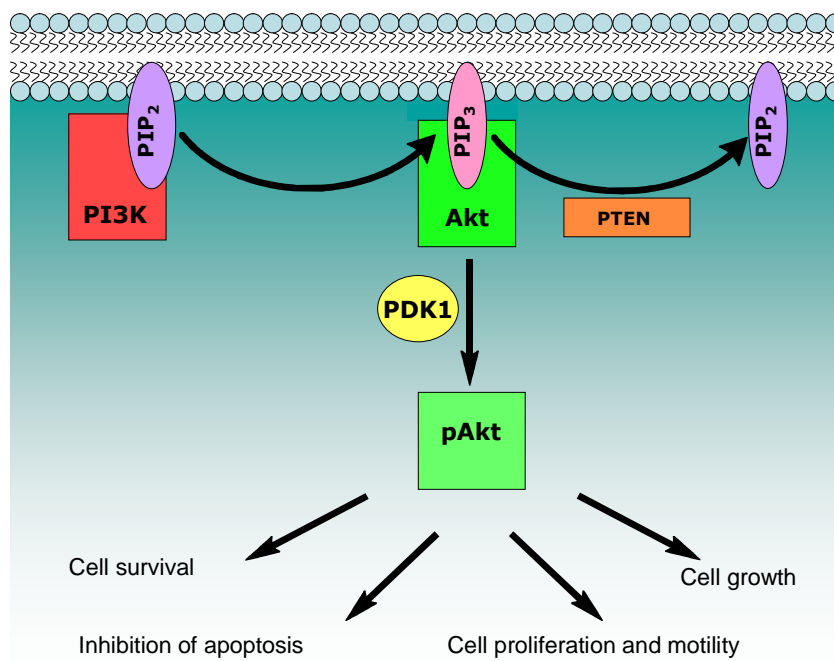


Figure 1.7: PI3K-Akt pathway^{61,62}

PTEN (phosphatase and tensin homolog) is the main negative regulator of this pathway, dephosphorylating PIP₃ to PIP₂ thus keeping the amount of activated Akt to a normal level. Deletion or mutation of PTEN has been shown in a large number of studies to be involved in the onset or progression of a number of human cancers including but not limited to lung,⁶³ thyroid,^{64,65} breast,⁶⁶ prostate⁶⁷, melanoma⁶⁸ and lymphoid carcinomas.⁶⁹

There is data to suggest that kigamicin D blocks the PI3K-Akt pathway evidenced by the inhibition of expression of phosphorylated Akt observed in treated cells.

Lu *et al*⁴⁷ carried out studies to analyse the mechanism of action of kigamicin D in which they stimulated the phosphorylation of Akt in nutrient deprived cells before adding kigamicin D. They found that there was significant inhibition of Akt phosphorylation. They also probed the activation of Akt *in vivo*. Tumours from nude mice grown over a period of six weeks, both with and without treatment with kigamicin D, were excised and subjected to analysis. These results mimicked the results found *in vitro*, providing support for the hypothesis that kigamicin D inhibits the activation of Akt.

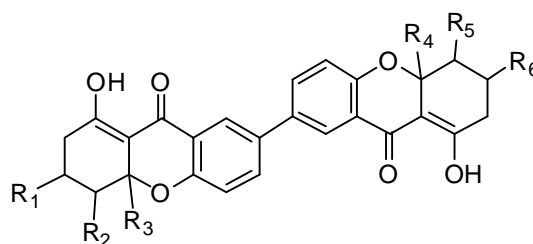
These results were supported by Hata *et al*⁵⁶ who also observed that there was diminished expression of phosphorylated Akt after treatment with kigamicin under conditions of nutrient deprivation. However the authors suggested that it inhibits more than one pathway and is not specific, as they found that kigamicin also inhibited the phosphorylation of ERK. The authors noted that kigamicin was found to induce necrosis, whereas typical ERK inhibitors induce cell death by apoptosis and so perhaps inhibition of ERK phosphorylation was not the cause of kigamicin's toxicity under nutrient deprived conditions.

1.4 Structurally Related Natural Products

In order to understand which part of the kigamicins is the active pharmacophore, we must first examine other structurally related natural products with potent biological activity. There are a number of polycyclic xanthone containing natural products; their biological activity and syntheses have been studied extensively.⁷⁰ Focus here is on those natural products containing the tetrahydroxanthone nucleus structurally analogous to the kigamicins but less well studied than their xanthone counterparts.

1.4.1 Secalonic acids

Secalonic acids A-G (**18-24**) are an example of dimeric structures often described as ergochromes for which the tetrahydroxanthone forms a monomeric part of its dimer-like structure (Figure 1.8). The first isolation of the secalonic acids dates back to 1906.⁷⁰ The biological effects of the secalonic acids have been studied, and in particular, secalonic acid D. Unlike the other natural products described in this chapter, the secalonic acids have been shown to have adverse biological effects. It has been shown to induce cleft palate in the offspring of exposed mice.^{71,72} The compound has also been shown to have teratogenic effects including skeletal, ophthalmic and visceral malformations in newly born mice and it has been proposed that it could cause behavioural dysfunction in neonatal mice.⁷³ Ehrlich *et al*⁷⁴ reported that secalonic acid D from the *Penicillium oxalium* fungus commonly found to infect corn crops, was present in corn dust from four sampled grain storage elevators in the US at levels of 0.3 – 4.5 ppm. This research was further developed by Pussemier *et al*⁷⁵ who found secalonic acid D in grain dust exposed workers at dangerous levels.



(18)	R ₁ = $\text{---}\text{Me}$	R ₂ = $\text{---}\text{OH}$	R ₃ = $\text{---}\text{CO}_2\text{Me}$	R ₄ = $\text{---}\text{CO}_2\text{Me}$	R ₅ = $\text{---}\text{OH}$	R ₆ = $\text{---}\text{Me}$
(19)	R ₁ = $\text{---}\text{Me}$	R ₂ = $\text{---}\text{OH}$	R ₃ = $\text{---}\text{CO}_2\text{Me}$	R ₄ = $\text{---}\text{CO}_2\text{Me}$	R ₅ = $\text{---}\text{OH}$	R ₆ = $\text{---}\text{Me}$
(20)	R ₁ = $\text{---}\text{Me}$	R ₂ = $\text{---}\text{OH}$	R ₃ = $\text{---}\text{CO}_2\text{Me}$	R ₄ = $\text{---}\text{CO}_2\text{Me}$	R ₅ = $\text{---}\text{OH}$	R ₆ = $\text{---}\text{Me}$
(21)	R ₁ = $\text{---}\text{Me}$	R ₂ = $\text{---}\text{OH}$	R ₃ = $\text{---}\text{CO}_2\text{Me}$	R ₄ = $\text{---}\text{CO}_2\text{Me}$	R ₅ = $\text{---}\text{OH}$	R ₆ = $\text{---}\text{Me}$
(22)	R ₁ = $\text{---}\text{Me}$	R ₂ = $\text{---}\text{OH}$	R ₃ = $\text{---}\text{CO}_2\text{Me}$	R ₄ = $\text{---}\text{CO}_2\text{Me}$	R ₅ = $\text{---}\text{OH}$	R ₆ = $\text{---}\text{Me}$
(23)	R ₁ = $\text{---}\text{Me}$	R ₂ = $\text{---}\text{OH}$	R ₃ = $\text{---}\text{CO}_2\text{Me}$	R ₄ = $\text{---}\text{CO}_2\text{Me}$	R ₅ = $\text{---}\text{OH}$	R ₆ = $\text{---}\text{Me}$
(24)	R ₁ = $\text{---}\text{Me}$	R ₂ = $\text{---}\text{OH}$	R ₃ = $\text{---}\text{CO}_2\text{Me}$	R ₄ = $\text{---}\text{CO}_2\text{Me}$	R ₅ = $\text{---}\text{OH}$	R ₆ = $\text{---}\text{Me}$

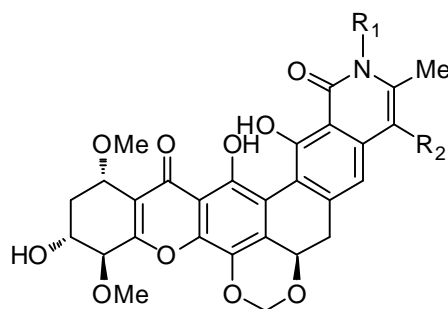
Figure 1.8: Structure of the secalonic acids

Secalonic acid A (**18**), however, has been found to have neuroprotective effects from colchine-induced apoptosis present in neurodegenerative diseases.⁷⁶ Secalonic acids B (**19**) and D (**21**) both exhibit potent cytotoxic activity to the B16 murine melanoma cell line (2.8 and 0.28 μM respectively).⁷⁷

To the best of our knowledge, despite much work on the monomeric components of the secalonic acids, there have been no total syntheses of any of these dimeric compounds.

1.4.2 Actinoplanones

The isolation and absolute structure determination of actinoplanones A and B (Figure 1.9) were described in 1988 by Noshino *et al.*⁷⁸ The natural product was isolated from the culture broth of a soil bacterium (*Actinoplanes* sp. R-304). The structure was determined using a wide range of spectroscopic methods. The same authors subsequently set out to isolate further analogues from the same culture broth.⁷⁹ Isolation was monitored using cytotoxicity against HeLa cells and the active fractions were purified using HPLC and preparative TLC. From this extraction, actinoplanones C-G were isolated and their structures identified. NOE experiments confirmed the relative configuration and Mosher's method⁸⁰ was employed to determine absolute configuration. Interestingly, the absolute configuration around the saturated ring is the same as for the kigamicins. The kigamicins also contain an acetal moiety in the same position in relation to the THX core and with the same absolute stereochemistry.



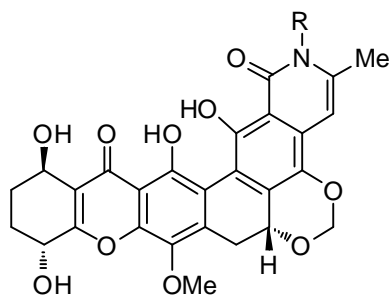
(25) Actinoplanone A	$R_1 = \text{NH}_2$	$R_2 = \text{Cl}$
(26) Actinoplanone B	$R_1 = \text{H}$	$R_2 = \text{Cl}$
(27) Actinoplanone C	$R_1 = \text{NH}_2$	$R_2 = \text{H}$
(28) Actinoplanone D	$R_1 = \text{H}$	$R_2 = \text{H}$
(29) Actinoplanone E	$R_1 = \text{N}=\text{C}(\text{CH}_3)_2$	$R_2 = \text{Cl}$
(30) Actinoplanone F	$R_1 = \text{N}=\text{C}(\text{CH}_3)\text{COCH}_3$	$R_2 = \text{Cl}$
(31) Actinoplanone G	$R_1 = \text{N}=\text{C}(\text{CH}_3)\text{COCH}_3$	$R_2 = \text{Cl}$

Figure 1.9: Structures of the actinoplanones

The actinoplanones A and B exhibited potent cytotoxicity against HeLa cells ($\text{IC}_{50} = 0.04 \text{ ng/mL}$; 5 ng/mL respectively) and actinoplanone C and G also demonstrated excellent cytotoxic activity ($\text{IC}_{50} = <0.04 \text{ ng/mL}$). Antifungal activity was also reported in the nanomolar range. Due to limited availability of material, only actinoplanones A, B and F were screened for antibacterial activity. Actinoplanone A showed strong activity against both Gram positive and Gram negative bacteria, whereas actinoplanone B and F were only active against Gram positive bacteria.

1.4.3 Simaomicin α and β

Simaomicin α and β are interesting natural products isolated in 1990 by Maiese *et al*⁸¹ from an *actinomycete* strain of bacteria. The structures were elucidated by Borders *et al*⁸² by a range of NMR techniques and x-ray crystallography.



32 R = Me
33 R = H

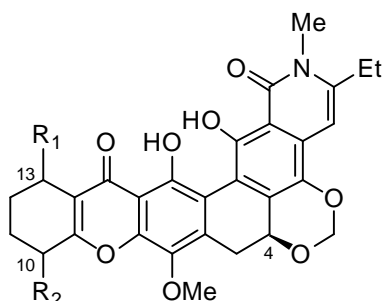
Figure 1.10: Structures of simaomicin α (32) and simaomicin β (33)

They have been reported to exhibit a wide range of biological activity. Initial analysis by Maiese⁸¹ showed that they displayed activity against Gram positive bacteria but not against Gram negative bacteria. They also reported antibiotic *in vitro* activity against a range of chicken coccidia, a type of parasite responsible for a significant economic loss to the poultry industry.⁸³ When tested *in vivo*, simaomicin α almost completely prevented lesions at only 1g/ton of medicated feed. Omura *et al*⁸⁴ reported simaomicin α to have extremely high *in vitro* potency against both drug resistant and drug sensitive strains of malaria ($IC_{50} = 0.045$ ng/mL and 0.0097 ng/mL respectively). They also reported strong cytotoxicity ($IC_{50} = 4$ ng/mL) against the human diploid embryonic cell line MRC-5. In 2009 Sugiyama *et al*⁸⁵ investigated the effect of simaomicin α on a variety of cancer cell lines and reported IC_{50} values in the nanomolar range against all tested cell lines.

To the best of our knowledge no synthetic work has been undertaken on this natural product.

1.4.4 Sch 42137

Three Sch 42137 compounds were isolated by Cooper *et al* in 1992⁸⁶ from a culture broth of *Actinoplanes* sp. SCC1906 isolated from a Brazilian soil sample.



- | | | |
|-----------------------------|----------------------|----------------------|
| (34) Sch 42137 (1) | R ₁ = OH | R ₂ = OH |
| (35) Sch 42137 (2) | R ₁ = OH | R ₂ = OAc |
| (36) Sch 42137 (3) | R ₁ = OAc | R ₂ = OH |

Figure 1.11: Structure of the Sch 42137 compounds

These compounds are active as antifungal agents with minimum inhibitory concentrations (MIC): **34**, 0.125 µg/mL; **35** and **36**, 1-2 µg/mL.

The authors conducted circular dichroism studies to establish the absolute configuration at C-4. Comparison to actinoplanone and lysolipin whose structures have been previously defined using CD spectra and single x-ray crystallography, provided evidence for absolute configuration at this centre. No effort, however, was made to establish the relative or absolute configuration at C-10 or C-13.

1.4.5 Ascherxanthonones A and B

Ascherxanthonone A was isolated from a culture of the fungus *Aschersonia* sp. BCC 8401 in 2005 by Isaka *et al.*⁸⁷ Chutrakul *et al.*⁸⁸ isolated Ascherxanthonone B alongside Ascherxanthonone A from the culture broth of *Aschersonia luteola* sp. BCC 8774 in 2009.

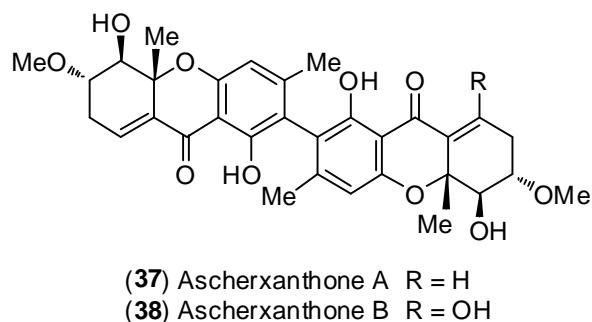


Figure 1.12: Structure of ascherxanthone A and B

The authors assigned the relative stereochemistry using NOE NMR experiments but attempts to synthesise Mosher's esters in order to assign the absolute configuration, were unsuccessful.

Ascherxanthone A was screened in a range of assays and was found to be a potent anti-malarial compound ($IC_{50} = 0.2 \mu\text{g/mL}$) and also a potent anti-cancer compound with activity against human epidermoid carcinoma cells ($IC_{50} = 1.70 \mu\text{g/mL}$), human breast cancer cells ($IC_{50} = 1.70 \mu\text{g/mL}$) and human lung cancer cells ($IC_{50} = 0.16 \mu\text{g/mL}$).

Ascherxanthone B is active against a rice blast fungus, *Magnaporthe grisea*, with an IC_{50} value of $0.58 \mu\text{g/mL}$, whereas ascherxanthone A showed no activity in this assay. Ascherxanthone B also displayed good activity *in vivo* in a rice plant infected with this pathogen.

1.4.6 Kibdelones

The kibdelones (Figure 1.13) were discovered and isolated by Capon *et al.*⁸⁹ from a rare *Kibdelosporangium* sp. MST-108465 soil bacteria. Screening of an organic extract from the culture broth of these bacteria revealed potent cytotoxic activity.⁹⁰

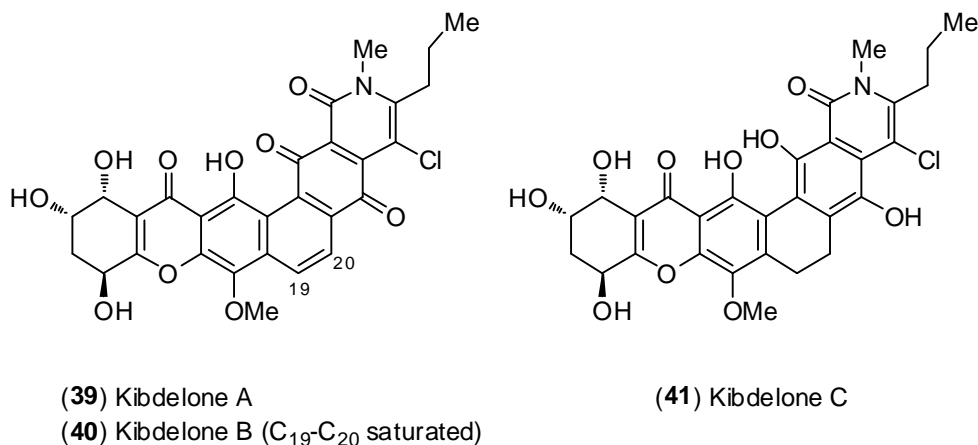
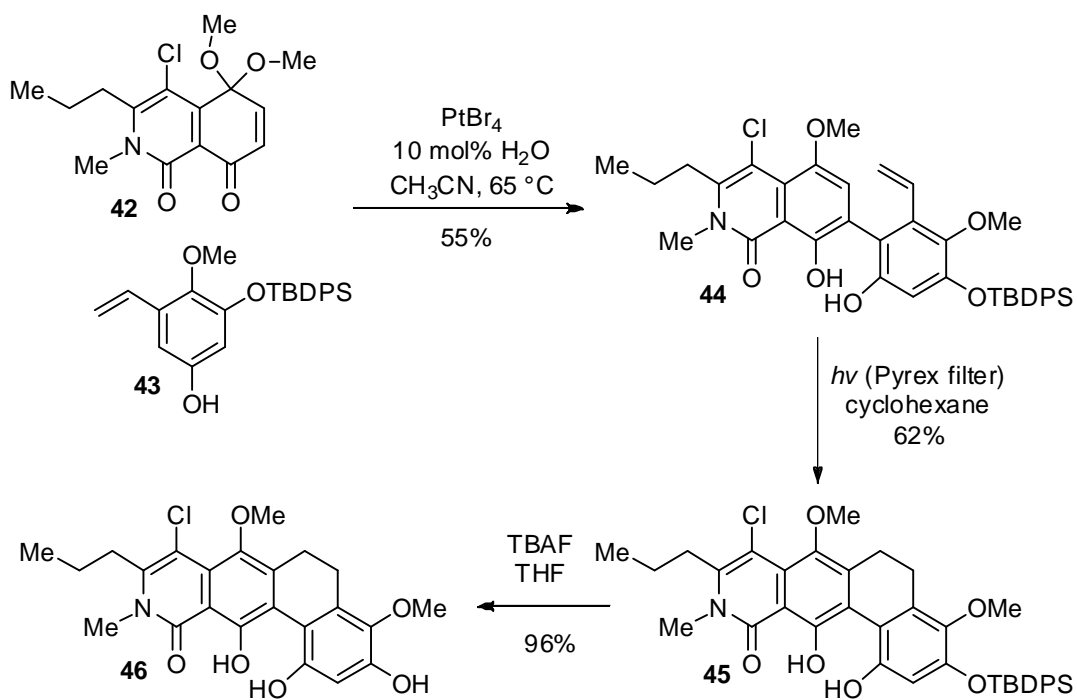


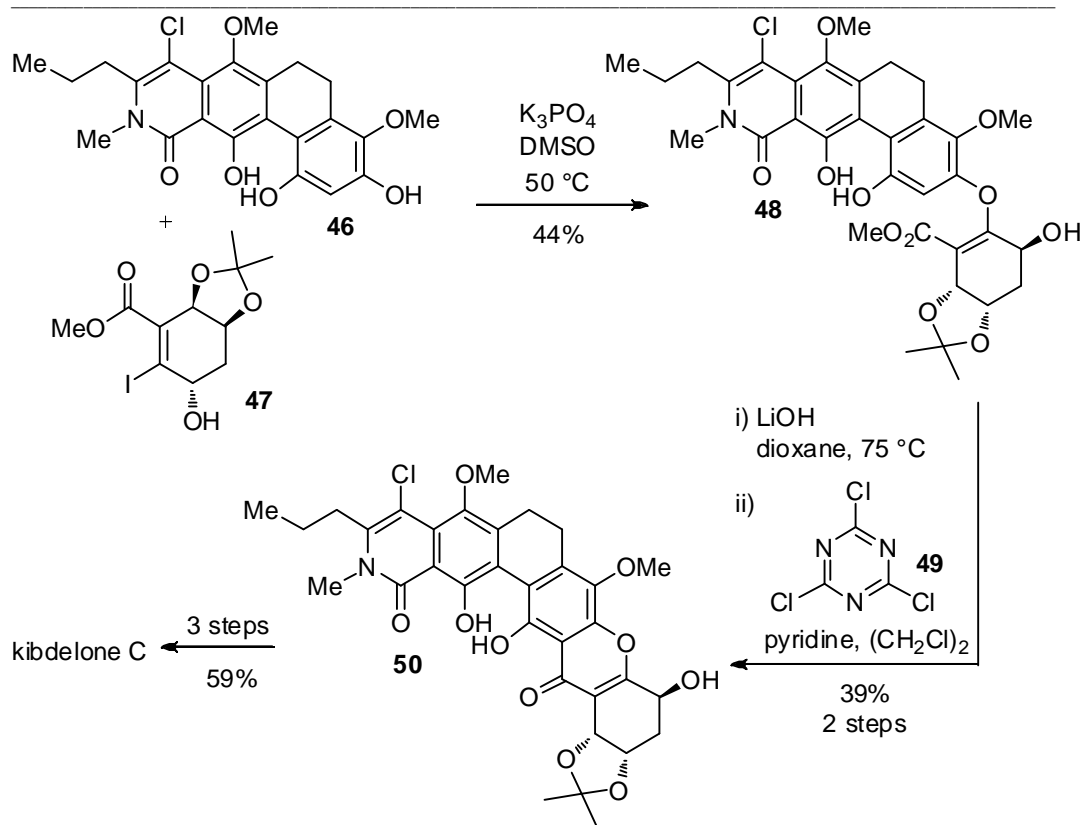
Figure 1.13: Structure of the kibdelones

A range of NMR and MS spectroscopic techniques allowed them to determine the structure of the kibdelones but the absolute stereochemical assignment was not established until Porco *et al.* completed the total synthesis in 2011 (described below).⁹¹ Comparison of the ¹H and ¹³C NMR, UV and optical rotations ($[\alpha]_D^{23} = +48^\circ$ synthetic, $+49^\circ$ natural (c = 0.5, CHCl₃)) of synthetic kibdelone C to that reported for the natural kibdelone, confirmed the absolute stereochemistry as that depicted (Figure 1.13). Interestingly, the absolute configuration at C-1 and C-4 is the same in the kibdelones as in the kigamicins and the actinoplanones.

There have been two reported syntheses of this natural product to date. Porco *et al.*⁹¹ and Ready *et al.*⁹² Both groups opted to construct the natural product in a convergent manner. Key steps in Porco's synthesis of fragment **46** were platinum mediated arylation of **42** and photocycloaddition of the resulting substrate **44**.⁹³

Scheme 1.2: Synthesis of **46**

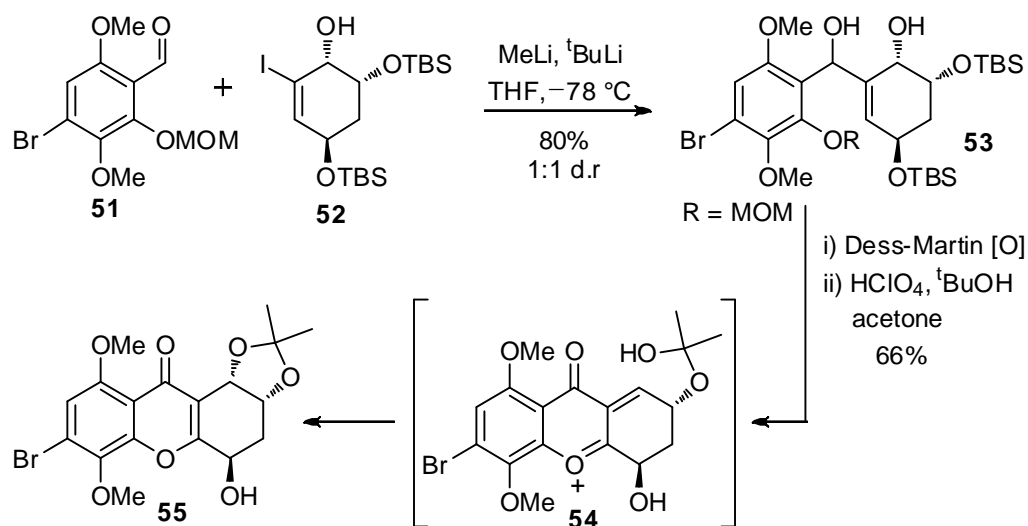
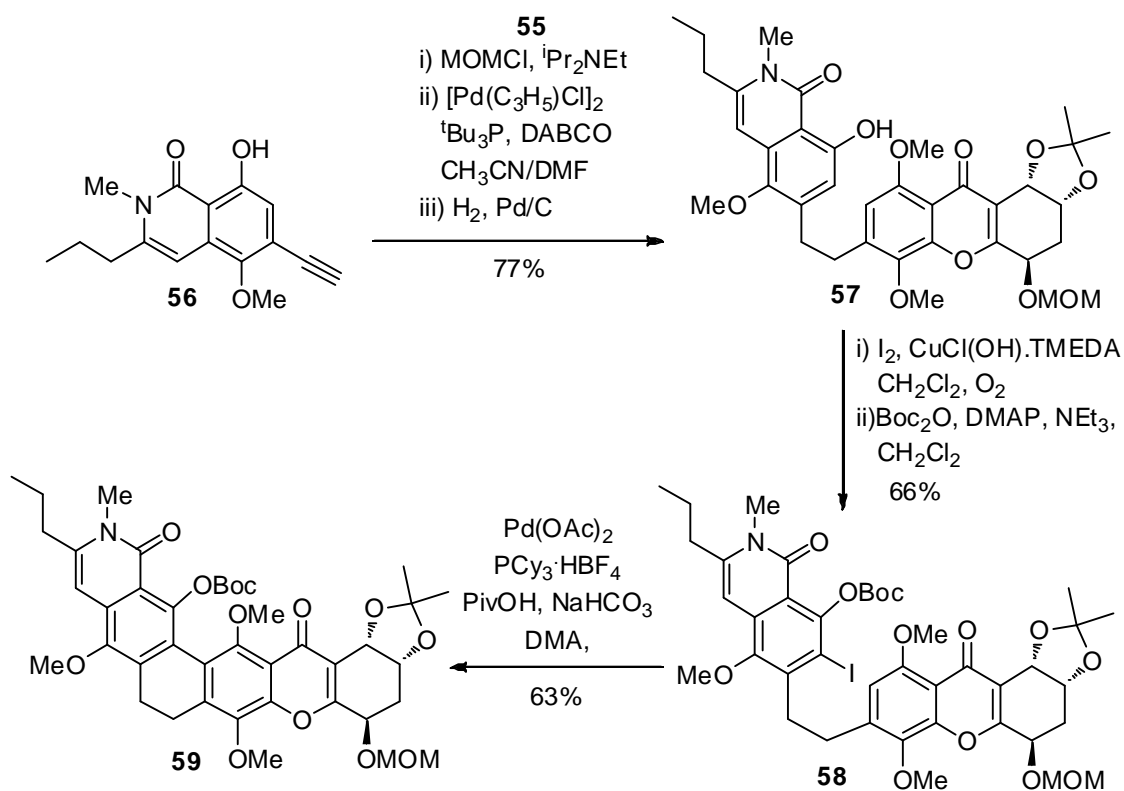
This fragment was then combined with **47** followed by cyclisation using cyanuric chloride **49** and pyridine in $(\text{CH}_2\text{Cl})_2$ to afford THX **50** in moderate yield. Kibdelone C (**41**) was formed in a further three steps and 59% yield.



Scheme 1.3: Final steps of Porco's kibelone C total synthesis

Ready and coworkers⁹² elected to begin the synthesis with formation of THX **55** by lithium-halogen exchange of **52** and addition into aldehyde **51**. Subsequent Dess Martin oxidation, deprotection of three hydroxyl groups, acid catalysed cyclisation and acetonide formation, provided **55** in 66% yield. The authors speculated that the cyclisation may occur through oxonium intermediate **54** (Scheme 1.4).

Sonogashira coupling of THX **55** and acetylene **56** combined the two halves of the natural product. Subsequent hydrogenation, copper catalysed iodination and C–H arylation provided the fused cyclic core. Kibelone C (**41**) was synthesised from **59** in four steps and 20% yield.

Scheme 1.4: THX formation by Ready *et al.*⁹²

Scheme 1.5: Final steps of Ready's kibelone C total synthesis

Initial biological screening of kibelone C was carried out by Capon *et al.*⁸⁹ They reported strong antibacterial activity against gram positive bacteria (LD₉₉ = 0.13

nM) and potent nematocidal activity ($LD_{99} = 8.5$ nM). They also reported anti-cancer activity with GI_{50} values of <0.3 nM against leukaemia and colon, CNS (central nervous system), melanoma, ovarian, renal, prostate and breast cancers.

Porco *et al*⁹³ tested the kibelones in the NCI 60-cell panel of human cancer cell lines and found potency in the nanomolar region against both leukaemia and renal cancer cell lines. This prompted them to investigate the total synthesis (as reported above). During the course of the total synthesis, they decided to test fragments of the natural product (**60** and **61**) in the NCI 60-cell panel in order to compare the biological activity.

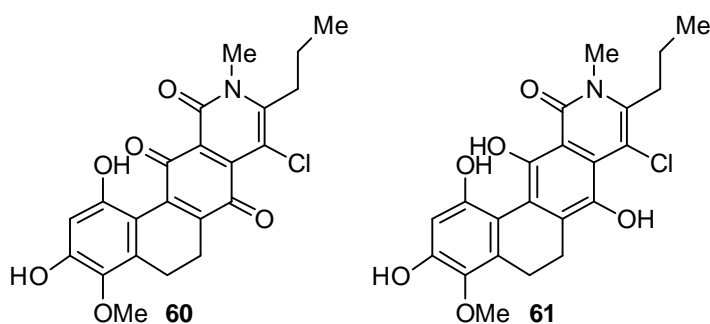


Figure 1.14: Kibelone analogues for biological screening

The fragments also showed anti-cancer properties, however they reported much lower potencies (4.5 μ M *cf.* 2.4 nM for the kibelones). The authors concluded that the missing tetrahydroxanthone may be important for high potency.

1.4.7 Globosuxanthonones A and B

Globosuxanthone B is a tetrahydroxanthone with a highly substituted saturated ring. It was isolated by Gunatilaka *et al* in 2006⁹⁴ from *Chaetomium globosum*, a fungal strain from the rhizosphere of *Opuntia leptocaulis*, a Christmas cactus. Globosuxanthone A, the corresponding dihydroxanthone, was also isolated. Both

were tested for cytotoxic activity and globosuxanthone A was found to have greater activity against all seven human cancer cell lines screened.

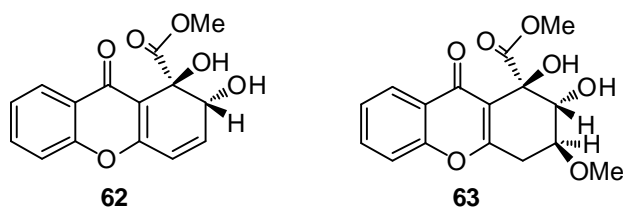


Figure 1.15: Structures of globosuxanthone A (62) and B (63)

1.4.8 Blennolides A, B and C

Blennolides A, B and C were originally isolated from a fungus (*Blennoria*) from the Canary Islands, by Krohn *et al* in 2008.⁹⁵

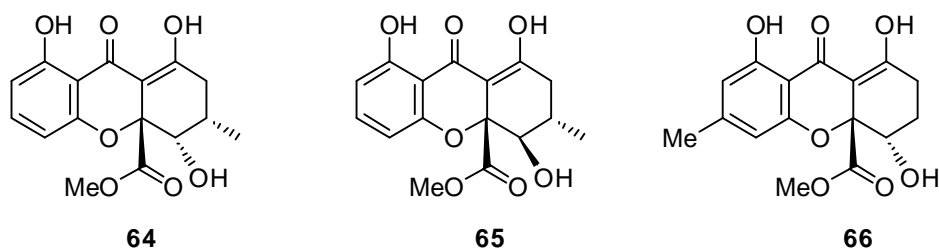
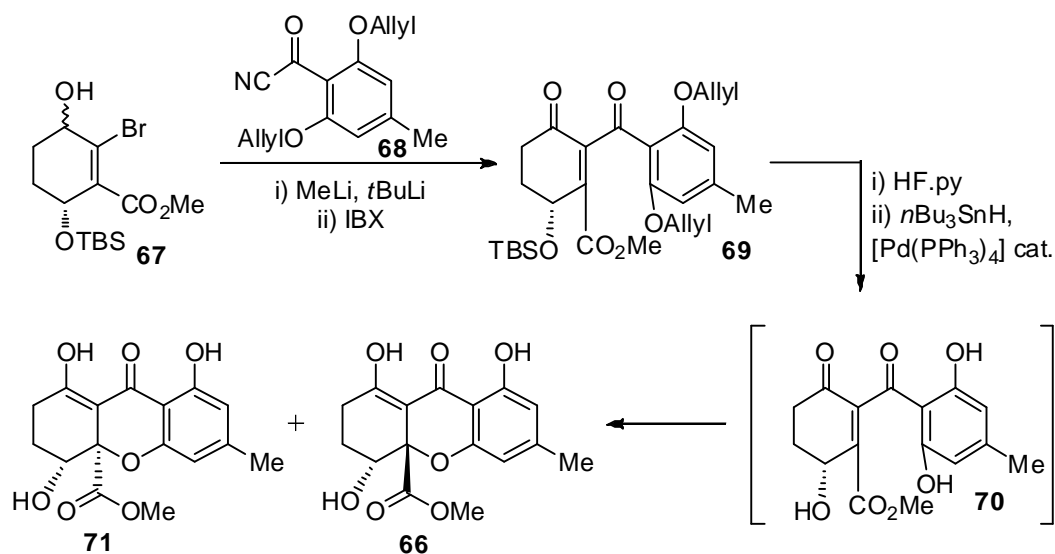


Figure 1.16: Structures of blennolides A (64), B (65) and C (66)

After some controversy surrounding the structure of these natural products, they were assigned as depicted in Figure 1.16 by Nicolaou *et al*⁹⁶ by total synthesis of blennolide C and comparison to data obtained for the original sample isolated by Krohn.⁹⁵

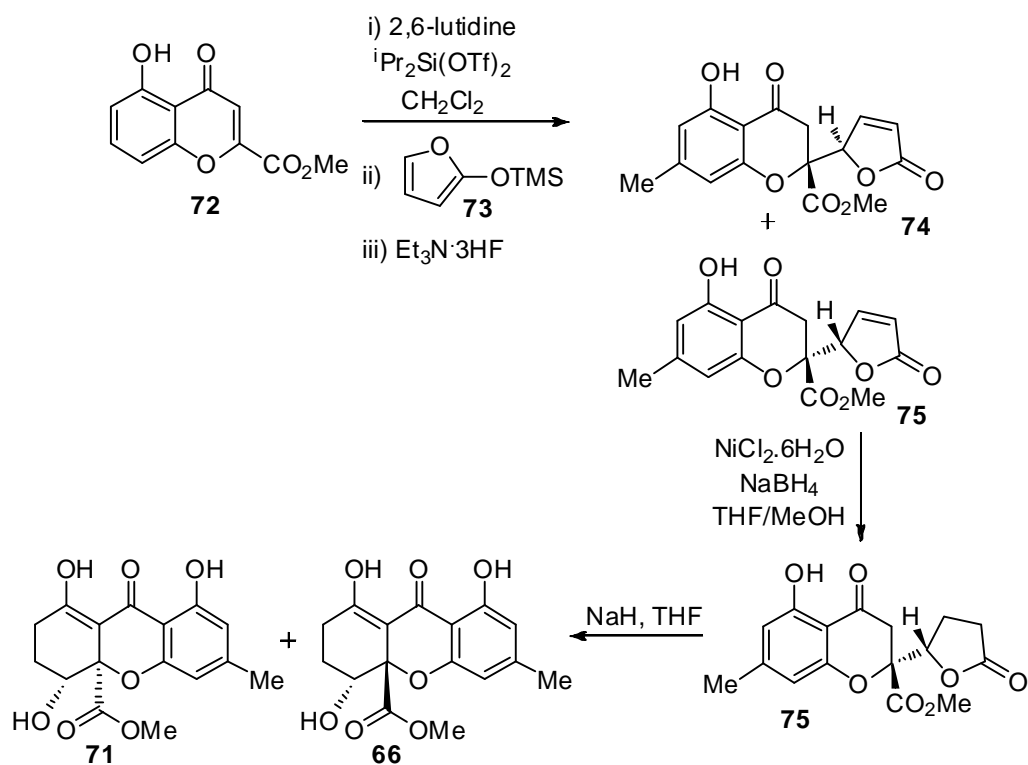
Blennolide A and B exhibit anti-algal activity, anti-fungal activity and also activity against Gram positive and Gram negative bacteria.⁹⁵

There are several reported syntheses of blennolide C⁹⁶⁻⁹⁸, only one for blennolide B and to the best of our knowledge, none for blennolide A. Nicolaou *et al*⁹⁶ used a domino deallylation-oxa-michael reaction as their key step from **69** synthesised by lithium-halogen exchange of **67** and addition into acyl cyanide **68** followed by oxidation to give desired diketone **69** (Scheme 1.6).



Scheme 1.6: Key steps in Nicolaou's synthesis of blennolide C⁹⁶

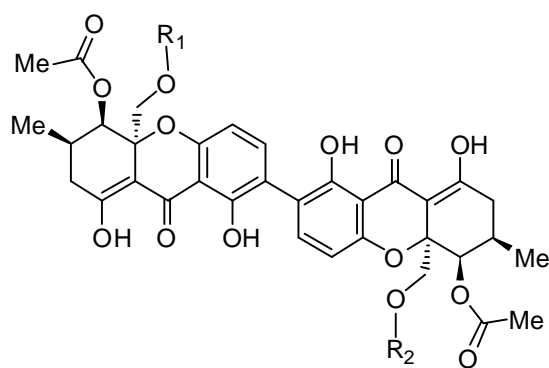
Porco *et al*⁹⁸ reported the synthesis of both blennolide B and C by vinylogous addition of siloxyfurans **73** to **72** and subsequent Dieckmann cyclisation, to provide the natural products in four steps (Scheme 1.7). Blennolide B was made in an analogous fashion.



Scheme 1.7: Key steps in Porco's synthesis of blennolide C

1.4.9 Dicerandrols A, B and C

Dicerandrols A, B and C were isolated from the fungus *Phomopsis* sp. PSU-D15 by Rukachaisirikul *et al*⁹⁹ in 2008 and also by Clardy *et al*¹⁰⁰ in 2001 from *Phomopsis longicolla* which is a fungus of the endangered mint *Dicerandra frutescens*.



- (76) Dicerandrol A: $\text{R}_1 = \text{H}$ $\text{R}_2 = \text{H}$
 (77) Dicerandrol B: $\text{R}_1 = \text{Ac}$ $\text{R}_2 = \text{H}$
 (78) Dicerandrol C: $\text{R}_1 = \text{Ac}$ $\text{R}_2 = \text{Ac}$

Figure 1.17: Structures of the dicerandrols¹⁰⁰

The biological activity of these compounds was assessed against *Staphylococcus aureus* and *Bascillus subtilis* bacteria, *Geotrichum candidum* fungus, *Saccharomyces cerevisiae* yeast, human colon tumour cell line HCT-116 and human lung tumour cell line A549. They found that all three compounds showed anti-bacterial activity but were inactive against the fungus and yeast. They also showed activity against both cancer cell lines ($IC_{50} = 1.8 - 7.0 \mu\text{g/mL}$).

1.5 Conclusions

Despite the improvements in prognosis for many cancers over the last decade, little such improvement has been realised for patients with pancreatic cancer. This is due in part, to the ability of the cancer cells to survive under austere conditions and the inability of the current chemotherapy drugs to demonstrate cytotoxicity under such conditions.

The new anti-austerity approach to selectively target cancer cells, opens up an exciting new avenue of research. The kigamicins are exciting lead structures in this research area and have shown efficacy both *in vitro* and *in vivo* with no obvious toxicity to normal cells. The THX nucleus forms the core of this natural product and many closely related polycyclic structures displaying potent biological activities, including cytotoxic activity. Simpler THXs – either monomeric or dimeric –display a range of interesting biological properties, including against cancer.

Thus, it is tempting to speculate that the THX nucleus of the kigamicins is responsible, at least in part, for the anti-austerity effects of the kigamicins.

In this thesis, we have set out to test this hypothesis through the synthesis of simplified kigamicin analogues that retain the THX nucleus and their evaluation in anti-austerity assays. Since mild methods for the synthesis of THXs are not especially well established, this has necessitated the development of innovative new chemical methods for the synthesis of these oxygen heterocycles.

Chapter 2:
Synthesis of
Tetrahydroxanthones

2.1 Initial Studies and Synthesis of Kigamicin Analogues

2.1.1 Introduction

As discussed in Chapter One, the tetrahydroxanthone (THX) nucleus forms the central core of many biologically active natural products including the kigamicins,¹⁰¹ kibdelones,⁹⁰ actinoplanones,⁷⁸ simaomicin α ,⁸² globosuxanthone B⁹⁴ and artopeden A¹⁰² (Figure 2.1). As such, it is reasonable to assume that the THX nucleus may be responsible, at least in part, for the biological activity of these natural products.

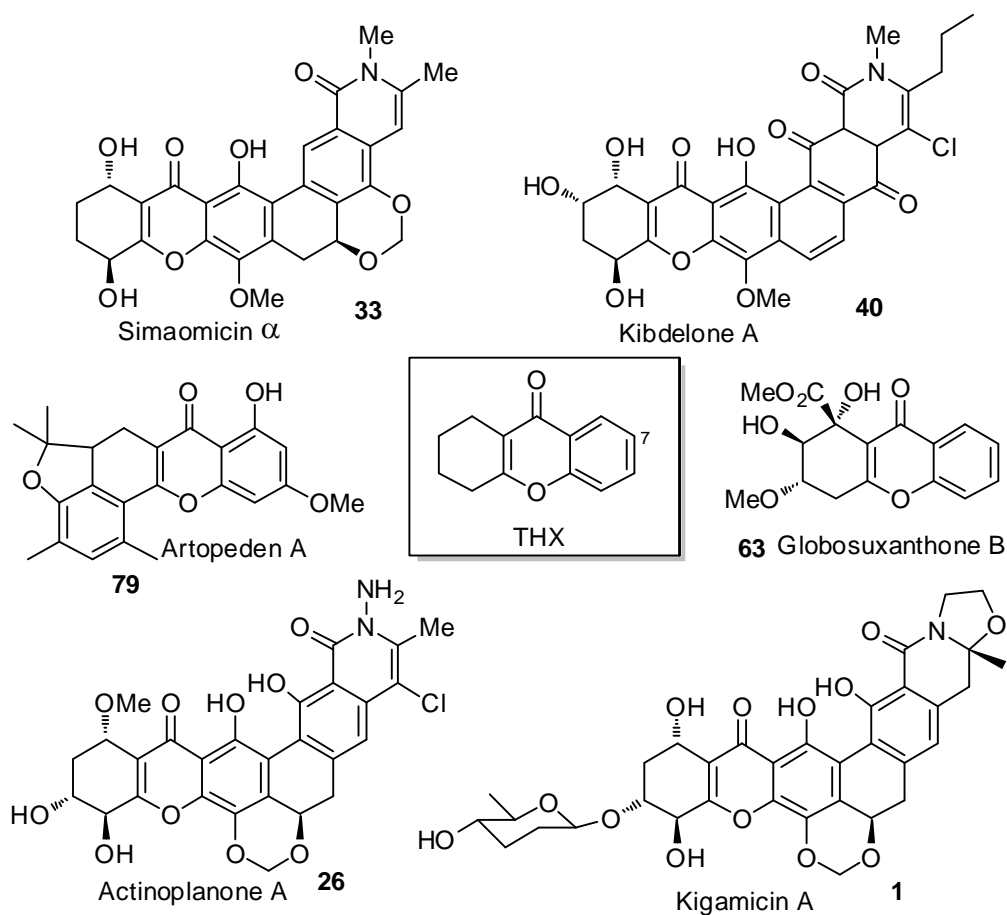


Figure 2.1: Natural products containing the THX core

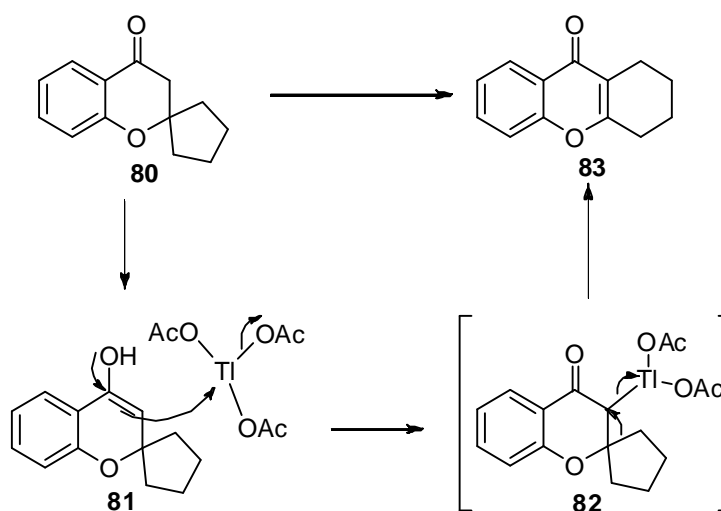
Clearly, the development of efficient routes to THXs is desirable so that analogues can be synthesised in order to investigate structure activity relationships. It is also

important that any such methodology allows for the incorporation of an aryl group at the 7-position of the THX – a key feature of many of these natural products.

This chapter focuses initially on the synthesis of 7-arylated THXs using existing methodology before exploring improved metal catalysed routes. Finally, tandem catalysis is developed utilising the developed metal catalysed strategies in partnership with conventional cross coupling reactions to facilitate the synthesis of 7-arylated THXs very directly.

2.1.2 Existing methodology for the synthesis of tetrahydroxanthenes

Kapil *et al*¹⁰³ reported the synthesis of THXs via the oxidation and alkyl migration of 2-spirochromanones. This method utilises thallium (III) nitrate or acetate to first oxidise 2-spirochromanone **80** prior to alkyl migration.¹⁰⁴ It is proposed that this migration is driven by the greater stability of the resulting conjugated THX **83**.

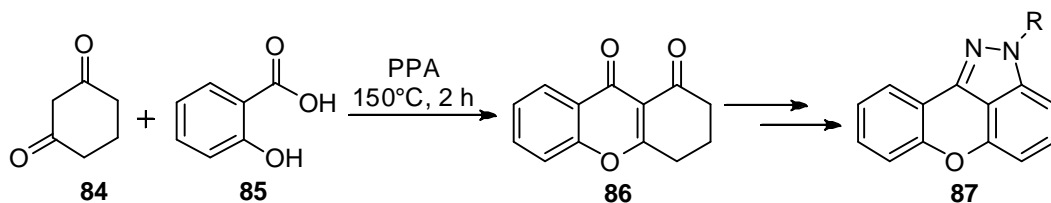


Scheme 2.1: Mechanism proposed for THX synthesis *via* spirochromanones¹⁰⁴

THXs have also been synthesised by Marakos *et al*¹⁰⁵ who created small libraries of compounds for biological screening and SAR studies. Their research was based

around aminoanthraquinones which exhibit potent anti-tumour properties. However, they have limited clinical use due to their cardiotoxic side effects. To this end, Marakos *et al* sought to create novel analogues including pyrazole-fused xanthenones **87** and amino derivatives thereof.

This involved the initial synthesis of xanthenes and tetrahydroxanthenes as precursors for the more elaborate biologically active molecules described above. The THX moiety was produced by heating 1,3-cyclohexanedione and salicylic acid with polyphosphoric acid at 150 °C.



Scheme 2.2: Synthesis of pyrazole-fused xanthenones via THX synthesis¹⁰⁵

In 1987, Watanabe and coworkers explored the synthesis of the chromone core of Khellin, a natural product with antispasmodic and coronary vasodilating properties (Figure 2.2).¹⁰⁶

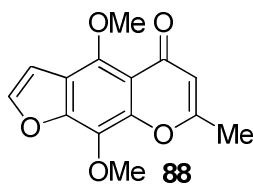
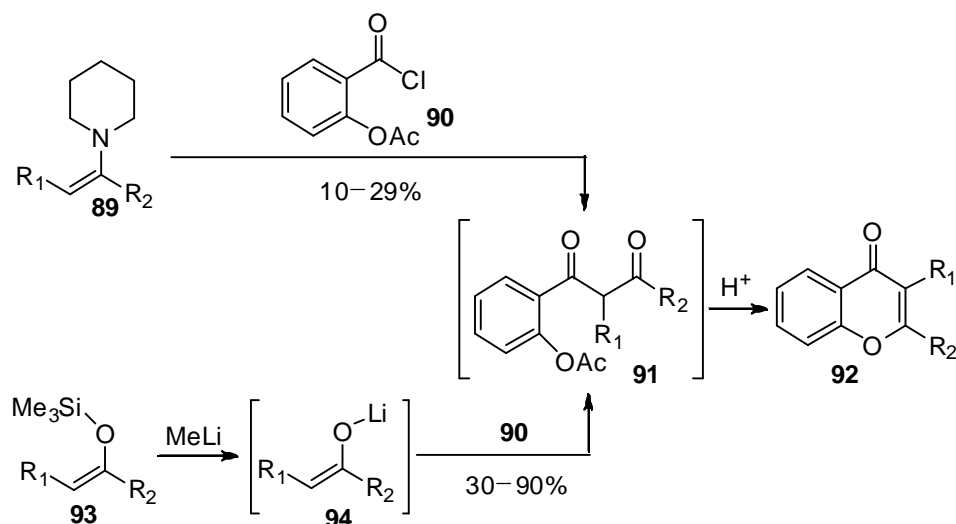


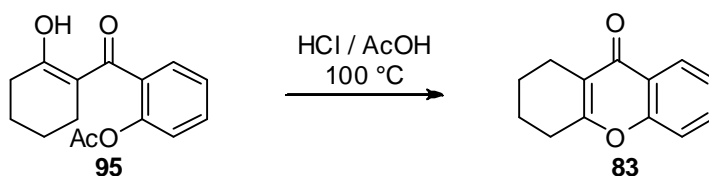
Figure 2.2: Khellin

To rapidly synthesise analogues for SAR studies, they investigated various routes to **92**, from the silyl enol ether **93** or enamine **89** (Scheme 2.3). Their findings revealed that either precursor was suitable but much greater yields were generally obtained using the lithium enolate method derived from the silyl enol ether.



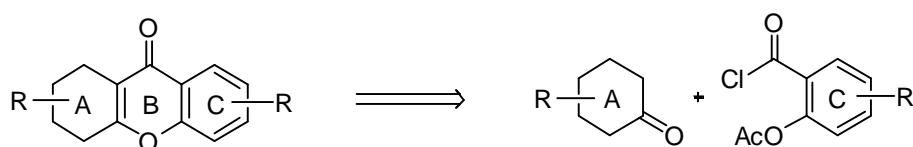
Scheme 2.3: Synthetic routes to chromones

In all these syntheses, the final step to form the xanthone or THX was acid catalysed dehydration. This method involves the deprotection of the acetate protecting group and cyclisation in one step by heating the precursor in concentrated acetic and hydrochloric acid to 100 °C.



Scheme 2.4: Acid catalysed dehydration

To make THXs rapidly, we wanted to explore a convergent synthesis whereby functionalised A and C rings could be brought together with assembly of ring B.

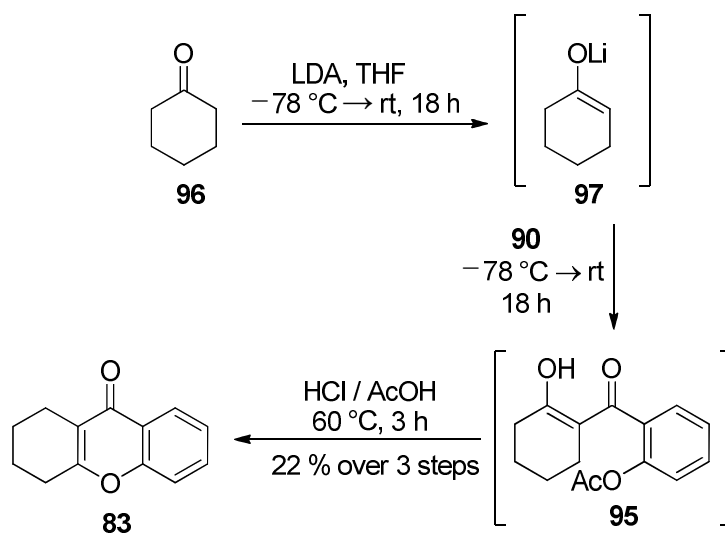


Scheme 2.5: Convergent synthesis to the THX

Encouraged by the good to excellent yields achieved in the aforementioned research by Watanabe *et al.*,¹⁰⁶ we sought to establish if this might provide a general route to THXs.

2.1.3 Tetrahydroxanthone synthesis by acid catalysed dehydration

Initially, we set about the synthesis of known THX **83** (Scheme 2.6). The lithium enolate **97** was formed directly from cyclohexanone **96** and not from the silyl enol ether as reported by Watanabe *et al.*¹⁰⁶ This was in order to minimise the number of steps in the synthesis. Enolate **97** was then added to acid chloride **90** to form **95**. This was not fully purified although an aqueous work-up was performed at this point to remove remaining diisopropylamine before the acid catalysed dehydration step.

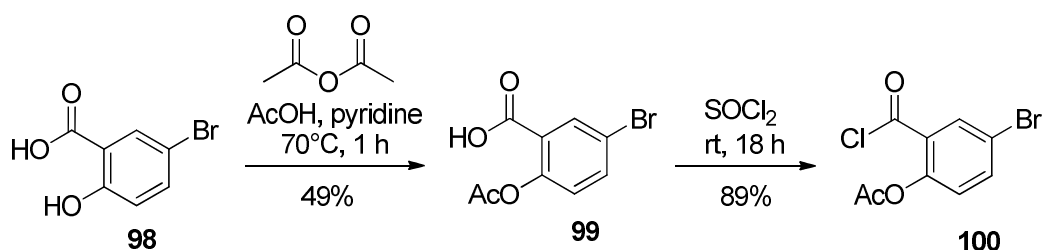


Scheme 2.6: Synthesis of the THX using acid

Disappointingly this reaction gave low yields (17-22%) compared with that reported by Watanabe *et al* (30-90%)¹⁰⁶ where enolate **97** was generated from the silyl enol ether (Scheme 2.3). Since **95** has a very acidic hydrogen, we were concerned that the product might be deprotonated. In order to improve the yield, the equivalents of LDA were increased from 1 to 1.5. This led to further side product

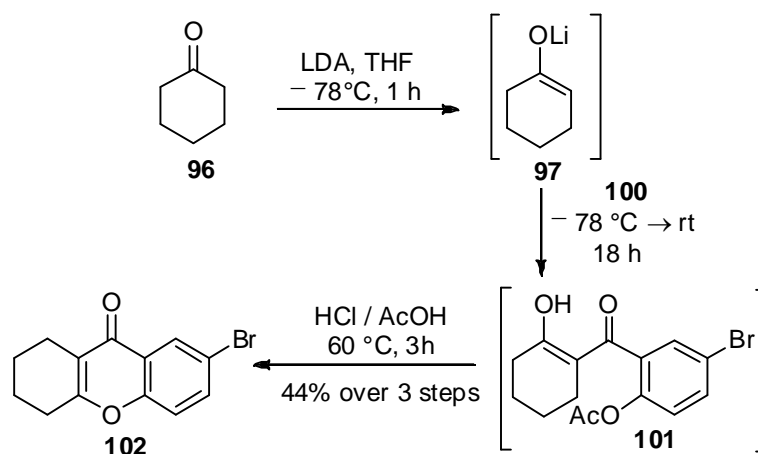
resulting from the addition of diisopropylamine (for LDA formation) to the acid chloride. The equivalents of acid chloride were increased to 1.5 but this did not result in an improved yield. The length of time for enolate formation was varied from 1 to 2 h but this had no effect. The base was changed to LiHMDS to try and minimise side products but unfortunately had no effect on the yield of reaction. In view of these results, lithium enolate **97** was generated from the silyl enol ether following the work of Watanabe¹⁰⁶ (Scheme 2.3). However, this resulted in no improvement to the yield.

We then attempted to introduce a bromine onto the 7-position of the aromatic ring of the THX in order to enable further elaboration of these compounds *via* cross coupling reactions. This was accomplished by treating 5-bromosalicylic acid **98** with acetic anhydride and acetic acid, followed by treatment **99** with thionyl chloride to give acid chloride **100**.



Scheme 2.7: Synthesis of the brominated acid chloride

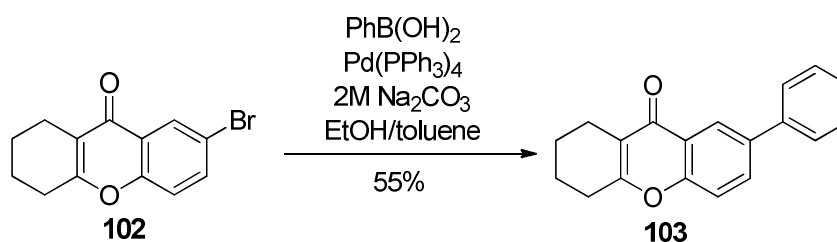
With bromide **100** in hand, the corresponding THX **102** was synthesised without problem but the yield for this reaction was comparably poor (22%). However, on scale up (9 g, 32 mmol), the yield improved to 44%.



Scheme 2.8: Synthesis of brominated THX

2.1.4 Suzuki-Miyaura couplings

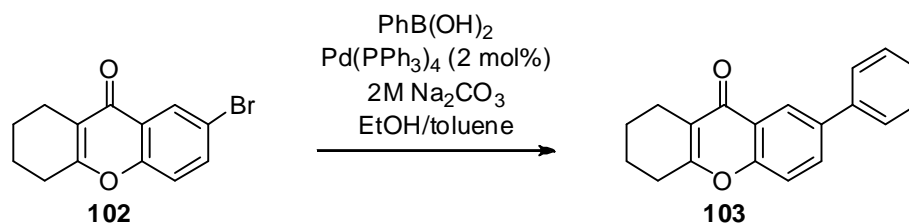
Next, we wished to carry out a series of Suzuki-Miyaura couplings in order to form 7-arylated THXs which might overlay well with the 7-aryl ring of the natural product. Such cross-coupling reactions have been thoroughly researched and a plethora of reaction conditions exist for this transformation.¹⁰⁷ Initially, we examined the coupling of bromide **102** with phenyl boronic acid (1 equiv.) using $\text{Pd}(\text{PPh}_3)_4$ (2 mol %) and 2M Na_2CO_3 (2 equiv.) in EtOH/toluene (1:1) (0.5 mM).¹⁰⁸ This provided **103** in an encouraging 55% yield.



Scheme 2.9: Suzuki-Miyaura reaction

The conditions for the Suzuki-Miyaura reaction were further optimised using phenyl boronic acid before applying them to other boronic acid substrates (Table 2.1).

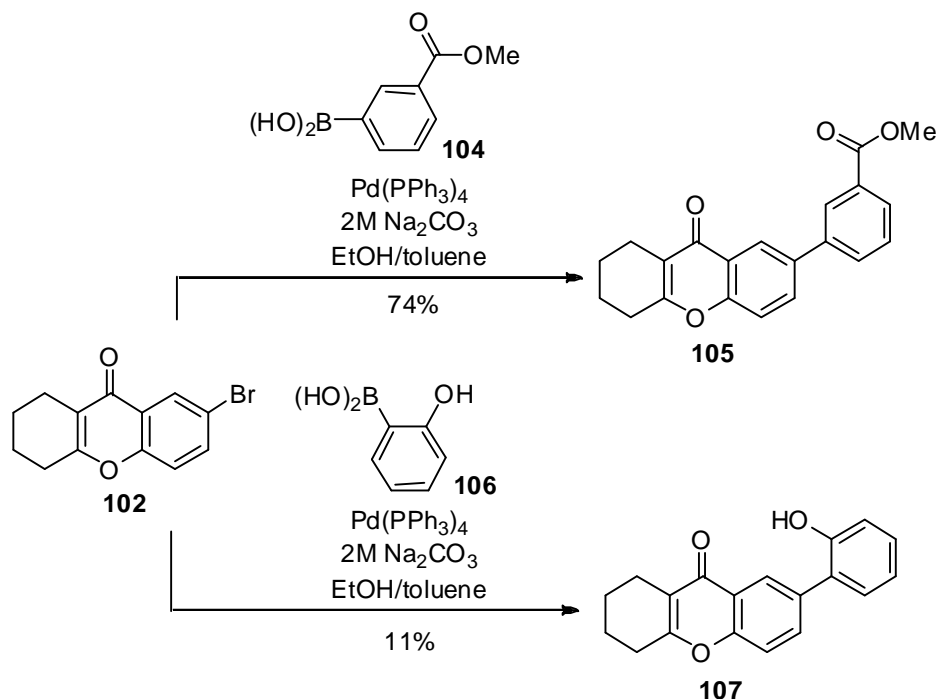
As shown in Table 2.1, the yield improved as the equivalents of boronic acid were increased (entry 5). However, increasing the equivalents of base had the opposite effect with two equivalents optimal. There was no appreciable difference in yield between reactions carried out in a microwave and reactions heated to reflux in a round-bottomed flask but due to shorter reaction times, microwave irradiation was used for all subsequent reactions.



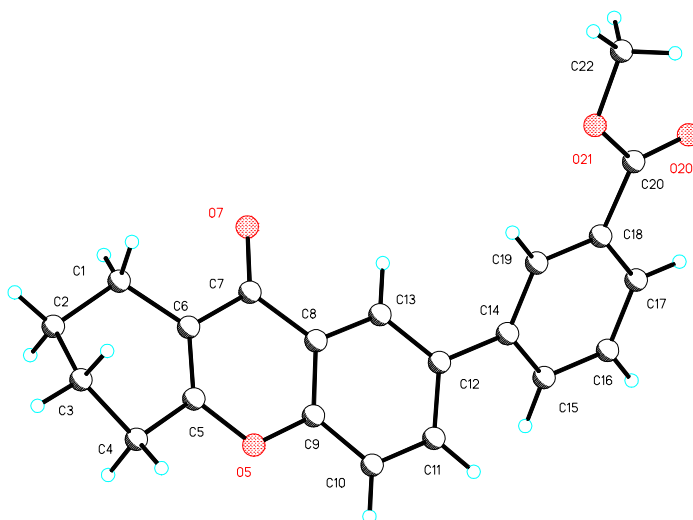
Entry	Boronic acid equiv.	2M Na ₂ CO ₃ equiv.	Reaction conditions	Yield (%)
1	1	2	thermal heating 90 °C, 1 h 45 min	55
2	2	2	thermal heating 90 °C, 1 h 45 min	67
3	2	2	microwave irradiation 300 W, 110 °C, 10 min	71
4	2	4	microwave irradiation 300 W, 110 °C, 10 min	52
5	3	2	microwave irradiation 300 W, 110 °C, 10 min	76

Table 2.1: Optimisation of Suzuki-Miyaura Couplings

The best yield obtained for the coupling of phenyl boronic acid with **102** was 76%. Different boronic acids were then used to test the substrate scope and produce derivatives **105** and **107**. A low yield was obtained for **107**, presumably due to the substituent *ortho* to the boronic acid (discussed in more detail in Section 2.2).

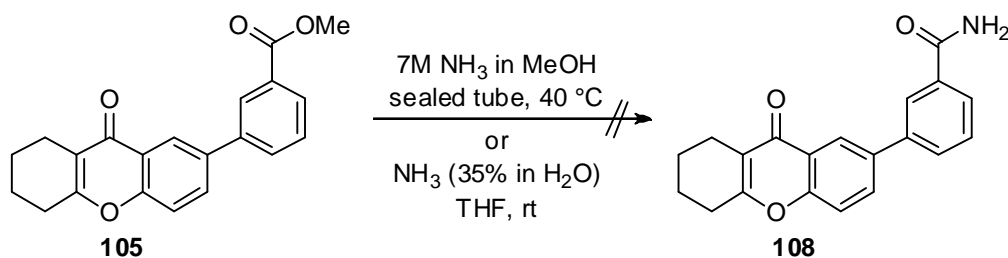
Scheme 2.10: Synthesis of derivatives **105** and **107**

The structures of **83**, **102**, **103** and **105** were all confirmed by ^1H and ^{13}C NMR spectroscopy, high resolution MS and elemental analysis. In the case of **83**, the data matched that reported in the literature.¹⁰⁹ A single crystal of compound **105** was grown from chloroform by slow evaporation and the structure unambiguously confirmed using single x-ray crystal diffraction (see Appendix I).

Figure 2.3: Crystal structure of compound **105**

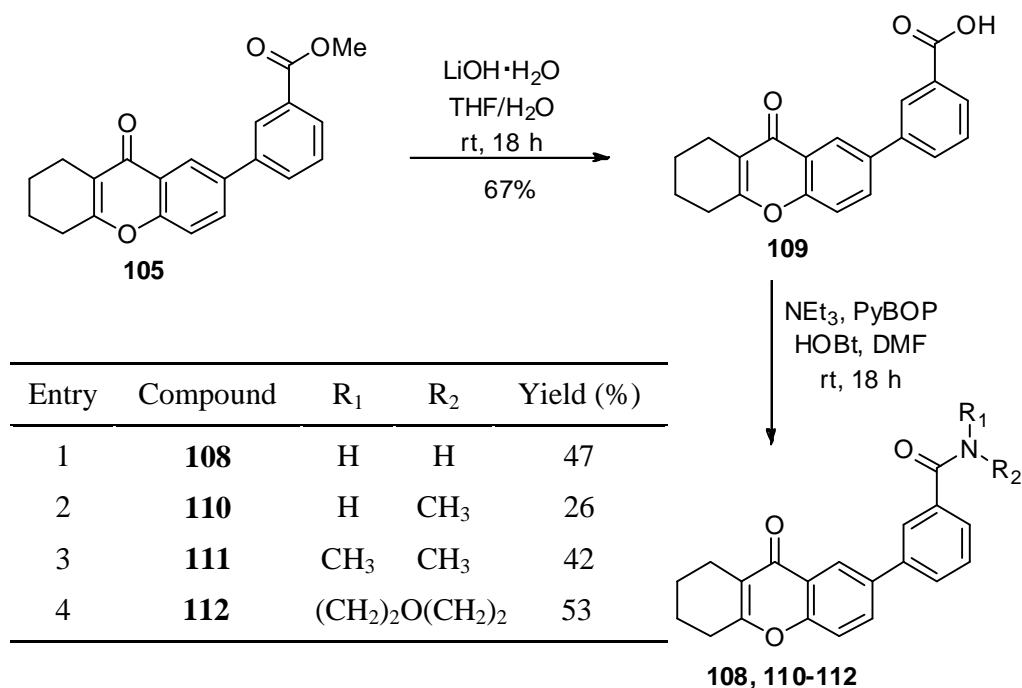
2.1.5 Amide couplings

With ester **105** in hand, we wished to make the corresponding amide which would further overlay kigamicin A, since an amide group is found in this position in the natural product (Figure 2.1). Initially, reactions between ester **105** and ammonia were attempted in MeOH and H₂O/THF but without success (Scheme 2.11).



Scheme 2.11: Attempted synthesis of amides

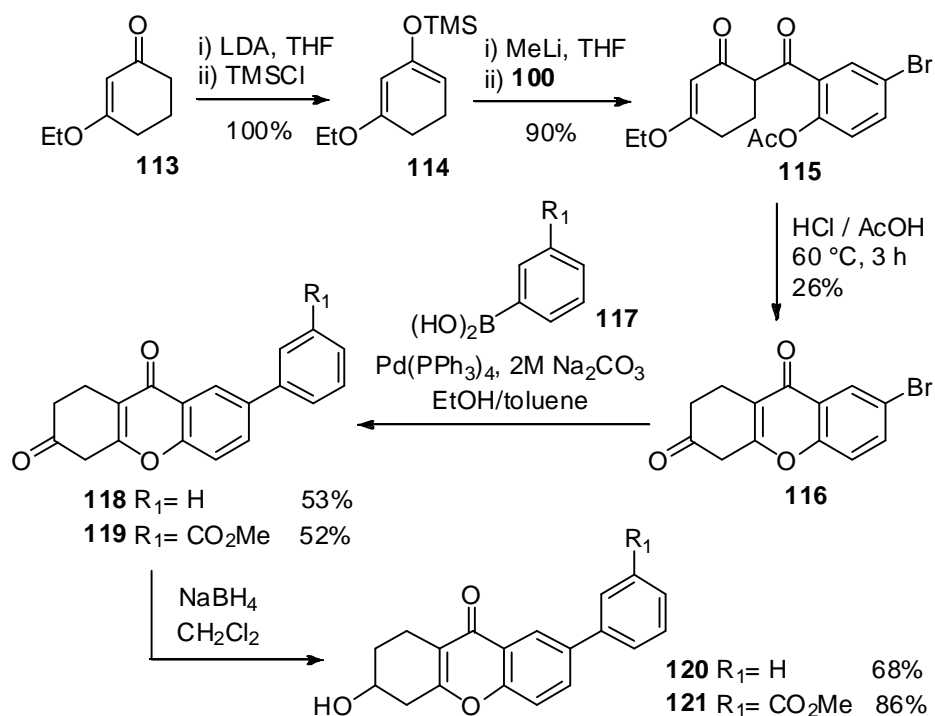
Subsequently, the ester was hydrolysed to the carboxylic acid before successfully undergoing conventional amide coupling. Several different analogues, namely **108** and **110-112** were synthesised in this manner (Scheme 2.12). These included a morpholine adduct **112**, which contains an additional oxygen and saturated ring to approximate the H ring of the natural product. Moderate to low yields were obtained for all of the amide couplings shown in Scheme 2.12, although no starting material or by-products were isolated. Despite this, there was sufficient material obtained for biological testing and therefore no alternative coupling reagents (such as DCC, EDC or HATU)¹¹⁰ were investigated.



Scheme 2.12: Hydrolysis and subsequent amide couplings

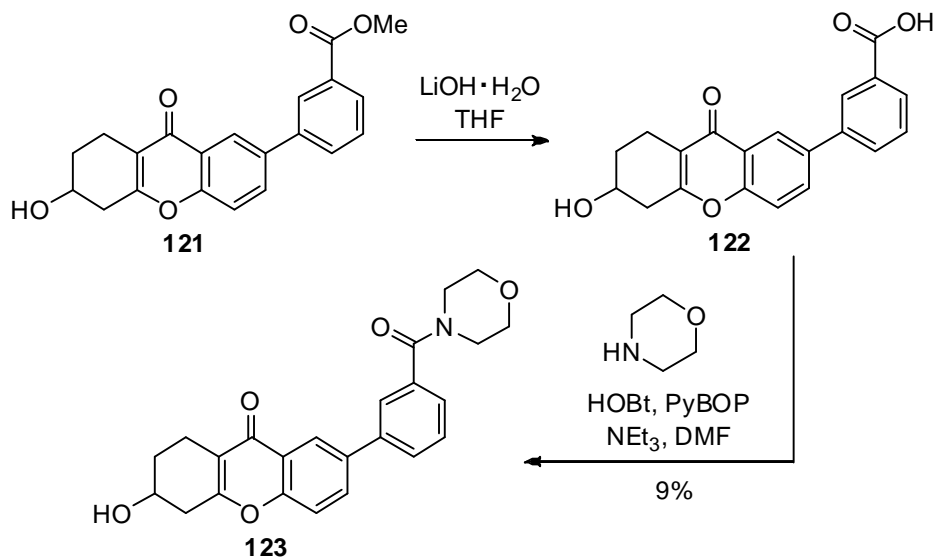
2.1.6 Initial library of natural product analogues

A further four analogues **118-119** were synthesised by a placement student, Chua Chun Kiang, under my supervision, that differed in the nature of the saturated A ring. An additional ketone group was incorporated into the A ring and the corresponding alcohol analogues were synthesised by final reduction of these ketones (Scheme 2.13).



Scheme 2.13: Synthesis of analogues

A further analogue **123** was also made by Chua Chun Kiang by hydrolysis and subsequent amide coupling of ester **121**.

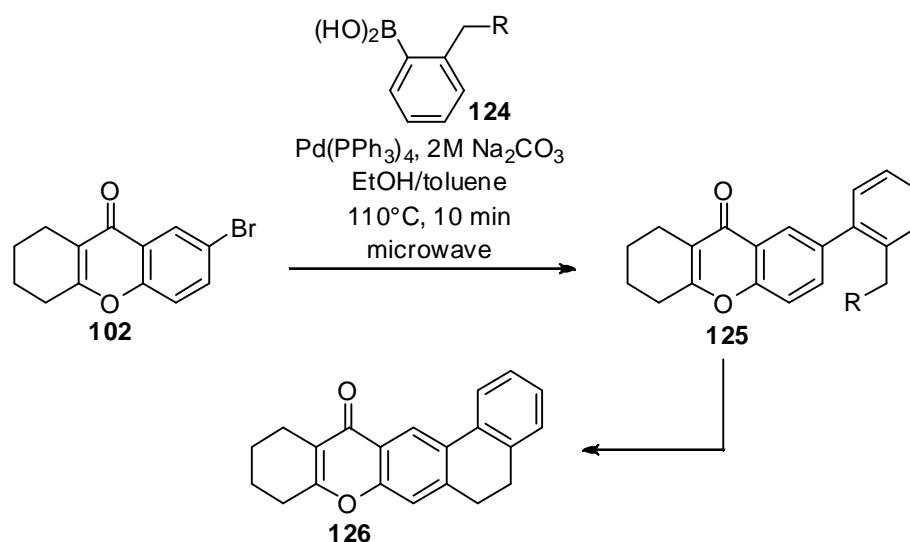


Scheme 2.14: Hydrolysis and amide coupling

The final library of analogues, along with kigamicin C itself (commercially available¹¹¹) were then tested for cytotoxicity against PANC-1 cells at the Peninsula Medical School (see Chapter Four).

2.2 Attempted Synthesis of the Natural Product E Ring

With this methodology in place, we wished to use *ortho* substituted boronic acids or esters in the cross couplings such that more complex analogues could be made and tested for biological activity. If an analogue could be synthesised with functionality *ortho* to the aryl-aryl bond, then the synthesis of the saturated E ring could be attempted (Scheme 2.15). This was thought to be desirable as it would further limit the number of rotatable bonds, an important concept in medicinal chemistry.¹¹²⁻¹¹⁴ Such a difference in conformational rigidity could have a large impact on the biological activity. Pentacycle **126** was expected to have a conformation much more akin to the natural product.

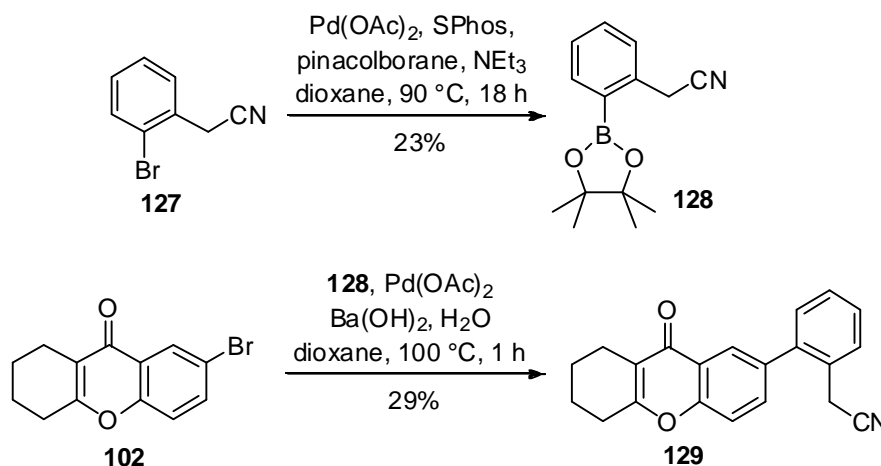


Scheme 2.15: Strategy to the synthesis of more complex analogues

Historically, the use of *ortho* substituted boronic acids in Suzuki-Miyaura reactions, often results in much longer reactions times and/or lower yields compared to *meta*

and *para* substituted derivatives. This can be attributed to the inherent steric hindrance which is particularly problematic during the transmetallation step of the catalytic cycle.¹¹⁵ Boronic acids used in Suzuki-Miyaura couplings can be prone to competitive hydrolytic deboronation and due to the longer reaction times with *ortho* substituted boronic acids, higher quantities of such side-product are often observed.^{116,117} Often, pinacol esters are used as they are less susceptible to hydrolytic deboronation, however this does not entirely solve this problem.¹¹⁶

Baudoin *et al*¹¹⁸ developed and optimised Suzuki-Miyaura reactions for the formation of *ortho* substituted pinacol esters, similar in structure to those required by us. Based on this work, boronic pinacol ester **128** was synthesised directly from **127** which was commercially available. The yield for this transformation was low, but provided sufficient quantities of **128** to test the subsequent steps.



Scheme 2.16: Synthesis of a functionalised 7-aryl THX containing a cyano moiety

With **128** in hand, a further Suzuki-Miyaura reaction was undertaken. Strong bases such as $\text{Ba}(\text{OH})_2$ have been shown to give higher yields for sterically encumbered substrates.^{107,119} Using $\text{Pd}(\text{OAc})_2$ in combination with $\text{Ba}(\text{OH})_2$ as a base, **129** was

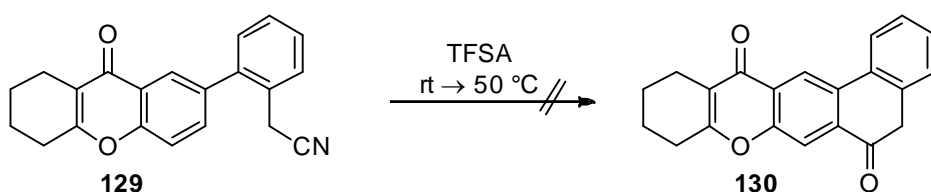
obtained in 29% yield. Despite the low yield, enough product was isolated cleanly to attempt ring closure.

Cyclisation was attempted using trifluoromethanesulphonic acid (TFSA) as similar cyclisations had been successfully reported in the literature by Nakamura *et al.*¹²⁰ They described the development of superacid catalysed cyclisations of arylcyanopropionates to give various carbocycles and it was hoped that similar reaction conditions could be applied here.



Scheme 2.17: Cyclisations by Nakamura¹²⁰

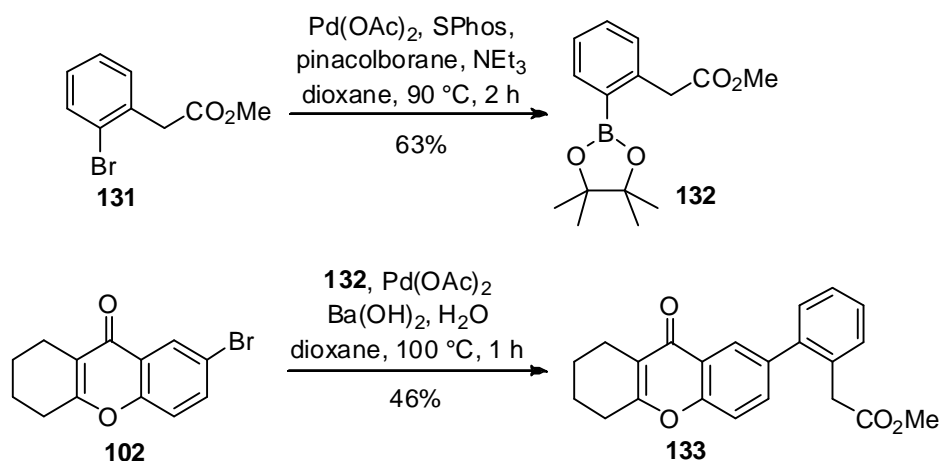
Nitrile **129** was added to ice-cold TFSA and then allowed to slowly warm to room temperature. After 3 h, there was no product apparent by crude ¹H NMR spectroscopy, only starting material was evident. The reaction was allowed to stir at room temperature overnight and then since no change was observed, the mixture was heated to 50 °C for a further 18 h.



Scheme 2.18: Attempted intramolecular cyclisation

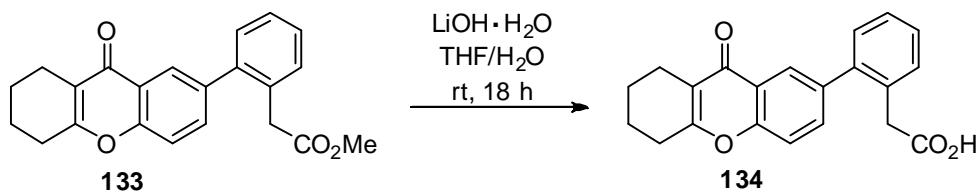
Since only **129** was isolated under these forcing reaction conditions, it was concluded that such nitriles are too unreactive for cyclisation to occur in these substrates.

To circumvent these problems, we decided to try the cyclisation *via* a more conventional Friedel Crafts process. For this, it was necessary to synthesise pinacol ester **132** containing a masked carboxylic acid moiety. The synthesis of **132** occurred in a much higher yield (63%) relative to its cyano analogue **128** (Scheme 2.16). With the pinacol ester **132** in hand, the subsequent Suzuki-Miyaura reaction provided **133** in an improved 46% yield.



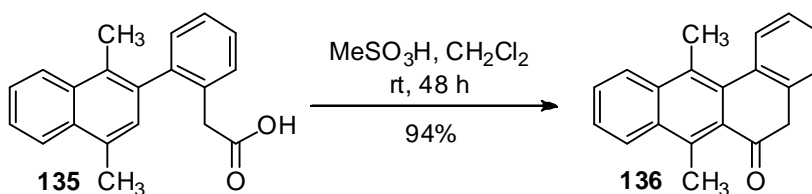
Scheme 2.19: Synthesis of a functionalised 7-aryl THX containing an ester moiety

Ester **133** was then hydrolysed using lithium hydroxide in a biphasic mixture of THF and H_2O . The reaction mixture was stirred at room temperature overnight and then subjected to an acidic aqueous work up to facilitate extraction of the acid into the organic phase. Further silica gel chromatography was not undertaken due to insolubility issues. However, by crude ^1H NMR spectroscopy, the methyl ester peak was no longer present and there was a broad peak at 10.78 ppm, indicative of a carboxylic acid hydrogen. There were only minor impurities present and therefore **134** was used without further purification.

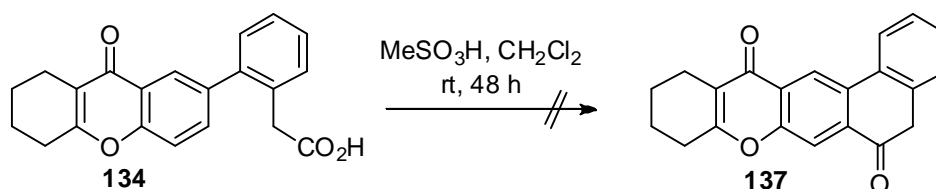


Scheme 2.20: Hydrolysis

Several methods were then attempted to realise cyclisation. The first of these was another strongly acidic method as reported by Sharma *et al* for the cyclisation of **135** to **136** in high yield (Scheme 2.21).¹²¹

Scheme 2.21: Cyclisation using methanesulphonic acid¹²¹

However, **137** was not isolated when these reaction conditions were applied to **134**.

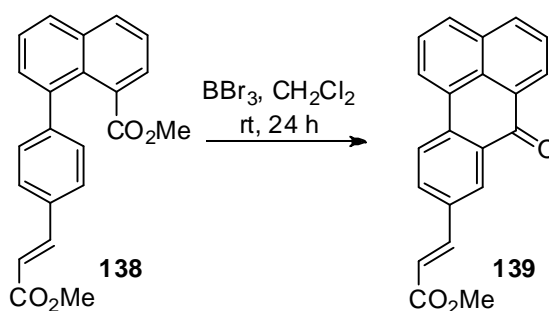


Scheme 2.22: Attempted cyclisation

Other reports in the literature for similar reactions include that of DeShong *et al*¹²² where the carboxylic acid was first converted to the acid chloride *in situ* before intramolecular Friedel Crafts reaction. This was attempted on **134** but as before, **137** was not isolated. This could be because the acid chloride didn't fully form before attempting the Friedel Crafts reaction. Due to being a one-pot process, the

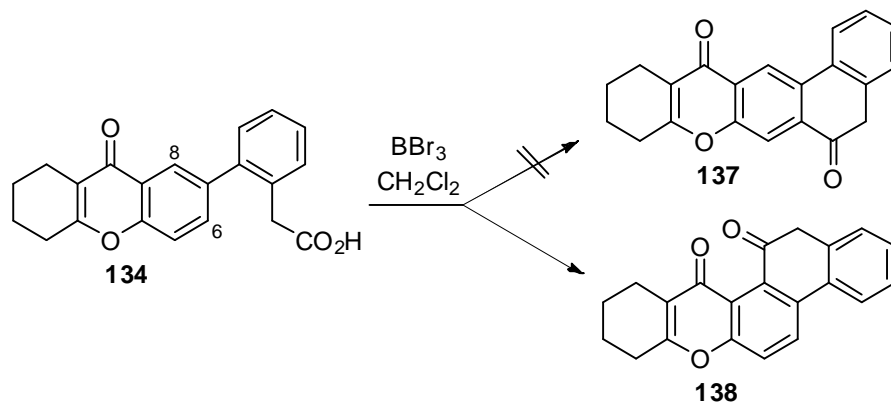
intermediate acid chloride was not isolated or characterised and therefore it was difficult to ascertain which step was problematic.

The final method attempted followed the work of Feldman *et al.*¹²³ They found that treating **138** with BBr_3 to remove the methyl groups, facilitated cyclisation to **139** (Scheme 2.23).



Scheme 2.23: Cyclisation using BBr_3

These conditions were applied to acid **134** and the reaction mixture was allowed to stir overnight at room temperature. The crude ^1H NMR spectrum showed a trace of one product forming with a large proportion of starting material remaining. Disappointingly, the product did not show the disappearance of the aromatic doublet of H-6 as expected but instead the singlet peak at H-8 which would only arise if regioisomer **138** had formed (Scheme 2.24).



Scheme 2.24: Attempted cyclisation and possible formation of alternative regioisomer

The formation of this isomer may arise from preferential coordination of both carbonyls to the Lewis acid during the cyclisation with loss of a bromide ion. Alternatively, it is possible that hydrogen bonding between the carboxylic acid hydrogen and the carbonyl of the THX encourages formation of this isomer (Figure 2.4).

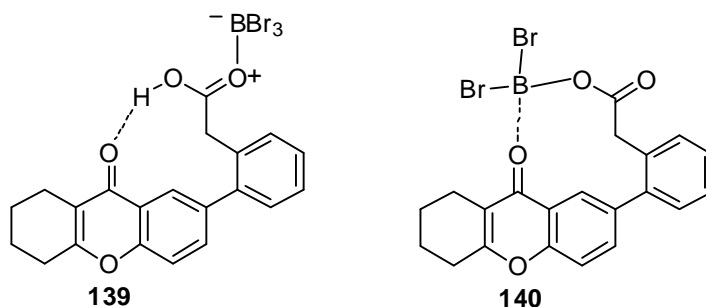


Figure 2.4: Possible hydrogen bonding or Lewis acid coordination

Disappointingly, treatment with further equivalents of BBr₃ and longer reaction times did not drive the reaction to completion. As such, we were unable to isolate sufficient quantities of **138** to verify its structure. Further work to produce analogues with an intact E ring was discontinued at this juncture.

2.3 Metal Catalysed Route to Tetrahydroxanthenes

2.3.1 Introduction

As described previously, current methods to THXs utilise very strong acids and harsh reaction conditions. Whilst this provides a rapid route to basic analogues containing the THX moiety, analogues with greater complexity that mimic the kigamicins more closely could not be made this way. In these cases, less forcing conditions would need to be developed. The natural product contains several acid sensitive functionalities, for example, the hydroxyl groups in the A ring at C-1 and C-4 which would be sensitive to acid catalysed dehydration and the cyclic acetal (D ring) would also potentially be sensitive to acid. On this basis, we concluded that it was necessary to develop a non-acidic route to THXs.

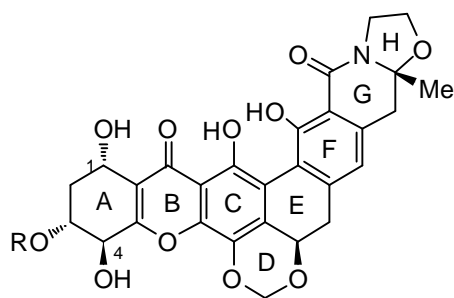
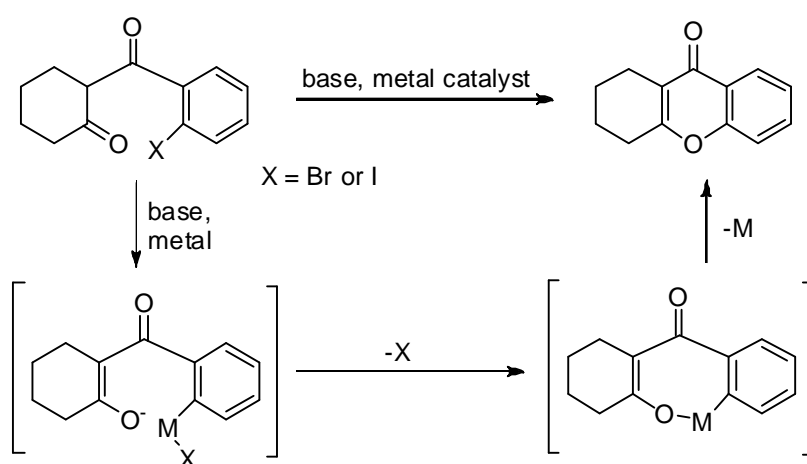


Figure 2.5: Kigamicin

We reasoned that the THX nucleus could be constructed *via* a metal-catalysed process, mediated for example, using copper or palladium. This would involve the use of a mild base and could provide a facile route which would be much more tolerant of a range of functional groups making way for the synthesis of libraries of analogues for biological screening. Such methodology could also be helpful in relation to the synthesis of the natural product itself. It is envisioned that the reaction would proceed *via* insertion of the metal into the aryl halide bond. This would be followed by the coordination of the enolate, formed after deprotonation, with the metal and subsequent reductive elimination to form the oxygen–aryl bond reforming the metal catalyst (Scheme 2.25).

Scheme 2.25: Proposed formation of the THX core *via* a metal catalysed route

2.3.2 Synthesis of substrates for investigation of metal catalysed cyclisation

Several different methods were explored for the synthesis of the substrates required for investigating the metal catalysed THX formation. The first of these, involved the addition of the lithium enolate of cyclohexanone to the appropriate acid chloride as shown in Scheme 2.26. This is analogous to the strategy used for synthesising the earlier precursors such as **83** and **102** for the acid catalysed dehydration method. In both cases, none of the diketone was observed, only the enol tautomer, presumably due to the hydrogen bonding between the enol proton and adjacent carbonyl oxygen. Evidence for this hydrogen bonding is also observed in the ^1H NMR where the highly deshielded enol proton appears at δ 15.82 ppm. It was assigned as enol **141a** instead of enol **141b** by NOE NMR experiments. Irradiation of the enol proton showed enhancement of the alkyl proton signals of C-4 but no effect on the aromatic protons.

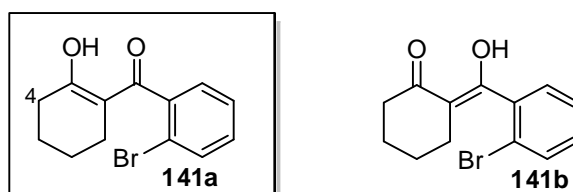
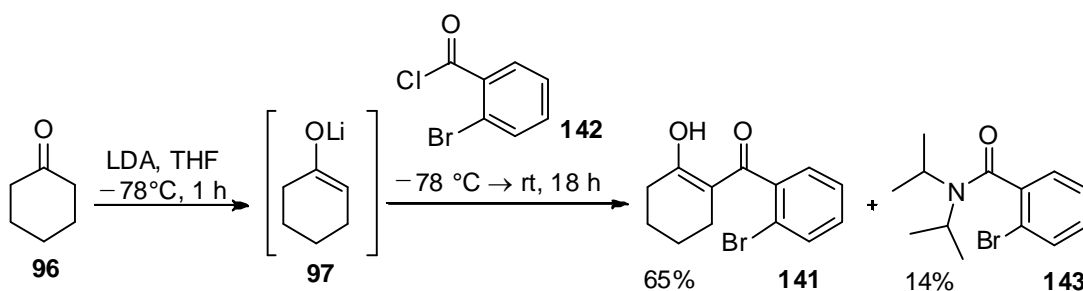


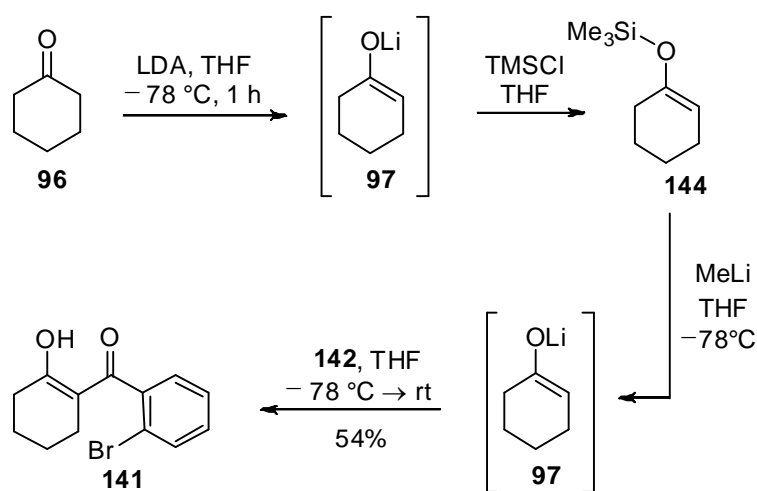
Figure 2.6: Possible enol tautomers

Alongside a 65% yield of **141**, a noticeable amount of **143** was observed, formed from the reaction of the LDA directly with acid chloride **142**.



Scheme 2.26: Acylation using LDA and side reaction

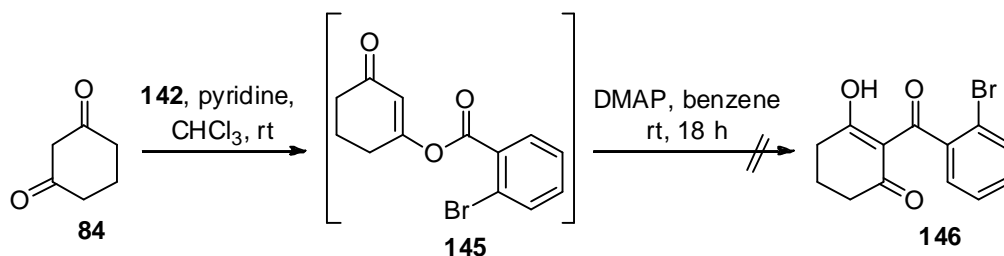
It was postulated that this could be avoided if the lithium enolate of cyclohexanone was trapped with TMSCl to give the silyl enol ether as described by Watanabe *et al.*¹⁰⁶ This could then be isolated and the lithium enolate regenerated using methyllithium to which the acid chloride could be added in the absence of diisopropylamine. Without this competing reaction, it was hoped that a higher yield would be observed. However this was not the case and in fact a slightly lower yield was obtained.



Scheme 2.27: Acylation *via* the silyl enol ether

Acylation was also attempted using cyclohexane-1,3-dione **84** in order to install the hydroxyl group present in the A ring at C-1 of the natural product. However, this resulted in predominantly *O*-acylation when the LDA method was used. The reaction was repeated using pyridine and before isolating the product, DMAP was added to isomerise any *O*-acylated **145** to *C*-acylated **146** (Scheme 2.28). This was based on work by Zaitsev *et al.*¹²⁴ where they achieved yields in excess of 90% using this approach. Disappointingly in our hands, this method failed to produce a significant yield of *C*-acylated **146**.

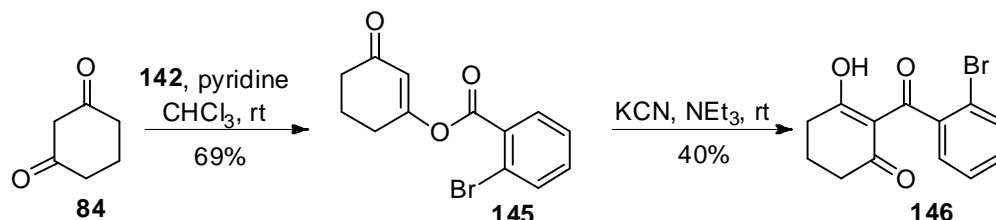
O-acylation is usually favoured when hard electrophiles such as acid chlorides are used.¹²⁵ However, the hard alkoxy anion of the enolate is bound tightly with the hard lithium counterion which leads to shielding of the anion.¹²⁶ This allows reaction through the carbon despite its ‘softer’ nature. However, in the case of the diketone **84**, the anion is further delocalised not only making the carbanion even softer in nature greatly reducing its ability to react with the hard acid chloride but also weakening the interaction between the alkoxy anion and lithium counterion creating more free enolate, thereby increasing reactivity through oxygen.¹²⁷



Scheme 2.28: Attempted acylation/isomerisation sequence

The conditions were then repeated but on this occasion the reaction was halted after the initial acylation step. No *C*-acylated product **146** was isolated but the *O*-acylated product **145** was isolated in 69% yield. In 1996, Burger *et al*¹²⁸ reported that after the initial *O*-acylation of cyclohexanedione, subsequent isomerisation could be realised using potassium cyanide and triethylamine in acetonitrile. No yield was quoted for this isomerisation but we decided to repeat the conditions on our substrate. Indeed the isomerisation did proceed but in only 40% yield. The *O*-acylated (**145**) and *C*-acylated (**146**) products were differentiated by ¹H and ¹³C NMR spectroscopy. The spectrum of **145** showed a peak at δ 6.06 ppm for the enone proton which was not present in the spectrum of **146**. The ¹³C NMR of **145** showed three peaks at δ 199.4, 169.9 and 162.6 ppm for the three quaternary carbons adjacent to oxygens whereas in **146**, they were much more similar (δ 198.1,

197.1 and 193.7) which would be expected for those in **146** considering the almost identical chemical environment of these quaternary carbons. It was therefore decided that the remaining substrates be synthesised according to the first method described, using LDA in THF.



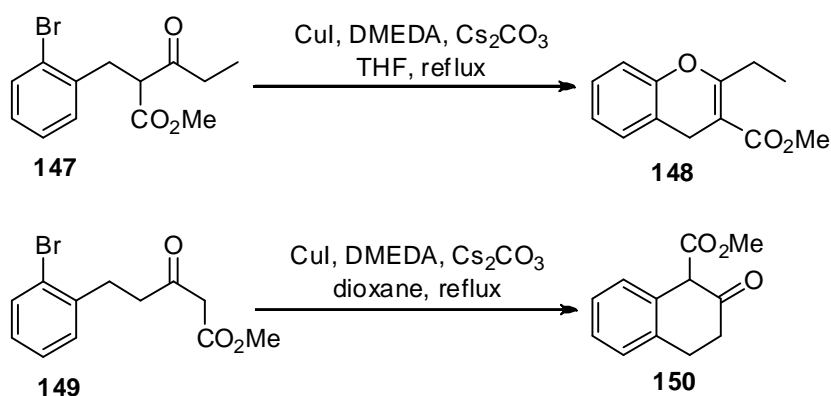
Scheme 2.29: *O*-Acylation followed by isomerisation¹²⁴

2.3.3 Formation of heterocycles using metal catalysis

There is no literature precedent for the metal catalysed cyclisation for the formation of THXs. However, the syntheses of other heterocycles namely benzopyrans and benzofurans using metal catalysis, most commonly using copper or palladium are known.

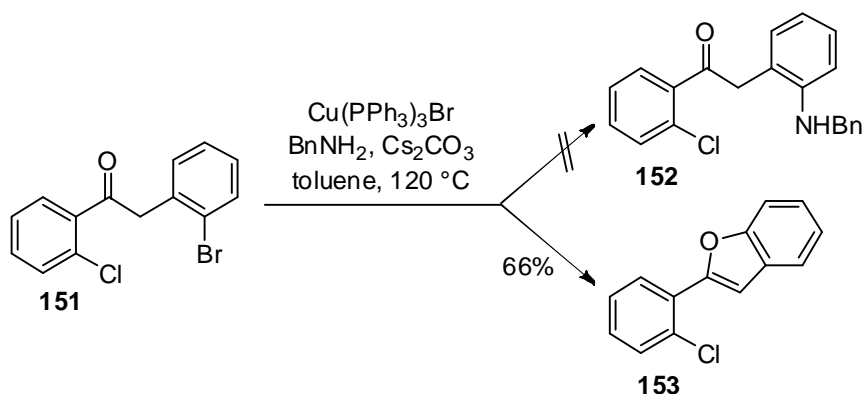
Li *et al*¹²⁹ demonstrated that depending on the structure of the substrate and on the reaction conditions, they could perform both *C*-arylation and *O*-arylation of β -keto esters to provide both 3,4-dihydronaphthalen-2(1*H*)-one derivatives (**150**) and benzopyrans (**148**) (Scheme 2.30). Initial studies involved the optimisation of the formation of benzopyrans *via* cyclisation utilising copper catalysis. Various copper sources were screened (Cu, CuI, CuCl) as well as different bases (Cs_2CO_3 , K_3PO_4 , DABCO, Na^tOBu) and different ligands (DMEDA, 1,10-phenanthroline, L-proline, PPh_3) were explored. The optimal conditions were found to be CuI (10 mol %), DMEDA (20 mol %) and Cs_2CO_3 (2 equiv.) in refluxing THF (Scheme 2.30).

In order to widen the scope of this reaction the authors reacted β -keto esters such as **149** under the same conditions to form benzopyran derivatives incorporating an exocyclic double bond. However, under these conditions, the reaction was very slow, so the solvent was changed to dioxane so higher temperatures could be employed. Under these conditions, only the *C*-arylated product **150** was observed (Scheme 2.30).



Scheme 2.30: *O*-arylation and *C*-arylation of β -keto esters¹²⁹

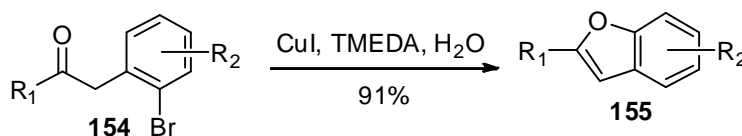
SanMartin *et al*¹³⁰ isolated an unexpected product in the reaction between deoxybenzoin **151** and benzylamine in the presence of a copper catalyst. Instead of the *N*-arylation product **152**, they had anticipated, benzofuran **153** was produced in 66% yield.



Scheme 2.31: Unexpected *O*-arylation

This prompted them to investigate the synthesis of benzofurans in this manner. Optimal conditions proved to be CuI (8.5 mol %) and TMEDA (3.5 equiv) in H₂O

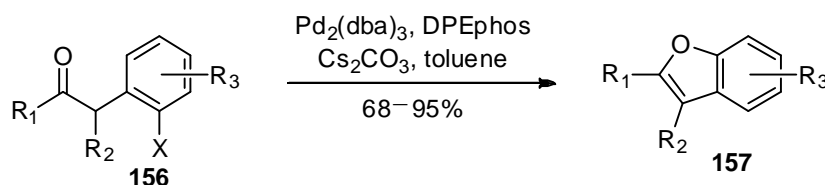
at 120 °C (Scheme 2.32). The use of H₂O gave the advantage of reduced cost and toxicity. The reaction was found to have wide scope with the exception that it is intolerant to electron donating substituents *para* to the bromine in **154**.



Scheme 2.32: Benzofuran synthesis

Palladium catalysis for benzofuran synthesis has also been reported. In 2004, Willis *et al*¹³¹ described the use of Pd₂(dba)₃ for this transformation. Initially, poor yields (<5%) were observed using xantphos as a ligand and Cs₂CO₃ as a base. Use of a stronger base (NaO^tBu) didn't improve the reaction and in this case no product was isolated. However, it was discovered that with DPEphos, the yield was markedly improved. The optimal conditions were: Pd₂(dba)₃ (2.5 mol %), DPEphos (6 mol %) and Cs₂CO₃ (2.2 equiv.) in toluene.

When examining the scope of this reaction it became apparent that although the catalyst, ligand and solvent were general to most substrates, the base required was substrate dependent. This chemistry has been extended to the synthesis of benzothiophenes.¹³²

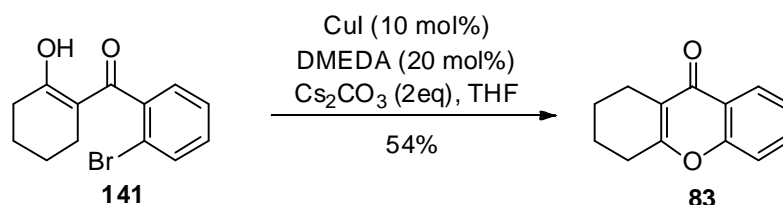


Scheme 2.33: Palladium catalysed benzofuran synthesis

2.4 Tetrahydroxanthone Formation using Copper Catalysis

From the above work, we imagined that the synthesis of THXs could potentially be realised using copper catalysis.

Compound **141** was chosen as a suitable substrate for model studies and once synthesised, was treated with copper iodide, DMEDA and Cs₂CO₃ in THF and heated to reflux for 18 h (Scheme 2.34). Encouragingly, at the first attempt, THX **83** was isolated in 54% yield.



Scheme 2.34: Copper catalysed cyclisation

2.4.1 Optimisation Studies

Optimisation was undertaken as shown in Table 2.2. The reaction time, base, equivalents of base, ligand and solvent were all changed. Only marginal improvement was realised when water was used as the solvent in place of THF (entry 8). However, no further improvements were realised.

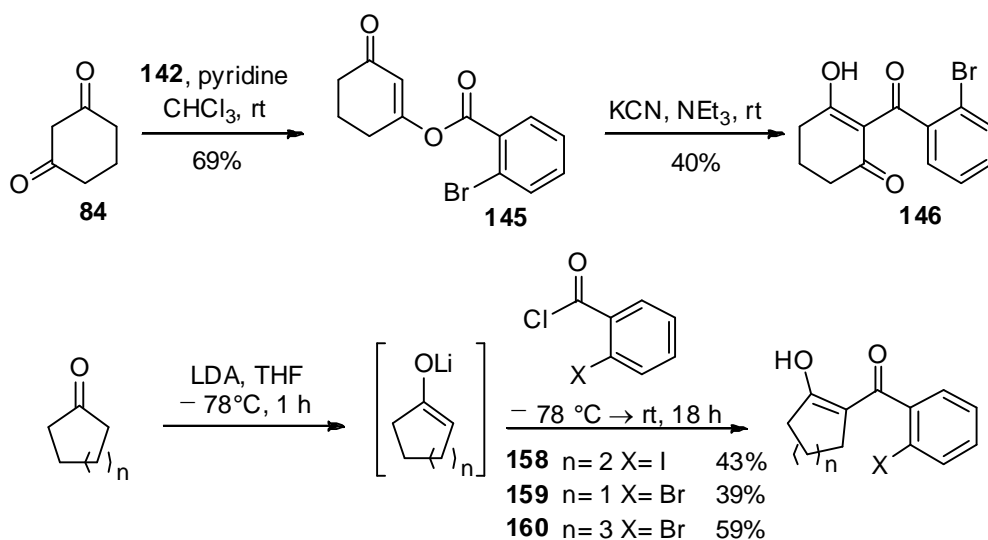
Entry	Base	Eq. base	Ligand	Solvent	Reaction time (h)	Yield (%)
1	Cs ₂ CO ₃	2	DMEDA	THF	18	54
2	Cs ₂ CO ₃	2	DMEDA	THF	48	27
3	none	none	DMEDA	THF	18	0
4	Cs ₂ CO ₃	2	TMEDA	THF	18	49
5	K ₃ PO ₄	2	DMEDA	THF	18	54
6	Cs ₂ CO ₃	2	<i>N,N</i> - dimethylglycine	THF	18	44
7	Cs ₂ CO ₃	2	DMEDA	CF ₃ CH ₂ OH	18	34
8	Cs ₂ CO ₃	2	DMEDA	H ₂ O	18	56
9	Cs ₂ CO ₃	2	DMEDA	DMF	18	46
10	Cs ₂ CO ₃	2	DMEDA	Dioxane	18	51

Table 2.2: Optimisation of Copper Iodide Catalysed Cyclisation

2.4.2 Scope of Copper Catalysed Cyclisation

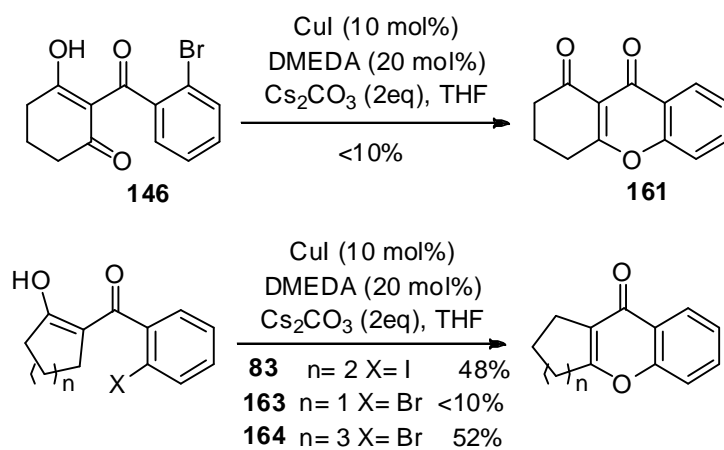
Despite moderate yields for this cyclisation, it was decided to synthesise a small number of other substrates (Figure 2.35). The purpose was not only to ascertain whether the reaction would tolerate different substrates but also if any of these substrates cyclised in higher yields.

These were all synthesised using the chemistry described in Section 2.3.2. Despite moderate to low yields, sufficient material was obtained to test the cyclisation step.



Scheme 2.35: Synthesis of substrates

All substrates were subjected to the optimal copper catalysed cyclisation conditions. Similar yields were achieved when **83** was formed from the iodide (48%) and **164** synthesised from cycloheptanone (52%). However, **161** and **163** were formed in poor yields (<10% yield in both cases).

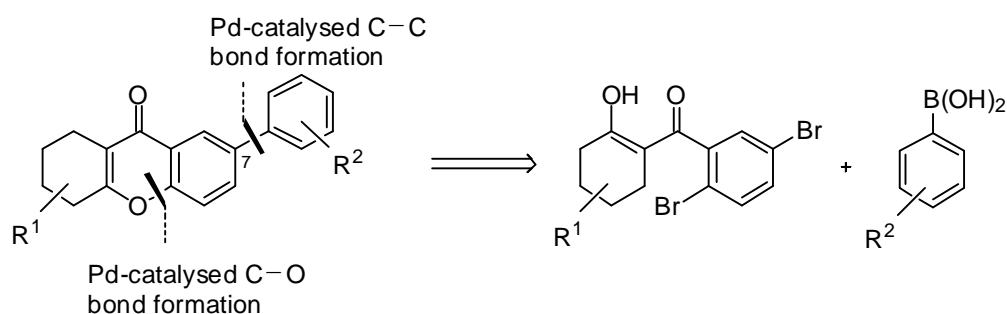


Scheme 2.36: Copper catalysed cyclisation

2.5 Tetrahydroxanthone Formation using Palladium Catalysis

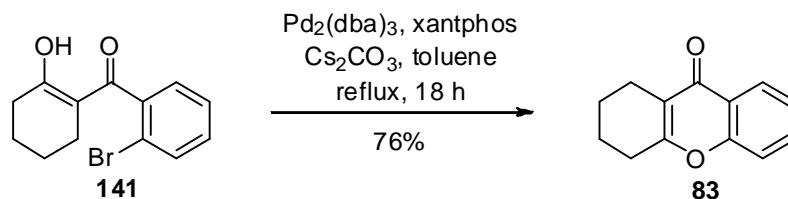
These results and the work described in Section 2.3.3, prompted us to study the THX formation using palladium catalysis in order to establish if the reaction could be improved.

We also reasoned that if palladium could be used, this would provide the opportunity to greatly extend the scope of the reaction. By manipulating the reaction conditions, it could be possible to incorporate the 7-aryl component concurrently *via* a Suzuki-Miyaura reaction. This would allow the synthesis of 7-arylated THX analogues *via* tandem catalysis¹³³⁻¹⁴⁰ by sequential C–O and C–C bond construction.



Scheme 2.37: Proposed tandem catalysis route to 7-arylated THXs

Initially it was important to determine if palladium could catalyse the cyclisation reaction. As previously described, Pd₂(dba)₃ had been reported to effect the cyclisation to oxygen heterocycles. Since xantphos was to hand, initial experiments were conducted with this ligand. Reaction of enol **141** with Pd₂(dba)₃, xantphos and caesium carbonate in toluene, gave **83** in an improved and very encouraging 76% yield (Scheme 2.38).

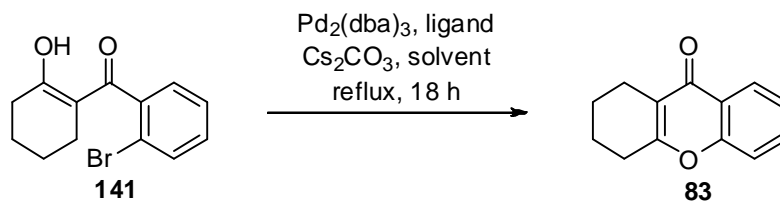


Scheme 2.38: Palladium catalysed cyclisation

2.5.1 Optimisation Studies

Encouraged by these results, we attempted to further improve the yield by variation of the solvent and ligand. The results are shown in Table 2.3.

An exploration of solvents resulted in an 11% improvement in yield when toluene was substituted by dioxane. The yield was improved once more through the consideration of different ligands (Figure 2.7). The use of Xphos in place of xantphos provided an excellent 93% yield (Table 2.3, entry 10). At this juncture, no further optimisation was conducted.



Entry	Ligand	Solvent	Yield (%)
1	Xantphos	Toluene	76
2	Xantphos	THF	76
3	Xantphos	H ₂ O	<25
4	Xantphos	DMF	62
5	Xantphos	Dioxane	87
6	DPEphos	Toluene	79
7	DPEphos	Dioxane	86
8	DPPB	Dioxane	83
9	Johnphos	Dioxane	82
10	Xphos	Dioxane	93

Table 2.3: Optimisation of palladium catalysed cyclisation

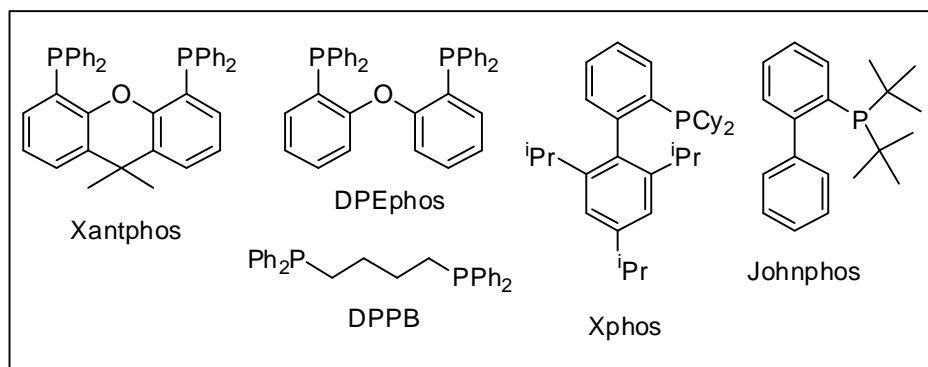


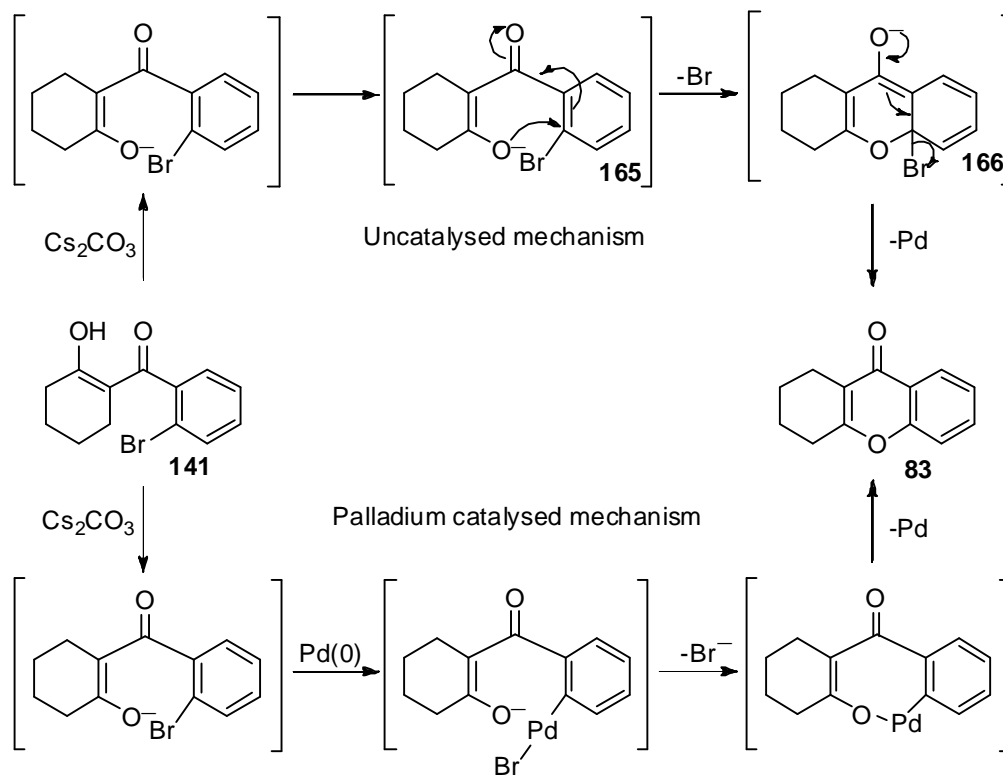
Figure 2.7: Ligands used for optimisation study

2.5.2 Catalysed versus uncatalysed reaction

For completion, we sought to establish the role of palladium in this reaction. To our initial surprise, the cyclisation still occurred in the absence of palladium and in high yield (86%). This prompted us to conduct studies surrounding the uncatalysed

reaction in order to ascertain whether the metal was playing a role in the reaction. Since the reaction was sensitive to the ligand used, we suspected that it did indeed play an important role.

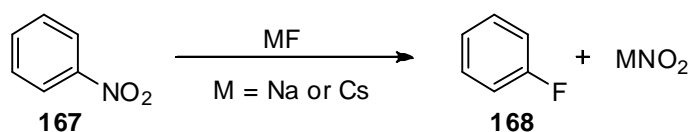
Considering the ability of the carbonyl group to stabilise negative charge through intermediates such as **165** and **166**, it is possible that the reaction proceeds *via* an S_NAr type mechanism.¹⁴¹⁻¹⁴³



Scheme 2.39: Proposed catalysed vs. uncatalysed reaction mechanisms

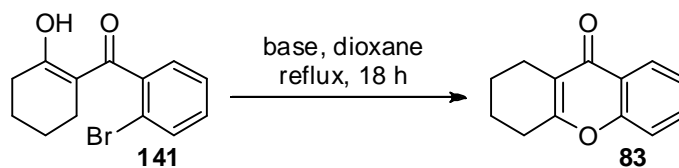
If the uncatalysed reaction is operating, then the reaction might be expected to be base dependent, specifically with respect to the nature of the counterion. We reasoned that if the enolate was highly covalent, then the reaction would be more likely to proceed *via* the catalysed route, due to the enolate being inherently less nucleophilic. If the enolate has more ionic character, then the uncatalysed reaction

would be faster. This has been illustrated by the work of Lee *et al*¹⁴⁴ who calculated the activation energies of a fluoridation S_NAr reaction in the presence of sodium or caesium counterions (Scheme 2.40). They reported that the strong interaction between the nucleophile and the sodium counterion greatly increased the activation energy (to ~39.1 kcal/mol) in comparison to that of the reaction with caesium as the counterion (~31.4 kcal/mol).



Scheme 2.40: Fluorination reaction with NaF or CsF

In order to test this hypothesis, we undertook a base screen to establish the effect of the counterion on the yields of the catalysed and uncatalysed reactions. Using **141**, a pair of reactions were conducted in parallel (heated in the same oil bath next to one another). In each reaction, the starting material was dissolved in dioxane and the base was added. To one of the reactions, Pd₂(dba)₃ and Xphos were then added. The reactions were heated to reflux for 18 h and then purified on silica gel to obtain the isolated yields for each reaction. The results are shown below in Table 2.4.



Base	Yield (%) catalysed ^[a]	Yield (%) uncatalysed
Cs ₂ CO ₃	85	92
CsF	85	82
K ₂ CO ₃	96	83
K ₃ PO ₄	49	65
NaO ^t Bu	51	0
Na ₂ CO ₃	85	0

[a] 2.5 mol% Pd₂(dba)₃ and 6 mol% Xphos

Table 2.4: Base screen

It is evident from the results of the base screen shown in Table 2.4, that with caesium as the counterion, the uncatalysed reaction proceeds equally well as the catalysed one. A potassium counterion also appears to enable the uncatalysed reaction to occur. However, using sodium *tert*-butoxide or carbonate, the uncatalysed reactions failed with complete recovery of starting material. Interestingly, the catalysed reactions still proceed under these conditions.

To provide further evidence, we examined the use of crown ethers which have been shown to coordinate to cations and in particular, 15-crown-5 which has been shown to coordinate specifically to sodium.¹⁴⁵ We postulated that if 15-crown-5 was added to the uncatalysed reaction involving a sodium counterion, it would bind to the sodium thus partially separating the counterion from the enolate anion. This in turn

would make the enolate more ionic in nature, and allow the uncatalysed reaction to proceed.

The reaction was performed as before with Na₂CO₃ as the base with 15-crown-5 added. The reaction was heated to reflux in dioxane overnight and was subjected to the same work up and purification. Instead of no conversion as seen in the absence of the crown ether, a 27% yield of **83** was obtained. Despite the low yield, this provides further evidence that increased ionic character of the enolate encourages the S_NAr process.

Next we investigated the reaction using caesium carbonate to establish whether the reaction with the palladium proceeds at a faster rate than in the absence of the transition metal. We had previously observed when undertaking the optimisation of the reaction, that using different ligands influenced the yield of the reaction which suggested that the palladium and ligand are taking an active role in the reaction mechanism.

To do this, we elected to study the extent of conversion to product, catalysed and uncatalysed at various time points in order to observe whether the palladium was increasing the rate of reaction. A third set of reactions were also carried out using twice the equivalents of palladium and ligand.

Initially, time course experiments were attempted, whereby an internal standard (1,3,5-trimethoxybenzene) was added. Aliquots of the reaction mixtures were taken every 10 min for the first hour, every 20 min for the second hour and every 30 min thereafter. Each sample was analysed by ¹H NMR spectroscopy. Despite changing

the equivalents of internal standard, there appeared to be loss of the internal standard towards the end of the reaction with minor or no peaks corresponding to this product remaining in the spectra. Overlapping starting material and product peaks meant comparison of the integration of these peaks to monitor the extent of conversion was also not possible. It was therefore decided that the reaction be followed by the more labour intensive manner of isolating the product at various time points.

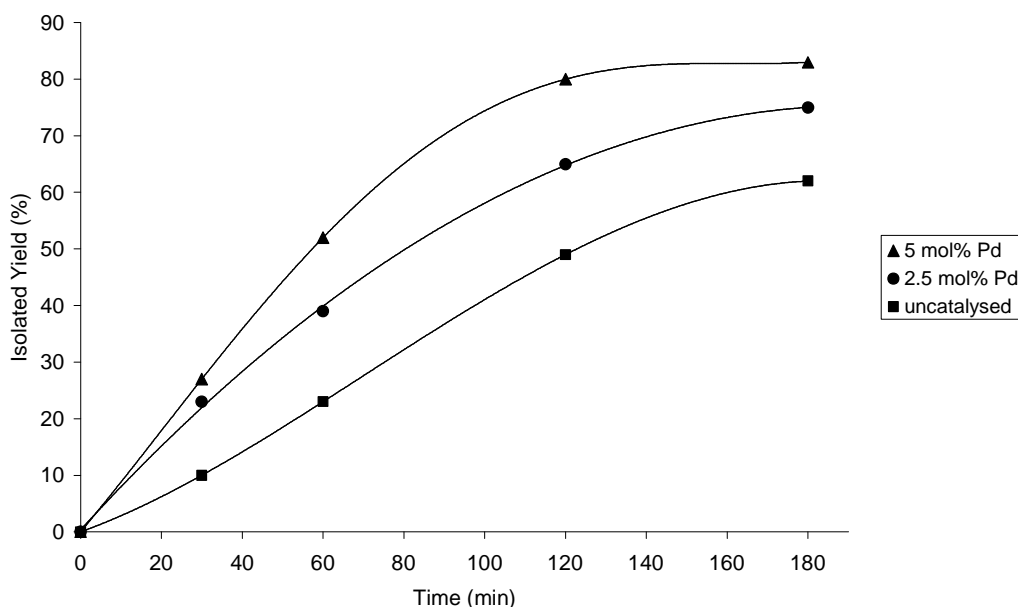
As before, the reactions were performed in pairs so that identical reaction conditions were achieved. The reactions were allowed to heat to reflux for 30 min, 1 h, 2, h and 3 h. Isolated yields were then determined for each reaction so that accurate comparisons could be made.

Time (min)	Yield (%) uncatalysed	Yield (%) 2.5 mol % Pd ^[a]	Yield (%) 5 mol% Pd ^[b]
0	0	0	0
30	10	23	27
60	23	39	52
120	49	65	80
180	62	75	83

[a] 2.5 mol% Pd₂(dba)₃ and 6 mol% Xphos, [b] 5 mol% Pd₂(dba)₃, 12 mol% Xphos

Table 2.5: Time course experiment

From Table 2.5, it is clear to see that cyclisation proceeds faster *via* a catalysed reaction mechanism with higher catalyst loading, leading to faster conversion to product. These results are also shown in the graph below (Graph 2.1).

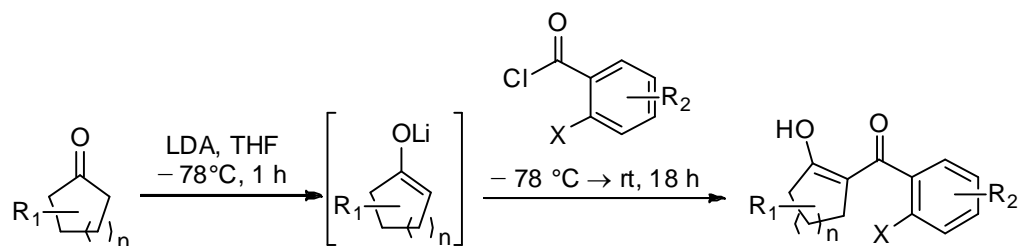


Graph 2.1: Graph to show intramolecular cyclisation: catalysed vs. uncatylsed

It is clear to see that whilst the reaction does work in the absence of catalyst, higher yields and faster conversions are achieved under palladium catalysis.

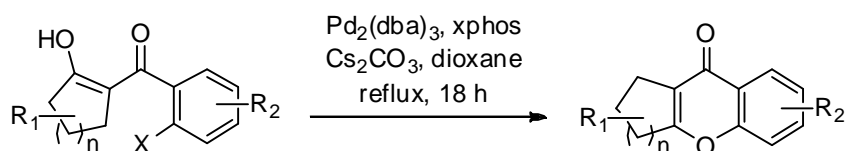
2.5.3 Scope of Palladium Catalysed Cyclisation

The scope of the reaction was then investigated. Various substrates were synthesised and isolated using the method described in Section 2.3.2 (Scheme 2.26). The size and substituents of the saturated ring were modified as well as substituents on the aromatic ring (Table 2.6). Despite moderate yields, sufficient material was isolated to test the subsequent cyclisations.



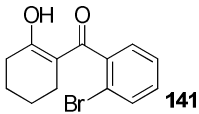
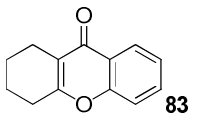
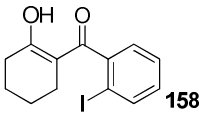
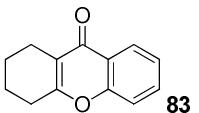
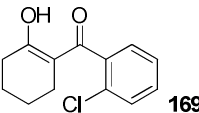
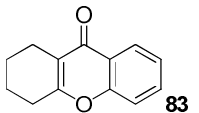
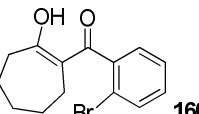
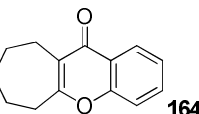
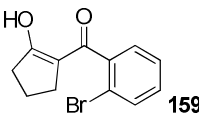
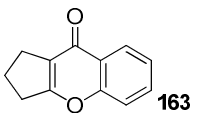
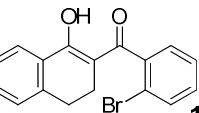
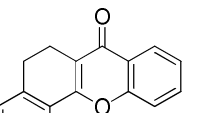
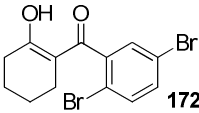
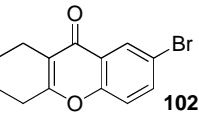
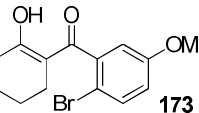
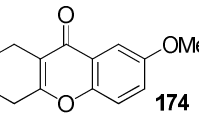
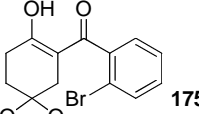
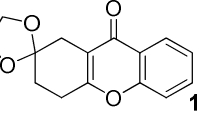
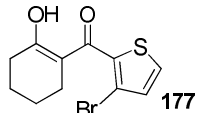
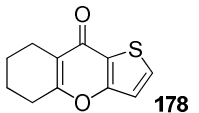
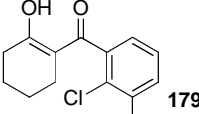
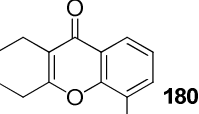
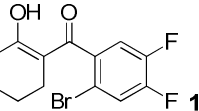
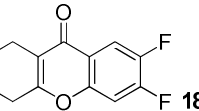
Scheme 2.41: Synthesis of substrates for cyclisation

The majority of substrates shown in Table 2.6 exist in enol form exclusively. However, two substrates exist as a mixture of the keto and enol forms. These are cyclopentanone derivative **159** (entry 5, 1:13 diketo:enol) and thiophene **177** (entry 10, 1:1 diketo:enol). Mechanistically, it should make no difference to the progress of the reaction as the substrate is deprotonated (and indeed in the case of entry 10, the cyclisation progressed in good yield (60%)). With the substrates in hand, they were subjected to our optimal cyclisation conditions and the results are shown in Table 2.6.



Scheme 2.42: Cyclisation

The results show a variety of functional groups are tolerated by this reaction. The reaction with chloride **169** proceeded in high yield (entry 3, 88%) although iodide **158** did not proceed as efficiently (entry 2, 54%). The substrate derived from cyclopentanone cyclised in a poor yield (entry 5, 23%) but all other substrates cyclised in good to excellent yields.

Entry	Substrate	Yield ^[a] (%)	Product	Yield ^[b] (%)
1		58		93
2		43		54
3		42		88
4		59		76
5		38		23
6		45		91
7		42		69
8		36		60
9		21		72
10		34		60
12		48		82
13		51		78

[a]Yield of substrate formation by C-acylation. [b] Yield of product formation by Pd catalysed cyclisation

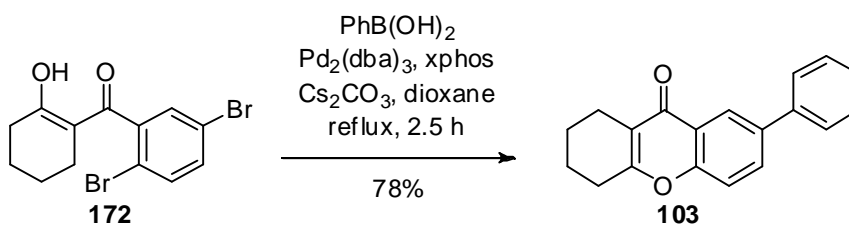
Table 2.6: Investigation of the scope of palladium catalysed cyclisation

As is evident from Table 2.6, the reaction tolerates a wide range of substrates including electron withdrawing (entry 12) and electron donating substituents (entry 8). It also tolerates acid sensitive groups such as the acetal functional group (entry 9) and additional heteroatoms in the aryl component (entry 10). Expansion of the saturated ring is tolerated, however, ring contraction resulted in a somewhat lower yield. This is perhaps due to increased ring strain in **163**.

Most encouragingly, entry 7 showed that the reaction tolerates substrates bearing two C–Br bonds with the palladium regioselectively inserting into the C–Br bond *ortho* to the carbonyl group. Some precedent for this kind of regioselectivity can be found in the literature.^{146,147} This gave us confidence to attempt the tandem catalysis described earlier (Scheme 2.37).

2.6 Tandem Catalysis

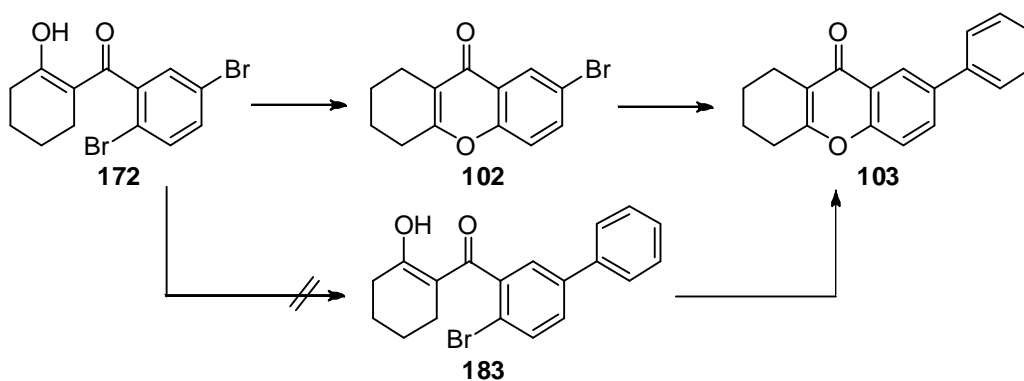
In order to test whether the Suzuki-Miyaura reaction would occur sequentially with cyclisation, dibromide **172** was treated under the same conditions as previously, with phenyl boronic acid (3 equiv.) added. The reaction mixture was heated to reflux and after 2.5 h, the reaction was complete as determined by TLC. Gratifyingly after work-up and purification by column chromatography, the 7-arylated THX **103** was isolated in 78% yield.



Scheme 2.43: One-pot synthesis of 7-aryl THX

2.6.1 Investigations into the Reaction Mechanism

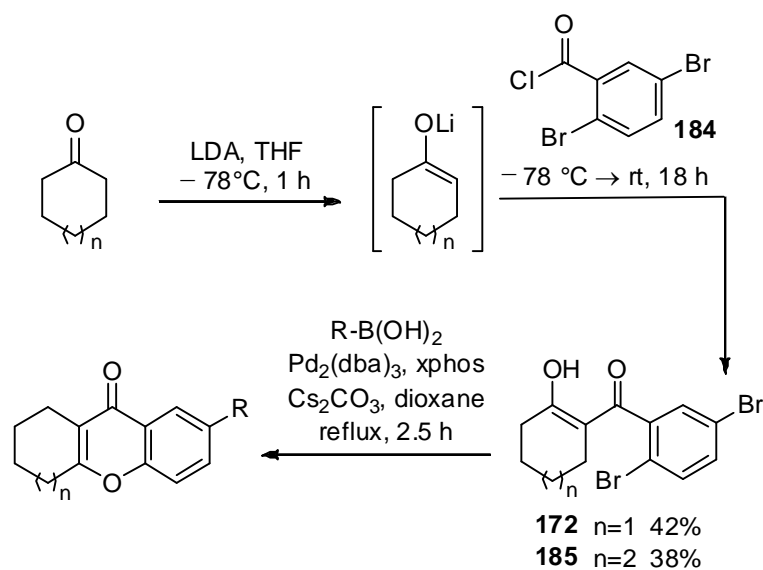
Time-course experiments were carried out by Ellanna Griffin (an undergraduate summer student) using GC-MS to monitor the reaction and the intermediates that were formed. Rapid consumption of starting material was observed with formation of the cyclised product **102**, i.e. where intramolecular C–O bond formation had occurred. Over time, this product was consumed and the Suzuki-Miyaura product **102** was observed. No trace of **183** resulting from initial C–C bond construction was observed (Scheme 2.44).



Scheme 2.44: Tandem catalysis pathway

2.6.2 Scope of tandem catalysis using Miyaura–Suzuki couplings

The scope of this reaction was probed and a small library of kigamicin analogues produced (Scheme 2.45 and Table 2.7). The reaction tolerates changes in the size of the saturated ring and different substituents on the aryl boronic acid.



Scheme 2.45: Synthesis of 7-aryl THXs by tandem catalysis

n	compound	R	Yield (%)
1	103		78
2	186		71
1	187		85
2	188		83
1	105		68
1	189		60

Table 2.7: Library of compounds by tandem catalysis

It should be noted that compounds **186** and **188** were synthesised from cycloheptanone by Ellanna Griffin, but the results are presented here for completeness.

Other substitution patterns were also tolerated, being made from dichloride substrates **194** and **195** (Scheme 2.46). This observation is important as there are

biologically active natural products with aryl groups in these positions such as isokibdelone C (**190**) and albobfungin (**191**) (Figure 2.8).^{89,148} The Suzuki-Miyaura reaction does not appear to proceed any less favourably using these aryl chlorides (Scheme 2.46).

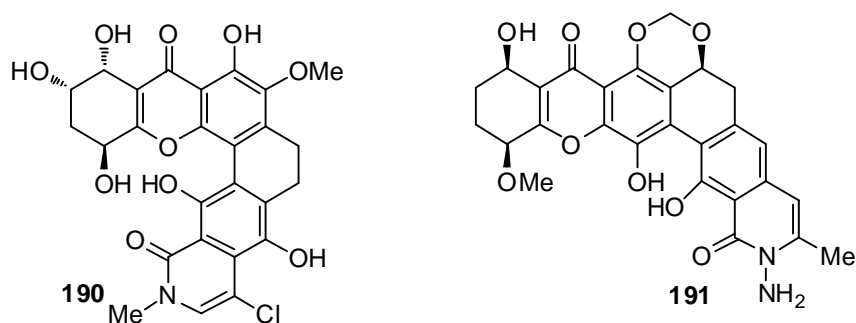
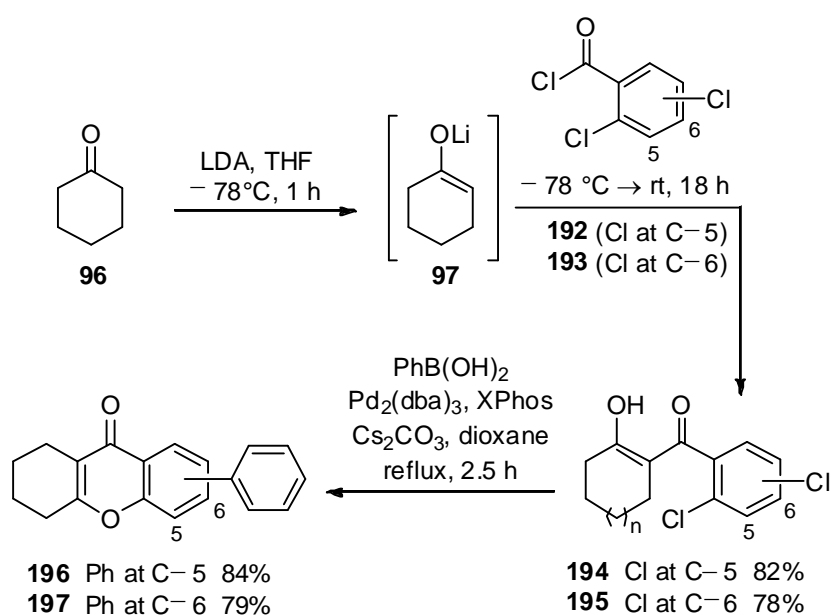


Figure 2.8: Isokibdelone C (**190**) and albobfungin (**191**)



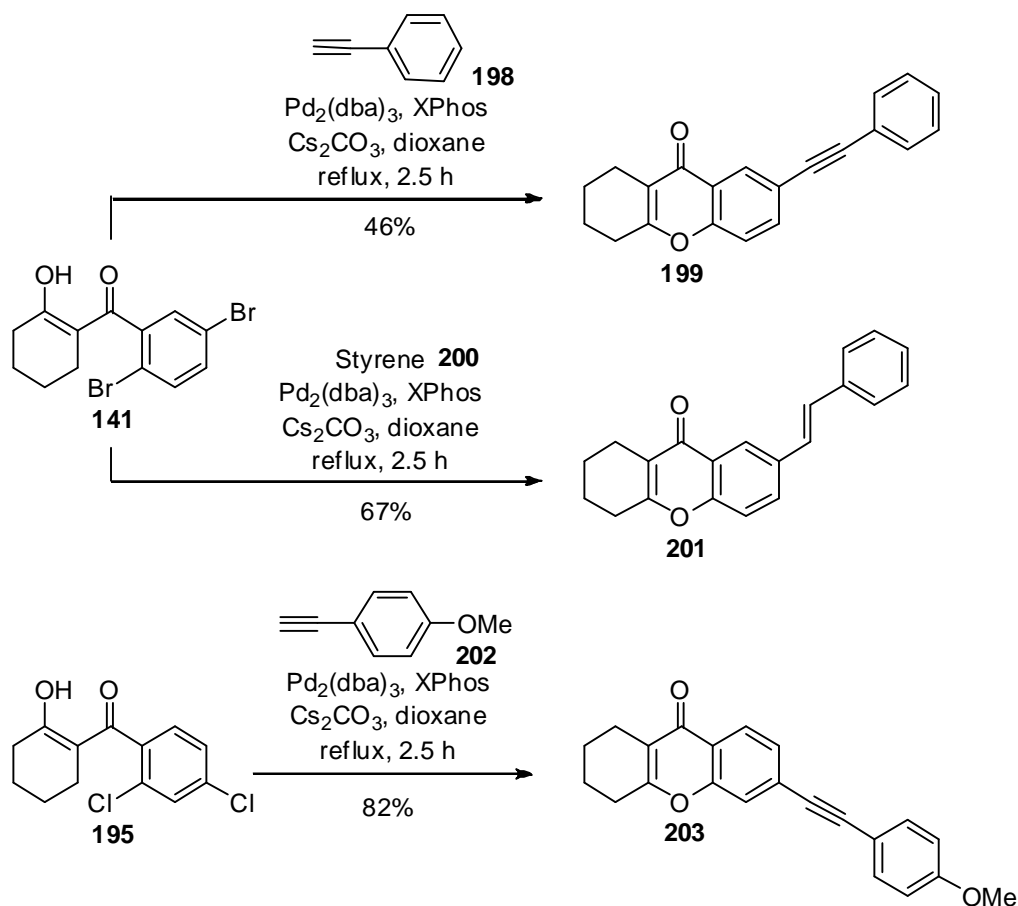
Scheme 2.46: 5 and 6-arylated THXs from dichloride substrates

2.6.3 Tandem catalysis using Sonogashira and Heck cross couplings

Subsequently we decided to investigate whether other palladium cross coupling reactions could be combined with THX formation. Due to time constraints, only a small number of examples were examined. Both Sonogashira couplings¹⁴⁹ and

Heck couplings¹⁵⁰ were achieved under the one-pot conditions, providing additional examples of the versatility of this reaction (Scheme 2.47).

The cyclisation with Sonagashira and Heck reactions were performed in an analogous way to the Suzuki-Miyaura couplings. The appropriate precursor was treated with Cs_2CO_3 , $\text{Pd}_2(\text{dba})_3$ and XPhos in dioxane followed by addition of alkyne or alkene. The Heck product **201** has tentatively been assigned as *trans*. This stereochemical outcome is normally preferred.¹⁵¹⁻¹⁵³ The ^1H NMR spectrum shows a singlet for the double bond hydrogens, clearly they are in very similar chemical environments. Despite re-running the ^1H NMR in various deuterated solvents (CDCl_3 , MeOD, $(\text{CD}_3)_2\text{CO}$, $\text{DMSO}-d_6$), the peak did not resolve into a pair of doublets that would have been used to assign stereochemistry more rigorously.

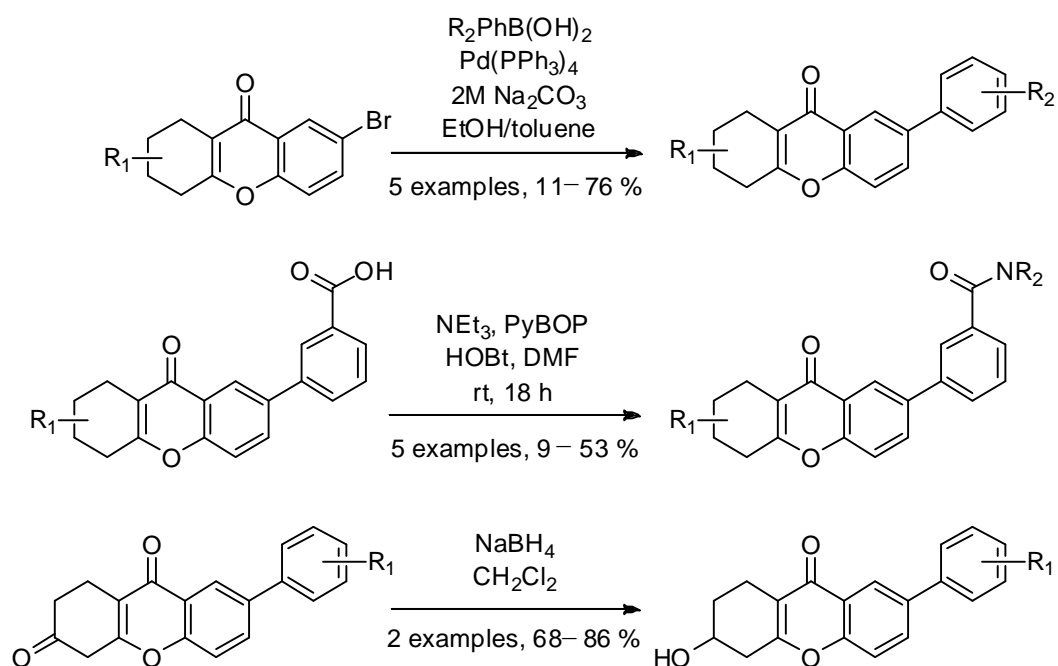


Scheme 2.47: Tandem catalysis utilising Sonagashira and Heck couplings

The Sonogashira coupling at both 5 and 6 positions of the THX were successful although it was noted that the yield was greatly increased when electron rich alkyne **202** was used, as is typical for this reaction.^{154,155} Electron rich substrates facilitate the nucleophilic addition of the alkyne to the palladium catalyst.

2.7 Conclusions and Future Work

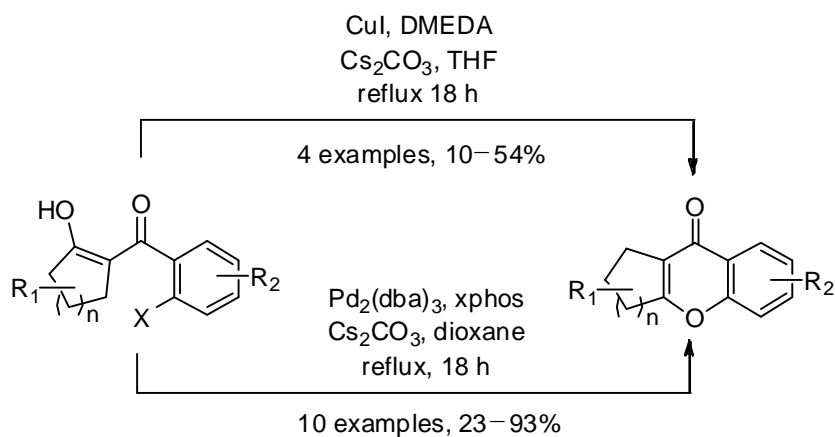
In summary, existing literature methods have been used for the formation of simple THXs that lie at the core of many natural products including the kigamicins. Subsequent optimisation of the Suzuki-Miyaura reaction of the brominated substrate allowed the synthesis of a total of twelve 7-arylated THXs whose biological activity is assessed in Chapter Four.



Scheme 2.48: Suzuki-Miyaura couplings and functional group interconversions

An improved approach using metal catalysis was investigated and it was found that both copper and palladium could be utilised for this cyclisation. After optimisation, it was observed that higher yields were obtained using palladium. The scope of both

reactions was also investigated providing access to a further eleven analogues of the natural product.



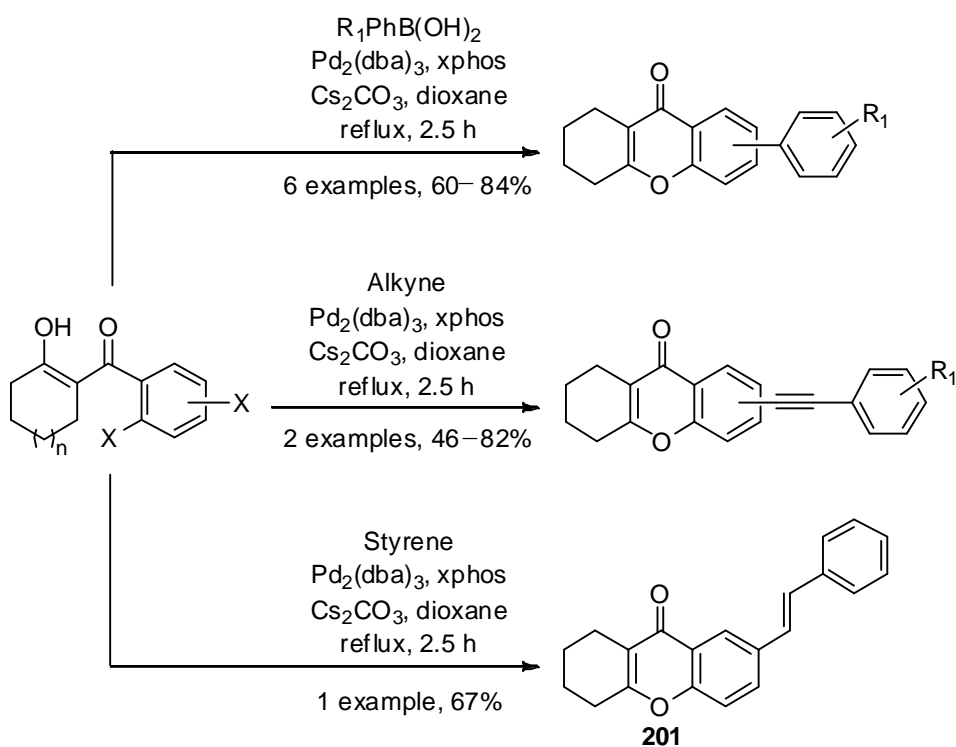
Scheme 2.49: Optimised analogues *via* copper and palladium catalysis

We discovered that the reaction also proceeds uncatalysed. After conducting a base screen, it was found that the uncatalysed reaction was base dependent and in particular on the nature of the enolate anion-counterion interaction. The catalysed reaction was found to proceed faster than the uncatalysed process, which was emphasised by a further increase in reaction rate with higher loading of palladium.

Copper catalysed processes have been reported to give very low yields or no product when there is an electron withdrawing group present promoting the competing S_NAr process.^{156,157} This was observed by us when investigating copper to form THXs. However, the uncatalysed reactions gave better yields than those containing copper. This is also illustrated in the work of Bowman *et al.*¹⁴¹ They observed that addition of copper to their S_NAr reaction hindered it completely by coordination to the anion. Lee *et al.*¹⁴⁴ suggest that in the presence of a strong counterion, the addition of H₂O decreases the activation energy of the reaction by coordinating to the counterion and thus partially neutralising the interaction

between the anion and counterion. This was evidenced in our work where the highest yield of 56% was observed in the copper reaction using H₂O as a solvent.

A one-pot reaction was undertaken whereby the C–C and C–O bonds were formed in the same reaction vessel. Good yields were obtained for this reaction and a further nine analogues were synthesised. Time-course GCMS analysis showed that the intramolecular C–O bond formation occurred first, followed by the intermolecular C–C bond formation. The scope of the tandem catalysis has been extended to include Sonagashira and Heck coupling reactions. Some of these results have been published.¹⁵⁸



Scheme 2.50: Scope of tandem catalysis

Future work should involve a more detailed investigation of the tandem catalysis using Sonogashira and Heck couplings, to fully test the scope of these one pot reactions.

Work should also be carried out to incorporate the hydroxyl and saccharide moieties surrounding the A ring of the natural product on the 7-arylated THX. As will be discussed in Chapter Four, another member of the group, Samiullah, synthesised a number of analogues containing functionalised A rings. However, they were not coupled to the 7-aryl group which overlays with the natural product. With these compounds in hand, direct comparisons could be made between the biological activity of the simple 7-arylated THX (**103**) and those containing functionalised A rings. Conclusions could then be drawn as to the importance of these groups in the bioactivity exhibited by the natural product.

Chapter 3:
Towards the Fused Rings of
the Kigamicins

3.1 Introduction

Alongside analogues based on the ABCF rings of the kigamicins, we also wanted to make compounds containing the central CDEF rings of the natural product (Figure 3.1). Moreover by combining the knowledge gained here with that acquired in Chapter 2, we would then be in a strong position to make the A-F rings of the natural product and could then target synthesis of the natural product itself.

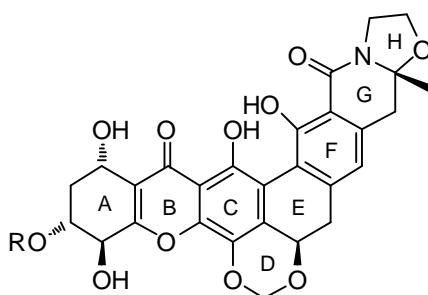


Figure 3.1: Kigamicin

3.2 Proposed Synthesis of the CDEF Rings of the Kigamicins

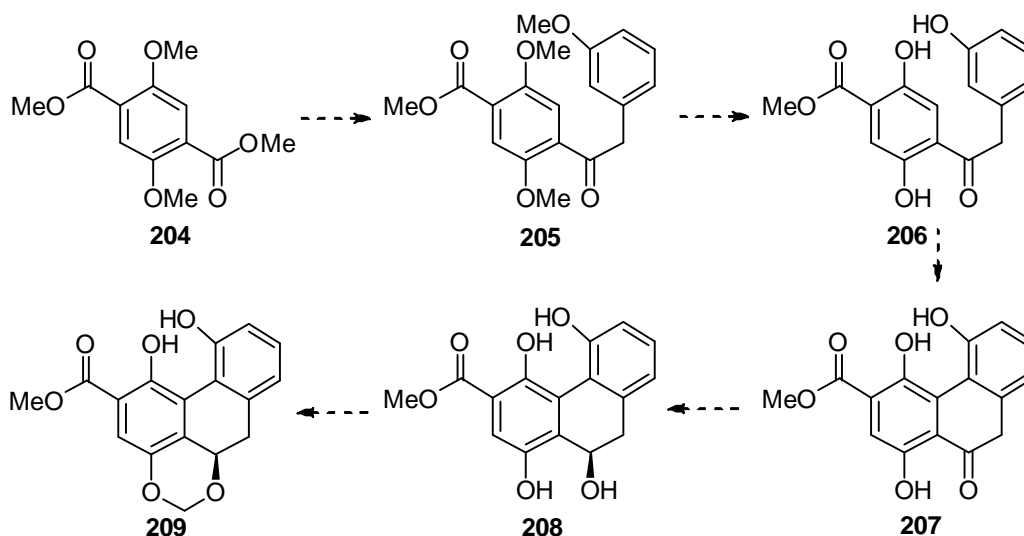
At the outset, we realised that the primary challenge to this piece of work was the hexa-substituted C ring of the natural product (Figure 3.1).

In Chapter Two, attempts were made to synthesise the E ring *via* Suzuki-Miyaura couplings of *ortho*-substituted boronic acids or their pinacol esters followed by Friedel Crafts cyclisation (Section 2.2). Given the limited success, we decided to explore alternative routes.

Literature suggested it would be possible to synthesise the aryl-aryl bond at C-7 of the THX (**206-207**) *via* an oxidative coupling directed by the two hydroxyl groups present *ortho* to the bond we wished to form (Scheme 3.1).¹⁵⁹⁻¹⁶¹ This is an

attractive strategy as it would allow for functionalisation at C-7 by C-H activation thus simplifying the substrate required.

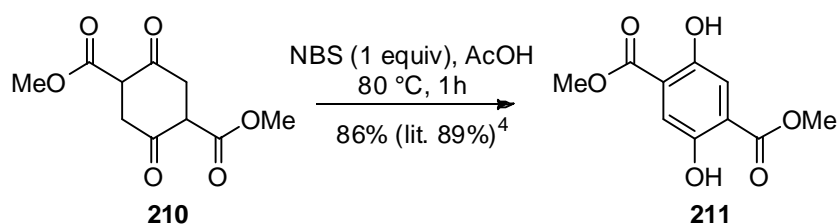
We anticipated that formation of substrate **206** required for the oxidative addition step might require some investigation, but that we could add to the carbonyl moiety of substrate **204** with a relevant nucleophile seemed plausible. Subsequent to oxidative coupling to form **207**, we expected that the enantioselective reduction to form alcohol **208** with the correct stereochemistry would be simple and the acetal formation to form **209** would also be facile. This would provide the CDEF rings of the natural product and efforts could then be directed towards the incorporation of the THX to this motif. To this end, it would be advantageous to incorporate a carbonyl functional group to the fused CDEF rings as shown in Scheme 3.1.



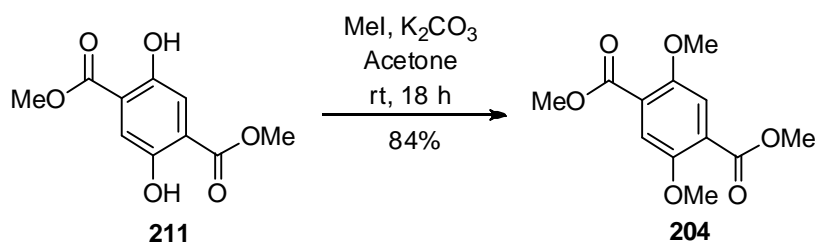
Scheme 3.1: Strategy to the central ring system

We chose to begin with simple symmetrical substrate **211** which had both the carbonyl groups and the hydroxyl groups we would require in the synthesis. This compound had been made previously by oxidation of dicarbonyl cyclohexanedione **210** which was commercially available.¹⁶² Dione **210** was dissolved in acetic acid

and heated to 80 °C before adding the *N*-bromosuccinimide (NBS). It was necessary to add the NBS in portions very carefully due to the evolution of HBr. This provided dimethyl dihydroxyterephthalate **211** in an excellent 86% yield (Scheme 3.2).

Scheme 3.2: Oxidation of **210**

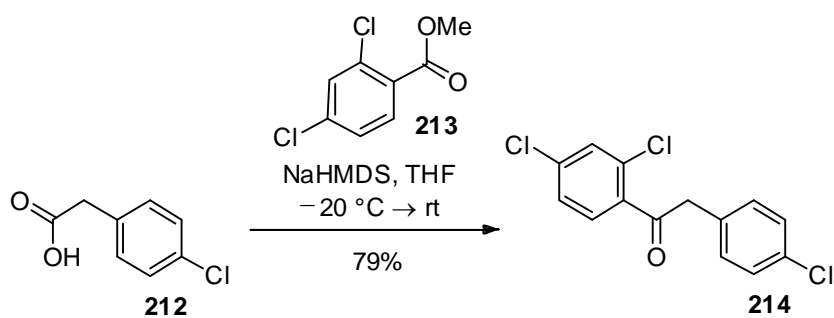
Next, we protected the hydroxyl groups of **211** as methyl ethers. This was easily accomplished using potassium carbonate and methyl iodide in acetone to give **204** in 84% yield (Scheme 3.3).



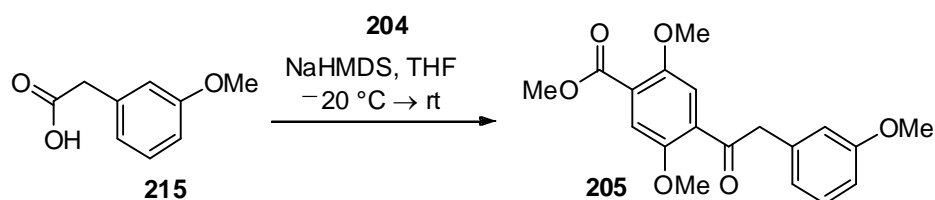
Scheme 3.3: Synthesis of the dimethoxy dimethylterephthalate

The synthesis was scaled up and gram quantities of **204** were produced so that various options could be explored.

Initial efforts focused on direct mono-addition to the ester. A variety of methods were considered. Debenham *et al*¹⁶³ successfully added the dianion of benzyl carboxylic acid **212** to ester **213** and after decarboxylation, isolated **214** in 79% yield (Scheme 3.4).

Scheme 3.4: Addition and decarboxylation¹⁶³

We attempted to use these conditions to add the dianion of 3-methoxyphenylacetic acid **215** to ester **204** (Scheme 3.4). The 3-methoxy substituent on **215** was necessary for directing oxidative addition later in the synthesis. Only a trace of product was observed under these conditions as determined by ¹H NMR spectroscopy of the crude material showing a marginal underintegration of the methyl ester peak and a small additional peak at 4.20 ppm which could correspond to the methylene of product **205**. However, only diester **204** was cleanly isolated. The conditions of the reaction were modified (Table 1); KHMDS and LiHMDS were used in place of NaHMDS, the equivalents of base were increased and the reaction temperature was gradually increased to reflux. In all of these reactions, only trace product could be detected and therefore it was decided that another method needed to be found.



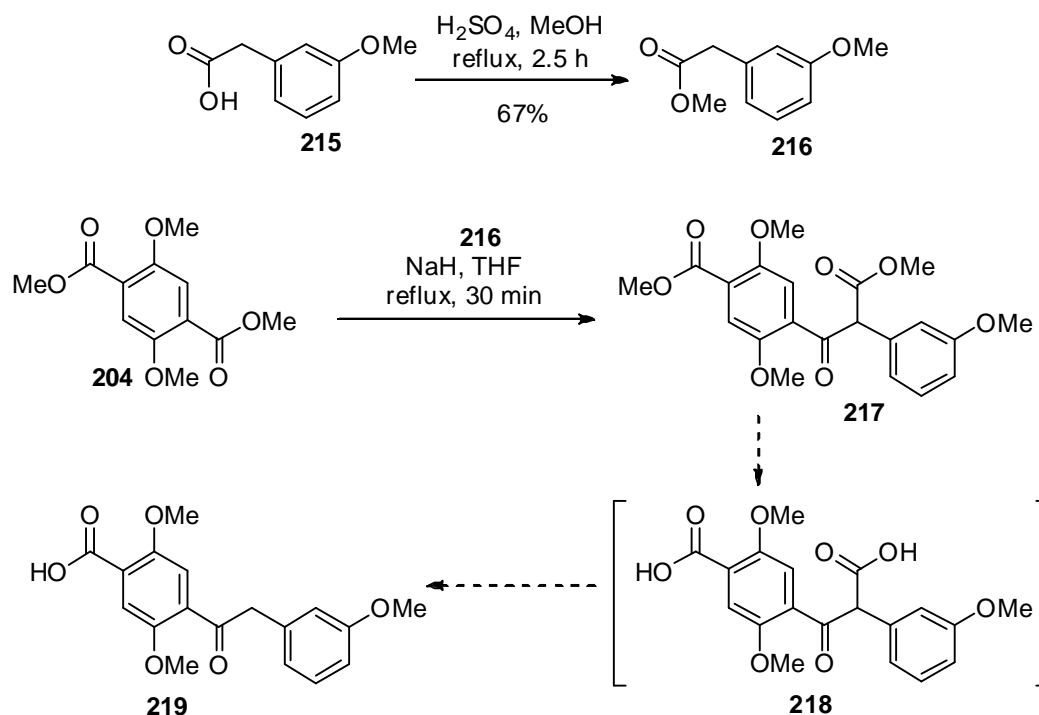
Scheme 3.5: Attempted dianion addition

entry	base	equiv. base	temp	time	result
1	NaHMDS	2	rt	18 h	trace product
2	LiHMDS	2	rt	18 h	trace product
3	LiHMDS	2	50 °C	18 h	trace product
4	LiHMDS	3	rt	18 h	trace product
5	LiHMDS	3	rt	60 h	trace product
6	KHMDS	2	rt → 50 °C	18 h	trace product
7	KHMDS	2	reflux	60 h	trace product

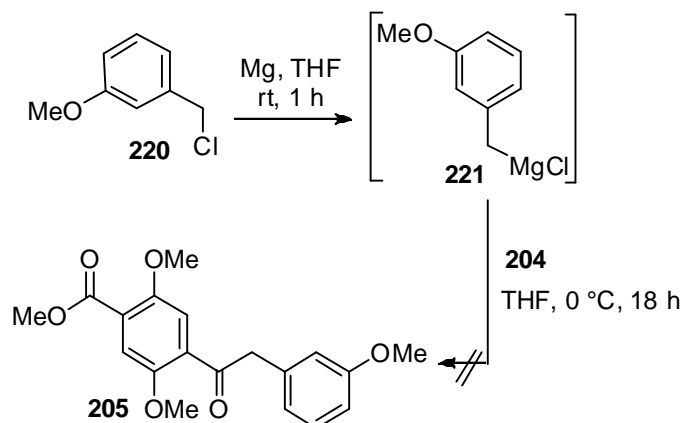
Table 1: Conditions used for attempted dianion addition

Next, a Claisen condensation of ester **216** with ester **204** was attempted. The resultant β -keto ester **217**, could then be hydrolysed to form the acid which would then decarboxylate to give **219** (Scheme 3.6). This is very similar to the above reaction but without the formation of the dianion which could potentially be a source of problems. Initially the ester **216** was synthesised from the carboxylic acid **215** in 67% yield.

The Claisen condensation was then attempted using NaH in THF.¹⁶⁴ Aqueous work up and purification on silica gel afforded very little product (<18%) which was not cleanly isolated. Both ¹H NMR spectroscopy and mass spectrometry confirmed that the correct product had formed but further optimisation was not undertaken due to the complex mixture of products formed and difficulty in isolation of **217**.

Scheme 3.6: Proposed route *via* Claisen condensation

As an alternative strategy, we explored monoaddition of a Grignard reagent to the diester. 2-Methoxybenzylchloride **220** was added to magnesium turnings in THF and the mixture was allowed to stir at room temperature until the magnesium had dissolved, indicating formation of Grignard **221**. This was then added dropwise to a solution of the starting material in THF at 0 °C. The reaction returned starting material with no indication of any product having formed. It was postulated that the failure of these reactions was due to the unreactive nature of ester **204**. The *ortho* substituted electron donating methoxy group could be making the ester less electrophilic towards nucleophiles. To test this theory, commercially available MeMgBr was reacted with diester **204** in THF and again no product was formed. This provides further evidence that the diester is unreactive and that failure of this reaction was not due to unsuccessful formation of the Grignard reagent.



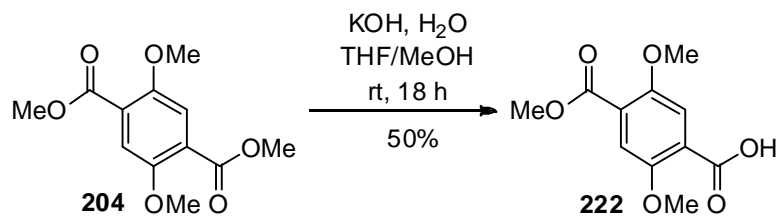
Scheme 3.7: Addition to the ester by a Grignard reagent

These results prompted us to re-evaluate our strategy. Next, attention turned to the conversion of one of the ester groups into the corresponding acid chloride or aldehyde, which would remove the symmetry in the molecule and make one of the carbonyl groups more electrophilic at the same time.

Treatment of diester **204** with aqueous sodium hydroxide in THF provided a mixture of products which was observed in the ^1H NMR spectrum of the crude material to be predominantly diester **204** and the corresponding diacid. The competing diacid formation could be encouraged in this biphasic mixture. Monohydrolysed product formed would be deprotonated and therefore more soluble in the aqueous phase. It could then be hydrolysed faster than the diester which is likely to be predominantly in the organic phase.

There have been examples in the literature such as the work by Valoti *et al*¹⁶⁵ where high yields of mono-acids are achieved by addition of MeOH to the reaction mixture. Following Valoti's work, diester **204** was therefore treated with aqueous potassium hydroxide in THF with an equal volume of MeOH added to aid the miscibility of the aqueous and organic phases. This gave product **222** in 50% yield.

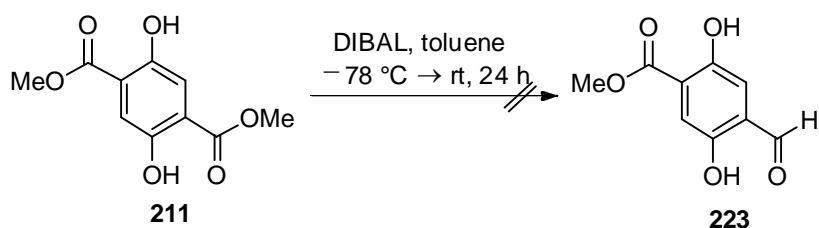
The low yield presumably reflects that diacid formation still competitively occurs but is much improved compared with the biphasic reaction.



Scheme 3.8: Mono-hydrolysis

Acid **222** was then converted to the corresponding acid chloride using thionyl chloride. We wished to add Grignard reagent **221** to this acid chloride but first attempted the reaction using MeMgBr in THF to test the reactivity of the substrate. Disappointingly, no product was apparent in the ¹H NMR of the crude material, only acid **222** and a complex mixture of other products in much smaller quantities. Due to the complex mixture, it was not attempted to isolate these products.

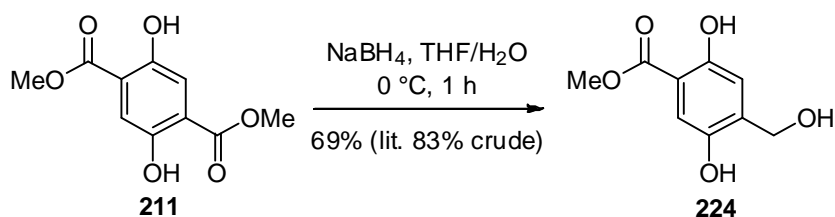
Our efforts then turned to the synthesis of mono-aldehyde **223**. To this end, direct reduction of ester **211** using DIBAL was attempted (Scheme 3.9). Instead of observing the aldehyde **223**, a complex mixture of products was observed; benzyl alcohol (resulting from over-reduction of one or both esters) and the dialdehyde as well as starting material.



Scheme 3.9: Attempted reduction to aldehyde

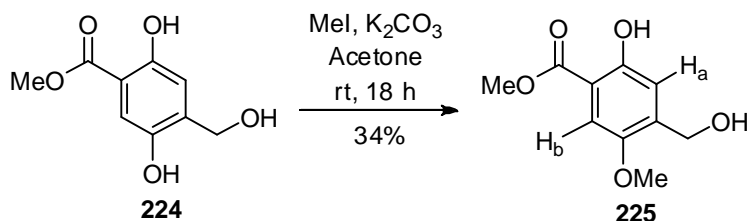
Reduction of **211** to benzyl alcohol **224** without reduction of the second ester moiety has been reported by Suzuki *et al.*¹⁶² This approach was investigated and the

diester was treated with NaBH₄ in THF/H₂O at 0 °C. The reaction was complete in 1 h and product **224** isolated in 69% yield.



Scheme 3.10: Reduction of diester

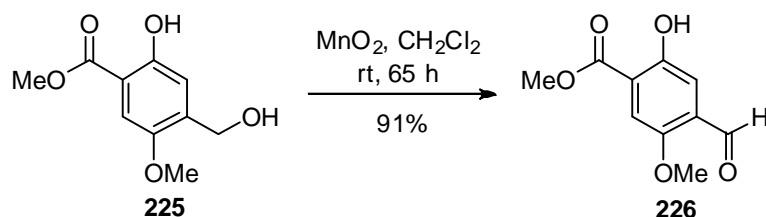
Next, oxidation of alcohol **224** was explored. A range of oxidising agents (MnO₂, PCC, IBX, DMP) were examined but no successful oxidation was realised, perhaps due to competitive oxidation of the hydroquinone. Selective protection of the hydroxyl groups was attempted. Alcohol **224** was treated with methyl iodide and potassium carbonate in acetone. However, the reaction did not go to completion and only mono-protected product **225** was observed in low yield.



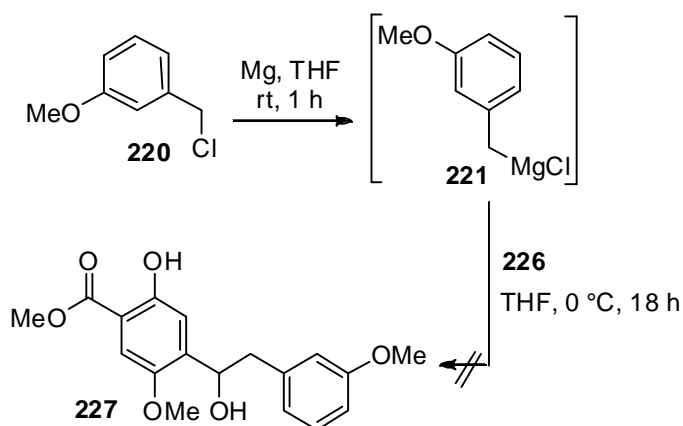
Scheme 3.11: Mono-protection

The hydroxyl group remaining unprotected was shown by NOE experiments to be as depicted in Scheme 3.11. Irradiation of the methylene group of the primary alcohol at 4.68 ppm (CH₂) enhanced an aromatic singlet at 6.99 ppm (H_a). When this signal was subsequently irradiated, both the phenolic hydroxyl group at 10.43 ppm (phenol) and the CH₂OH (4.68 ppm) were enhanced. Conversely, irradiation of the other aromatic hydrogen (7.23 ppm, H_b) enhanced the methyl ester (3.97 ppm) and ether (3.84 ppm). On this basis, we were able to confidently assign the site of the alkylation.

Oxidation of alcohol **225** with MnO_2 in CH_2Cl_2 at room temperature provided aldehyde **226** in 91% yield. The conversion was not therefore attempted using other oxidising agents. The high yield of oxidation of **225** is further evidence that oxidation to the hydroquinone is a problem of substrate **224** and protection of the phenolic hydroxyl group eliminates this side reaction.

Scheme 3.12: Oxidation using MnO_2

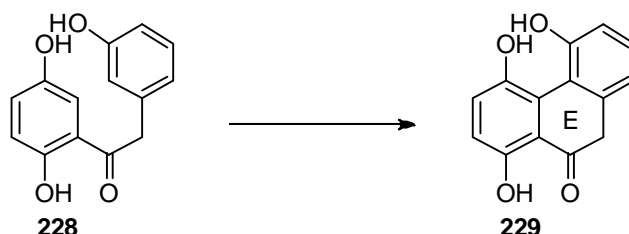
Next we attempted to selectively add a Grignard reagent to aldehyde **226**. The Grignard reagent derived from 2-methoxybenzylchloride **220** was made (Scheme 3.13) and was added to the aldehyde in THF. Unfortunately no reaction occurred and only starting material was isolated. This could have been due to the Grignard reagent not forming properly but reactions with commercial Grignard reagents were not investigated due to time constraints.



Scheme 3.13: Attempted addition of Grignard reagent to aldehyde

3.2.1 Synthesis of a model substrate for oxidative addition studies

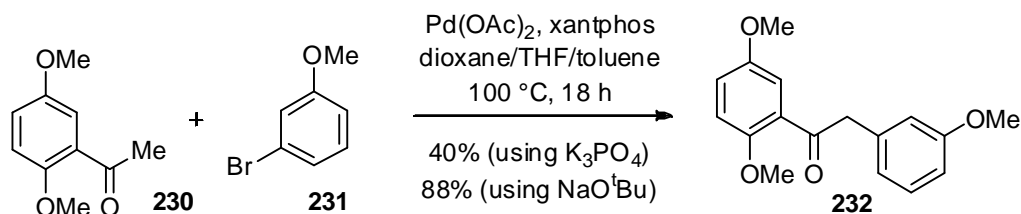
In parallel to the studies described above, we also targeted **229**, which could be used to study the oxidative cyclisation step for formation of the E ring of the natural product.



Scheme 3.14: Oxidative cyclisation to form the E ring

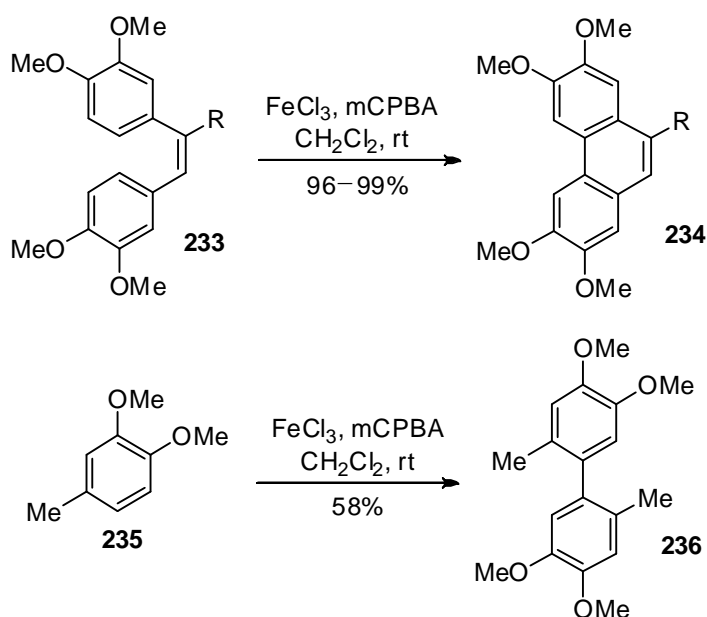
Desai *et al*¹⁶⁶ have developed a mild method using palladium catalysis for the α -arylation of ketones. The method was shown to be general and applicable to a wide array of substrates. This appeared an attractive method to assemble oxidative cyclisation precursor **228**.

2,5-Dimethoxyacetophenone **230** and 3-bromoanisole **231** were added to dioxane followed by Pd(OAc)₂, xantphos, K₃PO₄, THF and toluene according to Desai's conditions.¹⁶⁶ This reaction afforded **232** in a modest 40% yield. In 2000, Buchwald *et al*¹⁶⁷ reported the use of various conditions for the α -arylation of ketones. They established that the selection of base and ligand were very important with optimal conditions substrate specific.¹⁶⁷ They found higher yields when NaO^tBu was used, however, more sensitive substrates required weaker bases. Encouraged by their findings, we examined the use of NaO^tBu as base. When the reaction in Scheme 3.15 was repeated using NaO^tBu, **232** was isolated in a much improved 88% yield.



Scheme 3.15: Reaction using 2,5 dimethoxyacetophenone

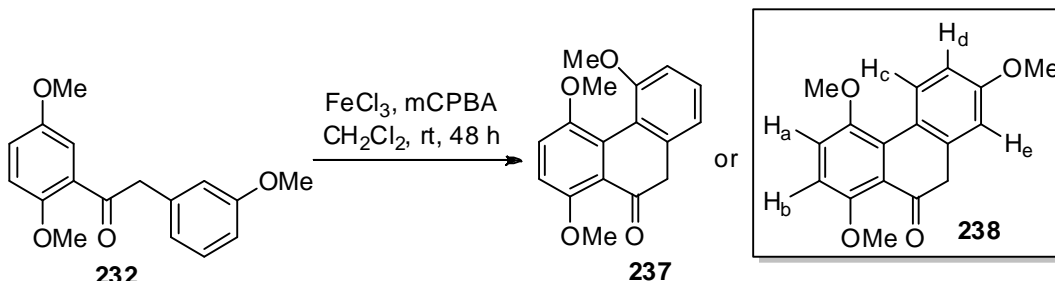
Next, we attempted oxidative cyclisation of ketone **232**. Wang *et al*¹⁶⁸ has reported similar oxidative couplings of aromatic compounds catalysed by FeCl_3 and mCPBA. This method offers advantages over historic methods¹⁶⁹ which use thallium, lead or vanadium salts¹⁷⁰⁻¹⁷⁴; its less expensive, less toxic and the reactions can occur under much milder conditions. They showed that the reaction provides excellent yields for intramolecular reactions and the scope can be extended to intermolecular reactions albeit in reduced yields (Scheme 3.16).



Scheme 3.16: Intermolecular and intramolecular coupling using iron

Treatment of **232** with FeCl_3 and mCPBA in CH_2Cl_2 at room temperature for 18 h returned predominantly starting material. The reaction was repeated increasing the reaction time to 48 h. In this case, there was much less starting material remaining

and one main product formed (2:1 starting material to product) but the product and starting material proved difficult to separate by chromatography. The major product was assigned as **238** (Scheme 3.17).

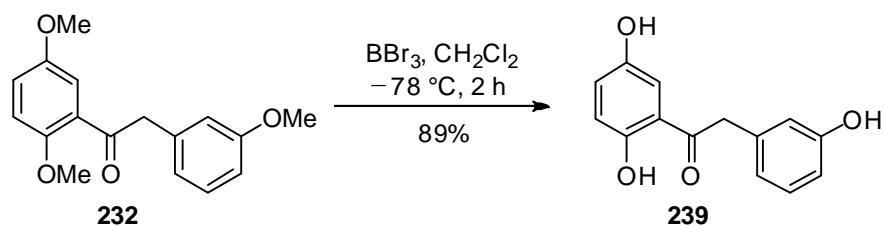


Scheme 3.17: Possible regioisomers from oxidative coupling

The ^1H NMR spectrum showed two doublets at 7.20 ppm and 6.80 ppm ($J = 7.8$ Hz) which coupled with one another assigned as H_a and H_b . There was also a doublet at 7.25 ppm with a small coupling (3.4 Hz) assigned as H_c , a doublet at 6.85 ppm with a larger coupling (9.0 Hz) assigned as H_c and a doublet doublet at 6.97 ppm with a small and large coupling (3.4 Hz and 9.0 Hz) assigned as H_d . The splitting pattern is fully consistent with the formation of **238**. If isomer **237** had been formed then with the methoxy group *ortho* to the bond formed, hydrogens would be expected to have one large J coupling. Isomer **238** could be formed preferentially due to less steric hindrance in comparison to **237**. The formation of this isomer is consistent with observations made by Wang *et al.*¹⁶⁸ The product could not be completely separated from the other fractions and could not therefore be fully characterised.

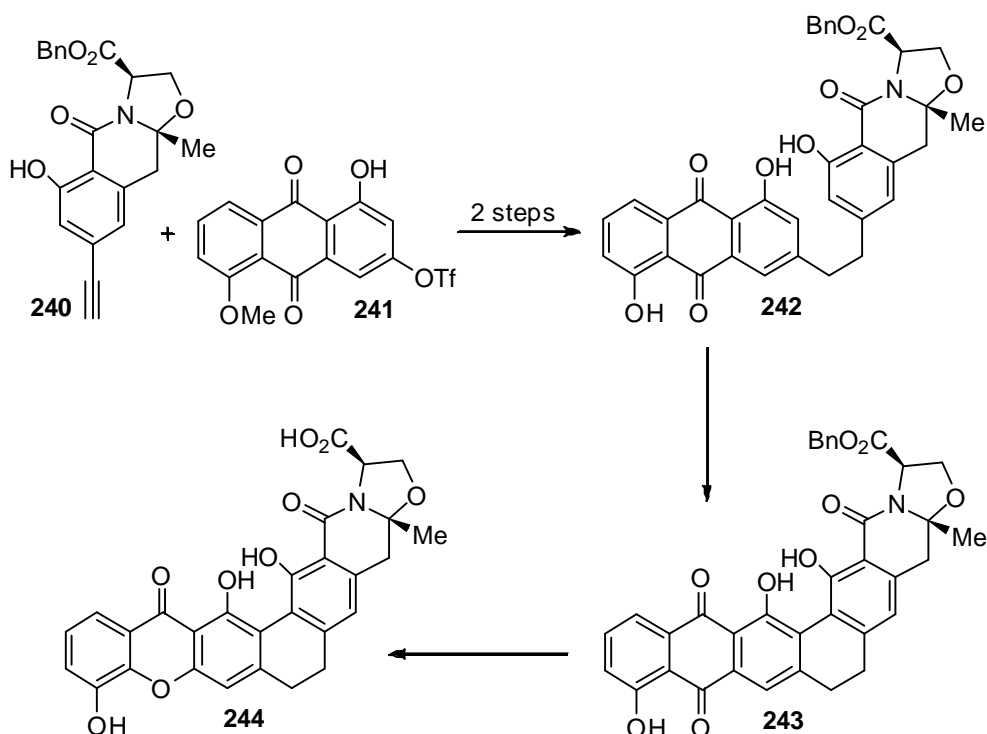
There is an abundance of literature examples for oxidative coupling reactions on substrates containing two hydroxyl moieties *ortho* to the bond forming.¹⁵⁹ We therefore set out to remove the methyl groups on our substrate and explore this

chemistry. This was performed using 3.5 equivalents of BBr_3 in CH_2Cl_2 at $-78\text{ }^\circ\text{C}$ which gave **239** in an excellent 89% yield (Scheme 3.18).



Scheme 3.18: Deprotection

Amongst the reported oxidative couplings of phenolic compounds is the total synthesis of TMC-66 by Hosokawa *et al*¹⁶¹ (Scheme 3.19). The structure of this compound is quite similar to the kigamicin natural products despite the lack of THX nucleus.



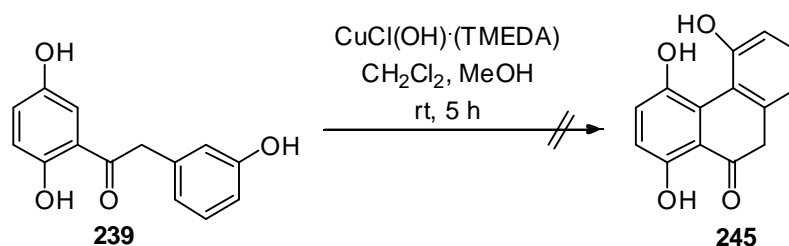
Scheme 3.19: Total synthesis of TMC-66¹⁶¹

The authors chose to construct the natural product using oxidative coupling (**242**-**243**) as the final step (excluding deprotection steps). They investigated a range of

oxidants and discovered that the only reagent that effected this transformation was $\text{CuCl}(\text{OH})\cdot(\text{TMEDA})$ which is a reagent developed by Koga *et al*¹⁷⁵ for the synthesis of binaphthol derivatives. The use of this reagent enabled Hosokawa to obtain **243** in 20% yield. Further modification to the reagent by replacement of TMEDA with *N*-methylimidazole (NMI) improved the yield to 89%.

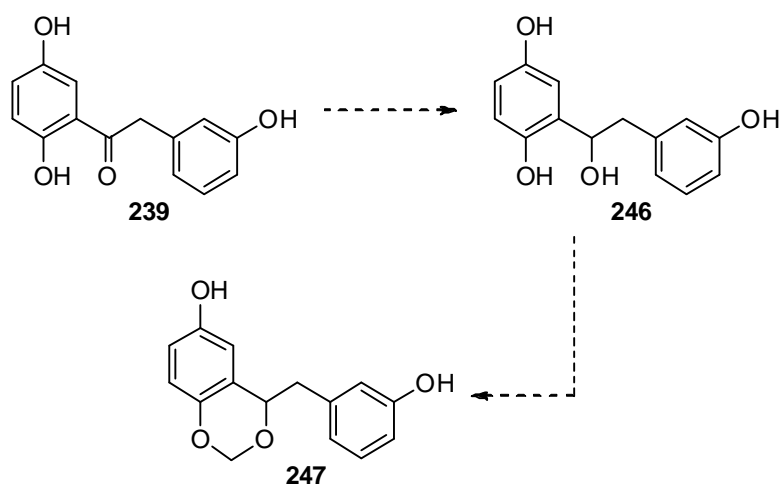
We set out to explore the use of $\text{CuCl}(\text{OH})\cdot(\text{TMEDA})$ and $\text{CuCl}(\text{OH})\cdot(\text{NMI})_2$ in the oxidative cyclisation of **239**. TMEDA was added to CuCl in MeOH and stirred in the presence of air at room temperature for 5 h. This provided a dark purple solid, whose appearance and melting point (m.p = 137-138 °C, lit. 137-138 °C) matched those described in the literature. This method was repeated with the substitution of NMI for TMEDA, however neither the appearance nor the melting point matched those described in the literature. Therefore, we proceeded with only $\text{CuCl}(\text{OH})\cdot(\text{TMEDA})$.

Substrate **239** was treated with $\text{CuCl}(\text{OH})\cdot(\text{TMEDA})$ under Hosokawa's conditions.¹⁶¹ ¹H NMR spectroscopy of the crude material showed no consumption of starting material. Triol **239** displayed poor solubility in CH_2Cl_2 and we were concerned that this might be the reason for the failure of the reaction. The reaction was therefore repeated with added MeOH to aid solubility of reagents, however this led to no improvement.



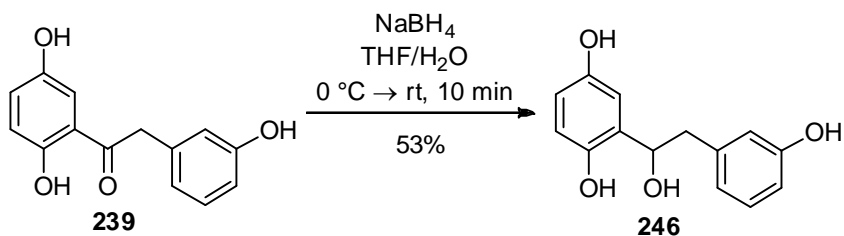
Scheme 3.20: Attempted oxidative coupling

To improve the solubility of the substrate, we sought to convert it into the corresponding acetal **247** (Scheme 3.21).



Scheme 3.21: Planned synthesis of acetal **247**

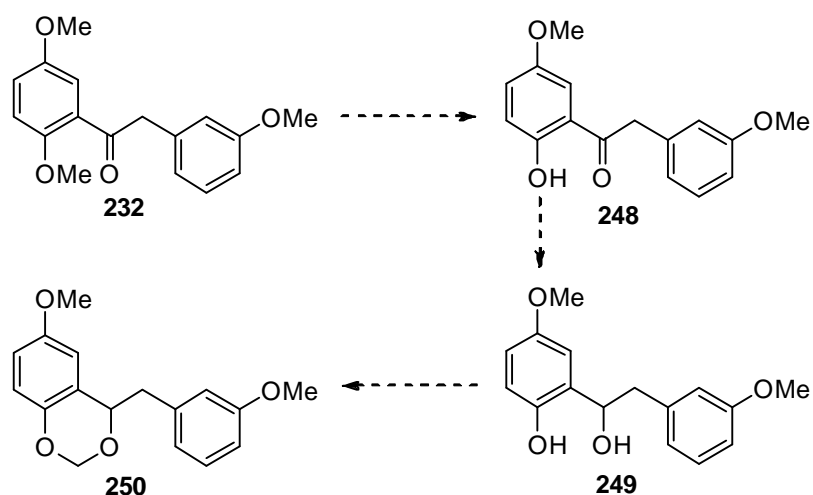
The reduction of ketone **239** was realised using NaBH_4 which gave **246** in 53% yield.



Scheme 3.22: Reduction using NaBH_4

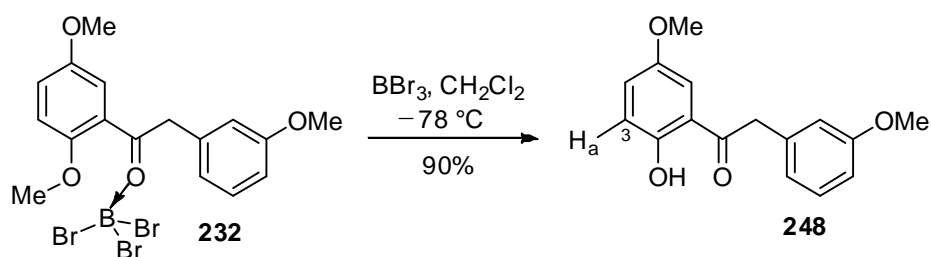
The main challenge with the purification and subsequent use of this compound was again its solubility.

The synthesis was therefore re-evaluated. It was decided to attempt the mono-deprotection of trimethoxy **232** prior to reduction of the ketone. It was hoped this would provide a more soluble compound for acetal formation (Scheme 3.23).



Scheme 3.23: Proposed synthesis

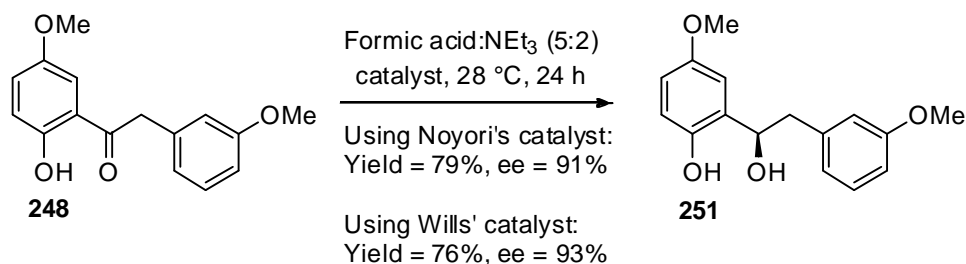
Ketone **232** was treated with 1.2 equivalents of BBr_3 in CH_2Cl_2 at -78°C . The solution was stirred at this temperature for 1 h before pouring over a mixture of ice and H_2O to quench, providing **248** in 90% yield. It was predicted that the boron of the BBr_3 would coordinate to the carbonyl leading to removal of the adjacent methyl group.¹⁷⁶



Scheme 3.24: Directed deprotection

Detailed NMR analysis using COSY, HMQC and HMBC techniques, confirmed the methyl group closest to the carbonyl oxygen was indeed removed. The doublet at 6.93 ppm ($J = 9.2$ Hz) is assigned as H_a as it is the only doublet with only a large coupling and no additional smaller coupling. H_a is shown to be attached to C-3 by HMQC and the hydroxyl group shows an interaction with C-3 by HMBC. Also, the hydroxyl hydrogen appeared at 11.82 ppm suggesting hydrogen bonding to the adjacent carbonyl oxygen atom.

Asymmetric reduction of ketone **248** to the *R*-enantiomer as shown in Scheme 3.25 was next examined.



Scheme 3.25: Enantioselective reduction

Initially, a ruthenium (II) based catalyst developed by Noyori^{177,178} (Figure 3.2) was utilised. This catalyst was made *in situ* by stirring (*p*-cymene) ruthenium(II)chloride dimer and (*R,R*)-TsDPEN in a 5:2 mixture of NEt₃: formic acid at 28 °C for 30 min before adding ketone **248**. Successful asymmetric reduction was achieved with this catalyst providing **251** in 79% yield and 91% ee. Concurrently, the reduction was attempted using a tethered catalyst developed by Wills *et al*¹⁷⁹⁻¹⁸¹ (Figure 3.2). A small sample of catalyst was kindly provided by this group and the reduction was realised in 76% yield and 93% ee.

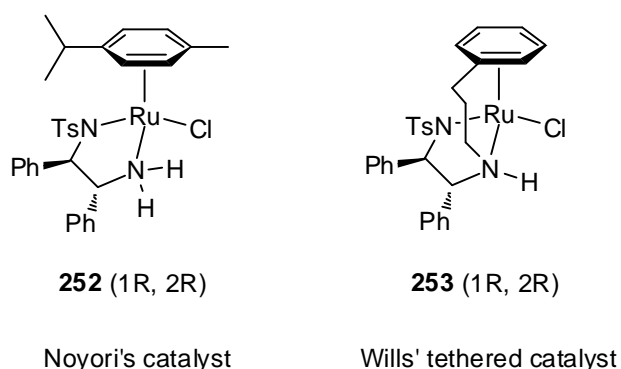


Figure 3.2: Ruthenium catalysts used for asymmetric reduction

The ee of **251** was determined using HPLC with a chiral AD column and eluting with 10% ⁱPrOH in *n*-hexane at 1.0 mL/min. Under these conditions, two separate

peaks of equal area were observed from the racemic substrate (the synthesis of which is described below). When chiral compound **251**, obtained using either Noyori or Wills' catalyst, was eluted under identical conditions, both peaks were again observed but one was major and one minor. The major peak was the same for **251** obtained using both catalysts which provides evidence that both catalysts provide the same enantiomer.

Product **251** has been tentatively assigned as the *R*-enantiomer. Wills' *et al*¹⁸⁰ describe the use of their tethered catalyst on a number of substrates and the (*R,R*) catalyst has been shown to provide the (*R*) product in most cases. In cases of acetophenone derivatives, excellent ee's are reported. It is believed that the reduction occurs *via* a 6-membered transition state (**254**) as depicted in Figure 3.3, where there is an edge-face CH/ π stabilising interaction. This directs the sense of reduction to give the preferred *R* product.

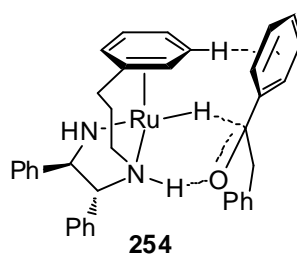
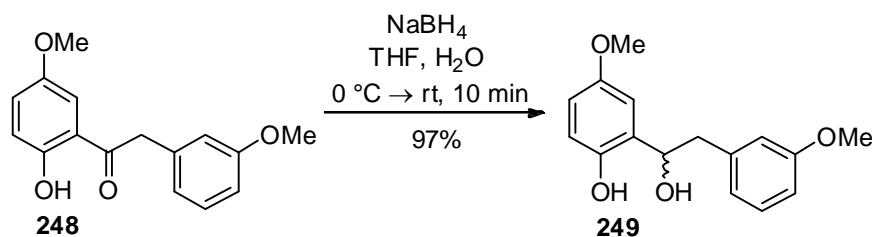


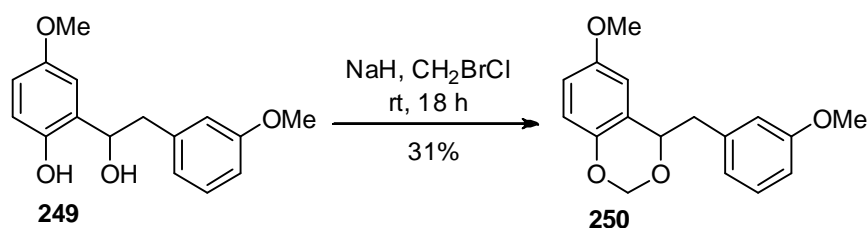
Figure 3.3: Transition state showing favourable CH/ π interaction

Alcohol **249** was also produced in racemic form using NaBH₄. (\pm) **249** was isolated in near quantitative yield.



Scheme 3.26: Reduction using NaBH₄

The cyclic acetal was then formed from the two hydroxyl groups. This step proved more challenging than we had anticipated. We attempted this reaction using paraformaldehyde with $\text{BF}_3 \cdot \text{OEt}^{182}$ or $\text{H}_2\text{SO}_4^{183,184}$, using *p*TsOH with dimethoxymethane in the presence of lithium bromide,^{185,186} and finally using sodium hydride with diiodomethane or bromochloromethane.¹⁸⁷ Most success was achieved with the latter conditions, which gave **250** in 31% yield (Scheme 3.27). Sufficient material was produced to examine further deprotection of the methyl ethers.



Scheme 3.27: Acetal formation

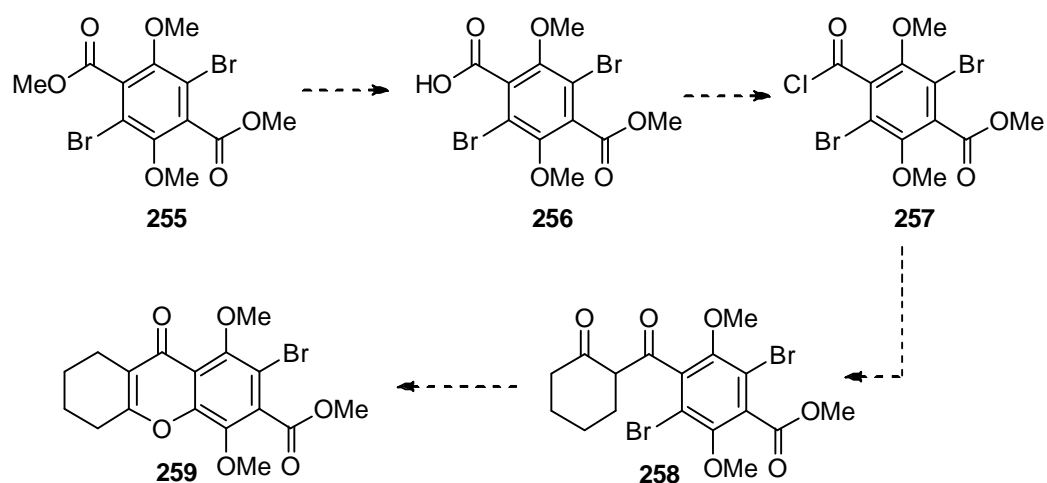
We had concerns using BBr_3 to protodemethylate **250**. However, Taylor *et al*¹⁸⁸ had achieved chemoselective protodemethylations in the presence of acetals in the total synthesis of preussomerins. On this basis, we elected to examine the use of BBr_3 for this transformation. Disappointingly upon treatment with BBr_3 , degradation of **250** was observed and no product could be isolated from the reaction mixture.

Seidel *et al*¹⁸⁹ had encountered difficulties with the deprotection of methyl ethers with BBr_3 and they reported 9-I-BBN as a much milder reagent for this transformation. However, when our substrate was treated with 9-I-BBN in CH_2Cl_2 at room temperature, no product was isolated. No success was encountered using LiCl in DMF at 85 °C.¹⁹⁰ No reaction occurred and only starting material was isolated. Use of AlCl_3 in CH_2Cl_2 was also ineffective.¹⁸⁸

Our final attempt at the deprotection of the methoxy groups was utilising NaSEt. The use of this reagent was developed by Mirrington *et al* in the 1970s.^{191,192} NaSEt was formed in situ from NaH and ethanethiol in DMF before adding **250**. The crude ¹H NMR spectrum showed the presence of the acetal group with the peaks for the methyl groups underintegrating. This suggested that the reaction was proceeding, albeit slowly but importantly without degradation of the acetal. Encouraged by these results, the reaction was repeated and heated to reflux for 68 h. Despite the much greater reaction time, there was still a large proportion of starting material visible by crude ¹H NMR spectroscopy, although even at reflux for this length of time, the acetal was still intact. Due to time constraints, this work wasn't pursued further.

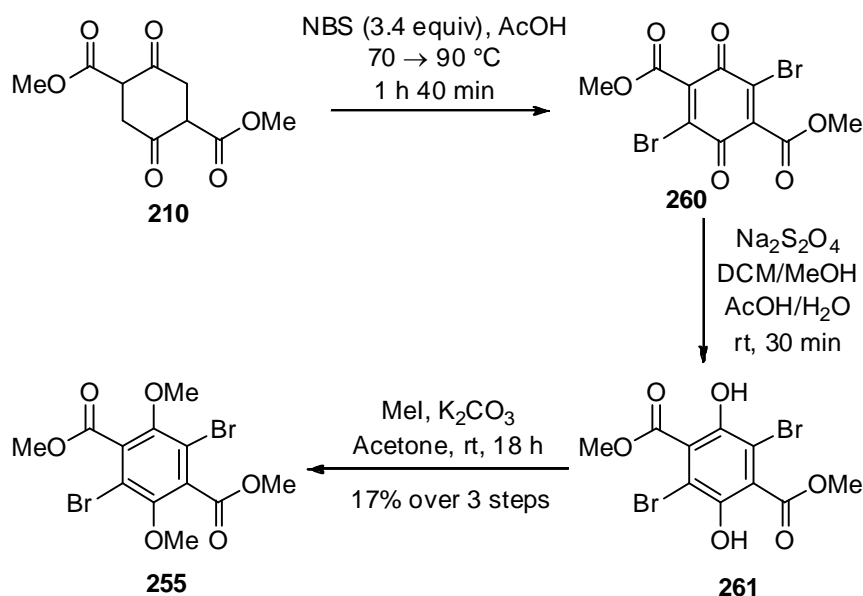
3.3 Attempted Synthesis of Hexa-Substituted THX Precursor

Based on the work carried out in Chapter Two, we wished to investigate the THX formation of a hexa-substituted system to evaluate whether this would be a valid route to more complex analogues (Scheme 3.28).



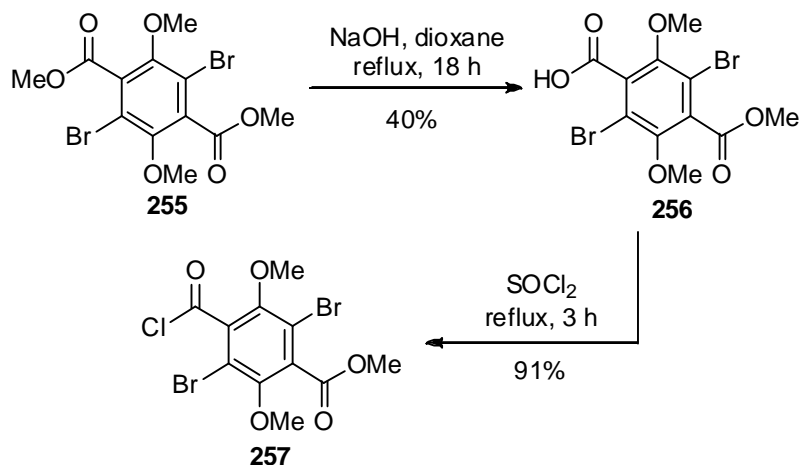
Scheme 3.28: Planned route to hexa-substituted THX **259**

Initially we oxidised the cyclohexanedione as in Section 3.2 (Scheme 3.2) but instead, an additional 3.4 equivalents of NBS were added in order to brominate **211** before reducing it to **261** with $\text{Na}_2\text{S}_2\text{O}_4$ (Scheme 3.29). This was carried out following the conditions of Hintermann *et al*¹⁹³, using NBS instead of NCS that they used to synthesise the chlorinated analogue. This material was methylated directly to give **255** in 17% yield over 3 steps.



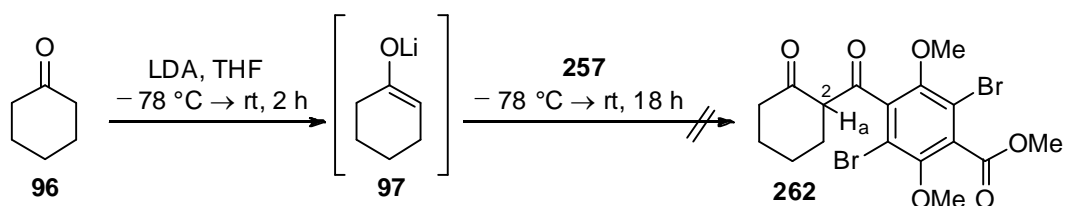
Scheme 3.29: Synthesis of dibrominated, hexa-substituted substrate

Initial attempts to monohydrolyse **255** under the conditions established earlier using KOH in methanol and THF returned clean starting material. The conditions were modified to those used by Hart *et al*¹⁹⁴ for monohydrolysis of a different diester. **255** was treated with NaOH in dioxane but at room temperature, again only starting material was returned. After heating to reflux for 3 h, **256** was isolated in 40% yield. Subsequent reaction with thionyl chloride at reflux gave the acid chloride in high yield (Scheme 3.30).



Scheme 3.30: Synthesis of acid chloride

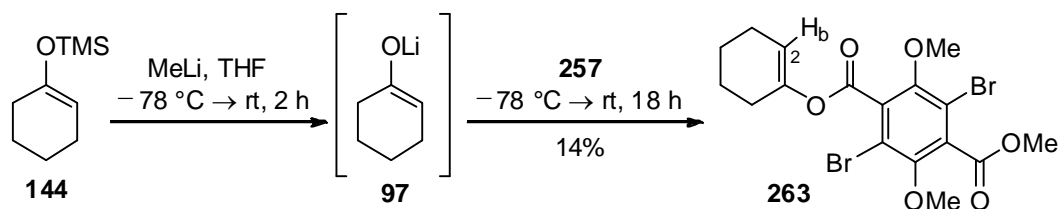
With the acid chloride in hand we sought to make THX precursor **262** through union with cyclohexanone **96**. Initial attempts by direct deprotonation of cyclohexanone with LDA were unsuccessful (Scheme 3.31).



Scheme 3.31: Attempted synthesis of THX precursor

However, when the lithium enolate was formed from the isolated silyl enol ether, the addition of the cyclohexanone component was accomplished in low yield (Scheme 3.32). Closer examination of the ^1H and ^{13}C NMR data, revealed that the *O*-acylated product **263** had been isolated instead of the *C*-acylated product (**262**). The alkene proton (H_b) appears at 5.61 ppm which is consistent with earlier *O*-acylated product **145** (6.06 ppm). If *C*-acylation had occurred, resulting in the enol tautomer, this proton would not be present. If *C*-acylation had resulted in diketone **262**, H_a would be expected in the same region as for diketone **159** and **177** (4.15 and 4.63 ppm) formed in Section 2.5.3. The ^{13}C NMR spectrum showed the carbon

signal for C-2 in **263** was at 115 ppm which is consistent with *O*-acylated product **145** formed earlier (118 ppm) (Scheme 2.29). The carbon signal at C-2 for diketone **159** and **177** was seen between 60 and 61 ppm. This result is perhaps not surprising due to the steric hindrance in acid chloride **257**. Isomerisation of **263** was not attempted due to limited material.



Scheme 3.32: Attempted synthesis from silyl enol ether

3.4 Conclusions

In summary, the E ring of the natural product has been formed by α -arylation of ketone **232** in high yield followed by aryl-aryl coupling of the C and F ring. The unwanted regioisomer was formed in this reaction with iron, but attempts to realise this transformation using copper catalysis were unsuccessful. Further investigation is required to establish if both isomers are formed in this reaction and if the correct isomer could be isolated.

Reduction of ketone **248** was achieved in high yield and ee and the resulting alcohol was converted to the cyclic acetal. This bodes well for the synthesis of the natural product.

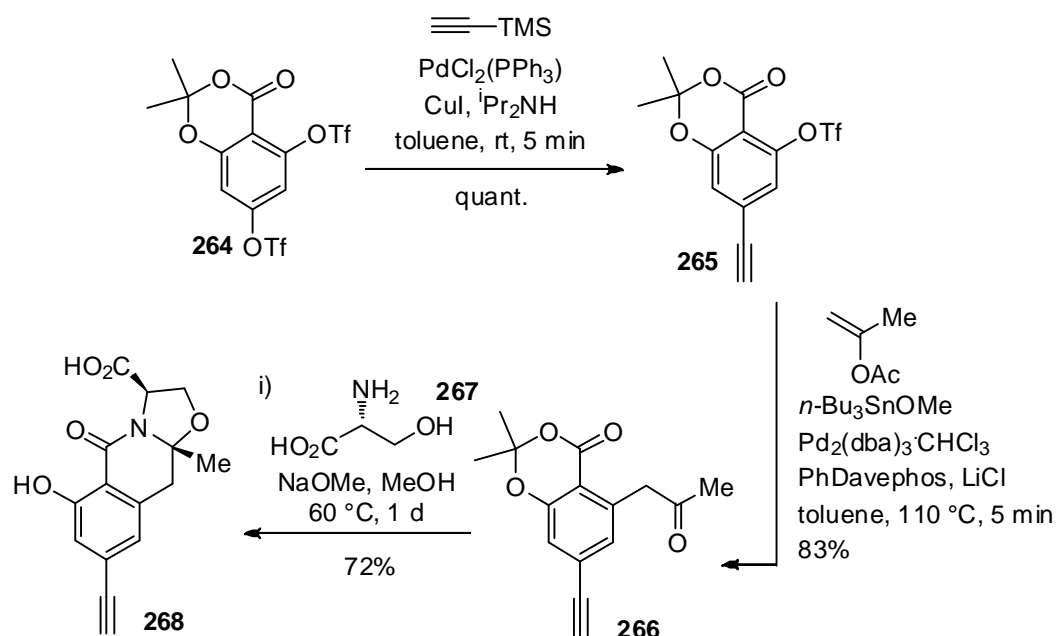
Deprotection of the methyl ethers in the presence of the acetal, was met with limited success although partial deprotection was observed when using NaSEt. Future work should include the optimisation of this process and subsequent oxidative couplings

of this substrate could then be investigated. It is anticipated that with free hydroxyl groups, *ortho* oxidative coupling could be achieved.

Synthesis of a hexa-substituted THX precursor was attempted but only *O*-acylated product was isolated and in low yield. Isomerisation to the *C*-acylated product could be attempted, although there may be limited success with this route due to inherent steric hindrance of this substrate.

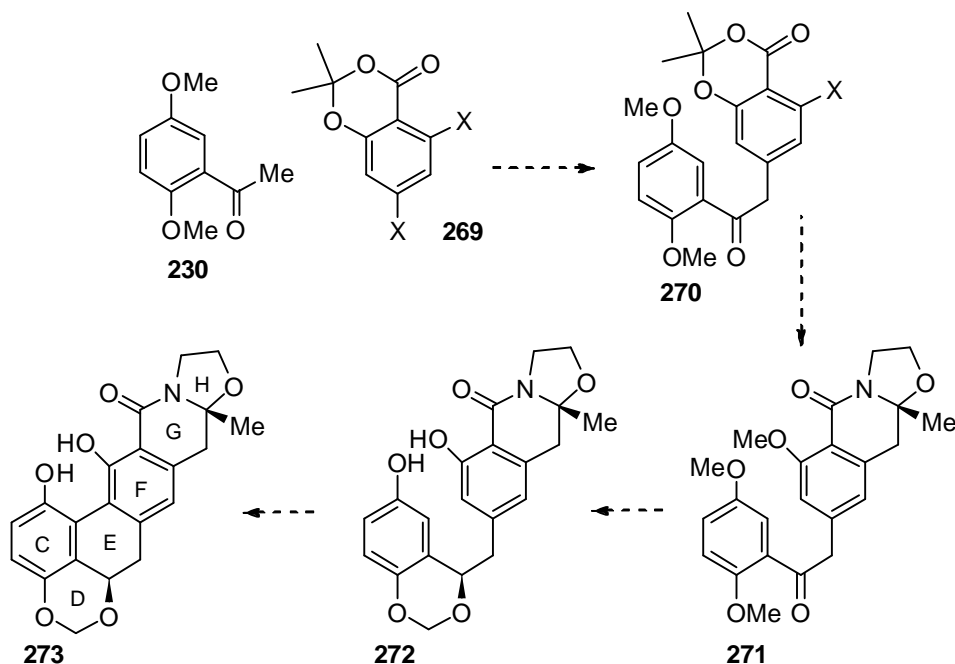
3.5 Future Work

Future work should involve optimisation and completion of the synthesis of the C-F rings of the natural product in the ways discussed above. Elaboration of this synthesis to include rings G and H of the natural product should then be explored. Analogous F-H rings have been made before by Hosokawa *et al*¹⁶¹ in the total synthesis of TMC-66 (Scheme 3.33).



Scheme 3.33: Synthetic steps as part of TMC-66 total synthesis

Combining this synthetic route with what has been learned throughout this chapter, it is hoped that the synthesis of rings C-H could be completed. Initial coupling of **269** with ketone **230** under the conditions developed in Section 3.2.1 should provide **270** in good yield. Following the synthetic steps described in Hosokawa's work,¹⁶¹ it is hoped that **271** could be made in a similar fashion. With **271** in hand, protodemethylation, enantioselective reduction and acetal formation would provide **272** for oxidative coupling to **273**.



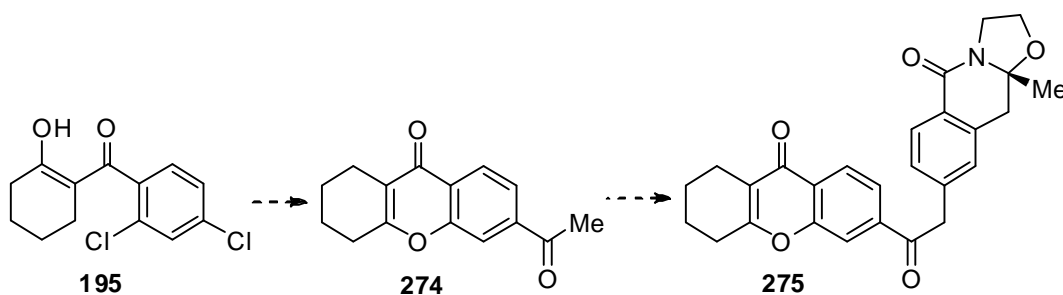
Scheme 3.34: Possible route to F-H rings of the kigamicins

To achieve this synthesis, there are two main challenges to overcome. The chiral centre in **271**; this is controlled by Hosokawa using the enantiomerically pure reagent **267**, however, a much simpler substrate, not incorporating a chiral centre, would be required in our synthesis. Achieving high enantioselectivity in this reaction will need to be investigated. Selective protodemethylation of **271** could also be problematic as there are two methyl ethers adjacent to carbonyl moieties.

Complete protodemethylation could be carried out on this substrate as an alternative.

This would provide complex analogues for biological screening but would also pave the way for total synthesis of the natural product.

In this Chapter, one of the key steps is the high yielding palladium catalysed arylation of ketone **232**. In order to combine the work here with the tandem catalysis developed in Chapter Two, a one-pot reaction involving both palladium catalysed THX formation and arylation should be attempted (Scheme 3.35). If successful, it could be possible to combine the THX A-C rings with the F-H rings of the natural product (Figure 3.35).



Scheme 3.35: Tandem catalysis involving THX formation and arylation

Further elaboration of the C ring followed by the steps described in Scheme 3.34 would allow for total synthesis of the A-H rings of the natural product.

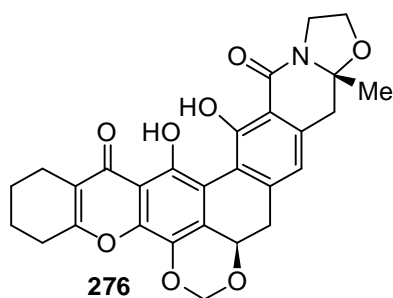


Figure 3.4: Kigamicin A-H rings

Chapter 4:

Biological Assays and

Development of Analogue SAR

4.1 Introduction

As described in Chapter 1, the kigamicins have shown cytotoxicity against the pancreatic cancer cell line PANC-1.⁵¹ Importantly, the natural product also shows selectivity, exhibiting a higher potency under nutrient deprived conditions in comparison to nutrient rich conditions. This is key, as this mimics the austere environment in which cancer cells survive in comparison to the nutrient rich conditions of the environment of healthy cells. Significantly, this selectivity is reversed in known chemotherapeutics with a reduced cytotoxic effect shown under austere conditions, as described in more detail in Chapter One. In this chapter, we report our own work to verify these findings for the natural product and the fuller testing of all the analogues produced in Chapter Two, in these assays.

4.2 Attempted Isolation of Kigamicin D

For the biological assays it was essential to have an authentic sample of kigamicin D for use as a positive control. This compound is not commercially available so we initially attempted to re-isolate the natural product from one of the producing bacterial strains.

The *Amycolatopsis* ML630-mF1 bacteria used by Kunimoto *et al*⁵¹ to isolate the kigamicins are not commercially available but there is a more recent report by Tan *et al*, suggesting that a different strain of bacteria, namely *Amycolatopsis regifaucium* sp. nov. also produces the kigamicins.¹⁹⁵ This bacteria is commercially available and was purchased from Leibniz Institute DSMZ¹¹¹ to establish if appreciable quantities of kigamicin D could be isolated using it.

Initial studies focused on the growth of the bacteria on two different types of agar to observe on which it grew more rapidly. It was inoculated onto GYM (glucose, yeast, malt) Streptomyces medium and GPHF medium. Successful growth was observed on both growth media but the bacteria grew faster on the GYM Streptomyces medium so this agar was selected for further studies.

The bacteria were inoculated from the agar into a liquid seed culture medium as described in the experimental section. After three days, this culture was used to inoculate the production medium. This was cultured for a further five days and subjected to centrifugation followed by an aqueous work up of the resulting supernatant.

Samples before and after inoculation and during the culture period were compared by TLC and LCMS analysis. No product was detected. The crude material from the broth extraction was analysed by HPLC and preparative TLC. No product was detected or isolated by either method but this could have been due to limited material.

This prompted us to scale up the bacteria culture ten fold in order to obtain further material for analysis. The UV absorbance showed a broad absorbance at 390 nm. For kigamicin D, the absorbance is reported to be 384 nm with the other kigamicin compounds absorbing at similar wavelengths. ¹H NMR spectroscopy showed many peaks, some of which could have corresponded to the natural product but nothing was conclusive. There were twelve components isolated by preparative TLC and despite obtaining a considerable quantity of mass spectrometry data using LCMS and MALDI-TOF methods, no mass ion corresponding to the natural product or

aglycone were observed. We concluded that the bacteria did not produce the kigamicins under our conditions. To make progress, we elected to purchase kigamicin C from Enzo Life Sciences. (£192 / 0.5 mg, Nov 2012) due to the almost identical biological activity reported compared with kigamicin D.⁵¹

4.3 Biological Assays

4.3.1 Introduction and assay development

In order for biological data to be obtained, we worked in collaboration with Dr Jackie Whatmore at the Peninsula Medical School in Exeter. With their experience and facilities for tissue culturing, I spent time here setting up our own anti-austerity assays to screen our compounds.

In 2000, Esumi *et al*⁴⁶ reported the high level of tolerance of PANC-1 cells to austere conditions. In this work, they incubated PANC-1 cells in Dulbecco's modified Eagles medium (DMEM) and nutrient deprived media (NDM) and used the trypan blue exclusion method to determine cell viability. In 2003, Kunimoto *et al*⁵¹ reported the isolation, physico-chemical properties and biological activity of the kigamicins and in 2004, Lu *et al*⁴⁷ described this biological activity in more detail. In both reports, the anti-austerity effect of the kigamicins was determined following the procedures and NDM composition described by Esumi,⁴⁶ but cell viability was measured using WST (water soluble tetrazolium) colourimetric assays. We tried to follow both methods as closely as possible in this work.

Commercially sourced PANC-1 cells were maintained in Dulbecco's modified Eagle's medium (DMEM) supplemented with foetal bovine serum, glutamine and gentamicin according to the experimental procedure in Chapter 5. These cells were

adherent, growing attached to the bottom of the plastic flask used to culture them. To feed the cells, the media was simply removed every 2-3 days and replaced with fresh media. When approximately 80% confluence was reached (when approximately 80% of the surface area on the base of the flask was covered with cells), the cells were passaged by trypsinisation. In order to passage the cells (divide them into new flasks to provide them more space to grow), the media was removed and the cells washed using PBS (phosphate buffered saline) warmed to 37 °C. The PBS was removed and the cells were treated with 1 mL trypsin solution (0.2 mg/mL) which is an enzyme used to detach the cells from the flask. After 5 min incubation at 37 °C under 5% CO₂/ 95% air atmosphere, the bottom of the flask was gently tapped to encourage detachment. DMEM (10 mL) was then added to neutralise the trypsin and the cell suspension was centrifuged at 200 g for 5 min. The media/trypsin mixture was removed and the cell pellet was resuspended in 10 mL fresh media before dividing between new flasks.

Each flask of cells was checked on a daily basis for levels of confluency and also for signs of infection or contamination.

4.3.2 Trypan blue assay

At the outset, it was important to test kigamicin C against the PANC-1 cell line and to obtain results comparable to those published in the literature.^{47,51} This would validate the published biological activity of kigamicin C in both DMEM and NDM and confirm the variability of the assay in our laboratory. Kigamicin C could then be used as a positive control and direct comparisons could be made between its potency/selectivity and those of the analogues synthesised.

It was decided that the first experiments would utilise the trypan blue exclusion method following the original work by Esumi.⁴⁶ Trypan blue is a diazo dye (Figure 4.1)¹⁹⁶ which the cells can be treated with. Live cells with viable cell membranes will not allow the dye to pass through the membrane. However, the cell membranes of dead cells are no longer viable and intact and therefore the dye can easily pass into the cells and stain them blue. Under the microscope, it is then obvious as to which cells are alive and which are dead. This can be quantitatively measured by counting the cells using a haemocytometer.

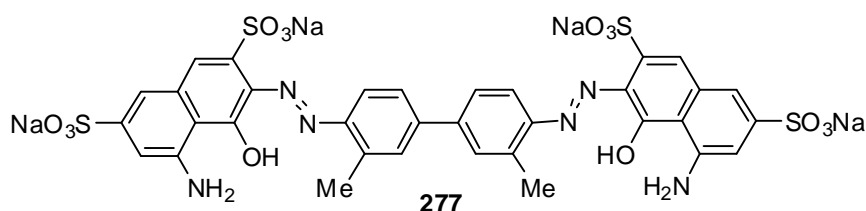


Figure 4.1: Trypan Blue Dye¹⁹⁶

We wished to measure the levels of PANC-1 cell death at various concentrations of kigamicin C, in both DMEM and NDM with control experiments using just DMSO in NDM at the same concentrations. DMSO was used to dissolve kigamicin C and all the other analogues tested hence it was important to establish that at the concentrations tested, it was having no detrimental effect to the cells and any effects observed were directly due to kigamicin C. Interestingly, this control experiment was seemingly not carried out by Lu⁴⁷ or Kunimoto.⁵¹

Initially cells were seeded into a 6 well plate and incubated at 37 °C under a 5% CO₂ / 95% air atmosphere. Once confluency was reached, the cells were treated with kigamicin C at 0 µg/mL, 0.01 µg/mL, 0.1 µg/mL, 1.0 µg/mL and 10.0 µg/mL in DMEM and separately NDM with a control experiment of DMSO in NDM also at the same concentrations. The cells were then incubated for 24 h before

trypsinising and staining with trypan blue dye. Counting both live and dead cells under the microscope allowed percentage cell death to be calculated for each different condition.

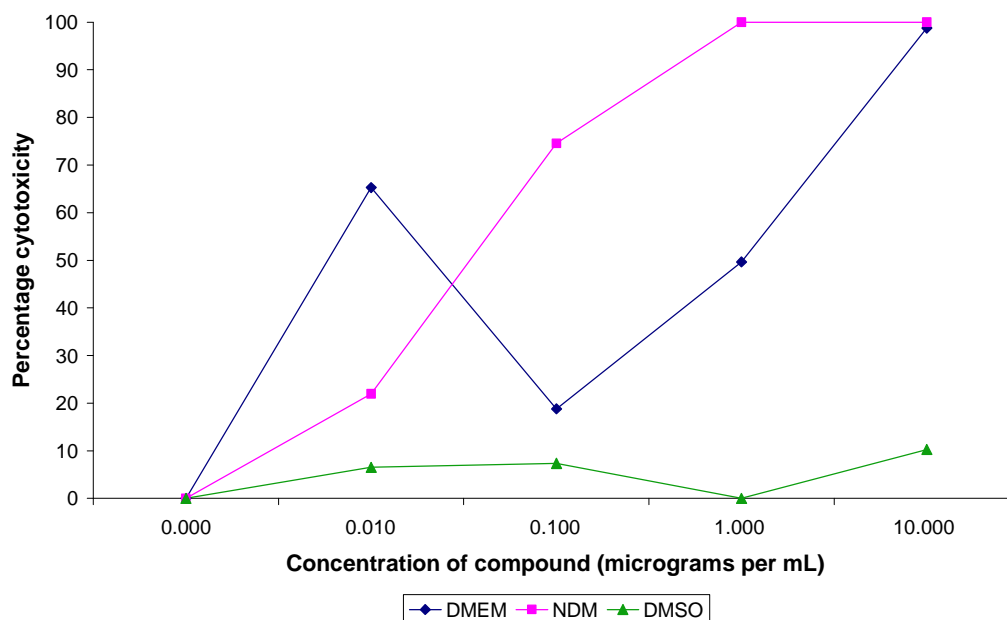
Although the trypan blue exclusion method is a very simple method and our results clearly revealed cell death induced by kigamicin C, it is very labour intensive and time consuming due to the manual cell counting of every well in each plate. The experiment was therefore only carried out in duplicate and no statistical analysis could be carried out. The results obtained were plotted and the IC₅₀ values measured from this (Table 4.1). There is considerable opportunity for human error as is reflected by the anomalous result at 0.01 µg/mL in DMEM (Graph 4.1). Having said this, the overall results clearly showed the expected trend both qualitatively and quantitatively which matched the literature data (Graph 4.1 and Table 4.1).

Media	IC ₅₀ Measured (µM)	Literature IC ₅₀ (µM)
DMEM	1.31	1.24
NDM	0.07	0.012

Table 4.1: Comparison with literature values^{51,57}

The plates containing DMEM with various concentrations of kigamicin C showed that at very low concentrations, the cells survived but at higher concentrations, the cells died with only 1% cell survival at 10 µg/mL. In the NDM, the same trend was observed but lower concentrations of the kigamicin C killed the cells and with no cell survival at only 1 µg/mL. At 0.1 µg/mL there was only 25% cell survival. This assay shows that the cells are more susceptible to kigamicin C under nutrient deprived conditions. The control experiment carried out with increasing

concentrations of DMSO alone, showed that even at the highest concentration used in the experiment, the cells survived, showing that at these concentrations DMSO was not toxic.



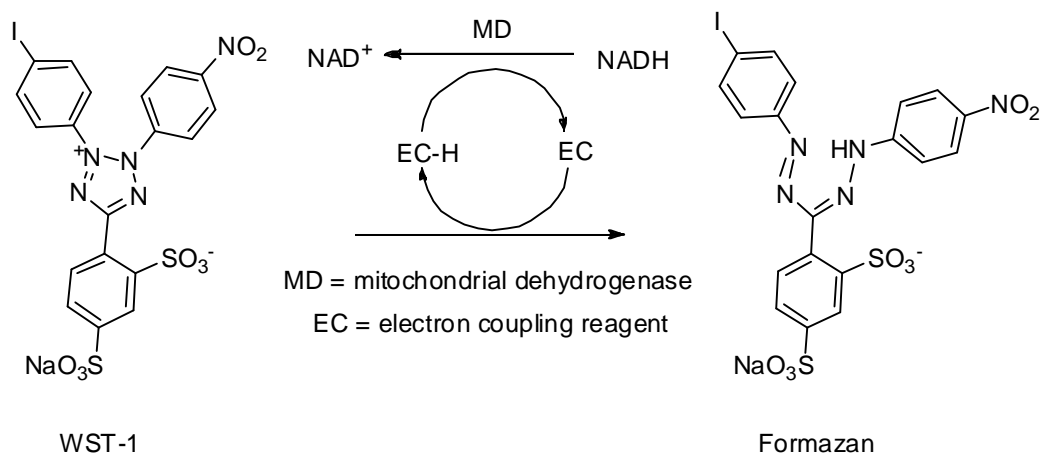
Graph 4.1: Cytotoxicity of kigamicin C on PANC-1 cells

4.3.3 WST-1 colourimetric assay

The trypan blue exclusion method is not suitable for high throughput work because it is too labour intensive. We required a method that would allow for analogues to be rapidly tested and all experiments to be carried out at least in triplicate.

It was decided to repeat the experiment using a WST-1 cell death assay as described by Kunimoto.⁵¹ WST-1 is a tetrazolium salt which can be converted to formazan by living cells. Metabolically active cells can oxidise NADH to NAD⁺ which in turn reduces WST-1 to formazan (Scheme 4.1).¹⁹⁷ Increase in the production of formazan dye is therefore directly linked to the number of viable cells present in each well of the plate. WST-1 reagent is pale red and formazan a dark red so the

absorbance can be measured to determine how much formazan has been produced using an ELISA microplate reader at 490 nm.



Scheme 4.1: Conversion of WST-1 reagent to formazan by living cells¹⁹⁷

Despite there being an abundance of other available and widely used assays, the WST-1 assay has the advantage that the formazan compound produced is water soluble and therefore dissolves in the culture media. In contrast, other assays such as MTT¹⁹⁸ involve additional steps in the assay where the crystals formed must be redissolved in DMSO for analysis. The WST-1 assay avoids these additional steps which reduces the time required for the assay and also avoids additional sources of error.

In this assay, the cells were seeded in a 96 well plate at 1×10^4 cells and 100 μ L medium per well and incubated at 37 °C under a 5% CO₂ / 95% air atmosphere for 24 h. In order to establish number of cells per well, the cells were trypsinised from the flask they were grown in, centrifuged and resuspended in 10 mL of medium. A small aliquot of cell suspension was further diluted (100 μ L of cell suspension added to 100 μ L of medium) before counting cells using a haemocytometer. Once

the concentration of cells per mL was known, the dilution factor could be calculated based on total number of cells and total volume of medium required.

After 24 h incubation, the DMEM was removed and each well was washed with 100 μ L PBS and this was then also removed. As with the trypan blue exclusion method, serial dilutions of kigamicin C were prepared at 0 μ g/mL, 0.001 μ g/mL, 0.01 μ g/mL, 0.1 μ g/mL, 1.0 μ g/mL and 10.0 μ g/mL in both DMEM and NDM. The cells were treated with these concentrations and each condition run in quadruplicate. After 24 h incubation at 37 °C under a 5% CO₂ / 95% air atmosphere, the WST-1 reagent was added. After 1 h incubation, the absorbance of the wells was read using the ELISA microplate reader and the results recorded.

Initial results showed the expected trend from the wells with DMEM and kigamicin but results from all the wells containing NDM showed no difference in absorbance between the control (with no kigamicin C) and the wells containing the kigamicin C. This implies that none of the cells in any of the wells were metabolising WST-1 to formazan which implies 100% cell death in all wells including the controls. There is literature suggesting that the cells should survive up to 72 h in NDM ⁴⁶ with no cell death at all after just 24 h and this is what we had observed and measured using the trypan blue exclusion method. Under the microscope it appeared that the cells with no kigamicin were alive even though the assay suggested they were not metabolising the WST-1 reagent. Although this is a qualitative observation, it was obvious that there wasn't 100% cell death as the results indicated.

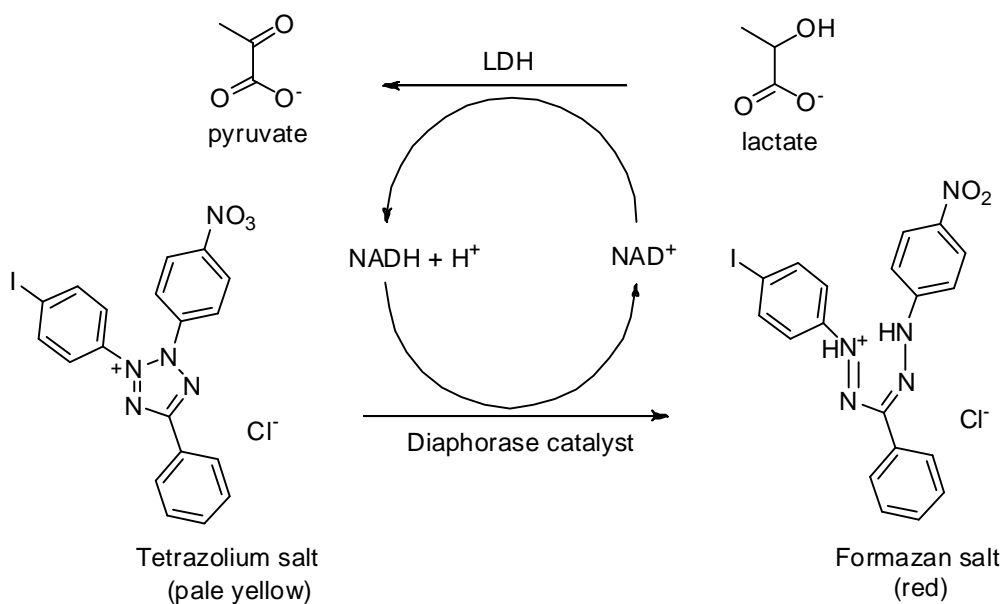
After 24 h starvation it was possible that the cells were just metabolising very slowly. The experiment was repeated but the same results were obtained. Cells were then seeded at 2×10^4 cells per well and 3×10^4 cells per well, in case there weren't enough cells per well to metabolise the reagent to a significant level to be observed. Fresh NDM medium was prepared and sterile filtered, different volumes (10 μ L, 20 μ L, 50 μ L and 100 μ L) of WST-1 reagent were added and different incubation periods were allowed both with the kigamicin (16 h and 24 h) and also with the WST-1 reagent (1 h, 2 h, 3 h and 4 h) but there was no change in the results. Another explanation for the results could be that the reagent wasn't compatible with the NDM. There is literature to suggest that in some cases, the inhibition of the WST-1 reagent has been observed despite metabolically active cells present.¹⁹⁹ After many attempts to modify the procedure, it was decided to purchase a different cytotoxicity detection kit.

4.3.4 Lactate dehydrogenase assay

Due to the problems encountered using the WST-1 cell assay, we sought a cell death assay that would not be reliant upon metabolism of a reagent by the cells or on such sensitive assay reagents. It was therefore decided that the lactate dehydrogenase cell death assay²⁰⁰ would be appropriate for our requirements. This assay has been reported for the determination of cell viability previously in an anti-austerity assay for PANC-1 cells,⁴⁸ however, it has not been used previously to determine the biological activity of the kigamicins.

Lactate dehydrogenase is a soluble enzyme present in the cytoplasm of normal cells. As previously explained, when a cell dies, the cell membrane loses its integrity. In this case, the lactate dehydrogenase present in the cell can leak out of

the cell cytoplasm and into the media surrounding the cell.²⁰¹ By adding lactate to the media, any lactate dehydrogenase present will oxidise the lactate to pyruvate. This will initiate the reduction of NAD^+ to $\text{NADH} + \text{H}^+$. In the presence of added diaphorase catalyst, the H^+ generated and hydride from the NADH is transferred to the tetrazolium salt thus reducing it to the formazan salt (Scheme 4.2).²⁰²



Scheme 4.2: Mechanism of reaction induced using LDH reagent²⁰²

The tetrazolium is a very pale yellow and the formazan salt is a dark red and so it is very easy to observe in which wells of the plate there is the most lactate dehydrogenase present. Not only is the change observed qualitatively but it can also be measured quantitatively using an ELISA microplate reader. Given that there is a direct link between concentration of lactate dehydrogenase in the media and cell death, the absorbance measured can be used to determine the percentage cytotoxicity of each well of a given plate.

Initial studies again focused on use of kigamicin C in both DMEM and NDM at various concentrations alongside a control containing DMSO in NDM at the same concentrations. Cells were seeded at 3×10^4 cells per well in a 96 well plate in

DMEM, which was then incubated at 37 °C under a 5% CO₂ / 95% air atmosphere for 24 h. The DMEM was then removed and the cells were washed with PBS (warmed to 37 °C). The cells were then treated with serial dilutions of kigamicin C or DMSO. Kigamicin C was tested up to 10 µg/mL for a direct comparison to be made with the literature. However, we wished to test the analogues synthesised up to a concentration of 100 µg/mL and therefore the DMSO control experiment was also carried out at this concentration.

Blank controls (containing only media), low controls (containing untreated cells) and high controls (containing lysed cells to determine maximum cellular LDH levels) were all included in the plate. Each concentration was carried out in quadruplicate for this first study and each experiment was carried out on at least three separate occasions.

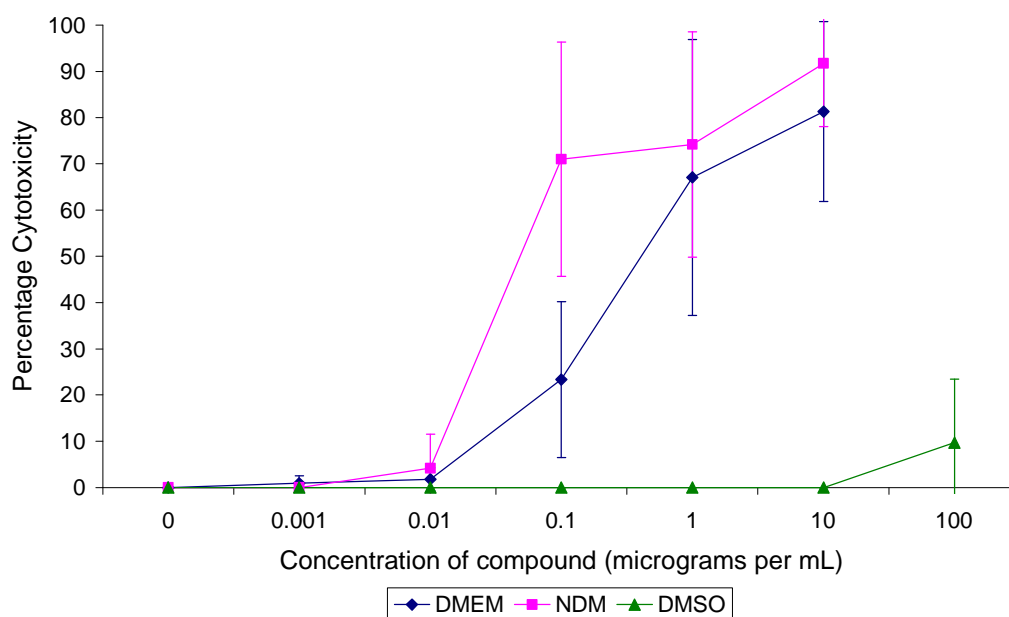
The plate was allowed to incubate for 24 h at 37 °C under a 5% CO₂ / 95% air atmosphere. At this point, the plate was centrifuged in order for any dead cells to be driven to the bottom of the plate and then 80 µL of supernatant was transferred to a new plate. This was to keep the assay cell free as there is potential for the cells to interfere with the absorbance measurements. The assay reagents as described in the experimental section were mixed immediately prior to use and 80 µL of the mixture was added per well of the plate. The plate was immediately covered to protect it from the light and allowed to stand at room temperature for 30 min. Meanwhile, the wells containing the untreated cells were lysed using a 2% (v/v) Triton X solution in DMEM or NDM as appropriate. After 5 min at room temperature, the plate was centrifuged and the supernatant mixed with the reagents as described above. This was used as the high control to ascertain the maximum cellular LDH levels. After

30 min incubation with the reagent, the absorbances of the wells were immediately read with the ELISA microplate reader and the results recorded. Percentage cytotoxicity could then be calculated for each compound according to the formula in Figure 4.2.

$$\frac{\text{Absorbance measured} - \text{Low control}}{\text{High control} - \text{Low control}} \times 100 = \text{Percentage Cytotoxicity}$$

Figure 4.2: Formula used to calculate percentage cytotoxicity

Once calculated, this data was plotted in a graph with error bars (Graph 4.2) and the IC₅₀ of kigamicin C was measured. This was compared with the potency values published for kigamicin C (Table 4.2).^{51,57}



Graph 4.2: Cytotoxicity of kigamicin C on PANC-1 cells

Media	IC ₅₀ Measured (µM)	Literature IC ₅₀ (µM)
DMEM	0.80	1.24
NDM	0.089	0.012

Table 4.2: Comparison with literature values^{51,57}

This shows that the results obtained in our assay are comparable to that of literature values which validates our assay and it could therefore be conducted in the same way for the analogues synthesised.

4.4 Assay Results for Kigamicin Analogues

4.4.1 Introduction

With the assay running successfully, the analogues could then be tested for cytotoxicity against the PANC-1 cell line.

Each plate was set out similarly to the initial kigamicin screen but with a row for a higher concentration (100 µg/mL) of compound to be added. Each plate could contain two different analogues to be tested, one in each half of the plate. The plates contained the same blank, low and high controls and the assay was carried out as described previously. Each condition was assayed in triplicate and each experiment was carried out on at least three separate occasions.

4.4.2 Results for the first generation analogues

The percentage cytotoxicity for each condition was calculated and the results compiled for each analogue in DMEM and NDM. The results of any active compounds can be seen in graphs in Appendix II. The trends observed from the graphs are described herein.

Compounds **118**, **120**, **110** and **108** showed no cytotoxicity at any concentration up to 100 µg/mL in either DMEM or NDM (Figure 4.3).

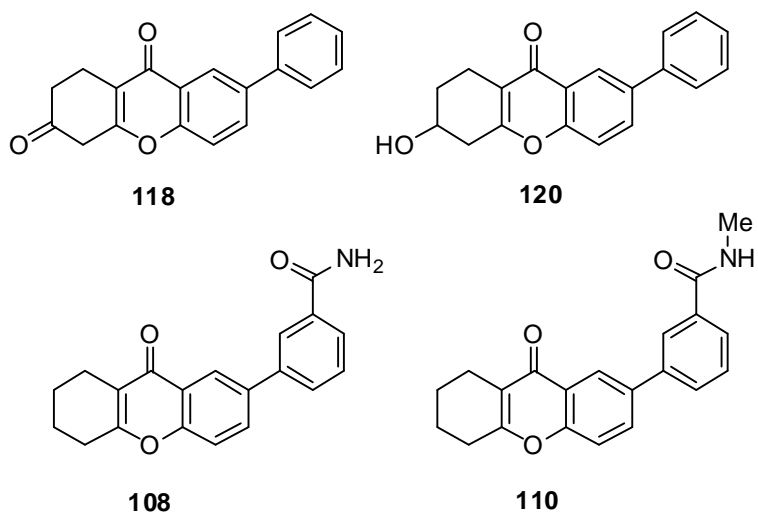


Figure 4.3: Inactive compounds

Compounds **123** and **105** showed no activity in DMEM at all and very weak potency (<50%) in NDM but only at the highest concentration of 100 $\mu\text{g/mL}$. Compound **107** showed very similar activity to that of **123** and **105** but with reversed selectivity showing weak potency in DMEM at 100 $\mu\text{g/mL}$.

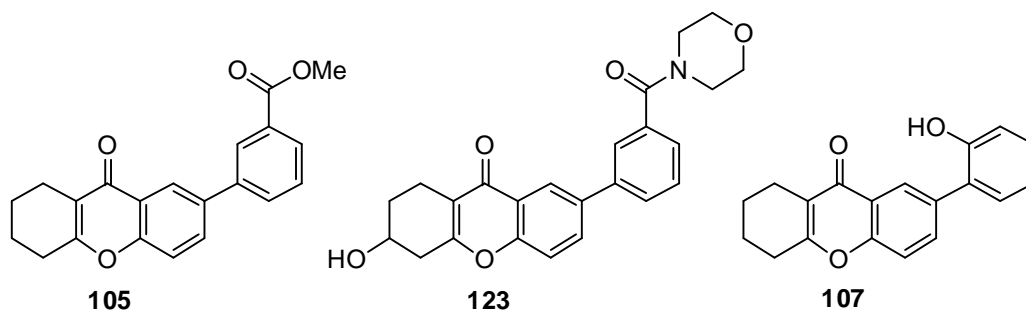


Figure 4.4: Compounds with very little activity

Compound **111** showed approximately 90% cytotoxicity at 100 $\mu\text{g/mL}$ in both NDM and DMEM indicating no selectivity between the two media despite the high cytotoxicity at the highest concentration. Compound **112** and **121** showed very similar activity, showing almost 100% cytotoxicity in NDM at 100 $\mu\text{g/mL}$. The selectivity of **121** was superior however with 27% cell death in DMEM whereas **112** showed 56% cell death in DMEM.

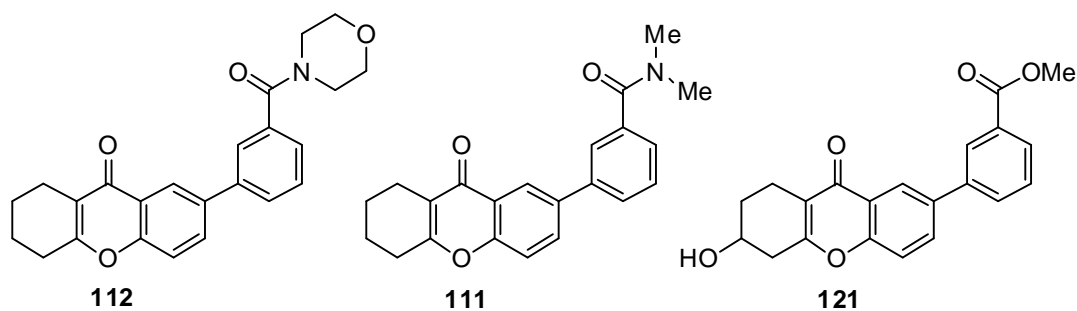


Figure 4.5: Compounds with high potency in NDM

Compound **119** showed 35% cytotoxicity at 10 $\mu\text{g/mL}$ in NDM with no toxic effects to cells in DMEM at the same concentration. However, curiously there appears to be no activity at 100 $\mu\text{g/mL}$ in either media. In some plates, crystals were observed under the microscope at 100 $\mu\text{g/mL}$ which could suggest that the compound precipitated at high concentrations when added to the aqueous media. This could explain the apparent loss of activity at 100 $\mu\text{g/mL}$.

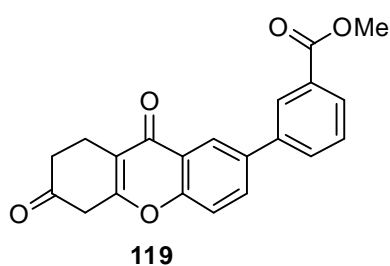


Figure 4.6: Compound 119

Despite being the simplest analogue, **103** showed more potency and selectivity than any of the other analogues screened and was the only compound other than the natural product to show significant activity at concentrations below 100 $\mu\text{g/mL}$.

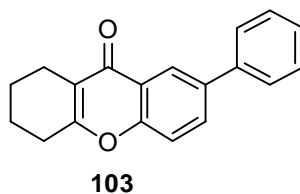
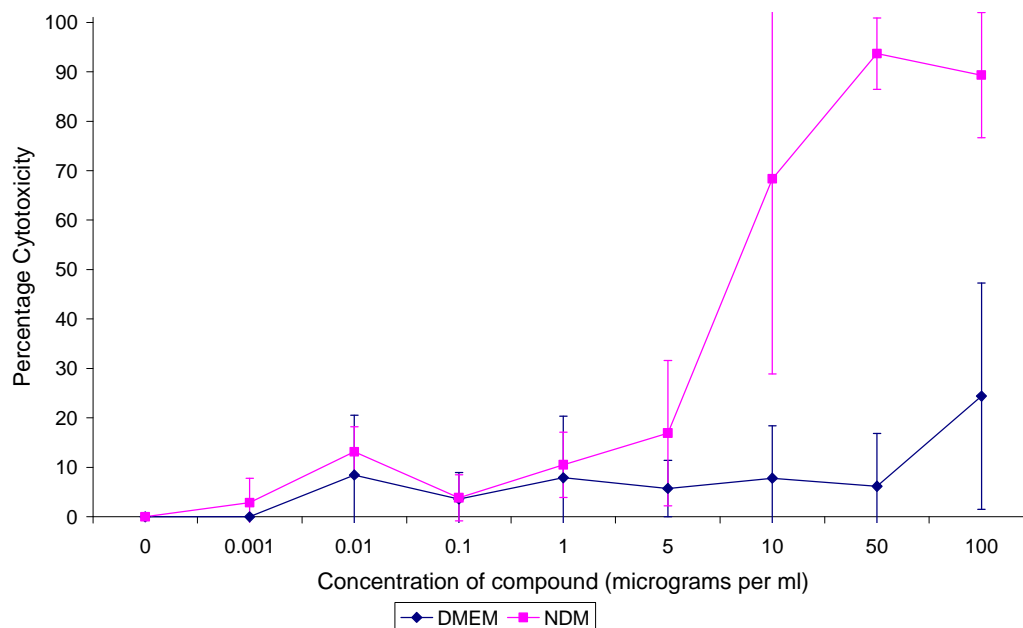


Figure 4.7: Most active analogue

There was 72% cell death at 10 $\mu\text{g/mL}$ in NDM with no significant cell death observed in DMEM at this concentration. Cytotoxic effects were only observed in DMEM at 100 $\mu\text{g/mL}$ and only 40% cell death was observed (see Appendix II for graph).

We decided to re-evaluate this compound at more concentrations, as there was a large increase in cell death between 1 $\mu\text{g/mL}$ and 10 $\mu\text{g/mL}$ in NDM and between 10 $\mu\text{g/mL}$ and 100 $\mu\text{g/mL}$ in DMEM. It was decided to screen this compound at 5 $\mu\text{g/mL}$ and 50 $\mu\text{g/mL}$ as well as the concentrations normally dosed. Pleasingly the results showed that there was 17% cytotoxicity at 5 $\mu\text{g/mL}$ and almost complete cell death at just 50 $\mu\text{g/mL}$ in NDM whereas in DMEM no cell death was observed until 100 $\mu\text{g/mL}$ (Graph 4.3).



Graph 4.3: Cytotoxicity of 103 on PANC-1 cells

From the graph, the IC₅₀ values in the different media could be calculated. For this compound, the IC₅₀ against PANC-1 cells in DMEM was >362 μM and 24 μM in NDM.

To our disappointment, there was no immediately obvious trend between the analogues to show which functional groups were needed for biological activity. The more bulky tertiary amide groups were more active than the primary or secondary amides. When an ester moiety was incorporated, activity improved when a hydroxyl group was added to the saturated ring, however when the hydroxyl group was added in the same position on the analogues with the amide moiety, the potency was reduced.

The IC₅₀ values of the most potent analogue (**103**) and three other analogues showing activity against the PANC-1 cells were compared to the natural product (Table 4.3).

Compound	IC ₅₀ in DMEM (μM) ^a	IC ₅₀ in NDM (μM) ^a	Selectivity ^b
Kigamicin C (RMM = 809)	0.8	0.089	9.0
103 (RMM = 276)	>362	24	>15.1
121 (RMM = 350)	>286	155	>1.8
112 (RMM = 389)	229	121	1.9
111 (RMM = 347)	174	157	1.1

^a estimated from concentration plots. ^b IC₅₀ in DMEM / IC₅₀ in NDM

Table 4.3: PANC-1 cell cytotoxicity data for the most active compounds

As is clear from Table 4.3, the analogues synthesised show somewhat reduced potency compared to the natural product. Even the most potent analogue identified is 300 fold less potent. However, encouragingly **103** shows greater selectivity than that of kigamicin C between cells grown in DMEM and those subjected to more austere growing conditions.

4.4.3 Results for the second generation analogues

A selection of quite simple analogues were tested in the second screen as **103** was shown from the first screen to be the most active. The analogues included those with a ring expanded and contracted saturated ring of the THX, a 7-aryl xanthone and also analogues with a naphthalene, acetal or methyl substituents resulting from the one-pot methodology developed as described in Chapter Two (Figure 4.8). Analogues **278**, **186**, **279** and **188** were synthesised by Ellanna Griffin.

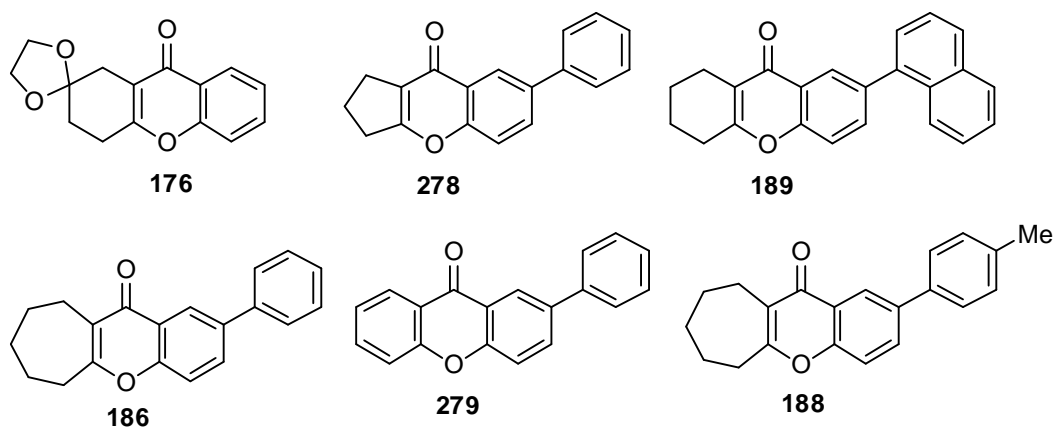


Figure 4.8: Analogues for screening

Analogues synthesised by another group member, Samiullah, were also screened. These all contained modifications to the saturated ring of the THX (Figure 4.9). It was hoped they would provide an insight into the role of the hydroxyl and sugar

moieties surrounding the saturated ring and whether they formed part of the pharmacophore of the natural product.

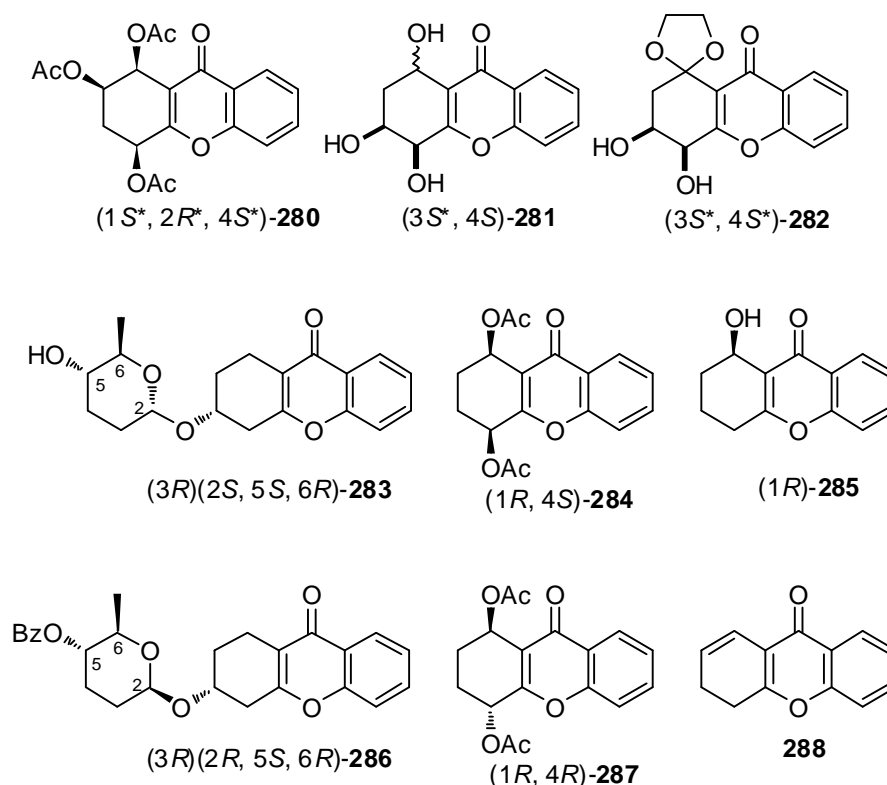


Figure 4.9: Samiullah's analogues

As with the screening of the first generation of analogues, the assay was validated using a positive control. On this occasion, due to limited material, kigamicin C was rechecked against **103**, then **103** was used as the positive control in the remaining assays.

For this screen, the analogues were tested at four concentrations instead of the seven concentrations used in the first screen. This was to enable a higher throughput of samples. Any compounds showing good activity and/or selectivity could be retested but inactive compounds could be immediately eliminated from further testing. The compounds were therefore tested at 0 µg/mL, 0.01 µg/mL, 1.0 µg/mL, 100.0 µg/mL. The assay itself was carried out as previously described.

From the analogues shown in Figure 4.8, **189** and **176** showed no activity in either DMEM or NDM at all. Compound **279**, however, showed quite high potency at the highest concentration. Despite this, there was very little selectivity shown between the types of media used. In contrast, **186** and **278** both showed good selectivity but the potency was poor with less than 40% cell death observed in both cases in DMEM at 100 $\mu\text{g/mL}$. **188** showed less than 20% cytotoxicity and no selectivity.

Disappointingly, the majority of the analogues synthesised by Samiullah were also inactive. Compounds **282** and **284** were both selective and showed no activity at all in DMEM (Figure 4.10). In NDM, both displayed weak potency at the highest concentration dosed (100.0 $\mu\text{g/mL}$) but not exceeding 40% cytotoxicity.

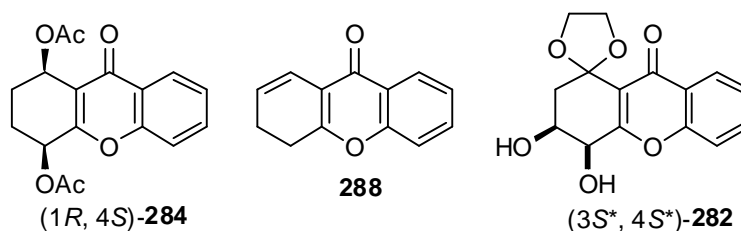


Figure 4.10: Compounds with activity

The only other analogue that showed any activity was **288** (Figure 4.10). Despite this compound showing only weak activity at 100 $\mu\text{g/mL}$, due to excess material available, it was possible to screen it at a very high concentration (1 mg/mL) in addition to the standard concentrations screened. At 1 mg/mL, it caused 85% cell death in NDM and only 22% cell death in DMEM. Clearly this compound is not very potent but exhibits some selectivity.

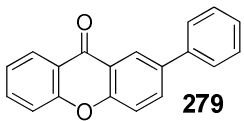
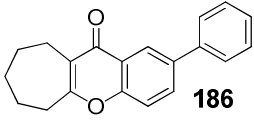
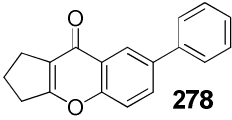
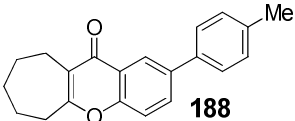
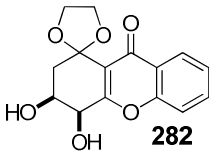
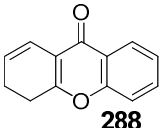
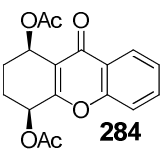
Compound tested	% Cytotoxicity at 100 µg/mL	
	In DMEM	In NDM
 279	49	65
 186	0	35
 278	0	14
 188	16	16
 282	0	10
 288	1	29
 284	2	36

Table 4.4: Most active second generation analogues

4.5 Kibdelone C and Analogues

The kibdelone natural products as described in Chapter One, are very similar in structure to the kigamicins.⁹⁰ In 2011, Porco and coworkers⁹³ reported their work on the synthesis and biological evaluation of the ABCD ring fragments of the kibdelones. This was later followed by the realisation of the total synthesis of kibdelone C by the same group.⁹¹ The ABCD ring fragments **60** and **61** (Figure 4.11) were screened in the NCI 60 human tumour cell line screen²⁰³ and were found to have GI₅₀ values of 4.5 µM compared to kibdelone C which they found to be 100

fold more potent at 2.4 nM. They concluded that the anti-cancer potency must lie in part in the THX portion of the natural product not found in their analogues. We were intrigued to find out what potency the kibelones and ABCD fragments would exhibit in our assay using the PANC-1 cell line as they have not been previously screened in an anti-austerity assay.

We sought to establish a collaboration with the Porco group in order that we might be able to obtain a sample of these compounds to screen in our assay. We were successful and were kindly provided with a small sample of **41**, **289**, **60** and **61** (Figure 4.11).

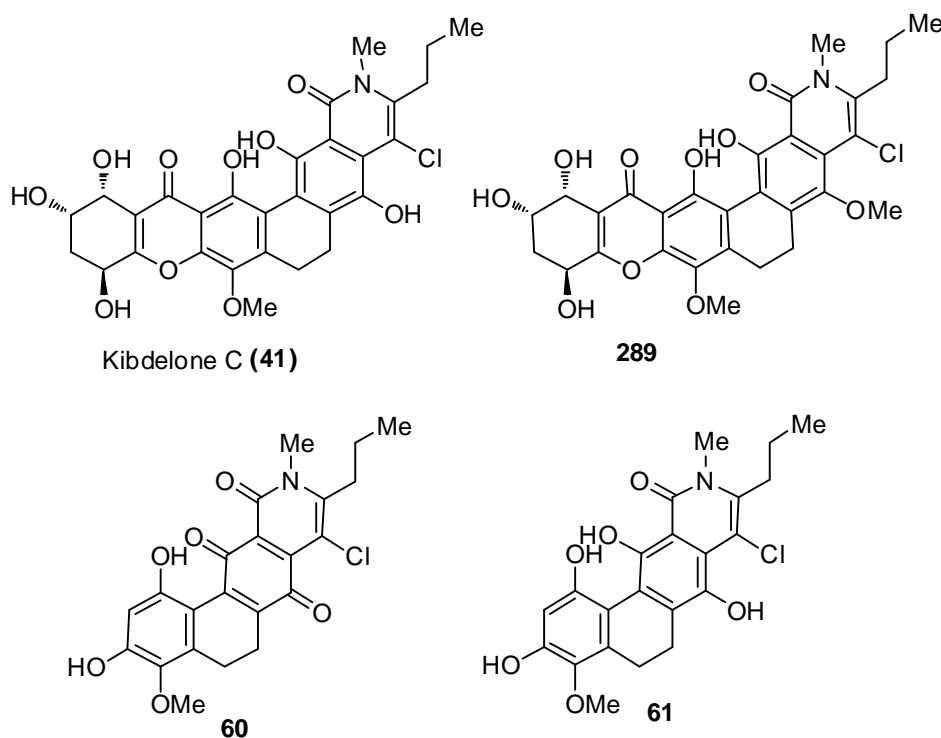


Figure 4.11: Kibdelone C related compounds

We tested these compounds in parallel with the analogues in the second compound screen against the PANC-1 cell line. These compounds were anticipated to have high potency and they were screened at all seven concentrations at the first pass.

The results are summarised in graph form (Appendix II) and in Table 4.5 showing the comparison with kigamicin C and our most potent synthetic analogue of the kigamicins.

The ABCD quinone and hydroquinone (**60** and **61**) both showed very similar results with no activity at 1 µg/mL in either media. At 10 µg/mL there was greater than 50% cell death in NDM for both compounds with very little if any activity in the DMEM. At 100 µg/mL there was complete cell death in NDM.

Kibdelone C and methyl ether analogue **289** of this natural product both exhibited much higher potency than that of the smaller analogues lacking the THX moiety. Cell death could be observed from 0.1 µg/mL in NDM when cells were dosed with **289** and from as low as 0.01 µg/mL in NDM when treated with kibdelone C (**41**) itself. Compound **289** exhibited greater selectivity than the natural product only achieving 51% cell death in DMEM at the maximum concentration whereas 100% cell death was reached at 10 µg/mL in DMEM with kibdelone C.

Compound	IC ₅₀ (µM) ^a		Selectivity ^b
	DMEM	NDM	
Kigamicin C (RMM = 809)	0.8	0.089	9.0
103 (RMM = 276)	>362	24	>15.1
Kibdelone C (RMM = 585.5)	6.7	0.69	9.7
289 (RMM = 600.5)	160	1.45	110.3
60 (RMM = 429.5)	142	16	8.9
61 (RMM = 431.5)	218	20	10.9

^a estimated from concentration plots ^b IC₅₀ in DMEM / IC₅₀ in NDM

Table 4.5: Comparing Kigamicin and Kibdelone analogues

The results show that the most potent compound against the PANC-1 cell line is kigamicin C although **289** exhibits excellent selectivity and good potency.

4.6 Conclusions and Future Work

In this chapter, we have discussed the attempted isolation of kigamicin C from *Amycolatopsis regifaucium* strain of bacteria. This involved the culture of this bacteria and extraction from the culture broth. Despite using different analytical techniques, no evidence for the production of the kigamicins could be obtained.

The PANC-1 cell line was utilised to test the potency of the analogues and the natural product itself. The trypan blue exclusion method was used to show the effect of kigamicin C on pancreatic cancer cells under normal conditions and also those of nutrient deprivation. It was found that these results were very similar to those already published for the natural product.⁵¹ However, this assay was not suitable for high throughput screening and therefore was not further investigated.

The WST-1 cell death assay was undertaken in accordance with earlier work by Kunimoto⁵¹ in this field. Despite obtaining results analogous to those found with the trypan blue exclusion method in DMEM, the assay failed to provide any reliable results when tested in NDM and this assay method was thus abandoned.

The LDH assay was successfully implemented for the screening of kigamicin C. The results showed that the data matched that of the trypan blue exclusion method and also correlated with potencies previously reported.⁵¹ This assay was then utilised to screen a further twelve analogues made in Chapter 2, or provided by coworkers.

There were mixed results from the assay with THX analogues exhibiting varying potencies and selectivities between the two media. The most potent analogue identified was **103**. This compound exhibited high cytotoxicity at 100µg/mL and in our hands, greater selectivity than the kigamicin C itself.

The second compound screen (fifteen compounds) was composed of some similar compounds but also those with substituents on the saturated ring of the THX. Disappointingly, none of the compounds showed better potency or selectivity than that of **103**.

Kibdelone C, **41**, the methyl ether analogue **289**, the ABCD quinone **60** and hydroquinone **61** were obtained from Porco and coworkers at Boston University. The cancer cells were also treated with these compounds and screened in our assay. The results showed for the first time that structurally related kibdelones are also active in anti-austerity assays.

From our work, we can conclude that some structures bearing the THX nucleus can display anti-austerity activity. However, the fact that small structural changes (eg. **103** to **120**) lead to a complete loss of activity, perhaps suggests that the situation is complex and that the THX nucleus per se is not responsible for activity. The fact that the ABCD fragments of kibdelone C (devoid of the THX) are active at similar levels of potency/selectivity supports this suggestion. Work to more fully address the origins of bioselectivity of the natural products is needed.

Other 7-arylated natural products (as described in Chapter One) should be procured if possible and screened in our assay to ascertain if these also exhibit anti-austerity

activity. Synthetic analogues of these compounds could be made in order to obtain more information about the pharmacophore of this family of compounds.

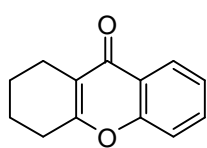
Kigamicin is known to inhibit the phosphorylation of Akt suggesting inhibition of the PI3K-Akt pathway as discussed in Chapter One. However the molecular target is not known. To further understand the activity of the analogues and indeed the kibdelones, it is vital to discover if they target the same pathway as the kigamicins. In order to do this Western-Blot analysis should be undertaken to observe if they also inhibit the phosphorylation of Akt. Flow cytometry should also be carried out to determine whether the analogues induce necrosis (as kigamicin) or apoptosis to cancer cells. This would give some indication that they have a similar mode of action. Although target pathway cannot be inferred from this information, if the analogues induce apoptotic cell death or if they do not inhibit phosphorylation of Akt, this would strongly suggest they are acting in a different way to the natural product.

Chapter 5:

Experimental

General Information

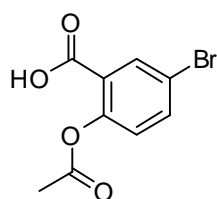
Anhydrous solvents were purchased in Sure/SealTM bottles from Sigma-Aldrich Co. All other solvents and reagents were used as received or purified by standard protocols. Petroleum ether refers to the fraction of petroleum ether having a boiling point between 40-60°C. All experiments were performed under an inert atmosphere in oven-dried or flame-dried glassware as required. Column chromatography was carried out using Matrex silica 60. Thin layer chromatography was performed on pre-coated aluminium-backed plates (Merck Kieselgel 60 F₂₅₄) and were visualised using UV light and staining with potassium permanganate or ceric ammonium molybdate followed by heating. Melting points were recorded on a Gallenkamp MPD350 apparatus and are reported as observed. Single crystal X-ray diffraction data were obtained using a Siemens SMART XRD system or an Oxford Diffraction Gemini XRD system. Optical rotations were measured with an AA1000 polarimeter and are quoted in 10⁻¹ deg cm² g⁻¹. Chiral HPLC was conducted using a Hewlett Packard 1050 Series machine using a chiral AD column (10% ⁱPrOH/*n*-hexane: 1.0 mL/min). Infrared spectra were recorded on a Perkin Elmer Paragon 1000 FT-IR Spectrometer with internal calibration and are given in cm⁻¹. ¹H and ¹³C NMR spectra were recorded at 300 MHz and 75 MHz respectively on a Bruker Spectrospin DPX300; at 400 MHz and 100 MHz respectively on a Bruker Spectrospin DPX400; at 500 MHz and 125 MHz respectively on a Bruker Spectrospin DPX500 and at 600 MHz and 150 MHz respectively on a Bruker Spectrospin DPX600. Chemical shifts are reported in ppm using TMS as the internal standard. Signals are reported as singlets (s), doublets (d), triplets (t) etc which refer to the spin-spin coupling patterns. Coupling constants are reported in Hertz. High resolution mass spectra were obtained using a Bruker ESI-Micro TOF instrument. Warwick Analytical Service carried out all elemental analysis.

1,2,3,4-Tetrahydro-xanthen-9-one (by acid catalysed dehydration) (83)

i Pr₂NH (0.45 mL, 5.0 mmol) and *n*-BuLi (1.6 M in hexane) (3.1 mL, 5.0 mmol) were added to THF (10 mL) at -78 °C under nitrogen. The solution was allowed to stir for 5 min before addition of cyclohexanone (0.53 mL, 5.0 mmol). The solution was stirred at -78 °C for 2 h. Acetylsalicyloyl chloride (1.02 g, 5.0 mmol) was dissolved in THF (10 mL) and added to the reaction mixture which continued to stir at -78 °C for 5 h before allowing to warm to room temperature overnight. The solvent was removed *in vacuo* and the residue treated with a saturated aqueous solution of NH₄Cl (20 mL). The aqueous phase was extracted with toluene (3 x 30 mL), washed with brine (2 x 20 mL), dried (MgSO₄), filtered and the solvent removed *in vacuo*. The brown oily residue was then treated with HCl: AcOH 1:20 (3 mL mmol⁻¹) and heated to 60 °C for 1 h. The mixture was allowed to cool to room temperature and poured over ice (15 g). The aqueous phase was extracted with toluene (3 x 30 mL), washed with a saturated aqueous solution of NaHCO₃ (30 mL), dried (MgSO₄), filtered and the solvent removed *in vacuo* to give an orange oil which solidified on standing at room temperature. The crude material was purified by column chromatography eluting with 10% EtOAc in petroleum ether to give a white solid. Trituration with Et₂O provided the title compound as a white solid (226 mg, 22%). m.p. 104-105 °C (lit. m.p. 100-101 °C); R_f = 0.35 (10% EtOAc in petroleum ether); IR (film) 2946, 1619, 1607, 1462, 1408, 765 cm⁻¹; δ_H (400 MHz, CDCl₃) 8.20 (1H, d, *J* = 7.8, ArH), 7.60 (1H, t, *J* = 7.8, ArH), 7.41-7.31 (2H, m, ArH), 2.72-2.64 (2H, m, CH₂), 2.63-2.55 (2H, m, CH₂), 1.93-1.83 (2H, m, CH₂), 1.83-1.73 (2H, m, CH₂). δ_C (100 MHz, CDCl₃) 177.7 (C=O), 163.8 (=CCO), 155.9 (C, Ar), 132.9 (CH, Ar), 125.7 (CH, Ar), 124.4 (CH, Ar), 123.2 (C, Ar), 118.4 (=CO), 117.6 (CH, Ar), 28.2 (CH₂), 21.6 (CH₂), 21.5 (CH₂), 21.0 (CH₂); MS (ES⁺) *m/z* 223 [MNa⁺]; HRMS (ES⁺) calcd. for

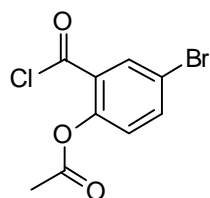
$C_{13}H_{12}NaO_2$ [MNa^+]: 223.0730; found: 223.0728. Anal. calcd. for $C_{13}H_{12}O_2$: C 77.98; H 6.04 %. Found C 77.68; H 6.03 %. Data is in accordance with literature values.^{109,204}

2-Acetoxy-5-bromobenzoic acid (**99**)



Acetic anhydride (1.6 mL, 16.6 mmol) and pyridine (80 μ l, 1.0 mmol) were added to a suspension of 5-bromosalicylic acid (2.0 g, 9.2 mmol) in acetic acid (18 mL). The mixture was stirred at room temperature for 18 h before filtering the resultant white precipitate (985 mg, 49%). m.p. 153-155 °C; IR (film) 2878, 1760, 1660, 1595, 1296, 866 cm^{-1} ; δ_H (400 MHz, $CDCl_3$) 10.91 (1H, s, OH), 7.76 (1H, dd, $J = 2.4, 8.6$, ArH), 8.27 (1H, d, $J = 2.4$, ArH), 7.06 (1H, d, $J = 8.6$, ArH), 2.37 (3H, s, CH_3); δ_C (100 MHz, $CDCl_3$) 169.4 (C=O), 168.5 (C=O), 150.3 (C, Ar), 137.8 (CH, Ar), 135.2 (CH, Ar), 125.8 (CH, Ar), 123.8 (C, Ar), 119.2 (C, Ar), 20.9 (CH_3); MS (ES^+) m/z 280 [MNa^+ , ^{79}Br], 282 [MNa^+ , ^{81}Br]; HRMS (ES^+) calcd. for $C_9H_7BrNaO_4$ [MNa^+ , ^{79}Br]: 280.9420; found: 280.9417. Data is in accordance with literature values.²⁰⁵

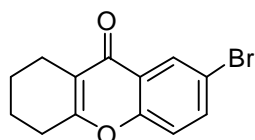
Acetic acid 4-bromo-2-chlorocarbonyl-phenyl ester (**100**)



Carboxylic acid **99** (10 g, 39 mmol) was treated with thionyl chloride (26.3 mL, 360 mmol) and heated to 70°C for 1 h. The mixture was allowed to cool to room temperature before removing excess thionyl chloride *in vacuo*. The resultant bright yellow solid was recrystallised from hexane to give the title compound as a pale yellow solid (9.49 g, 89%). m.p. 60-61 °C; IR (film) 1751, 1464, 1370, 1176, 882, 841, 747 cm^{-1} ; δ_H (400 MHz, $CDCl_3$) 8.32 (1H, d, $J = 2.3$, ArH), 7.78 (1H, dd, $J =$

2.3, 8.6, ArH), 7.06 (1H, d, $J = 8.6$, ArH), 2.35 (3H, s, CH₃); δ_C (100 MHz, CDCl₃) 169.5 (C=O), 168.7 (C=O), 150.4 (C, Ar), 135.3 (CH, Ar), 126.1 (CH, Ar), 126.0 (CH, Ar), 123.9 (C, Ar), 119.3 (C, Ar), 21.1 (CH₃).

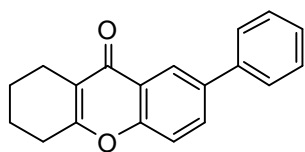
7-Bromo-1,2,3,4-tetrahydro-xanthen-9-one (102)



ⁱPr₂NH (4.5 mL, 32 mmol) and *n*-BuLi (1.6 M in hexane) (20.3 mL, 32 mmol) were added to THF (90 mL) at -78 °C under nitrogen. The solution was stirred at -78 °C for 5 min before addition of cyclohexanone (3.3 mL, 32 mmol). The solution was stirred at -78 °C for 1 h. Acid chloride **100** (9.0 g, 32 mmol) was dissolved in THF (90 mL) and added to the reaction mixture which continued to stir at -78 °C for 5 h before allowing to warm to room temperature overnight. The solvent was removed *in vacuo* and the residue treated with a saturated aqueous solution of NH₄Cl (200 mL). The product was extracted with toluene (2 x 200 mL), washed with brine (2 x 200 mL), dried (MgSO₄), filtered and the solvent removed *in vacuo*. The orange oily residue was then treated with HCl:AcOH 1:20 (3 mL/mmol) and heated to 60° C for 3 h. The mixture was allowed to cool to room temperature and poured over ice (150 g). The aqueous phase was extracted with toluene (2 x 200 mL), washed with a saturated aqueous solution of NaHCO₃ (200 mL), dried (MgSO₄) and filtered. The solvent was removed *in vacuo* to give an orange oil which solidified on standing at room temperature overnight. The crude material was recrystallised from MeOH to give the title compound as a pale orange solid (4.02 g, 44%). m.p. 150-151 °C; IR (film) 2940, 1627, 1602, 1435, 1304, 826, 648 cm⁻¹; δ_H (400 MHz, CDCl₃) 8.30 (1H, d, $J = 2.2$, ArH), 7.67 (1H, dd, $J = 2.2, 8.8$, ArH), 7.28 (1H, d, $J = 8.8$, ArH), 2.71-2.62 (2H, m, CH₂), 2.61-2.51 (2H, m, CH₂), 1.93-1.83 (2H, m, CH₂), 1.81-1.72 (2H, m, CH₂); δ_C (100 MHz, CDCl₃) 176.4 (C=O), 164.2 (=CCO), 154.7 (C, Ar),

135.9 (CH, Ar), 128.3 (CH, Ar), 124.5 (C, Ar), 119.6 (CH, Ar), 118.7 (C, Ar), 117.7 (=CO), 28.2 (CH₂), 21.8 (CH₂), 21.5 (CH₂), 21.0 (CH₂); MS (ES⁺) *m/z* 301 [MNa⁺, ⁷⁹Br], 303 [MNa⁺, ⁸¹Br]; HRMS (ES⁺) calcd. for C₁₃H₁₁BrNaO₂ [MNa⁺, ⁷⁹Br]: 300.9835; found: 300.9835. Anal. calcd. for C₁₃H₁₁O₂Br: C 55.94; H 3.97; Br 28.63 %. Found C 55.74; H 3.96; Br 28.79 %.

7-Phenyl-1,2,3,4-tetrahydro-xanthen-9-one (103)

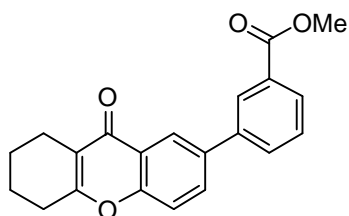


Pd(PPh₃)₄ (8 mg, 0.007 mmol) was added to a biphasic mixture of **102** (100 mg, 0.36 mmol) and phenylboronic acid (88 mg, 0.72 mmol) in ethanol (1.5 mL), toluene (1.5 mL) and 2M Na₂CO₃ (0.36 mL). Mixture subjected to microwave irradiation (300W) for 10 min at 110 °C. The solvent was removed *in vacuo* before adding H₂O (10 mL). The aqueous phase was extracted with EtOAc (10 mL) and washed with H₂O (10 mL) and brine (10 mL). The organic phase was dried (MgSO₄), filtered and solvent removed *in vacuo* to give a dark yellow oil. The crude material was purified using column chromatography eluting with 10% EtOAc in petroleum ether to give the title compound as a white solid (70 mg, 71%). m.p. 120-121 °C; R_f = 0.19 (10% EtOAc in petroleum ether); IR (film) 2934, 1640, 1608, 1471, 1149, 824, 764, 700, 610 cm⁻¹; δ_H (400 MHz, CDCl₃) 8.42 (1H, d, *J* = 2.3, ArH), 7.88 (1H, dd, *J* = 2.3, 8.7, ArH), 7.66 (2H, d, *J* = 7.5, ArH), 7.46 (3H, m, ArH), 7.37 (1H, t, *J* = 7.5, ArH), 2.74-2.66 (2H, m, CH₂), 2.65-2.56 (2H, m, CH₂), 1.94-1.84 (2H, m, CH₂), 1.83-1.74 (2H, m, CH₂); δ_C (100 MHz, CDCl₃) 177.8 (C=O), 163.9 (=C), 155.3 (C, Ar), 139.6 (C, Ar), 137.5 (C, Ar), 131.8 (CH, Ar), 128.9 (CH, Ar), 127.6 (CH, Ar), 127.2 (CH, Ar), 123.6 (CH, Ar), 123.3 (C, Ar), 118.5 (=C), 118.1 (CH, Ar), 28.2 (CH₂), 21.9 (CH₂), 21.7 (CH₂), 21.1 (CH₂); MS (ES⁺) *m/z* 299

[MNa⁺]; HRMS (ES⁺) calcd. for C₁₉H₁₆O₂ [MNa⁺]: 299.1043; found: 299.1053.

Anal. calcd. for C₁₉H₁₆NaO₂: C 82.58; H 5.84 %. Found: C 82.29; H 5.85 %.

3-(9-Oxo-5,7,8,9-tetrahydro-6H-xanthen-2-yl)benzoic acid methyl ester (**105**)



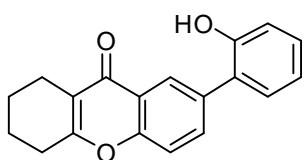
Pd(PPh₃)₄ (8 mg, 0.007 mmol) was added to a biphasic mixture of **102** (100 mg, 0.36 mmol) and 3-methoxycarbonylphenylboronic acid (196 mg, 1.07 mmol) in ethanol (1.5 mL), toluene (1.5 mL) and

2M Na₂CO₃ (0.36 mL). Mixture subjected to microwave irradiation (300W) for 10 min at 110 °C. The solvent was removed *in vacuo* before adding H₂O (5 mL). The aqueous phase was extracted with EtOAc (3 x 5 mL), washed with H₂O (5 mL) and brine (2 x 5 mL), dried (MgSO₄), filtered and solvent removed *in vacuo*. The crude material was purified using column chromatography eluting with 25% EtOAc in petroleum ether to give the title compound as a pale yellow solid (72 mg, 61%). m.p. 138-140 °C; R_f = 0.10 (20% EtOAc in petroleum ether); IR (film) 2941, 1711, 1636, 1610, 1299, 1239, 819, 764 cm⁻¹; δ_H (400 MHz, CDCl₃) 8.44 (1H, d, *J* = 2.0, ArH), 8.32 (1H, s, ArH), 8.04 (1H, d, *J* = 7.9, ArH), 7.86 (2H, dt, *J* = 2.0, 7.9, ArH), 7.53 (1H, t, *J* = 7.9, ArH), 7.47 (1H, d, *J* = 8.5, ArH), 3.95 (3H, s, OCH₃), 2.75-2.66 (2H, m, CH₂), 2.66-2.55 (2H, m, CH₂), 1.96-1.84 (2H, m, CH₂), 1.84-1.71 (2H, m, CH₂); δ_C (100 MHz, CDCl₃) 177.7 (C=O), 166.9 (C=O), 164.0 (=C), 155.6 (C, Ar), 139.9 (C, Ar), 136.4 (C, Ar), 131.8 (CH, Ar), 131.5 (CH, Ar), 130.9 (C, Ar), 129.1 (CH, Ar), 128.7 (CH, Ar), 128.2 (CH, Ar), 123.8 (CH, Ar), 123.4 (C, Ar), 118.6 (=C), 118.3 (CH, Ar), 52.2 (OCH₃), 28.2 (CH₂), 21.9 (CH₂), 21.7 (CH₂), 21.1 (CH₂); MS (ES⁺) *m/z* 357 [MNa⁺]; HRMS (ES⁺) calcd. for C₂₁H₁₈NaO₄ [MNa⁺]: 357.1097; found: 357.1089. Anal. calcd. for C₂₁H₁₈O₄: C 75.06; H 5.43 %.

Found: C 75.43; H 5.43 %. Slow evaporation of chloroform provided crystals suitable for X-ray analysis (*see Appendix I*)

Crystal Data. C₂₁H₁₈O₄, *M* = 334.35, monoclinic, *a* = 12.2467(2) Å, *b* = 7.47592(13) Å, *c* = 17.7579(3) Å, *U* = 1614.63(5) Å³, *T* = 100(2) K, space group P2₁/c, *Z* = 4, μ(MoKα) = 0.095, 21519 reflections measured, 5502 unique (*R*_{int} = 0.0309) which were used in all calculations. The final *wR*₂ was 0.1072 and *R*₁ was 0.0429 (>2 sigma (I)).

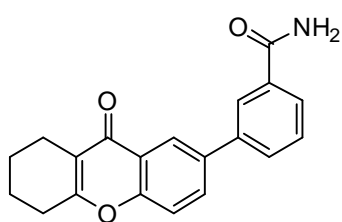
7-(2-Hydroxy-phenyl)-1,2,3,4-tetrahydro-xanthen-9-one (107)



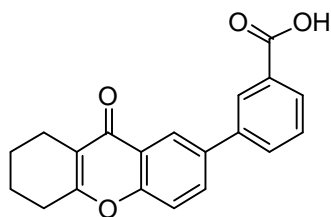
Pd(PPh₃)₄ (16 mg, 0.014 mmol) was added to a biphasic mixture of **102** (200 mg, 0.72 mmol) and 2-hydroxybenzene boronic acid (296 mg, 2.14 mmol) in ethanol (3 mL), toluene (3 mL) and 2M Na₂CO₃ (0.72 mL). Half of this mixture at a time was subjected to microwave irradiation (300 W) for 10 min at 110°C. The mixtures were recombined and the solvent was removed *in vacuo* before adding H₂O (20 mL). The aqueous phase was extracted with EtOAc (20 mL), washed with H₂O (20 mL), brine (20 mL), dried (MgSO₄), filtered and solvent removed *in vacuo*. The crude material was purified using column chromatography eluting with 25% EtOAc in petroleum ether. Trituration of the resultant solid with MeOH provided the title compound as a brown solid (22 mg, 11%). *R*_f = 0.20 (25% EtOAc in petroleum ether); δ_H (400 MHz, CDCl₃) 8.20 (1H, d, *J* = 2.3, ArH), 7.96 (1H, dd, *J* = 2.3, 8.8, ArH), 7.60 (1H, d, *J* = 8.8, ArH), 7.33 (1H, dd, *J* = 1.7, 7.6, ArH), 7.20 (1H, dt, *J* = 1.7, 7.6, ArH), 6.98 (1H, d, *J* = 7.6, ArH), 6.90 (1H, t, *J* = 7.6, ArH), 2.73 (2H, t, *J* = 6.3, CH₂), 2.46 (2H, t, *J* = 6.3, CH₂), 1.88-1.80 (2H, m, CH₂), 1.76-1.68 (2H, m, CH₂); δ_C (100 MHz, CDCl₃): δ 176.8 (C=O), 164.4 (=C), 155.8 (C, Ar), 154.6 (C, Ar), 135.8 (C, Ar), 135.0 (CH, Ar), 130.6 (CH, Ar), 129.4 (CH, Ar),

126.5 (C, Ar), 125.0 (CH, Ar), 122.5 (C, Ar), 119.5 (CH, Ar), 117.9 (=C), 117.8 (CH, Ar), 117.0 (CH, Ar), 27.9 (CH₂), 21.8 (CH₂), 21.6 (CH₂), 21.3 (CH₂); MS (ES⁺) *m/z* 293 [MH⁺]; HRMS (ES⁺) calcd. for C₁₉H₁₇O₃ (M+H)⁺: 293.1172; found: 293.1160.

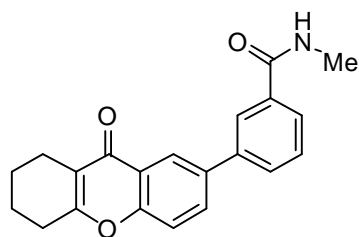
3-(9-Oxo-5,7,8,9-tetrahydro-6H-xanthen-2-yl)benzamide (108)



Carboxylic acid **109** (100 mg, 0.30 mmol) was dissolved in DMF (10 mL) and NEt₃ (92 μl, 0.66 mmol), HOBt (53 mg, 0.39 mL), PyBOP (187 mg, 0.36 mmol) and NH₃ (35% in H₂O) (41 μl, 0.75 mmol) were added. The reaction mixture was stirred at room temperature for 18 h. H₂O (25 mL) and EtOAc (25 mL) were added and the organic phase was separated and washed with 1.5M HCl (5 mL), H₂O (25 mL) and a saturated aqueous solution of NaHCO₃ (25 mL). The organic phase was dried (MgSO₄), filtered and the solvent removed *in vacuo*. The resultant yellow solid was triturated with DCM and filtered to give the title compound as a pale yellow solid (45 mg, 31% over 2 steps). m.p. 233-235 °C; IR (film) 3344, 3152, 2358, 1682, 1624, 1597, 1454, 802 cm⁻¹; δ_H (500 MHz, CDCl₃) 8.32 (1H, d, *J* = 1.9, ArH), 8.25 (1H, s, ArH), 8.20 (1H, br s, NH), 8.13 (1H, dd, *J* = 1.9, 7.0, ArH), 7.93-7.89 (2H, m, ArH), 7.70 (1H, d, *J* = 7.0, ArH), 7.59 (1H, t, *J* = 6.2, ArH), 7.47 (1H, br s, NH), 2.76-2.70 (2H, m, CH₂), 2.49-2.44 (2H, m, CH₂), 1.87-1.80 (2H, m, CH₂), 1.75-1.68 (2H, m, CH₂); δ_C (125 MHz, CDCl₃) 176.7 (C=O), 168.1 (H₂NC=O), 164.7 (=C), 155.4 (C, Ar), 139.1 (C, Ar), 136.5 (C, Ar), 135.6 (C, Ar), 132.6 (CH, Ar), 130.0 (CH, Ar), 129.6 (CH, Ar), 127.5 (CH, Ar), 126.2 (CH, Ar), 123.2 (CH, Ar), 123.0 (C, Ar), 119.3 (CH, Ar), 118.1 (=C), 28.0 (CH₂), 21.8 (CH₂), 21.5 (CH₂), 21.3 (CH₂); MS (ES⁺) *m/z* 320 [MH⁺]; HRMS (ES⁺) calcd. for C₂₀H₁₈NO₃ [MH⁺]: 320.1281; found: 320.1280

3-(9-Oxo-5,7,8,9-tetrahydro-6H-xanthen-2-yl)benzoic acid (109)

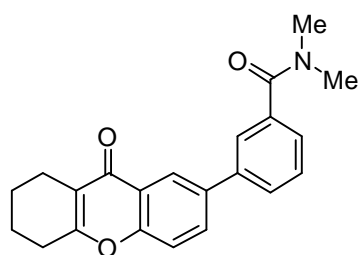
Ester **105** (350 mg, 1.05 mmol) was dissolved in THF (17.5 mL) and H₂O (17.5 mL) and LiOH·H₂O (220 mg, 5.25 mmol) was added. The mixture was stirred for 18 h at room temperature. The solvent was partially removed *in vacuo* before adding H₂O (5 mL) and adjusting to pH 1 using 1.5 M HCl. The aqueous phase was extracted with EtOAc (5 x 10 mL), dried (MgSO₄), filtered and the solvent removed *in vacuo* to give the title compound as a yellow solid (226 mg, 67%). The crude material was used without further purification. δ_{H} (400 MHz, DMSO-*d*₆) 13.10 (1H, brs, CO₂H), 8.25-8.22 (2H, m, ArH), 8.11 (1H, dd, *J* = 2.4, 8.8, ArH), 8.04-7.95 (2H, m, ArH), 7.69 (1H, d, *J* = 8.8, ArH), 7.64 (1H, t, *J* = 7.7, ArH), 2.75-2.70 (2H, m, CH₂), 2.48-2.43 (2H, m, CH₂), 1.87-1.79 (2H, m, CH₂), 1.75-1.67 (2H, m, CH₂); MS (ES⁺) *m/z* 321 [MH⁺].

N-Methyl-3-(9-oxo-5,7,8,9-tetrahydro-6H-xanthen-2-yl)benzamide (110)

Carboxylic acid **109** (180 mg, 0.56 mmol) was dissolved in DMF (30 mL) and NEt₃ (172 μ l, 1.24 mmol), HOBT (99 mg, 0.73 mmol), PyBOP (354 mg, 0.68 mmol) and methylamine (2M in THF) (0.72 mL, 1.41 mmol) were added. The reaction mixture was stirred for 18 h at room temperature. H₂O (40 mL) and EtOAc (40 mL) were added and the organic phase separated and washed with 1.5M HCl (10 mL), H₂O (40 mL) and a saturated aqueous solution of NaHCO₃ (2 x 40 mL). The organic phase was dried (MgSO₄), filtered and the solvent removed *in vacuo*. The resultant off-white solid was triturated with DCM and filtered to give the title compound as a white solid (16 mg, 6% over 2 steps). m.p. 248-249 °C; IR (film) 3379, 2940, 2358, 1660, 1630, 1606,

1444, 1149, 752 cm^{-1} ; δ_{H} (400 MHz, CDCl_3) 8.43 (1H, d, $J = 2.3$, ArH), 8.05 (1H, s, ArH), 7.89 (1H, dd, $J = 2.3, 8.7$, ArH), 7.79 (2H, d, $J = 7.8$, ArH), 7.54 (1H, d, $J = 7.8$, ArH), 7.49 (1H, d, $J = 8.7$, ArH), 6.40 (1H, br s, NH), 3.09 (3H, d, $J = 4.8$, NCH_3), 2.77-2.70 (2H, m, CH_2), 2.66-2.60 (2H, m, CH_2), 1.97-1.89 (2H, m, CH_2), 1.85-1.77 (2H, m, CH_2); δ_{C} (150 MHz, CDCl_3): δ 177.7 (C=O), 168.0 (RNC=O), 164.1 (=C), 155.5 (C, Ar), 140.0 (C, Ar), 136.5 (C, Ar), 135.5 (C, Ar), 131.8 (CH, Ar), 129.9 (CH, Ar), 129.2 (CH, Ar), 126.1 (CH, Ar), 125.5 (CH, Ar), 123.7 (CH, Ar), 123.3 (C, Ar), 118.6 (=C), 118.4 (CH, Ar), 28.2 (CH_2), 26.9 (CH_3), 21.9 (CH_2), 21.6 (CH_2), 21.0 (CH_2); MS (ES^+) m/z 334 [MH^+]; HRMS (ES^+) calcd. for $\text{C}_{21}\text{H}_{20}\text{NO}_3$ ($\text{M}+\text{H}$) $^+$: 334.1438; found: 334.1438.

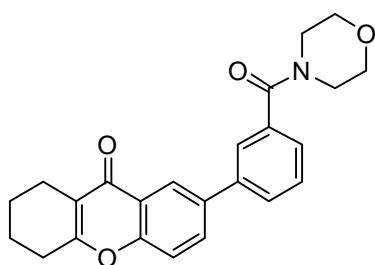
N,N-Dimethyl-3-(9-oxo-5,7,8,9-tetrahydro-6H-xanthen-2-yl)benzamide (111)



Carboxylic acid **109** (60 mg, 0.19 mmol) was dissolved in DMF (10 mL) and NEt_3 (52 μl , 0.41 mmol), HOBt (34 mg, 0.24 mmol), PyBOP (117 mg, 0.23 mmol) and dimethylamine (2M in MeOH) (0.24 mL, 0.47 mmol) were added. The reaction mixture was stirred for 18 h at room temperature. H_2O (50 mL) and EtOAc (30 mL) were added and the organic phase separated and washed with 1.5M HCl (5 mL), H_2O (50 mL) and a saturated aqueous solution of NaHCO_3 (2 x 30 mL) and brine (30 mL). The organic phase was dried (MgSO_4), filtered and the solvent removed *in vacuo*. The resultant off-white solid was purified using column chromatography eluting with 75% EtOAc in petroleum ether to give the title compound as a white solid (27 mg, 18% over 2 steps). IR (film) 2920, 1631, 1607, 1444, 807, 614 cm^{-1} ; δ_{H} (400 MHz, CDCl_3) 8.41 (1H, d, $J = 2.3$, ArH), 7.85 (1H, dd, $J = 2.3, 8.7$, ArH), 7.70 (2H, m, ArH), 7.53-7.43 (2H, m, ArH), 7.40 (1H, d, $J = 7.7$, ArH), 3.15 (3H, br s, NCH_3), 3.03 (3H, br s, NCH_3),

2.74-2.66 (2H, m, CH₂), 2.64-2.57 (2H, m, CH₂), 1.94-1.85 (2H, m, CH₂), 1.83-1.73 (2H, m, CH₂); δ_C (100 MHz, CDCl₃) 177.6 (C=O), 171.4 (RNC=O), 164.0 (=C), 155.5 (C, Ar), 139.9 (C, Ar), 137.2 (C, Ar), 136.7 (C, Ar), 131.8 (CH, Ar), 129.0 (CH, Ar), 128.2 (CH, Ar), 126.2 (CH, Ar), 125.8 (CH, Ar), 123.8 (CH, Ar), 123.3 (C, Ar), 118.6 (=C), 118.3 (CH, Ar), 39.7 (CH₃), 35.4 (CH₃), 28.2 (CH₂), 21.9 (CH₂), 21.7 (CH₂), 21.1 (CH₂); MS (ES⁺) m/z 370 [MNa⁺]; HRMS (ES⁺) calcd. for C₂₂H₂₁NNaO₃ (M+Na)⁺: 370.1414; found: 370.1423.

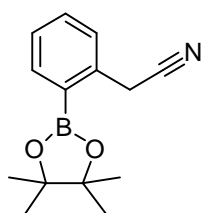
7-[3-(Morpholine-4-carbonyl)-phenyl]-1,2,3,4-tetrahydro-xanthen-9-one (112)



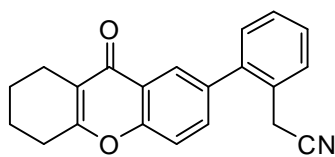
Carboxylic acid **109** (60 mg, 0.19 mmol) was dissolved in DMF (10 mL) and NEt₃ (57 μ l, 0.41 mmol), HOBt (34 mg, 0.24 mmol), PyBOP (117 mg, 0.23 mmol) and morpholine (41 μ l, 0.47 mmol) were added. The reaction mixture was stirred for 18 h at room temperature. H₂O (50 mL) and EtOAc (30 mL) were added and the organic phase separated and washed with 1.5M HCl (5 mL), H₂O (50 mL), a saturated aqueous solution of NaHCO₃ (2 x 30 mL) and brine (30 mL). The organic phase was dried (MgSO₄), filtered and the solvent removed *in vacuo* to give a yellow oil which solidified on standing at room temperature. The solid was purified using column chromatography eluting with 75% EtOAc in petroleum ether to give the title compound as a white solid (39 mg, 36% over 2 steps). m.p. 174-175 °C; IR (film) 2933, 1632, 1611, 1447, 1106, 613 cm⁻¹; δ_H (400 MHz, CDCl₃) 8.40 (1H, d, J = 2.3, ArH), 7.82 (1H, dd, J = 2.3, 8.8, ArH), 7.74-7.67 (2H, m, ArH), 7.51 (1H, t, J = 7.7, ArH), 7.47 (1H, d, J = 8.8, ArH), 7.39 (1H, d, J = 7.7, ArH), 3.94-3.41 (8H, br m, CH₂), 2.74-2.66 (2H, m, CH₂), 2.64-2.58 (2H, m, CH₂), 1.94-1.86 (2H, m, CH₂), 1.83-1.74 (2H, m, CH₂); δ_C (400 MHz, CDCl₃) 177.6 (C=O), 170.2 (RNC=O), 164.0 (=C), 155.6 (C, Ar), 140.2

(C, Ar), 136.4 (C, Ar), 136.2 (C, Ar), 131.7 (CH, Ar), 129.2 (CH, Ar), 128.6 (CH, Ar), 126.1 (CH, Ar), 125.8 (CH, Ar), 123.8 (CH, Ar), 123.3 (C, Ar), 118.6 (=C), 118.4 (CH, Ar), 66.9 (4 x CH₂), 28.2 (CH₂), 21.9 (CH₂), 21.7 (CH₂), 21.1 (CH₂); MS (ES⁺) *m/z* 412 [MNa⁺]; HRMS (ES⁺) calcd. for C₂₄H₂₃NNaO₄ [MNa⁺]: 412.1519; found: 412.1512.

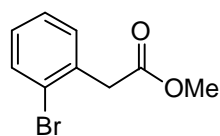
[2-(4,4,5,5-Tetramethyl-[1,3,2]dioxaborolan-2-yl)-phenyl]acetonitrile (128)



Triethylamine (0.98 mL, 7.06 mmol), Pd(OAc)₂ (20 mg, 0.09 mmol) and SPhos (145 mg, 0.35 mmol) added to a stirred solution of 2-bromophenylacetonitrile (0.23 mL, 1.77 mmol) in dioxane (4 mL). Pinacolborane (0.76 mL, 5.30 mmol) then added dropwise. Reaction mixture heated to 90 °C for 1 h. After allowing the mixture to cool to room temperature, a saturated aqueous solution of NH₄Cl (10 mL) was added to quench. The product was extracted with Et₂O (2 x 20 mL), dried (MgSO₄), filtered and the solvent removed *in vacuo*. The resultant black oil was purified using column chromatography eluting with 3% EtOAc in petroleum ether to give the title compound as an off-white solid (100 mg, 23%). *R*_f = 0.30 (5% EtOAc in petroleum ether); δ_H (400 MHz, CDCl₃) δ 7.90 (1H, d, *J* = 7.3, ArH), 7.51-7.44 (2H, m, ArH), 7.38 (1H, dt, *J* = 1.7, 7.3, ArH), 4.11 (2H, s, CH₂), 1.37 (12H, s, CH₃); δ_C (100 MHz, CDCl₃) 136.9 (CH, Ar), 136.7 (C, Ar), 131.9 (CH, Ar), 128.6 (CH, Ar), 127.3 (CH, Ar), 119.0 (CN), 84.1 (OC(CH₃)₂), 24.9 (4 x CH₃), 23.6 (CH₂); MS (ES⁺) *m/z* 338 [MNa⁺]. Data is in accordance with literature values.²⁰⁶

[2-(9-Oxo-5,7,8,9-tetrahydro-6H-xanthen-2-yl)-phenyl]acetonitrile (129)

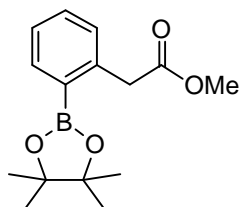
Boronic ester **128** (115 mg, 0.41 mmol) added to a stirring mixture of compound **Y** (100 mg, 0.41 mmol), Pd(OAc)₂ (4.5 mg, 0.02 mmol) and Ba(OH)₂·8H₂O (390 mg, 1.23 mmol) in dioxane (1 mL). The reaction mixture was heated to 100 °C for 1 h. After allowing the mixture to cool to room temperature, the mixture was filtered through Celite[®] washing with CH₂Cl₂ (2 x 20 mL). The combined organic phases were washed with brine (20 mL), dried (MgSO₄), filtered and the solvent removed *in vacuo* to give a yellow oil which solidified on standing at room temperature. The resulting solid was purified using column chromatography eluting with 20% EtOAc in petroleum ether to give an off-white residue which was triturated with Et₂O and filtered off to give the title compound as a white solid (38 mg, 29%). δ_H (300 MHz, CDCl₃) δ 8.10 (1H, d, *J* = 2.2, ArH), 7.60-7.53 (2H, m, ArH), 7.49 (1H, d, *J* = 8.6, ArH), 7.45-7.40 (2H, m, ArH), 7.33-7.29 (1H, m, ArH), 3.65 (2H, s, CH₂CN), 2.76-2.68 (2H, m, CH₂), 2.64-2.56 (2H, m, CH₂), 1.96-1.85 (2H, m, CH₂), 1.84-1.74 (2H, m, CH₂); δ_C (125 MHz, CDCl₃) 177.6 (C=O), 164.3 (=C), 155.5 (C), 140.5 (C), 136.3 (C), 133.8 (CH, Ar), 130.8 (CH, Ar), 129.3 (CH, Ar), 128.8 (CH, Ar), 128.6 (CH, Ar), 127.9 (C), 125.9 (CH, Ar), 123.3 (C), 118.9 (CN), 118.4 (CH, Ar), 118.0 (=C), 28.3 (CH₂), 22.3 (CH₂CN), 22.0 (CH₂), 21.8 (CH₂), 21.2 (CH₂); MS (ES⁺) *m/z* 338 [MNa⁺]; HRMS (ES⁺) calcd. for C₂₁H₁₇NNaO₂ [MNa⁺]: 338.1151; found: 338.1150.

(2-Bromo-phenyl)acetic acid methyl ester (131)

2-Bromo-phenylacetic acid (3.0 g, 14.0 mmol) dissolved in MeOH (20 mL) and treated with concentrated HCl (0.1 mL). The solution was heated to reflux for 2 h. After allowing the

reaction mixture to cool to room temperature the organic solvent was removed *in vacuo*. The product was extracted with Et₂O (100 mL) and washed with a saturated aqueous solution of NaHCO₃ (100 mL) and brine (100 mL). The organic phase was dried (MgSO₄), filtered and the solvent removed *in vacuo* to give the title compound as a colourless oil (3.02 g, 94%). δ_{H} (300 MHz, CDCl₃) δ 7.58 (1H, d, J = 7.8, ArH), 7.31-7.27 (2H, m, ArH), 7.20-7.10 (1H, m, ArH), 3.81 (2H, s, CH₂), 3.73 (3H, s, CH₃); δ_{C} (100 MHz, CDCl₃) 171.1 (C=O), 134.3 (C, Ar), 133.0 (CH, Ar), 131.6 (CH, Ar), 129.0 (CH, Ar), 127.7 (CH, Ar), 125.2 (C, Ar), 52.3 (CH₃), 41.6 (CH₂); MS (ES⁺) m/z 251 [MNa⁺, ⁷⁹Br], 253 [MNa⁺, ⁸¹Br]; HRMS (ES⁺) calcd. for C₉H₉BrNaO₂ [MNa⁺, ⁸¹Br]: 252.9658; found: 252.9668. Data is in accordance with literature values.²⁰⁷

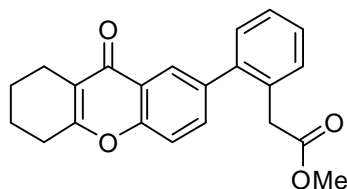
[2-(4,4,5,5-Tetramethyl-[1,3,2]dioxaborolan-2-yl)-phenyl]acetic acid methyl ester (132)



Triethylamine (4.9 mL, 34.9 mmol), Pd(OAc)₂ and cyclohexyl JohnPhos (612 mg, 1.75 mmol) added to a stirring solution of **131** in dioxane (20 mL). Pinacolborane (3.8 mL, 26.2 mmol) then added dropwise. The reaction mixture was heated to 90 °C for 2 h. After allowing the reaction mixture to cool to room temperature, the solvent was removed *in vacuo*. An aqueous saturated solution of NH₄Cl (5 mL) was added to quench the reaction and the product was extracted with Et₂O (50 mL). The organic phase was washed with H₂O (2 x 50 mL), dried (MgSO₄), filtered and the solvent was removed *in vacuo* to give an orange oil. Purified using column chromatography eluting with 5% EtOAc in petroleum ether to give the title compound as an orange solid (1.5 g, 63%). m.p. 67-68 °C; IR (film) 2975, 2924, 1739, 1342, 1143, 658 cm⁻¹; δ_{H} (400 MHz, CDCl₃) 7.84 (1H, d, J = 7.6, ArH), 7.39

(1H, t, $J = 7.6$, ArH), 7.28 (1H, t, $J = 7.6$, ArH), 7.20 (1H, d, $J = 7.6$, ArH), 3.99 (2H, s, CH₂), 3.67 (3H, s, CH₃), 1.33 (12H, s, CH₃); δ_C (75 MHz, CDCl₃) 173.0 (C=O), 140.5 (C, Ar), 136.2 (CH, Ar), 131.1 (CH, Ar), 130.2 (CH, Ar), 127.2 (C, Ar), 126.5 (CH, Ar), 83.7 (OC(CH₃)₂), 51.8 (CO₂CH₃), 41.1 (CH₂), 25.0 (CH₃); MS (ES⁺) m/z 277 [MH⁺]. Data is in accordance with literature values.²⁰⁸

[2-(9-Oxo-5,7,8,9-tetrahydro-6-*H*-xanthen-2-yl)phenyl]acetic acid methyl ester (133)

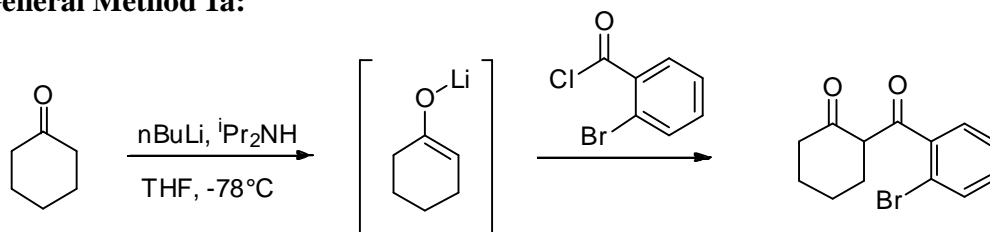


Boronic ester **132** (200 mg, 0.71 mmol), compound Y (394 mg, 1.42 mmol), Pd(OAc)₂ (8 mg, 0.04 mmol) and 2M Na₂CO₃ (1.07 mL, 2.14 mmol) dissolved in H₂O (0.3 mL) and dioxane (1.7 mL) and the reaction mixture heated to 100 °C for 1 h. After allowing the reaction mixture to cool to room temperature, the mixture was filtered through Celite[®] washing with CH₂Cl₂ (2 x 20 mL). The combined organic phases were washed with brine (20 mL), dried (MgSO₄), filtered and the solvent removed *in vacuo* to give a black oil. Purified using column chromatography eluting with 10% EtOAc in petroleum ether to give the title compound as a colourless oil (115 mg, 46%). δ_H (400 MHz, CDCl₃) δ 8.14 (1H, d, $J = 2.1$, ArH), 7.60 (1H, dd, $J = 2.1, 8.6$, ArH), 7.44 (1H, d, $J = 8.6$, ArH), 7.41-7.33 (3H, m, ArH), 7.31-7.28 (1H, m, ArH), 2.74-2.68 (2H, m, CH₂), 2.64-2.58 (2H, m, CH₂), 1.94-1.86 (2H, m, CH₂), 1.83-1.75 (2H, m, CH₂), 3.64 (3H, s, CH₃), 3.60 (2H, s, CH₂CO₂Me); δ_C (100 MHz, CDCl₃) 177.6 (C=O), 172.1 (CO₂Me), 164.0 (=C), 155.1 (C, Ar), 141.1 (C, Ar), 137.5 (C, Ar), 134.1 (CH, Ar), 131.9 (C, Ar), 130.5 (CH, Ar), 130.4 (CH, Ar), 128.0 (CH, Ar), 127.4 (CH, Ar), 126.0 (CH, Ar), 122.9 (C, Ar), 118.6 (=C), 117.6 (CH, Ar), 52.1 (CO₂CH₃), 38.9 (CH₂CO₂Me), 28.2

(CH₂), 21.9 (CH₂), 21.7 (CH₂), 21.1 (CH₂); MS (ES⁺) *m/z* 371 [MNa⁺]; HRMS (ES⁺) calcd. for C₂₂H₂₀NaO₄ [MNa⁺]: 371.1254; found: 371.1252.

Acylation using lithium diisopropylamide

General Method 1a:



Lithium diisopropylamide (2M in THF/heptane/ethylbenzene) (1.0 molar equiv) in THF (2-10 mL) was cooled to -78 °C whereupon the relevant ketone (1.0 molar equiv) was added. The solution was stirred at -78 °C for 1 h before addition of the acid chloride (1.0 molar equiv). The solution was then allowed to warm to room temperature and stirred at room temperature for 5 h. 2M HCl (10 mL) was added and the product was extracted with DCM (2 x 10 mL) and dried (MgSO₄). Removal of the solvent and purification gave the title compounds predominantly in the enol form with the exception of compound **177** (50:50 enol:diketone forms) and compound **159** (13:1 enol:diketone forms).

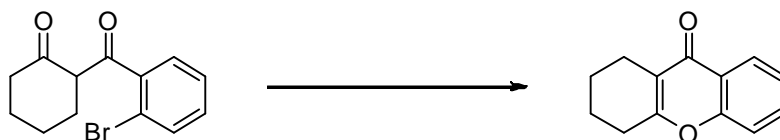
General Method 1b:

Diisopropylamine (2.0 molar equiv) in THF (10 mL) was cooled to -78 °C and *n*-BuLi (2.5M in hexane) (2.0 molar equiv) was added. The solution was stirred for 5 min before adding cyclohexanone (2.0 molar equiv). The solution was stirred at -78 °C for 1 h before addition of the acid chloride (1.0 molar equiv). The solution was then allowed to warm to room temperature and stirred at room temperature for 18 h. 2M HCl (15 mL) was added and the product was extracted with EtOAc (3 x 50 mL)

and dried (MgSO_4). Removal of the solvent and purification gave the title compounds predominantly in the enol form.

Copper catalysed synthesis of tetrahydroxanthenes

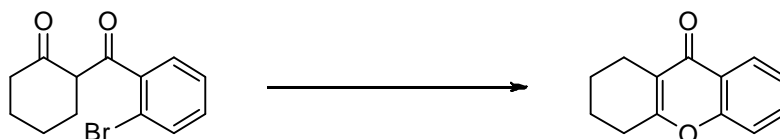
General Method 2:



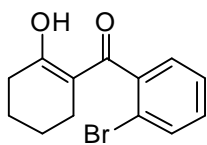
The appropriate ketone (1.0 molar equiv) was dissolved in THF (0.10 mol dm^{-3}) and CuI (0.1 molar equiv), DMEDA (0.2 molar equiv) and Cs_2CO_3 (2.0 molar equiv) were added. The mixture was heated to reflux for 18 h. After all the mixture to cool to room temperature it was filtered over Celite[®] washing with EtOAc (5 x 10 mL). The combined organic phases were dried (MgSO_4) and filtered. Removal of the solvent *in vacuo* and purification provided the title compounds.

Palladium catalysed synthesis of tetrahydroxanthenes

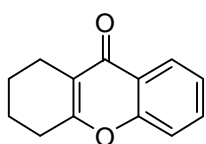
General Method 3:



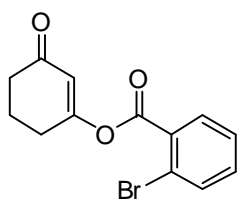
The appropriate ketone (1.0 molar equiv) was dissolved in dioxane ($0.29\text{-}0.37 \text{ mol dm}^{-3}$) and $\text{Pd}_2(\text{dba})_3$ (2.5 mol%), Cs_2CO_3 (2.2 molar equiv), and Xphos (6.0 mol%) were added. The mixture was heated to reflux for 18 h. After allowing the mixture to cool to room temperature it was filtered over Celite[®] washing with CH_2Cl_2 (5 x 10 mL). The combined organic phases were dried (MgSO_4) and filtered. Removal of the solvent *in vacuo* and purification provided the title compounds.

(2-Bromophenyl)(2-hydroxycyclohex-1-enyl)methanone (141)

To lithium diisopropylamide (2M in THF/heptane/ethylbenzene, 4.55 mL, 9.10 mmol) and cyclohexanone (0.94 mL, 9.10 mmol) in THF (10 mL) was added 2-bromo-benzoyl chloride (1.19 mL, 9.10 mmol) according to General Method 1a. Workup followed by column chromatography eluting with 3% EtOAc in petroleum ether gave the title compound as a white solid (1.48 g, 58%). m.p. 62-63 °C (lit. m.p 63-64 °C); $R_f = 0.29$ (5% EtOAc in petroleum ether); IR (film) 2933, 1575, 1406, 1315, 936, 742 cm^{-1} ; δ_{H} (400 MHz, CDCl_3) 15.82 (1H, s, OH), 7.58 (1H, d, $J = 7.8$ Hz, ArH), 7.40-7.33 (1H, m, ArH), 7.29-7.22 (1H, m, ArH), 7.22-7.17 (1H, m, ArH), 2.50-2.43 (2H, m, CH_2), 2.10-2.01 (2H, m, CH_2), 1.78-1.69 (2H, m, CH_2), 1.65-1.56 (2H, m, CH_2); δ_{C} (100 MHz, CDCl_3) 192.9 (C=O), 187.4 (COH), 139.3 (C, Ar), 132.8 (CH, Ar), 130.4 (CH, Ar), 127.6 (CH, Ar), 127.5 (CH, Ar), 118.9 (C, Ar), 107.6 (=C), 32.1 (CH_2), 24.6 (CH_2), 22.9 (CH_2), 21.6 (CH_2); MS (ES^+) m/z 303 [MNa^+ , ^{79}Br], 305 [MNa^+ , ^{81}Br]; HRMS (ES^+) calcd. for $\text{C}_{13}\text{H}_{13}\text{BrNaO}_2$ [MNa^+ , ^{81}Br]: 304.9971; found: 304.9971. Anal. Calcd. for $\text{C}_{13}\text{H}_{13}\text{O}_2\text{Br}$: C 55.54; H 4.66 %. Found: C 55.38; H 4.60 %. Data is in accordance with literature values.²⁰⁹

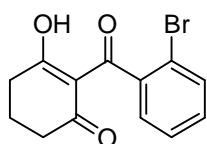
1,2,3,4-Tetrahydro-xanthen-9-one (83)

141 (100 mg, 0.36 mmol) was dissolved in dioxane (1 mL) and $\text{Pd}_2(\text{dba})_3$ (8 mg, 0.009 mmol), Xphos (10 mg, 0.021 mmol) and Cs_2CO_3 (255 mg, 0.75 mmol) added according to General Method 2. Workup followed by column chromatography eluting with 5% EtOAc in petroleum ether gave the title compound as a white solid (66 mg, 93%). Data as previously reported.

2-Bromo-benzoic acid 3-oxo-cyclohex-1-enyl ester (145)

Pyridine (0.17 mL, 2.09 mmol) and 2-bromobenzoyl chloride (0.30 mL, 2.28 mmol) added to a stirring solution of 1,3-cyclohexanedione (213 mg, 1.90 mmol) in chloroform (4 mL).

The reaction mixture was stirred at room temperature for 2 h. The solution was washed with H₂O (20 mL) and further extracted with DCM (10 mL). The combined organic phases were dried (MgSO₄) and filtered and the solvent was removed *in vacuo* to give the title compound as a white solid (465 mg, 69%). R_f = 0.21 (10% EtOAc in petroleum ether); δ_H (400 MHz, CDCl₃) 7.93-7.88 (1H, m, ArH), 7.75-7.70 (1H, m, ArH), 7.46-7.39 (2H, m, ArH), 6.06 (1H, s, =CH), 2.74-2.69 (2H, m, CH₂), 2.50-2.44 (2H, m, CH₂), 2.18-2.10 (2H, m, CH₂); δ_C (100 MHz, CDCl₃) 199.4 (C=O), 169.9 (OC=), 162.6 (CO₂R), 134.9 (CH, Ar), 133.8 (CH, Ar), 132.1 (CH, Ar), 130.4 (C, Ar), 127.6 (CH, Ar), 122.6 (C, Ar), 118.2 (=CH), 36.9 (CH₂), 28.4 (CH₂), 21.4 (CH₂).

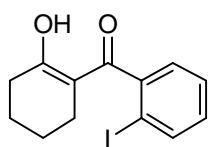
2-(2-Bromo-benzoyl)cyclohexane-1,3-dione (146)

Triethylamine (0.09 mL, 0.0007 mmol) and KCN (0.33 mg, 0.005 mmol) added to a stirring solution of compound **145** in MeCN (1 mL). The reaction mixture was stirred at room

temperature for 18 h. The solvent was then removed *in vacuo*. The resulting residue was dissolved in EtOAc (3 mL) and 2M HCl (3 mL) added. The mixture was stirred at room temperature for 5 min. The organic layer was separated and washed with a saturated aqueous solution of NaHCO₃ (2 x 5 mL). The aqueous layer was then neutralised using 2M HCl and re-extracted with EtOAc (10 mL). The organic layer was dried (MgSO₄), filtered and the solvent removed *in vacuo* to give a colourless oil which solidified on standing at room temperature. The solid was recrystallised

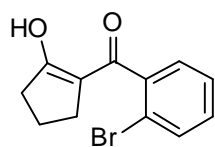
from MeOH and filtered to give the title compound as a white solid (40 mg, 40%). δ_{H} (300 MHz, CDCl_3) enol proton not observed, 7.56 (1H, d, $J = 7.7$, ArH), 7.38 (1H, t, $J = 7.7$, ArH), 7.29 (1H, t, $J = 7.7$, ArH), 7.18 (1H, dd, $J = 1.6, 7.7$, ArH), 2.84-2.73 (2H, m, CH_2), 2.52-2.40 (2H, m, CH_2), 2.05 (2H, p, $J = 6.5$, CH_2); δ_{C} (100 MHz, CDCl_3) 198.1 (ArC=O), 197.1 ($\text{H}_2\text{CC}=\text{O}$), 193.7 (COH), 141.0 (C, Ar), 132.5 (CH, Ar), 130.7 (CH, Ar), 127.4 (CH, Ar), 127.2 (CH, Ar), 118.4 (C, Ar), 114.0 (=C), 37.9 (CH_2), 32.6 (CH_2), 19.2 (CH_2); MS (ES^+) m/z 317 [MNa^+ , ^{79}Br], 319 [MNa^+ , ^{81}Br].

(2-Iodophenyl)(2-hydroxycyclohex-1-enyl)methanone (158)



To lithium diisopropylamide (2M in THF/heptane/ethylbenzene, 0.90 mL, 1.88 mmol) and cyclohexanone (0.19 mL, 1.88 mmol) in THF (2 mL) was added 2-iodo-benzoyl chloride (500 mg, 1.88 mmol) according to General Method 1a. Workup followed by column chromatography eluting with 3% EtOAc in petroleum ether gave the title compound as a white solid (262 mg, 43%). $R_f = 0.46$ (5% EtOAc in petroleum ether); δ_{H} (300 MHz, CDCl_3) 15.84 (1H, s, OH), 7.85 (1H, dd, $J = 1.4, 7.9$ Hz, ArH), 7.40 (1H, dt, $J = 1.4, 7.9$, ArH), 7.16 (1H, dd, $J = 1.4, 7.9$, ArH), 7.08 (1H, dt, $J = 1.4, 7.9$, ArH), 2.47 (2H, m, CH_2), 2.03 (2H, m, CH_2), 1.80-1.70 (2H, m, CH_2), 1.68-1.57 (2H, m, CH_2).

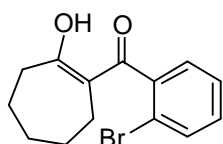
(2-Bromophenyl)(2-hydroxycyclopent-1-enyl)methanone (159)



To lithium diisopropylamide (2M in THF/heptane/ethylbenzene, 2.28 mL, 4.56 mmol) and cyclopentanone (0.40 mL, 4.56 mmol) in THF (5.0 mL) was added 2-bromo-benzoyl chloride (0.60 mL, 4.56 mmol) according to General Method 1a. Workup followed by column

chromatography eluting with 2 % EtOAc in petroleum ether gave the title compound as a yellow oil (467 mg, 38%). Mixture of enol to diketone (13:1). $R_f = 0.27$ (5% EtOAc in petroleum ether); IR (film) 2933, 1582, 1241, 743 cm^{-1} ; δ_H (400 MHz, CDCl_3) enol: 13.48 (1H, s, OH), 7.62 (1H, d, $J = 7.9$ Hz, ArH), 7.41-7.32 (2H, m, ArH), 7.31-7.24 (1H, m, ArH), 2.50 (2H, t, $J = 7.9$, CH_2), 2.45 (2H, t, $J = 7.9$, CH_2), 1.93 (2H, p, $J = 7.9$, CH_2), diketone: δ 7.65-7.58 (1H, m, ArH), 7.47 (1H, dd, $J = 1.8, 7.7$, ArH), 7.42-7.39 (1H, m, ArH), 7.32-7.30 (1H, m, ArH), 4.15 (1H, t, $J = 8.8$, CH), 2.37-2.31 (4H, m, CH_2), 2.2-2.15 (2H, m, CH_2); δ_C (100 MHz, CDCl_3) enol: 209.4 (C=O), 169.4 (COH), 135.0 (C, Ar), 133.2 (CH, Ar), 131.1 (CH, Ar), 129.6 (CH, Ar), 127.4 (CH, Ar), 120.7 (C, Ar), 111.7 (=C), 38.0 (CH_2), 26.5 (CH_2), 20.9 (CH_2), diketone (no quaternary carbons observed): 133.5 (CH, Ar), 131.9 (CH, Ar), 129.4 (CH, Ar), 127.6 (CH, Ar), 61.4 (CHCO), 38.9 (CH_2), 27.4 (CH_2), 22.6 (CH_2); MS (ES^+) m/z 267 [MH^+ , ^{79}Br], 269 [MH^+ , ^{81}Br]; HRMS (ES^+) calcd. for $\text{C}_{12}\text{H}_{12}\text{O}_2\text{Br}$ [MH^+ , ^{81}Br]: 268.9995; found: 268.9990.

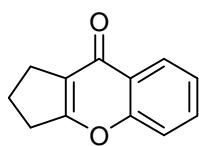
(2-Bromophenyl)((Z)-2-hydroxycyclohept-1-enyl)methanone (160)



To lithium diisopropylamide (2M in THF/heptane/ethylbenzene, 1.4 mL, 2.86 mmol) and cycloheptanone (0.54 mL, 4.56 mmol) in THF (5.0 mL) was added 2-bromo-benzoyl chloride (0.60 mL, 4.56 mmol) according to General Method 1a. Workup followed by column chromatography eluting with 5% EtOAc in petroleum ether gave the title compound as a pale pink oil (788 mg, 59%). $R_f = 0.44$ (10% EtOAc in petroleum ether); IR (film) 2932, 1592, 1245, 943, 742 cm^{-1} ; δ_H (300 MHz, CDCl_3) 16.26 (1H, s, OH), 7.61 (1H, d, $J = 8.0$, ArH), 7.41-7.32 (1H, m, ArH), 7.31-7.20 (2H, m, ArH), 2.66 (2H, br s, CH_2), 2.15 (2H, br s, CH_2), 1.74 (4H, br s, CH_2), 1.61 (1H, br s, CH_2), 1.47 (1H, br s, CH_2); δ_C (100 MHz, CDCl_3) 179.6 (C=O), 178.3 (COH), 137.4 (C),

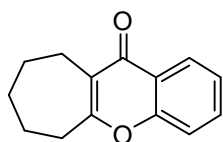
132.9 (CH, Ar), 130.5 (CH, Ar), 128.9 (CH, Ar), 127.4 (CH, Ar), 120.6 (C), 112.6 (C), 42.0 (CH₂), 31.1 (CH₂), 29.1 (CH₂), 27.7 (CH₂), 24.8 (CH₂); MS (ES⁺) *m/z* 295 [MH⁺, ⁷⁹Br], 297 [MH⁺, ⁸¹Br]; HRMS (ES⁺) calcd. for C₁₄H₁₆BrO₂ [MH⁺, ⁷⁹Br]: 295.0328; found: 295.0327.

2,3-Dihydro-1H-cyclopenta[b]chromen-9-one (163)



159 (100 mg, 0.37 mmol) was dissolved in dioxane (1 mL) and Pd₂(dba)₃ (9 mg, 0.009 mmol), Xphos (11 mg, 0.021 mmol) and Cs₂CO₃ (268 mg, 0.82 mmol) added according to General Method 2. Workup followed by column chromatography eluting with 10% EtOAc in petroleum ether gave the title compound as a white solid (16 mg, 23%). m.p. 118-121 °C; IR (film) 2954, 2354, 1639, 1607, 1461, 1429, 762 cm⁻¹; δ_H (400 MHz, CDCl₃) 8.24 (1H, d, *J* = 7.7, ArH), 7.61 (1H, t, *J* = 7.7, ArH), 7.43 (1H, d, *J* = 7.7, ArH), 7.38 (1H, t, *J* = 7.7, ArH), 3.02-2.94 (2H, m, CH₂), 2.91-2.83 (2H, m, CH₂), 2.13 (2H, p, *J* = 7.4, CH₂); δ_C (75 MHz, CDCl₃) 175.7 (C=O), 169.0 (=C), 156.4 (C, Ar), 132.1 (CH, Ar), 125.2 (CH, Ar), 124.2 (CH, Ar), 123.6 (C, Ar), 120.4 (=C), 117.3 (CH, Ar), 31.7 (CH₂), 25.5 (CH₂), 18.9 (CH₂); MS (ES⁺) *m/z* 187 [MH⁺]; HRMS (ES⁺) calcd. for C₁₂H₁₁O₂ [MH⁺]: 187.0754; found 187.0754.

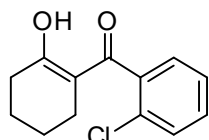
7,8,9,10-Tetrahydro-6H-5-oxa-cyclohepta[b]naphthalen-11-one (164)



160 (100 mg, 0.34 mmol) was dissolved in dioxane (1 mL) and Pd₂(dba)₃ (8 mg, 0.008 mmol), Xphos (12 mg, 0.02 mmol) and Cs₂CO₃ (243 mg, 0.75 mmol) added according to General Method 2. Workup followed by column chromatography eluting with 10% EtOAc in petroleum ether gave the title compound as a yellow solid (55 mg, 75%). m.p. 84-85 °C (lit. m.p 82-83 °C) ; R_f = 0.44 (10% EtOAc in petroleum ether); IR (film)

2922, 2840, 2360, 1624, 1464, 1400, 1606, 757 cm^{-1} . δ_{H} (400 MHz, CDCl_3) 8.21 (1H, dd, $J = 1.2, 7.9$, ArH), 7.60 (1H, dt, $J = 1.2, 7.9$, ArH), 7.41-7.31 (2H, m, ArH), 2.90-2.83 (2H, m, CH_2), 2.83-2.76 (2H, m, CH_2), 1.91-2.80 (2H, m, CH_2), 1.80-1.71 (2H, m, CH_2), 1.66-1.57 (2H, m, CH_2); δ_{C} (100 MHz, CDCl_3) 177.1 (C=O), 169.0 (=C), 155.7 (C, Ar), 132.8 (CH, Ar), 126.1 (CH, Ar), 124.6 (CH, Ar), 123.0 (C, Ar), 122.8 (=C), 117.8 (CH, Ar), 34.8 (CH_2), 32.0 (CH_2), 26.4 (CH_2), 25.0 (CH_2), 22.3 (CH_2); MS (ES^+) m/z 215 [MH^+]; HRMS (ES^+) calcd. for $\text{C}_{14}\text{H}_{15}\text{O}_2$ [MH^+]: 215.1067; found: 215.1069. Data is in accordance with literature values.¹⁰⁹

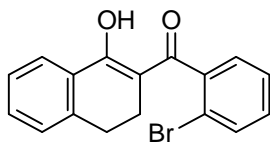
(2-Chlorophenyl)(2-hydroxycyclohex-1-enyl)methanone (169)



To lithium diisopropylamide (2M in THF/heptane/ethylbenzene, 1.4 mL, 2.86 mmol) and cyclohexanone (0.30 mL, 2.86 mmol) in THF (2.50 mL) was added 2-chloro-benzoyl chloride (0.36 mL, 2.86 mmol) according to General Method 1a. Workup followed by column chromatography eluting with 5% EtOAc in petroleum ether gave an off-white solid which was triturated with hexane and filtered off to give the title compound as a white solid (286 mg, 42%). m.p. 69-70 °C; $R_f = 0.35$ (5% EtOAc in petroleum ether); IR (film) 2937, 1575, 1406, 1317, 1279, 1243, 745 cm^{-1} ; δ_{H} (300 MHz, CDCl_3) 15.88 (1H, s, OH), 7.44-7.28 (3H, m, ArH), 7.27-7.19 (1H, m, ArH), 2.52-2.42 (2H, m, CH_2), 2.12-2.02 (2H, m, CH_2), 1.80-1.66 (2H, m, CH_2), 1.67-1.53 (2H, m, CH_2); δ_{C} (100 MHz, CDCl_3) 191.9 (C=O), 187.5 (C-OH), 137.2 (C, Ar), 130.3 (CH, Ar), 130.2 (C, Ar), 129.7 (CH, Ar), 127.7 (CH, Ar), 127.1 (CH, Ar), 108.0 (C, Ar), 32.1 (CH_2), 24.4 (CH_2), 22.8 (CH_2), 21.6 (CH_2). MS (ES^+) m/z 237 [MH^+ , ^{35}Cl], 239 [MH^+ , ^{37}Cl]; HRMS (ES^+) calcd. for $\text{C}_{13}\text{H}_{14}\text{ClO}_2$ [MH^+ , ^{35}Cl]: 237.0677;

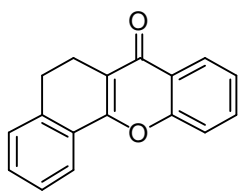
found: 237.0674. Anal. calcd. for $C_{13}H_{13}O_2Cl$: C 65.97; H 5.54; Cl 14.98 %. Found: C 65.83; H 5.55; Cl 14.90 %. Data is in accordance with literature values.²¹⁰

(2-Bromophenyl)(1,2-dihydro-4-hydroxynaphthalen-3-yl)methanone (170)



To lithium diisopropylamide (2M in THF/heptane/ethylbenzene, 2.28 mL, 4.56 mmol) and α -tetralone (0.61 mL, 4.56 mmol) in THF (5 mL) was added 2-bromo-benzoyl chloride (0.60 mL, 4.56 mmol) according to General Method 1a. Workup followed by column chromatography eluting with 2% EtOAc in petroleum ether gave the title compound as a white solid (672 mg, 45%). m.p. 53-56 °C; R_f = 0.22 (5% EtOAc in petroleum ether); IR (film) 2933, 2843, 1595, 1246, 762 cm^{-1} ; δ_H (400 MHz, $CDCl_3$) 16.23 (1H, s, OH), 8.05 (1H, d, J = 7.8 Hz, ArH), 7.64 (1H, d, J = 7.8, ArH), 7.49-7.26 (5H, m, ArH), 7.21 (1H, d, J = 7.8, ArH), 2.88-2.80 (2H, m, CH_2), 2.42 (2H, br s, CH_2); δ_C (100 MHz, $CDCl_3$) 185.8 (C=O), 182.4 (C-OH), 141.8 (C, Ar), 138.1 (C, Ar), 132.9 (CH, Ar), 132.8 (CH, Ar), 131.6 (C, Ar), 130.7 (CH, Ar), 128.6 (CH, Ar), 127.9 (CH, Ar), 127.6 (CH, Ar), 127.0 (CH, Ar), 126.5 (CH, Ar), 120.0 (C, Ar), 107.0 (CCO), 28.5 (CH_2), 23.4 (CH_2); MS (ES^+) m/z 329 [MH^+ , ^{79}Br], 331 [MH^+ , ^{81}Br]; HRMS (ES^+) calcd. for $C_{17}H_{14}BrO_2$ [MH^+ , ^{79}Br]: 329.0172; found 329.0165.

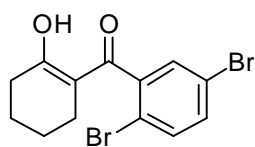
5,6-Dihydro-benzo[c]xanthen-7-one (171)



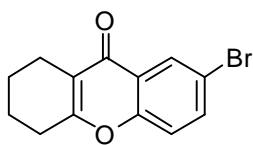
170 (100 mg, 0.30 mmol) was dissolved in dioxane (1 mL) and $Pd_2(dba)_3$ (7 mg, 0.008 mmol), Xphos (9 mg, 0.018 mmol) and Cs_2CO_3 (218 mg, 0.67 mmol) added according to General Method 2. Workup followed by column chromatography eluting with 5% EtOAc in petroleum ether gave the title compound as a white solid (68 mg, 91%). m.p. 143-

144 °C; $R_f = 0.12$ (5% EtOAc in petroleum ether); IR (film) 3064, 2926, 1624, 1606, 1559, 1463, 753 cm^{-1} ; δ_{H} (300 MHz, CDCl_3) 8.27 (1H, dd, $J = 1.5, 8.0$, ArH), 8.02, 7.93 (1H, m, ArH), 7.68 (1H, dt, $J = 1.6, 7.8$, ArH), 7.55 (1H, d, $J = 8.0$, ArH), 7.45-7.34 (3H m, ArH), 7.32-7.25 (1H, m, ArH), 2.96 (4H, s, CH_2); δ_{C} (100 MHz, CDCl_3) 176.6 (C=O), 157.1 (=C), 155.0 (C, Ar), 138.8 (C, Ar), 132.6 (CH, Ar), 130.5 (CH, Ar), 127.8 (C, Ar), 127.6 (CH, Ar), 126.3 (CH, Ar), 125.2 (CH, Ar), 124.2 (CH, Ar), 123.2 (CH, Ar), 123.0 (C, Ar), 117.3 (CH, Ar), 116.0 (=C), 26.5 (CH_2), 18.3 (CH_2). MS (ES^+) m/z 249 [MH^+]; HRMS (ES^+) calcd. for $\text{C}_{17}\text{H}_{13}\text{O}_2$ [MH^+]: 249.0901; found: 249.0909.

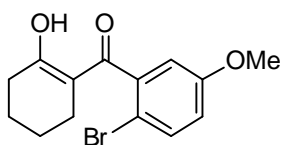
(2,5-Dibromophenyl)(2-hydroxycyclohex-1-enyl)methanone (172)



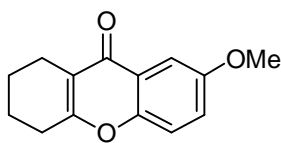
To lithium diisopropylamide (2M in THF/heptane/ethylbenzene, 0.97 mL, 1.95 mmol) and cyclohexanone (0.2 mL, 1.95 mmol) in THF (5.8 mL) was added 2,5-dibromobenzoyl chloride (582 mg, 1.95 mmol) according to General Method 1a. Workup followed by column chromatography eluting with 2% EtOAc in petroleum ether gave the title compound as a white solid (298 mg, 42%). m.p. 75-77 °C $R_f = 0.5$ (10% EtOAc in petroleum ether); IR (film) 29938, 2852, 1566, 813 cm^{-1} ; δ_{H} (400 MHz, CDCl_3) 15.66 (1H, s, OH), 7.45 (1H, d, $J = 8.8$ Hz, ArH), 7.40-7.32 (2H, m, ArH), 2.47 (2H t, $J = 6.5$, CH_2), 2.11-2.02 (2H, m, CH_2), 1.79-1.70 (2H, m, CH_2), 1.67-1.57 (2H, m, CH_2); δ_{C} (100 MHz, CDCl_3) 191.3 (C=O), 187.7 (COH), 141.0 (C, Ar), 134.3 (CH, Ar), 133.4 (CH, Ar), 130.4 (CH, Ar), 121.09 (C, Ar), 117.7 (C, Ar), 107.4 (CCO), 32.0 (CH_2), 24.5 (CH_2), 22.8 (CH_2), 21.5 (CH_2). MS (ES^+) m/z 381 [MNa^+ , ^{79}Br , ^{79}Br], 383 [MNa^+ , ^{79}Br , ^{81}Br], 385 [MNa^+ , ^{81}Br , ^{81}Br]; HRMS (ES^+) calcd. for $\text{C}_{13}\text{H}_{12}\text{Br}_2\text{NaO}_2$ [MNa^+ , ^{79}Br , ^{81}Br]: 382.9076; found 382.9075.

7-Bromo-1,2,3,4-tetrahydro-xanthen-9-one (102)

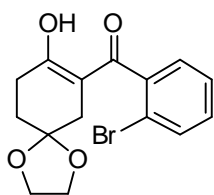
102 (100 mg, 0.28 mmol) was dissolved in dioxane (1 mL) and Pd₂(dba)₃ (6 mg, 0.007 mmol), Xphos (8 mg, 0.017 mmol) and Cs₂CO₃ (199 mg, 0.61 mmol) added according to General Method 2. Workup followed by column chromatography eluting with 5% EtOAc in petroleum ether gave the title compound as a white solid (54 mg, 69%). Data as previously reported.

(2-Bromo-5-methoxyphenyl)(2-hydroxycyclohex-1-enyl)methanone (173)

To lithium diisopropylamide (2M in THF/heptane/ethylbenzene, 1.00 mL, 2.00 mmol) and cyclohexanone (0.21 mL, 2.00 mmol) in THF (5 mL) was added 2-bromo, 5-methoxybenzoyl chloride (500 mg, 2.00 mmol) according to General Method 1a. Workup followed by column chromatography eluting with 5% EtOAc in petroleum ether gave the title compound as a colourless oil (223 mg, 36%). R_f = 0.64 (10% EtOAc in petroleum ether); IR (film) 2934, 1703, 1567, 1463, 1412, 1309, 1238, 1016, 730 cm⁻¹; δ_H (300 MHz, CDCl₃) 15.77 (1H, s, OH), 7.45 (1H, d, *J* = 9.0 Hz, ArH), 6.81 (1H, dd, *J* = 3.1, 9.0, ArH), 6.74 (1H, d, *J* = 3.1, ArH), 3.79 (3H, s, OCH₃), 2.49-2.41 (2H, m, CH₂), 2.11-2.02 (2H, m, CH₂), 1.78-1.67 (2H, m, CH₂), 1.65-1.55 (2H, m, CH₂); δ_C (75 MHz, CDCl₃): δ 199.9 (C=O), 187.1 (C-OH), 159.0 (C, Ar), 140.0 (C, Ar), 133.7 (CH, Ar), 116.5 (CH, Ar), 112.8 (CH, Ar), 109.0 (C, Ar), 107.5 (CCO), 55.6 (CH₃), 32.0 (CH₂), 24.5 (CH₂), 22.8 (CH₂), 21.6 (CH₂); MS (ES⁺) *m/z* 333 [MNa⁺, ⁷⁹Br], 335 [MNa⁺, ⁸¹Br]; HRMS (ES⁺) calcd. for C₁₄H₁₅BrNaO₃ [MNa⁺, ⁷⁹Br]: 333.0097; found: 333.0099.

7-Methoxy-1,2,3,4-tetrahydro-xanthen-9-one (174)

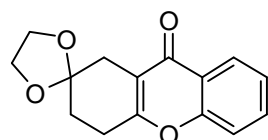
173 (100 mg, 0.34 mmol) was dissolved in dioxane (1 mL) and Pd₂(dba)₃ (8 mg, 0.008 mmol), Xphos (10 mg, 0.02 mmol) and Cs₂CO₃ (243 mg, 0.75 mmol) added according to General Method 2. Workup followed by column chromatography eluting with 5% EtOAc in petroleum ether gave the title compound as a white solid (47 mg, 60%). m.p. 102-104 °C (lit. m.p 116 °C); R_f 0.41 (10% EtOAc in petroleum ether); IR (film) 2940, 1609, 1484, 1438, 1030, 820, 758 cm⁻¹; δ_H (300 MHz, CDCl₃) 7.56 (1H, d, *J* = 3.0, ArH), 7.30 (1H, d, *J* = 8.9, ArH), 7.19 (1H, dd, *J* = 3.0, 8.9, ArH), 3.89 (3H, s, OCH₃), 2.70-2.62 (2H, m, CH₂), 2.62-2.54 (2H, m, CH₂), 1.92-1.82 (2H, m, CH₂), 1.82-1.70 (2H, m, CH₂); δ_C (75 MHz, CDCl₃) 176.9 (C=O), 163.0 (=C), 155.7 (C, Ar), 150.1 (C, Ar), 123.0 (C, Ar), 122.4 (CH, Ar), 118.4 (CH, Ar), 117.0 (=C), 104.2 (CH, Ar), 55.2 (CH₃), 27.5 (CH₂), 21.3 (CH₂), 21.1 (CH₂), 20.5 (CH₂); MS (ES⁺) *m/z* 231 [MH⁺]; HRMS (ES⁺) calcd. for C₁₄H₁₅O₃ [MH⁺]: 231.1016; found: 231.1014. Data is in accordance with literature values.²¹¹

7-(2-Bromo-benzoyl)-1,4-dioxaspiro[4.5]decan-8-one (175)

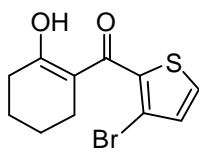
To lithium diisopropylamide (2M in THF/heptane/ethylbenzene, 1.14 mL, 2.28 mmol) and 1,4-cyclohexadione monoethylene acetal (355 mg, 2.28 mmol) in THF (2.5 mL) was added 2-bromo-benzoyl chloride (0.30 mL, 2.28 mmol) according to General Method 1a. Workup followed by column chromatography eluting with 50% DCM in petroleum ether gave the title compound as a white solid (159 mg, 21%). m.p. 106-107 °C; R_f = 0.19 (10% EtOAc in petroleum ether); IR (film) 2896, 1430, 1307, 1242, 1055, 947, 858, 1562, 775 cm⁻¹; δ_H (300 MHz, CDCl₃) 15.80 (1H, s, OH), 7.59 (1H, dd, *J* = 1.5, 7.7 Hz, ArH), 7.38 (1H, dt, *J* = 1.5, 7.7, ArH), 7.27 (1H, dt, *J* = 1.5, 7.7,

ArH), 7.21 (1H, dd, $J = 1.5, 7.7$, ArH), 3.96-3.89 (4H, m, 2CH₂), 2.69 (2H, t, $J = 6.9$, CH₂), 2.30 (2H, s, CH₂), 1.90 (2H, t, $J = 6.9$, CH₂); δ_C (100 MHz, CDCl₃): δ 192.6 (C=O), 186.3 (COH), 138.9 (C, Ar), 132.9 (CH, Ar), 130.7 (CH, Ar), 127.6 (CH, Ar), 127.6 (CH, Ar), 118.8 (C, Ar), 107.1 (OCO), 105.3 (CCO), 64.57 (2 x acetal CH₂), 34.3 (CH₂), 30.7 (CH₂), 30.0 (CH₂); MS (ES⁺) m/z 361 [MNa⁺, ⁷⁹Br], 363 [MNa⁺, ⁸¹Br]; HRMS (ES⁺) calcd. for C₁₅H₁₅BrNaO₄ [MNa⁺, ⁷⁹Br]: 361.0046; found 361.0047. Anal. calcd. for C₁₅H₁₅O₄Br: C 53.12; H 4.46 %. Found: C 52.98; H 4.46 %.

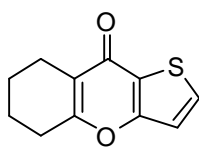
2-Dioxa-spiro-1,2,3,4-tetrahydro-xanthen-9-one (176)



175 (100 mg, 0.29 mmol) was dissolved in dioxane (1 mL) and Pd₂(dba)₃ (7 mg, 0.007 mmol), Xphos (8 mg, 0.018 mmol) and Cs₂CO₃ (211 mg, 0.65 mmol) added according to General Method 2. Workup followed by column chromatography eluting with hexane/ DCM/ acetone (10:3:1) gave the title compound as a white solid (55 mg, 72%). m.p. 182-183 °C; R_f = 0.16 (hexane/ DCM/ acetone 10:3:1); IR (film) 2890, 1608, 1466, 1148, 1094, 1060, 1003, 764 cm⁻¹; δ_H (400 MHz, CDCl₃) δ 8.18 (1H, dd, $J = 1.6, 7.8$, ArH), 7.62 (1H, dt, $J = 1.6, 7.8$, ArH), 7.43-7.31 (2H, m, ArH), 4.11-3.98 (4H, m, CH₂), 2.93 (2H, t, $J = 6.8$, CH₂), 2.81 (2H, s, CH₂), 2.04 (2H, t, $J = 6.8$, CH₂); δ_C (100 MHz, CDCl₃) 177.5 (C=O), 162.6 (=C), 155.9 (C, Ar), 133.2 (CH, Ar), 125.7 (CH, Ar), 124.6 (CH, Ar), 122.8 (C, Ar), 117.6 (CH, Ar), 116.0 (OCO), 107.1 (=C), 64.7 (2 x CH₂), 31.1 (CH₂), 30.7 (CH₂), 27.3 (CH₂); MS (ES⁺) m/z 259 [MH⁺]; HRMS (ES⁺) calcd. for C₁₅H₁₅O₄ [MH⁺]: 259.0965; found: 259.0962.

(3-Bromothiophen-2-yl)(2-hydroxycyclohex-1-enyl)methanone (177)

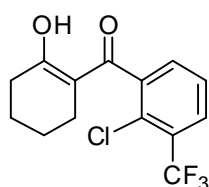
To lithium diisopropylamide (2M in THF/heptane/ethylbenzene, 2.10 mL, 4.26 mmol) and cyclohexanone (0.44 mL, 4.26 mmol) in THF (5 mL) was added 3-bromo-thiophene-2-carbonyl chloride (961 mg, 4.26 mmol) according to General Method 1a. Workup followed by column chromatography eluting with 5% EtOAc in petroleum ether gave the title compound as an orange oil (404 mg, 34%) as a mixture of the diketone and enol forms (1:1). $R_f = 0.62$ and 0.24 (10% EtOAc in petroleum ether); IR (film) 2939, 1706, 1652, 872 cm^{-1} ; δ_H (400 MHz, CDCl_3) 16.11 (1H, s, OH), 7.53 (1H, d, $J = 5.3$ Hz, diketone ArH), 7.39 (1H, d, $J = 5.3$, enol ArH), 7.07 (1H, d, $J = 5.3$, diketone ArH), 7.00 (1H, d, $J = 5.3$, enol ArH), 4.63-4.57 (1H, m, diketone CH), 2.60-2.54 (2H, m, CH_2), 2.51-2.46 (2H, t, $J = 6.5$, CH_2), 2.41-2.36 (2H, t, $J = 6.5$, CH_2), 2.24-2.16 (2H, m, CH_2), 2.13-2.05 (2H, m, CH_2), 2.03-1.95 (2H, m, CH_2), 1.81-1.72 (2H, m, CH_2), 1.69-1.61 (2H, m, CH_2); δ_C (100 MHz, CDCl_3) 207.9 (diketone C=O), 190.9 (enol C=O), 189.9 (diketone COH), 182.3 (enol COH), 138.7 (C), 133.6 (CH, Ar), 133.2 (C), 132.8 (CH, Ar), 131.0 (CH, Ar), 127.9 (CH, Ar), 114.0 (C), 111.2 (C), 109.1 (C), 60.8 (enol HCCO), 42.8 (CH_2), 33.0 (CH_2), 29.8 (CH_2), 27.6 (CH_2), 25.3 (CH_2), 23.8 (CH_2), 23.0 (CH_2), 21.6 (CH_2); MS (ES^+) m/z 309 [MNa^+ , ^{79}Br], 311 [MNa^+ , ^{81}Br]; HRMS (ES^+) calcd. for $\text{C}_{11}\text{H}_{11}\text{O}_2\text{BrS}$ [MNa^+ , ^{79}Br]: 310.9535; found: 310.9537.

5,6,7,8-Tetrahydro-4-oxa-1-thia-cyclopenta[b]naphthalen-9-one (178)

177 (100 mg, 0.35 mmol) was dissolved in dioxane (1 mL) and $\text{Pd}_2(\text{dba})_3$ (8 mg, 0.009 mmol), Xphos (10 mg, 0.02 mmol) and Cs_2CO_3 (250 mg, 0.77 mmol) added according to General Method 2. Workup followed by column chromatography eluting with 20% EtOAc in

petroleum ether gave the title compound as a white solid (43 mg, 60%). m.p. 148-149 °C; $R_f = 0.56$ (20% EtOAc in petroleum ether); IR (film) 3066, 2944, 1598, 1460, 1419, 1139, 1032, 750 cm^{-1} ; δ_H (400 MHz, CDCl_3) 7.62 (1H, d, $J = 5.4$, ArH), 7.07 (1H, d, $J = 5.4$, ArH), 2.73-2.64 (2H, m, CH_2), 2.63-2.55 (2H, m, CH_2), 1.93-1.82 (2H, m, CH_2), 1.82-1.72 (2H, m, CH_2); δ_C (100 MHz, CDCl_3) 174.1 (C=O), 162.6 (=C), 158.3 (C, Ar), 131.3 (CH, Ar), 123.9 (C, Ar), 118.6 (=C), 117.6 (CH, Ar), 27.8 (CH_2), 22.0 (CH_2), 21.7 (CH_2), 21.1 (CH_2); MS (ES^+) m/z 207 [MH^+]; HRMS (ES^+) calcd. for $\text{C}_{11}\text{H}_{11}\text{O}_2\text{S}$ [MH^+]: 207.0474; found: 207.0471.

(2-Chloro-3-(trifluoromethyl)phenyl)(2-hydroxycyclohex-1-enyl)methanone

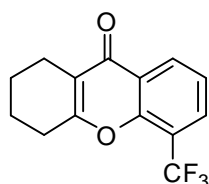


(179)

To lithium diisopropylamide (2M in THF/heptane/ethylbenzene, 1.03 mL, 2.06 mmol) and cyclohexanone (0.21 mL, 2.06 mmol) in THF (5 mL) was added 2-chloro-3 (trifluoromethyl)benzoyl chloride (500 mg, 2.06 mmol) according to General Method 1a. Workup followed by column chromatography eluting with 5% EtOAc in petroleum ether gave the title compound as a colourless oil which crystallised on standing at room temperature (298 mg, 48%). m.p. 80-81 °C; $R_f = 0.52$ (10% EtOAc in petroleum ether); IR (film) 2938, 2360, 1559, 1304, 1118, 816, 743 cm^{-1} ; δ_H (400 MHz, CDCl_3) 15.70 (1H, s, OH), 7.75 (1H, d, $J = 7.6$ Hz, ArH), 7.50-7.38 (2H, m, ArH), 2.53-2.45 (2H, m, CH_2), 2.03 (2H, br s, CH_2), 1.79-1.71 (2H, m, CH_2), 1.66-1.58 (2H, m, CH_2); δ_C (100 MHz, CDCl_3) 191.1 (C=O), 187.5 (COH), 139.8 (C, Ar), 130.9 (CH, Ar), 129.3 (q, $^2J_{\text{FC}} = 32$, C- CF_3), 128.6 (q, $^3J_{\text{FC}} = 5$, CH, Ar), 127.1 (CH, Ar), 122.7 (q, $^1J_{\text{FC}} = 272$, CF_3), 107.8 (CCO), 32.0 (CH_2), 24.3 (CH_2), 22.7 (CH_2), 21.5 (CH_2); MS (ES^+) m/z 305 [MH^+ , ^{35}Cl], 307 [MH^+ , ^{37}Cl]; HRMS (ES^+) calcd. for $\text{C}_{14}\text{H}_{13}\text{ClF}_3\text{O}_2$ [MH^+ ,

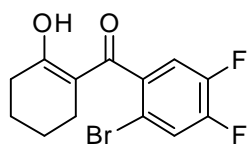
³⁵Cl]: 305.0551; found 305.0549. Anal. calcd. for C₁₄H₁₂O₂ClF₃: C 55.19; H 3.97
%. Found: C 55.07; H 3.96 %.

5-Trifluoromethyl-1,2,3,4-tetrahydro-xanthen-9-one (180)



179 (100 mg, 0.33 mmol) was dissolved in dioxane (1 mL) and Pd₂(dba)₃ (8 mg, 0.008 mmol), Xphos (9 mg, 0.020 mmol) and Cs₂CO₃ (235 mg, 0.72 mmol) added according to General Method 2. Workup followed by column chromatography eluting with 10% EtOAc in petroleum ether gave the title compound as a white solid (72 mg, 82%). m.p. 138-140 °C. R_f = 0.49 (10% EtOAc in petroleum ether); IR (film) 2936, 2361, 1640, 1607, 1414, 1304, 1111, 759 cm⁻¹; δ_H (300 MHz, CDCl₃) 8.38 (1H, dd, *J* = 1.2, 7.6, ArH), 7.89 (1H, dd, *J* = 1.2, 7.6, ArH), 7.40 (1H, t, *J* = 7.6, ArH), 2.78-2.68 (2H, m, CH₂), 2.64-1.54 (2H, m, CH₂), 1.96-1.85 (2H, m, CH₂), 1.85-1.72 (2H, m, CH₂); δ_C (75 MHz, CDCl₃) 176.4 (C=O), 164.1 (=C), 152.7 (C, Ar), 130.4 (q, ³J_{FC} = 5, CH), 130.1 (CH, Ar), 122.8 (q, ¹J_{FC} = 271, CF₃), 124.0 (C, Ar), 123.5 (CH, Ar), 119.4 (q, ²J_{FC} = 32, CCF₃), 119.2 (=C), 28.0 (CH₂), 21.7 (CH₂), 21.4 (CH₂), 20.9 (CH₂); MS (ES⁺) *m/z* 291 [MNa⁺]; HRMS (ESI) calcd. for C₁₄H₁₁F₃NaO₂ [MNa⁺]: 291.0603; found: 291.0602.

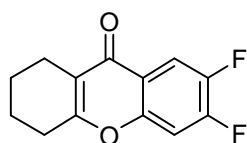
(2-Bromo-4,5-difluorophenyl)(2-hydroxycyclohex-1-enyl)methanone (181)



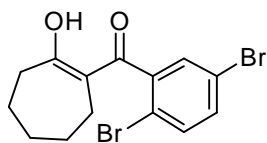
To lithium diisopropylamide (2M in THF/heptane/ethylbenzene, 1.76 mL, 3.50 mmol) and cyclohexanone (0.37 mL, 3.50 mmol) in THF (9 mL) was added 2-bromo-4,5-difluoro-benzoyl chloride (900 mg, 3.50 mmol) according to General Method 1a. Workup followed by column chromatography eluting with 1% EtOAc in petroleum ether gave the title compound as an off-white solid (567 mg,

51%). m.p. 92-94 °C; $R_f = 0.42$ (5% EtOAc in petroleum ether); IR (film) 3046, 2933, 1592, 1491, 1289, 786 cm^{-1} ; δ_{H} (400 MHz, CDCl_3) 15.65 (1H, s, OH), 7.44 (1H, dd, $J = 7.0, 9.0$ Hz, ArH), 7.07 (1H, dd, $J = 7.0, 9.0$, ArH), 2.51-2.46 (2H, m, CH_2), 2.09-2.04 (2H, m, CH_2), 1.79-1.72 (2H, m, CH_2), 1.67-1.59 (2H, m, CH_2); δ_{C} (100 MHz, CDCl_3) 190.4 (C=O), 188.2 (COH), 150.3 (dd, $^1J_{\text{FC}} = 253$, $^2J_{\text{FC}} = 13$, CF), 149.7 (dd, $^1J_{\text{FC}} = 253$, $^2J_{\text{FC}} = 13$, CF), 135.9 (dd, $^3J_{\text{FC}} = 9$, $^5J_{\text{FC}} = 5$, C), 122.1 (d, $^2J_{\text{FC}} = 20$, CH), 116.7 (d, $^2J_{\text{FC}} = 20$, CH), 113.1 (dd, $^3J_{\text{FC}} = 7$, $^5J_{\text{FC}} = 4$, C), 107.4 (CCO), 32.1 (CH_2), 24.5 (CH_2), 22.8 (CH_2), 21.5 (CH_2); MS (ES^+) m/z 339 [MNa^+ , ^{79}Br], 341 [MNa^+ , ^{81}Br]; HRMS (ES^+) calcd. for $\text{C}_{13}\text{H}_{11}\text{BrF}_2\text{NaO}_2$ [MNa^+ , ^{81}Br]: 340.9782; found: 340.9786.

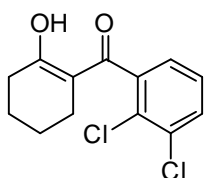
6,7-Difluoro-1,2,3,4-tetrahydro-xanthen-9-one (182)



181 (100 mg, 0.32 mmol) was dissolved in dioxane (1 mL) and $\text{Pd}_2(\text{dba})_3$ (8 mg, 0.008 mmol), Xphos (9 mg, 0.019 mmol) and Cs_2CO_3 (226 mg, 0.69 mmol) added according to General Method 2. Workup followed by column chromatography eluting with 10% EtOAc in petroleum ether gave the title compound as a white solid (58 mg, 78%). m.p. 151-152 °C; $R_f = 0.49$ (10% EtOAc in petroleum ether); IR (film) 3044, 2945, 1617, 1588, 1459, 1144, 892, 756 cm^{-1} ; δ_{H} (300 MHz, CDCl_3) 7.93 (1H, dd, $J = 8.8, 10.4$, ArH), 7.19 (1H, dd, $J = 6.2, 10.4$, ArH), 2.71-2.61 (2H, m, CH_2), 2.61-2.50 (2H, m, CH_2), 1.94-1.82 (2H, m, CH_2), 1.82-1.70 (2H, m, CH_2); δ_{C} (75 MHz, CDCl_3) 176.1 (C=O), 164.5 (=C), 153.5 (dd, $^1J_{\text{FC}} = 271$, $^2J_{\text{FC}} = 16$, CF), 152.3 (C, Ar), 148.1 (dd, $^1J_{\text{FC}} = 248$, $^2J_{\text{FC}} = 14$, CF), 120.0 (C, Ar), 118.2 (=C), 112.9 (d, $^2J_{\text{FC}} = 18$, CH), 106.6 (d, $^2J_{\text{FC}} = 21$, CH), 28.0 (CH_2), 21.8 (CH_2), 21.5 (CH_2), 20.9 (CH_2); MS (ES^+) m/z 259 [MNa^+]; HRMS (ES^+) calcd. for $\text{C}_{13}\text{H}_{10}\text{F}_2\text{NaO}_2$ [MNa^+]: 259.0541; found: 259.0539.

(2,5-Dibromophenyl)((Z)-2-hydroxycyclohept-1-enyl)methanone (185)

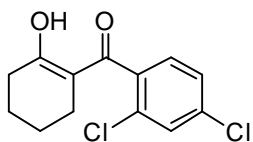
To lithium diisopropylamide (2M in THF/heptane/ethylbenzene, 7.0 mL, 0.014 mol) and cycloheptanone (1.67 mL, 0.014 mol) in THF (15 mL) was added 2,5-dibromo-benzoyl chloride (4.23 g, 0.014 mol) according to General Method 1. Workup followed by column chromatography (0.5% EtOAc in petroleum ether) gave the title compound as a white solid (2.00 g, 38%). m.p. 106 °C; IR (film) 2924, 1565, 810 cm^{-1} ; δ_{H} (300 MHz, CDCl_3) 16.10 (1H, s, OH), 7.47 (1H, m, ArH), 7.38 (1H, m, ArH), 7.36 (1H, m, ArH), 2.49 (2H, m, CH_2), 1.98 (2H, m, CH_2), 1.57 (4H, m, CH_2); δ_{C} (300 MHz, CDCl_3) 204.3 (C=O), 177.4 (COH), 138.5 (C), 133.7 (CH), 132.9 (CH), 131.0 (CH), 120.7 (C), 118.8 (C), 112.0 (C), 41.2 (CH_2), 30.9 (CH_2), 28.4 (CH_2), 27.0 (CH_2), 24.2 (CH_2); MS (ES^+) m/z 372 [MH^+]; HRMS (ES^+) calcd. for $\text{C}_{14}\text{H}_{14}\text{O}_2\text{Br}_2$ [MH^+]: 372.9433; found: 372.9433.

(2,3-Dichloro-phenyl)-(2-hydroxy-cyclohex-1-enyl)methanone (194)

To diisopropylamine (2.7 mL, 19.09 mmol), *n*-BuLi (2.5 M in hexane, 7.6 mL, 19.09 mmol) and cyclohexanone (2.0 mL, 19.09 mmol) in THF (10 mL) was added 2,3 dichlorobenzoyl chloride (1.3 mL, 9.55 mmol) according to General Method 1b. Workup followed by column chromatography eluting with 35% EtOAc in petroleum ether gave the title compound as a white solid (2.12 g, 82%). m.p. 101-102 °C; IR (film) 2935, 1557, 1410, 1316, 1153, 900, 795 cm^{-1} ; δ_{H} (400 MHz, CDCl_3) 15.71 (1H, s, enol), 7.50 (1H, dd, $J = 1.5, 7.8$, ArH), 7.27 (1H, t, $J = 7.8$, ArH), 7.13 (1H, dd, $J = 1.5, 7.8$, ArH), 2.48 (2H, t, $J = 6.5$, CH_2), 2.05 (2H, brs, CH_2), 1.78-1.70 (2H, m, CH_2), 1.64-1.57 (2H, m, CH_2); δ_{C} (100 MHz, CDCl_3) 191.6 (C=O), 187.4 (COH), 139.4 (C, Ar), 133.7 (C, Ar), 131.0 (CH, Ar), 128.8 (C, Ar), 127.9 (CH, Ar), 125.7 (CH, Ar),

107.8 (=C), 32.0 (CH₂), 24.4 (CH₂), 22.8 (CH₂), 21.6 (CH₂); MS (ES⁺) *m/z* 271 [MH⁺, ³⁵Cl, ³⁵Cl], 273 [MH⁺, ³⁵Cl, ³⁷Cl], 275 [MH⁺, ³⁷Cl, ³⁷Cl]; HRMS (ES⁺) calcd. for C₁₃H₁₂Cl₂NaO₂ [MNa⁺, ³⁵Cl, ³⁵Cl]: 293.0107; found 293.0106.

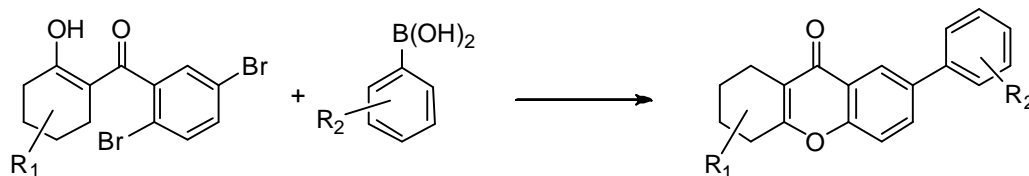
(2,4-Dichloro-phenyl)-(2-hydroxy-cyclohex-1-enyl)methanone (195)



To diisopropylamine (2.7 mL, 19.09 mmol), *n*-BuLi (2.5 M in hexane, 7.6 mL, 19.09 mmol) and cyclohexanone (2.0 mL, 19.09 mmol) in THF (10 mL) was added 2,4 dichlorobenzoyl chloride (1.3 mL, 9.55 mmol) according to General Method 1b. Workup followed by column chromatography eluting with 35% DCM in petroleum ether gave a pale pink oil which solidified on standing at room temperature. Trituration with Et₂O and filtration gave the title compound as a white solid (2.02 g, 78%). m.p. 62-63 °C; IR (film) 2951, 1584, 1409, 1100, 822, 781 cm⁻¹; δ_H (400 MHz, CDCl₃) 15.81 (1H, s, enol), 7.44 (1H,d, *J* = 2.0, ArH), 7.31 (1H, dd, *J* = 2.0, 8.1, ArH), 7.18 (1H, d, *J* = 8.1, ArH); δ_C (100 MHz, CDCl₃) 190.7 (C=O), 188.1 (COH), 135.8 (C, Ar), 131.4 (C, Ar), 129.8 (CH, Ar), 128.8 (CH, Ar), 127.4 (CH, Ar), 108.1 (=C), 32.3 (CH₂), 24.5 (CH₂), 22.9 (CH₂), 21.7 (CH₂), one quaternary carbon not observed; MS (ES⁺) *m/z* 271 [MH⁺, ³⁵Cl, ³⁵Cl], 273 [MH⁺, ³⁵Cl, ³⁷Cl], 275 [MH⁺, ³⁷Cl, ³⁷Cl]; HRMS (ES⁺) calcd. for C₁₃H₁₂Cl₂NaO₂ [MNa⁺, ³⁵Cl, ³⁵Cl]: 293.0107; found 293.0108.

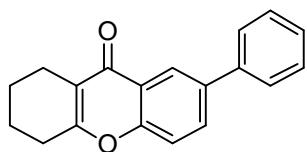
Synthesis of 7-arylated tetrahydroxanthenes by sequential C–O and C–C bond construction

General Method 4:

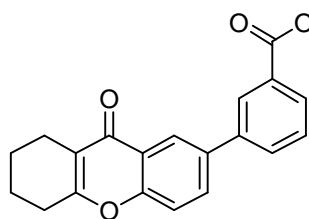


Ketone (1.0 molar equiv) was dissolved in dioxane (1 mL) and $\text{Pd}_2(\text{dba})_3$ (2.5 mol%), Cs_2CO_3 (2.2 molar equiv), Xphos (6 mol%) and the appropriate boronic acid (3.0 molar equiv), alkyne (1.3 equiv.) or alkene (5 equiv.) were added. The mixture was heated to reflux for 2.5 h. After allowing the mixture to cool to room temperature, the mixture was filtered through Celite[®] washing with CH_2Cl_2 (5 x 10 mL). The combined organic phases were dried (MgSO_4), filtered and the solvent removed *in vacuo*. Column chromatography provided the title compounds.

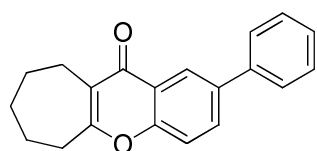
7-Phenyl-1,2,3,4-tetrahydro-xanthen-9-one (103)



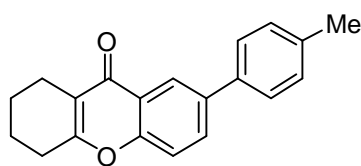
172 (100 mg, 0.28 mmol) was dissolved in dioxane (1 mL) and $\text{Pd}_2(\text{dba})_3$ (6 mg, 0.007 mmol), Xphos (8 mg, 0.02 mmol), Cs_2CO_3 (199 mg, 0.61 mmol) and phenyl boronic acid (102 mg, 0.83 mmol) added according to General Method 4. Workup followed by column chromatography (10% EtOAc in petroleum ether) gave the title compound as a white solid (60 mg, 78%). Data as previously reported.

3-(9-Oxo-5,7,8,9-tetrahydro-6H-xanthen-2-yl)benzoic acid methyl ester (105)

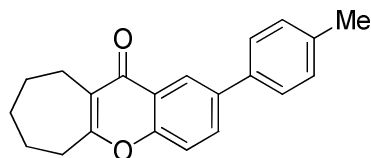
172 (30 mg, 0.08 mmol) was dissolved in dioxane (1 mL) and Pd₂(dba)₃ (2 mg, 0.002 mmol), Xphos (2 mg, 0.005 mmol), Cs₂CO₃ (60 mg, 0.18 mmol) and 3-methoxycarbonyl phenylboronic acid (45 mg, 0.25 mmol) added according to General Method 4. Workup followed by column chromatography (10% EtOAc in petroleum ether) gave the title compound as a white solid (19 mg, 68%). Data as previously reported.

7,8,9,10-Tetrahydro-2-phenylcyclohepta[b]chromen-11(6H)-one (186)

185 (100 mg, 0.27 mmol) was dissolved in dioxane (1 mL) and Pd₂(dba)₃ (6 mg, 0.007 mmol), Xphos (8 mg, 0.02 mmol) Cs₂CO₃ (192 mg, 0.59 mmol) and phenylboronic acid (98 mg, 0.80 mmol) added according to General Method 4. Workup followed by column chromatography (hexane/ acetone/ ether 8:1:1) gave the title compound as a white solid (55 mg, 71%). m.p. 148 °C; IR (film) 2918, 1611, 1146, 830, 765, 698 cm⁻¹; δ_H (400 MHz, CDCl₃) 8.43 (1H, d, *J* = 2.3, ArH), 7.86 (1H, dd, *J* = 2.3, 6.5, ArH), 7.67 (2H, d, *J* = 6.5, ArH), 7.48 (3H, t, *J* = 6.5, ArH), 7.39 (1H, t, *J* = 6.5, ArH), 2.92-2.86 (2H, m, CH₂), 2.86-2.79 (2H, m, CH₂), 1.92-1.83 (2H, m, CH₂), 1.82-1.73 (2H, m, CH₂), 1.68-1.57 (2H, m, CH₂); δ_C (100 MHz, CDCl₃) 177.1 (C=O), 169.0 (=C), 155.2 (C), 139.7 (C, Ar), 137.7 (C, Ar), 131.8 (CH, Ar), 128.9 (CH, Ar), 127.6 (CH, Ar), 127.2 (CH, Ar), 124.0 (CH, Ar), 123.1 (C, Ar), 123.0 (C, Ar), 118.3 (CH, Ar), 34.8 (CH₂), 32.0 (CH₂), 26.5 (CH₂), 25.0 (CH₂), 22.4 (CH₂); MS (ES⁺) *m/z* 291 [MH⁺]; HRMS (ES⁺) calcd. for C₂₀H₁₈O₂ [MH⁺]: 291.1380; found: 291.1391.

7-*p*-Tolyl-1,2,3,4-tetrahydro-xanthen-9-one (187)

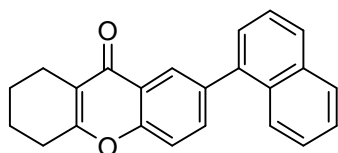
172 (100 mg, 0.28 mmol) was dissolved in dioxane (1 mL) and Pd₂(dba)₃ (6 mg, 0.007 mmol), Xphos (8 mg, 0.02 mmol), Cs₂CO₃ (199 mg, 0.61 mmol) and *p*-tolylboronic acid (113 mg, 0.83 mmol) added according to General Method 4. Workup followed by column chromatography (5% EtOAc in petroleum ether) gave the title compound as a white solid (69 mg, 85%). m.p. 154-155 °C; IR (film) 2933, 1625, 1607, 1463, 1407, 1146, 810, 752, 702, 668 cm⁻¹; δ_H (400 MHz, CDCl₃) 8.39 (1H, d, *J* = 2.2, ArH), 7.83 (1H, dd, *J* = 2.2, 8.2, ArH), 7.56 (2H, d, *J* = 8.2, ArH), 7.43 (1H, d, *J* = 8.2, ArH), 7.27 (2H, d, *J* = 8.2, ArH), 2.73-2.65 (2H, m, CH₂), 2.65-2.58 (2H, m, CH₂), 2.40 (2H, m, CH₂), 1.94-1.84 (2H, m, CH₂), 1.83-1.74 (2H, m, CH₂); δ_C (100 MHz, CDCl₃) 177.8 (C=O), 163.8 (=C), 155.2 (C, Ar), 137.5 (C, Ar), 137.4 (C, Ar), 137.4 (C, Ar), 136.8 (C, Ar), 131.7 (2 x CH, Ar), 129.7 (2 x CH, Ar), 127.0 (CH, Ar), 123.3 (CH, Ar), 118.4 (=C), 118.1 (CH, Ar), 28.2 (CH₂), 22.0 (CH₂), 21.7 (CH₃), 21.1 (CH₂), 21.1 (CH₂); MS (ES⁺) *m/z* 313 [MNa⁺]; HRMS (ES⁺) calcd. for C₂₀H₁₈NaO₂ [MNa⁺]: 313.1199; found: 313.1194.

7,8,9,10-Tetrahydro-2-*p*-tolylcyclohepta[*b*]chromen-11(6H)-one (188)

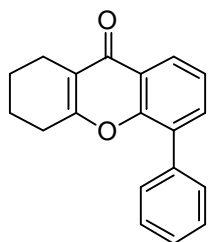
185 (100 mg, 0.27 mmol) was dissolved in dioxane (1 mL) and Pd₂(dba)₃ (6 mg, 0.007 mmol), Xphos (8 mg, 0.02 mmol), Cs₂CO₃ (192 mg, 0.59 mmol) and *p*-tolylboronic acid (109 mg, 0.80 mmol) added according to General Method 4. Workup followed by column chromatography (5% EtOAc in petroleum ether) gave the title compound as a white solid (70 mg, 85%). m.p. 148 °C; IR (film) 2924, 1606, 1444, 1149, 804, 698 cm⁻¹; δ_H (300 MHz, CDCl₃) 8.40 (1H, d, *J* = 2.2, ArH), 7.83 (1H, dd, *J* = 2.2, 8.7, ArH), 7.55 (2H, d, *J* = 7.5, ArH), 7.43 (1H, d, *J* = 8.7,

ArH), 7.26 (2H, d, $J = 7.5$, ArH), 2.91-2.85 (2H, m, CH₂), 2.85-2.78 (2H, m, CH₂), 2.10 (3H, s, CH₃), 1.92-1.82 (2H, m, CH₂), 1.82-1.72 (2H, m, CH₂) 1.67-1.58 (2H, m, CH₂); δ_C (75 MHz, CDCl₃) 176.5 (C=O), 168.4 (=C), 154.4 (C, Ar), 137.0 (C, Ar), 136.9 (C, Ar), 136.2 (C, Ar), 131.0 (CH, Ar), 129.0 (2 x CH, Ar), 126.4 (2 x CH, Ar), 123.0 (CH, Ar), 122.4 (=C), 122.3 (C, Ar), 117.6 (CH, Ar), 34.2 (CH₂), 31.4 (CH₂), 25.8 (CH₂), 24.4 (CH₂), 21.8 (CH₂), 20.5 (CH₃); MS (ES⁺) m/z 327 [MNa⁺]; HRMS (ES⁺) calcd. for C₂₁H₂₀O₂ [MNa⁺]: 327.1356; found: 327.1351.

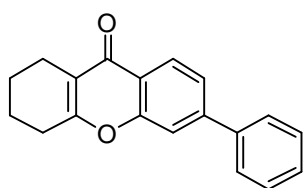
7-Naphthalen-1-yl-1,2,3,4-tetrahydro-xanthen-9-one (189)



172 (100 mg, 0.28 mmol) was dissolved in dioxane (1 mL) and Pd₂(dba)₃ (6 mg, 0.007 mmol), Xphos (8 mg, 0.02 mmol), Cs₂CO₃ (199 mg, 0.61 mmol) and naphthylene boronic acid (143 mg, 0.83 mmol) added according to General Method 4. Workup followed by column chromatography (5% EtOAc in petroleum ether) gave the title compound as a white solid (55 mg, 60%). m.p. 171-173 °C; $R_f = 0.27$ (5% EtOAc in petroleum ether); IR (film) 2935, 1640, 1606, 1151, 768 cm⁻¹; δ_H (300 MHz, CDCl₃) 8.34 (1H, d, $J = 2.1$, ArH), 7.91 (2H, t, $J = 8.5$, ArH), 7.83 (1H, d, $J = 8.5$, ArH), 7.75 (1H, dd, $J = 2.1, 8.5$, ArH), 7.58-7.38 (5H, m, ArH), 2.78-2.67 (2H, m, CH₂), 2.67-2.56 (2H, m, CH₂), 1.97-1.85 (2H, m, CH₂), 1.85-1.74 (2H, m, CH₂); δ_C (100 MHz, CDCl₃) 177.7 (C=O), 164.0 (=C), 155.3 (C, Ar), 138.7 (C, Ar), 137.1 (C, Ar), 134.9 (CH, Ar), 133.8 (C, Ar), 131.5 (C, Ar), 128.4 (CH, Ar), 128.1 (CH, Ar), 127.4 (CH, Ar), 126.7 (CH, Ar), 126.3 (CH, Ar), 125.9 (CH, Ar), 125.6 (CH, Ar), 125.4 (CH, Ar), 123.1 (C, Ar), 118.6 (=C), 117.6 (CH, Ar), 28.2 (CH₂), 22.0 (CH₂), 21.7 (CH₂), 21.1 (CH₂); MS (ES⁺) m/z 327 [MH⁺]; HRMS (ES⁺) calcd. for C₂₃H₁₈NaO₂ [MNa⁺]: 349.1199; found: 349.1196.

5-Phenyl-1,2,3,4-tetrahydro-xanthen-9-one (196)

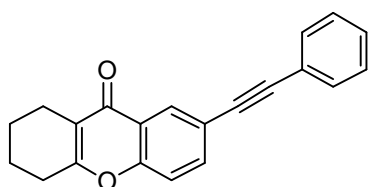
194 (100 mg, 0.37 mmol) was dissolved in dioxane (1 mL) and Pd₂(dba)₃ (8 mg, 0.009 mmol), Xphos (11 mg, 0.02 mmol), Cs₂CO₃ (264 mg, 0.81 mmol) and phenyl boronic acid (135 mg, 1.11 mmol) added according to General Method 2. Workup followed by column chromatography (10% EtOAc in petroleum ether) gave the title compound as an off-white solid (86 mg, 84%). m.p. 152 °C; IR (film) 2939, 1624, 1425, 1409, 1156, 758, 698 cm⁻¹; δ_H (400 MHz, CDCl₃) 8.22 (1H, dd, *J* = 1.7, 7.9, ArH), 7.65 (1H, dd, *J* = 1.7, 7.9, ArH), 7.58 (2H, d, *J* = 7.9, ArH), 7.50-7.45 (2H, m, ArH), 7.44-7.38 (2H, m, ArH), 2.64-2.57 (4H, m, CH₂), 1.89-1.81 (2H, m, CH₂), 1.80-1.73 (2H, m, CH₂); δ_C (100 MHz, CDCl₃) 177.9 (C=O), 164.0 (=C), 152.8 (C, Ar), 136.4 (C, Ar), 134.0 (CH, Ar), 131.1 (C, Ar), 129.6 (CH, Ar), 128.4 (CH, Ar), 127.9 (CH, Ar), 125.2 (CH, Ar), 124.4 (CH, Ar), 123.7 (C, Ar), 118.3 (=C), 28.2 (CH₂), 21.9 (CH₂), 21.7 (CH₂), 21.1 (CH₂); MS (ES⁺) *m/z* 277 [MH⁺]; HRMS (ES⁺) calcd. for C₁₉H₁₆NaO₂ [MNa⁺]: 299.1043; found: 299.1041.

6-Phenyl-1,2,3,4-tetrahydro-xanthen-9-one (197)

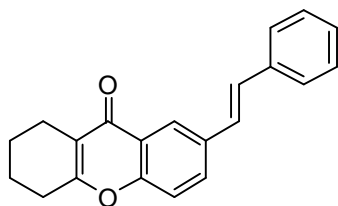
195 (100 mg, 0.37 mmol) was dissolved in dioxane (1 mL) and Pd₂(dba)₃ (8 mg, 0.009 mmol), Xphos (11 mg, 0.02 mmol), Cs₂CO₃ (264 mg, 0.81 mmol) and phenyl boronic acid (135 mg, 1.11 mmol) added according to General Method 2. Workup followed by column chromatography (10% EtOAc in petroleum ether) gave the title compound as a white solid (81 mg, 79%). m.p. 143-144 °C; IR (film) 2932, 1636, 1612, 1424, 1152, 754 cm⁻¹; δ_H (400 MHz, CDCl₃) 8.24 (1H, d, *J* = 7.2, ArH), 7.65 (2H, dd, *J* = 1.5, 7.2, ArH), 7.59 (2H, dd, *J* = 1.5, 7.2, ArH), 7.48 (2H, dt, *J* = 1.5, 7.2, ArH), 7.42 (1H, m, ArH), 2.72-2.66 (2H, m, CH₂), 2.64-2.58 (2H, m, CH₂),

1.94-1.84 (2H, m, CH₂), 1.82-1.74 (2H, m, CH₂); δ_{C} (100 MHz, CDCl₃) 177.6 (C=O), 164.0 (=C), 156.3 (C, Ar), 146.1 (C, Ar), 139.5 (C, Ar), 129.1 (CH, Ar), 128.6 (CH, Ar), 127.4 (CH, Ar), 126.3 (CH, Ar), 123.6 (CH, Ar), 122.0 (C, Ar), 118.6 (=C), 115.7 (CH), 28.3 (CH₂), 22.9 (CH₂), 21.8 (CH₂), 21.1 (CH₂); MS (ES⁺) m/z 277 [MH⁺]; HRMS (ES⁺) calcd. for C₁₉H₁₆NaO₂ [MNa⁺]: 299.1043; found: 299.1044.

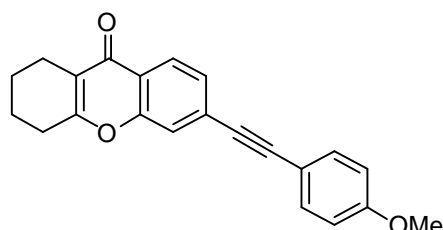
7-Phenylethynyl-1,2,3,4-tetrahydroxanthen-9-one (199)



172 (100 mg, 0.28 mmol) was dissolved in dioxane (1 mL) and Pd₂(dba)₃ (6 mg, 0.007 mmol), Xphos (8 mg, 0.02 mmol), Cs₂CO₃ (199 mg, 0.61 mmol) and phenylacetylene (0.04 mL, 0.36 mmol) was added according to General Method 2. Workup followed by column chromatography (10% EtOAc in petroleum ether) gave the title compound as a yellow solid (56 mg, 67%). m.p. 163-165 °C; IR (film) 3051, 2928, 1633, 1607, 1437, 1307, 1152, 833, 747, 686 cm⁻¹; δ_{H} (300 MHz, CDCl₃) 8.36 (1H, d, J = 2.2, ArH), 7.73 (1H, dd, J = 2.2, 8.7, ArH), 7.57-7.52 (2H, m, ArH), 7.39-7.33 (4H, m, ArH), 2.72-2.65 (2H, m, CH₂), 2.62-2.56 (2H, m, CH₂), 1.93-1.83 (2H, m, CH₂), 1.82-1.73 (2H, m, CH₂); δ_{C} (100 MHz, CDCl₃) 177.1 (C=O), 164.1 (=C), 155.5 (C, Ar), 135.8 (CH, Ar), 131.8 (CH, Ar), 129.3 (CH, Ar), 128.6 (CH, Ar), 128.5 (CH, Ar), 123.2 (C, Ar), 123.0 (C, Ar), 119.9 (C, Ar), 119.0 (=C), 118.1 (CH, Ar), 90.0 (\equiv C), 88.3 (\equiv C), 28.3 (CH₂), 22.0 (CH₂), 21.7 (CH₂), 21.1 (CH₂); MS (ES⁺) m/z 301 [MH⁺]; HRMS (ES⁺) calcd. for C₂₁H₁₆NaO₂ [MNa⁺]: 323.1043; found: 323.1040.

7-Styryl-1,2,3,4-tetrahydro-xanthen-9-one (201)

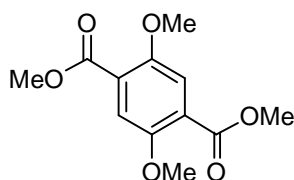
172 (100 mg, 0.28 mmol) was dissolved in dioxane (1 mL) and Pd₂(dba)₃ (6 mg, 0.07 mmol), Xphos (8 mg, 0.02 mmol), Cs₂CO₃ (199 mg, 0.61 mmol) and styrene (0.16 mL, 1.39 mmol) added according to General Method 2. Workup followed by column chromatography (10% EtOAc in petroleum ether) gave the title compound as a white solid (39 mg, 46%). m.p. 140-142 °C; IR (film) 2941, 1627, 1605, 1438, 813, 747, 687, 564 cm⁻¹; δ_H (300 MHz, CDCl₃) 8.28 (1H, d, *J* = 2.3, ArH), 7.77 (1H, dd, *J* = 2.3, 8.8, ArH), 7.53 (2H, d, *J* = 7.2, ArH), 7.41-7.34 (3H, m, ArH), 7.31-7.25 (1H, m, ArH), 7.16 (2H, s, HC=CH), 2.71-2.56 (4H, m, CH₂), 1.93-1.72 (4H, m, CH₂); δ_C (100 MHz, CDCl₃) 177.7 (C=O), 163.9 (=C), 155.4 (C, Ar), 137.7 (C, Ar), 134.0 (C, Ar), 130.9 (CH, Ar), 129.7 (=CAr), 128.8 (CH, Ar), 128.0 (CH, Ar), 127.2 (=CAr), 126.7 (CH, Ar), 123.3 (CH, Ar), 118.5 (=C), 118.2 (CH, Ar), 28.3 (CH₂), 22.0 (CH₂), 21.7 (CH₂), 21.1 (CH₂); MS (ES⁺) *m/z* 305 [MH⁺]; HRMS (ES⁺) calcd. for C₂₁H₁₈NaO₂ [MNa⁺]: 325.1199; found: 325.1197.

6-(4-Methoxy-phenylethynyl)-1,2,3,4-tetrahydroxanthen-9-one (203)

195 (100 mg, 0.37 mmol) was dissolved in dioxane (1 mL) and Pd₂(dba)₃ (8 mg, 0.009 mmol), Xphos (11 mg, 0.02 mmol), Cs₂CO₃ (264 mg, 0.81 mmol) and 4-methoxyphenylacetylene (0.06 mL, 0.48 mmol) added according to General Method 2. Workup followed by column chromatography (10% EtOAc in petroleum ether) gave the title compound as a yellow solid (122 mg, 82%). m.p. 139-140 °C; IR (film) 2938, 2209, 1624, 1614, 1603, 1251, 1151, 831 cm⁻¹; δ_H (300

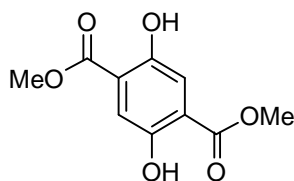
MHz, CDCl₃) 8.13 (1H, d, $J = 8.3$, ArH), 7.52-7.46 (3H, m, ArH), 7.43 (1H, dd, $J = 1.3, 8.3$, ArH), 6.89 (2H, d, $J = 8.7$, ArH), 3.83 (3H, s, OCH₃), 2.69-2.61 (2H, m, CH₂), 2.61-2.53 (2H, m, CH₂), 1.92-1.81 (2H, m, CH₂), 1.80-1.70 (2H, m, CH₂); δ_C (100 MHz, CDCl₃) 177.2 (C=O), 164.1 (=C), 162.2 (C, Ar), 155.6 (C, Ar), 133.4 (CH, Ar), 128.5 (C, Ar), 127.5 (CH, Ar), 125.7 (CH, Ar), 122.4 (C, Ar), 120.2 (CH, Ar), 118.8 (=C), 114.6 (CH, Ar), 114.2 (CH, Ar), 93.0 (\equiv C), 87.1 (\equiv C), 55.4 (CH₃), 28.2 (CH₂), 21.9 (CH₂), 21.7 (CH₂), 21.1 (CH₂); MS (ES⁺) m/z 331 [MH⁺]; HRMS (ES⁺) calcd. for C₂₂H₁₈NaO₃ [MNa⁺]: 353.1148; found: 353.1145.

2,5-Dimethoxy-terephthalic acid dimethyl ester (204)



K₂CO₃ (37 g, 0.27 mol) and MeI (24 mL, 0.39 mol) were added to a solution of **211** (8.82 g, 0.039 mol) in acetone (250 mL). The reaction mixture was stirred at room temperature for 65 h. The solids were filtered washing with acetone (50 mL) and the filtrate was concentration *in vacuo* to give a yellow solid. Trituration with Et₂O and filtration gave the title compound as a white solid (8.28 g, 84%). m.p. 142-143 °C; δ_H (400 MHz, CDCl₃) 7.40 (2H, s, ArH), 3.92 (6H, s, CH₃), 3.90 (6H, s, CH₃); δ_C (100 MHz, CDCl₃) 166.1 (C=O), 152.5 (C, Ar), 124.09 (C, Ar), 115.6 (CH, Ar), 56.9 (OCH₃), 52.6 (OCH₃); MS (ES⁺) m/z 255 [M+H⁺]. Data is in accordance with literature values.²¹²

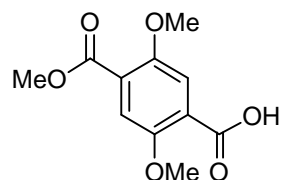
2,5-Dihydroxy-terephthalic acid dimethyl ester (211)



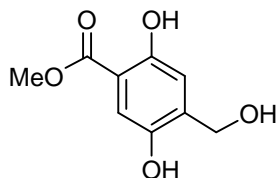
Dimethyl 2,5-dioxocyclohexane-1,4-dicarboxylate (1 g, 4.39 mmol) was added to AcOH (3 mL) and heated to 80 °C before adding NBS (780 mg, 4.39 mmol) carefully. After 1 h at 80 °C, the reaction mixture was allowed to cool to room temperature

and the product was filtered washing with AcOH (2 mL), ^tBuOMe (2 mL) and H₂O (2 mL). The solid was dried to give the title compound as a yellow solid (852 mg, 86%). m.p. 173-177 °C (lit. m.p 176-177 °C); δ_H (300 MHz, CDCl₃) 10.07 (2H, s, OH), 7.47 (2H, s, ArH), 3.98 (6H, s, OCH₃); δ_C (100 MHz, CDCl₃) 169.6 (C=O), 153.0 (C, Ar), 118.5 (C, Ar), 117.9 (CH, Ar), 52.9 (CH₃); MS (ES⁻) *m/z* 225 [M-H⁺]; HRMS (ES⁻) calcd. for C₁₀H₁₀O₆ [M-H⁺]: 225.0405; found: 225.0397. Data is in accordance with literature values.¹⁹³

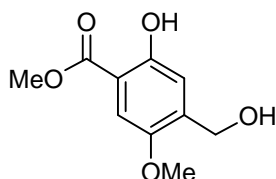
2,5-Dimethoxy-terephthalic acid monomethyl ester (222)



KOH (231 g, 4.13 mmol) dissolved in H₂O (2 mL) was added dropwise to a mixture of **204** (1 g, 3.94 mmol) in MeOH (5 mL) and THF (5 mL). The reaction mixture was stirred at room temperature for 18 h. The organic solvents were removed *in vacuo* and the resulting aqueous phase was extracted with EtOAc (2 x 10 mL) to remove any remaining starting material. The aqueous phase was then cooled to 0 °C, acidified using 2M HCl (3mL) and extracted with EtOAc (2 x 20 mL). The organic phase was separated, dried (MgSO₄), filtered and the solvent removed *in vacuo*. The resulting solid was purified using column chromatography eluting with 50% EtOAc in petroleum ether to give the title compound as a white solid (469 mg, 50%). m.p. 145-147 °C (lit. m.p 147-148 °C); IR (film) 2956, 1736, 1709, 1406, 1251, 1209, 1029 cm⁻¹; δ_H (300 MHz, CDCl₃) 10.87 (1H, brs, CO₂H), 7.80 (1H, s, ArH), 7.49 (1H, s, ArH), 4.10 (3H, s, CO₂CH₃), 3.95 (3H, s, OCH₃), 3.94 (3H, s, OCH₃); δ_C (100 MHz, CDCl₃) 165.7 (C=O), 164.6 (C=O), 153.6 (C, Ar), 151.2 (C, Ar), 125.5 (C, Ar), 121.3 (C, Ar), 116.8 (CH, Ar), 115.2 (CH, Ar), 57.5 (OCH₃), 56.8 (OCH₃), 52.8 (CO₂CH₃); MS (ES⁻) *m/z* 239 [M-H⁺]; HRMS (ES⁺) calcd. for C₁₁H₁₂NaO₆ [MNa⁺]: 263.0526; found: 263.0525.

2,5-Dihydroxy-4-hydroxymethyl-benzoic acid methyl ester (224)

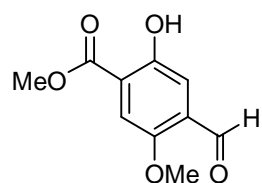
To a stirring solution of **211** (3.65 g, 16.15 mmol) in THF (70 mL) and H₂O (11 mL), cooled to 0 °C, was added NaBH₄ (1.83 g, 48.5 mmol). The reaction mixture was allowed to warm to room temperature and stirred for 1 h before recooling to 0 °C and quenching with 2M HCl until effervescence ceased (~15 mL). An aqueous saturated solution of NaHCO₃ (20 mL) was added to neutralise the mixture and the product was extracted with EtOAc (2 x 100 mL). The organic phase was washed with brine (50 mL), dried (MgSO₄), filtered and the solvent removed in vacuo to give the title compound as an off-white solid (2.2 g, 69%). m.p. 143-145 °C (lit. m.p 147-148 °C); IR (film) 3424, 1667, 1627, 1438, 1214, 1076, 788 cm⁻¹; δ_H (300 MHz, CD₃OD) 7.17 (1H, s, ArH), 6.95 (1H, s, ArH), 4.63 (2H, s, CH₂), 3.91 (3H, s, CH₃); δ_C (75 MHz, CDCl₃) 171.6 (C=O), 156.3 (C, Ar), 147.9 (C, Ar), 139.3 (C, Ar), 116.4 (CH, Ar), 114.5 (CH, Ar), 111.5 (C, Ar), 60.4 (CH₂), 52.6 (OCH₃); MS (ES⁺) *m/z* 221 [MNa⁺]; HRMS (ES⁺) calcd. for C₉H₁₀NaO₅ [MNa⁺]: 221.0420; found: 221.0423. Data is in accordance with literature values.¹⁶²

2-Hydroxy-4-hydroxymethyl-5-methoxy-benzoic acid methyl ester (225)

224 (350 mg, 1.77 mmol) was dissolved in acetone (7 mL) and K₂CO₃ (1.7 g, 12.37 mmol) was added followed by MeI (1.1 mL, 17.68 mmol). The reaction mixture was stirred at room temperature overnight. The solvent was removed in vacuo and treated with 2M HCl (10 mL) and extracted with DCM (3 x 10 mL). The organic phase was separated, dried (MgSO₄), filtered and the solvent removed in vacuo to give the title compound as a white solid (128 mg, 34%). m.p. 117-118 °C; IR (film) 2919, 1672, 1203, 1176, 1036, 788, 716 cm⁻¹; δ_H (300 MHz, CDCl₃) 10.43 (1H, s,

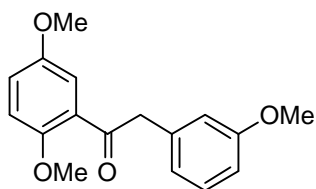
phenolic OH), 7.23 (1H, s, ArH), 6.99 (1H, s, ArH), 4.68 (2H, d, $J = 6.6$, CH₂), 3.97 (3H, s, CH₃), 3.84 (3H, s, CH₃), 2.29 (1H, t, $J = 6.6$, CH₂OH); δ_C (150 MHz, CDCl₃) 170.3 (C=O), 156.5 (C, Ar), 149.8 (C, Ar), 138.6 (C, Ar), 117.3 (CH, Ar), 110.6 (C, Ar), 109.4 (CH, Ar), 61.7 (CH₂), 55.9 (CH₃), 52.4 (CH₃); MS (ES⁺) m/z 213 [MH⁺]; HRMS (ES⁺) calcd. for C₁₀H₁₃O₅ [MH⁺]: 213.0757; found: 213.0756.

4-Formyl-2-hydroxy-5-methoxy-benzoic acid methyl ester (226)



225 (128 mg, 0.60 mmol) was dissolved in DCM (10 mL) and MnO₂ (525 mg, 6.04 mmol) was added. The reaction mixture was stirred at room temperature for 65 h before filtering through a plug of Celite[®] washing with DCM (3 x 10 mL). The solvent was removed *in vacuo* to give the title compound as a yellow solid (116 mg, 91%). m.p. 139-141 °C; IR (film) 3236, 1677, 1212, 893, 786, 707 cm⁻¹; δ_H (300 MHz, CDCl₃) 10.43 (1H, s, HC=O), 10.25 (1H, s, OH), 7.39 (1H, s, ArH), 7.38 (1H, s, ArH), 3.99 (3H, s, CH₃), 3.90 (3H, s, CH₃); δ_C (100 MHz, CDCl₃) 189.3 (C=O), 169.6 (C=O), 155.3 (C, Ar), 153.7 (C, Ar), 130.4 (C, Ar), 117.1 (CH, Ar), 117.0 (C, Ar), 112.1 (CH, Ar), 56.3 (CH₃), 52.9 (CH₃); MS (ES⁺) m/z 233 [MNa⁺]; HRMS (ES⁺) calcd. for C₁₀H₁₀NaO₅ [MNa⁺]: 233.0420; found: 233.0423.

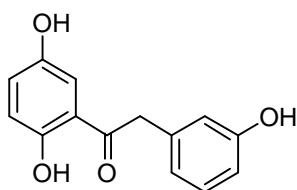
1-(2,5-Dimethoxy-phenyl)-2-(3-methoxy-phenyl)ethanone (232)



2,5-dimethoxyacetophenone (0.51 mL, 3.2 mmol), 3-bromoanisole (0.34 mL, 2.67 mmol), Pd(OAc)₂ (6 mg, 0.03 mmol), xantphos (31 mg, 0.05 mmol) and Na^tBuO (334 mg, 3.48 mmol) were combined in toluene (2.7 mL) and heated to 80 °C overnight. The reaction mixture was allowed to cool to room temperature and 2M HCl was added before extracting with Et₂O (2 x 10 mL). The organic phase was

washed with H₂O (20 mL), dried (MgSO₄), filtered and the solvent removed *in vacuo*. The resulting orange oil was purified by column chromatography eluting with 5% EtOAc in petroleum ether to give the title compound as a colourless oil (671 mg, 88%). IR (film) 2943, 2834, 1674, 1584, 1490, 1220, 1047, 1018; δ_{H} (300 MHz, CDCl₃) 7.26-7.18 (2H, m, ArH), 7.03 (1H, dd, $J = 3.2, 9.0$, ArH), 6.91 (1H, d, $J = 9.0$, ArH), 6.85-6.76 (2H, m, ArH), 4.30 (2H, s, CH₂), 3.89 (3H, s, CH₃), 3.79 (3H, s, CH₃), 3.78 (3H, s, CH₃); δ_{C} (100 MHz, CDCl₃) 199.6 (C=O), 159.7 (C, Ar), 153.6 (C, Ar), 153.0 (C, Ar), 136.8 (C, Ar), 129.4 (CH, Ar), 128.4 (C, Ar), 122.2 (CH, Ar), 120.2 (CH, Ar), 115.4 (CH, Ar), 114.4 (CH, Ar), 113.2 (CH, Ar), 112.2 (CH, Ar), 56.1 (CH₃), 55.9 (CH₃), 55.2 (CH₃), 50.2 (CH₃); MS (ES⁺) m/z 287 [MH⁺]; HRMS (ES⁺) calcd. for C₁₇H₁₉O₄ [MH⁺]: 287.1278; found: 287.1276.

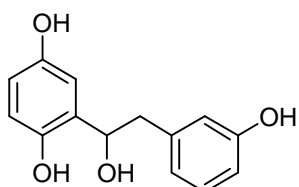
1-(2,5-Dihydroxy-phenyl)-2-(3-hydroxy-phenyl)ethanone (239)



232 (359 mg, 1.26 mmol) was dissolved in DCM and cooled to -78 °C. BBr₃ (1M in DCM) (4.39 mL, 4.39 mmol) was added cautiously and the reaction mixture was stirred at -78 °C for 6 h before allowing to warm to room temperature. The reaction mixture was poured over ice and H₂O (30 mL) and extracted with EtOAc (50 mL). The organic phase was separated, dried (MgSO₄), filtered and the solvent removed *in vacuo*. The resulting yellow solid was columned eluting with 50% EtOAc in petroleum ether to give the title compound as a yellow solid (272 mg, 89%). m.p. 170-171 °C; δ_{H} (400 MHz, CD₃OD) 7.32 (1H, d, $J = 3.0$, ArH), 7.12 (1H, t, $J = 8.0$, ArH), 6.99 (1H, dd, $J = 3.0, 9.0$, ArH), 6.79 (1H, d, $J = 9.0$, ArH), 6.74 (1H, d, $J = 8.0$, ArH), 6.73-6.71 (1H, m, ArH), 6.67 (1H, dd, $J = 2.4, 8.0$, ArH), 4.19 (2H, s, CH₂); δ_{C} (100 MHz, CDCl₃) 205.5 (C=O), 158.7 (C, Ar), 157.1 (C, Ar), 150.5 (C, Ar), 137.4 (C, Ar), 130.7 (CH, Ar), 126.0 (CH, Ar), 121.6 (CH, Ar), 120.1 (C, Ar),

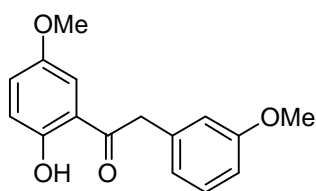
119.7 (CH, Ar), 117.2 (CH, Ar), 116.3 (CH, Ar), 114.9 (CH, Ar), 46.2 (CH₂). MS (ES⁺) *m/z* 267 [M+Na⁺]; HRMS (ES⁺) calcd. for C₁₄H₁₂NaO₄ [M+Na⁺]: 267.0628; found: 267.0627.

2-[1-Hydroxy-2-(3-hydroxy-phenyl)ethyl]benzene-1,4-diol (246)



239 (100 mg, 0.41 mmol) was dissolved in a mixture of THF (2 mL) and H₂O (0.3 mL) and cooled to 0 °C. NaBH₄ (46 mg, 1.23 mmol) added and once the effervescence had ceased, the reaction mixture was allowed to warm to room temperature for 10 min. The mixture was then recooled to 0 °C and was quenched with 2M HCl (5 mL) and was extracted with EtOAc (2 x 5 mL). The organic phase was separated, dried (MgSO₄), filtered and the solvent removed in vacuo to give the title compound as an orange oil (54 mg, 53 %). δ_H (400 MHz, CD₃OD) 7.05 (1H, t, *J* = 8.0, ArH), 6.72-6.67 (3H, m, ArH), 6.63-6.58 (2H, m, ArH), 6.52 (1H, dd, *J* = 3.0, 8.6, ArH), 5.08 (1H, dd, *J* = 4.6, 8.4, CHOH), 3.00 (1H, dd, *J* = 4.6, 13.6, CHH), 2.80 (1H, dd, *J* = 8.4, 13.6, CHH); δ_C (100 MHz, CDCl₃) 158.0 (C, Ar), 151.0 (C, Ar), 148.4 (C, Ar), 142.1 (C, Ar), 132.6 (C, Ar), 129.9 (CH, Ar), 121.9 (CH, Ar), 117.4 (CH, Ar), 116.9 (CH, Ar), 115.2 (CH, Ar), 114.4 (CH, Ar), 113.9 (CH, Ar), 72.5 (CHOH), 45.2 (CH₂); MS (ES⁻) *m/z* 245 [M-H⁺]; HRMS (ES⁺) calcd. for C₁₄H₁₄NaO₄ [MNa⁺]: 269.0784; found: 269.0783

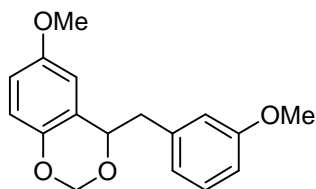
1-(2-Hydroxy-5-methoxy-phenyl)-2-(3-methoxy-phenyl)ethanone (248)



Compound **232** (4 g, 13.99 mmol) was dissolved in DCM (100 mL) and cooled to -78 °C. BBr₃ (1M in DCM) (16.78 mL, 16.78 mmol) was added and the reaction mixture was stirred at -78 °C for 1 h before warming to room temperature.

The mixture was subsequently poured over ice and H₂O (100 mL) and extracted with EtOAc (2 x 100 mL). The organic phase was separated, dried (MgSO₄), filtered and the solvent removed *in vacuo*. The resulting orange oil was purified by column chromatography eluting with 10% EtOAc in petroleum ether to give the title compound as a yellow oil which solidified on standing at room temperature (3.42 g, 90%). m.p. 48-49 °C; IR (film) 2956, 1592, 1485, 1258, 1228, 1040, 775 cm⁻¹; δ_H (400 MHz, CDCl₃) 11.82 (1H, s, OH), 7.31-7.25 (2H, m, ArH), 7.11 (1H, dd, *J* = 3.0, 9.0, ArH), 6.93 (1H, d, *J* = 9.2, ArH), 6.89-6.81 (3H, m, ArH), 4.25 (2H, s, CH₂), 3.80 (3H, s, OCH₃), 3.78 (3H, s, OCH₃); δ_C (100 MHz, CDCl₃) 203.4 (C=O), 160.0 (C, Ar), 157.4 (C, Ar), 151.8 (C, Ar), 135.5 (C, Ar), 129.9 (CH, Ar), 124.6 (CH, Ar), 121.8 (CH, Ar), 119.6 (CH, Ar), 118.6 (C, Ar), 115.2 (CH, Ar), 113.2 (CH, Ar), 112.7 (CH, Ar), 56.0 (CH₃), 55.6 (CH₃), 45.6 (CH₂); MS (ES⁻) *m/z* 271 [M-H⁺]; HRMS (ES⁻) calcd. for C₁₆H₁₅O₄ [M-H⁺]: 271.0976; found: 271.0982.

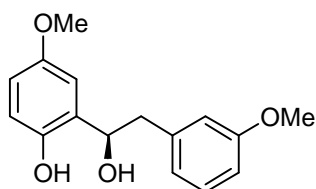
6-Methoxy-4-(3-methoxy-benzyl)-4H-benzo[1,3]dioxine (250)



249 (200 mg, 0.73 mmol) was dissolved in DMF and cooled to 0 °C. NaH (60% in mineral oil) (73 mg, 1.8 mmol) was added and the reaction mixture was allowed to warm to room temperature before adding bromochloromethane (0.07 mL, 1.09 mmol). Stirred at room temperature overnight and then quenched with an aqueous saturated solution of NH₄Cl (10 mL). The product was extracted with EtOAc (2 x 10 mL), washed with H₂O (10 mL), dried (MgSO₄), filtered and the solvent removed *in vacuo*. The resulting oil was purified by column chromatography eluting with 10% EtOAc in petroleum ether to give the title compound as a colourless oil (65 mg, 31%). IR (film) 3001, 2916, 2849, 2834, 1601, 1584, 1497, 1227, 1006 cm⁻¹; δ_H (300 MHz, CDCl₃) 7.73-7.67 (1H, m, ArH), 7.37-7.17 (4H, m,

ArH), 7.01 (1H, d, $J = 2.8$, ArH), 5.70 (1H, d, $J = 5.8$, acetal CHH), 5.61 (1H, dd, $J = 4.1$, 8.9, CHO), 5.52 (1H, d, $J = 5.8$, acetal CHH), 4.25 (3H, s, OCH₃), 4.18 (3H, s, OCH₃), 3.64 (1H, dd, $J = 4.1$, 14.3, CHH), 3.51 (1H, dd, $J = 8.9$, 14.3, CHH); δ_C (100 MHz, CDCl₃) 159.7 (C, Ar), 154.0 (C, Ar), 147.0 (C, Ar), 139.4 (C, Ar), 129.3 (CH, Ar), 125.4 (C, Ar), 121.9 (CH, Ar), 117.9 (CH, Ar), 115.4 (CH, Ar), 114.2 (CH, Ar), 112.1 (CH, Ar), 110.5 (CH, Ar), 89.4 (acetal CH₂), 75.6 (CHO), 55.8 (CH₃), 55.3 (CH₃), 42.4 (CH₂); MS (ES⁺) m/z 309 [MNa⁺]; HRMS (ES⁺) calcd. for C₁₇H₁₈NaO₄ [MNa⁺]: 309.1097; found: 309.1098.

2-[1-Hydroxy-2-(3-methoxy-phenyl)ethyl]-4-methoxy-phenol (**251**)

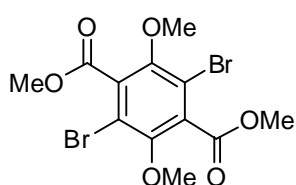


Using Will's catalyst: The tethered catalyst (**253**) (2.3 mg, 0.004 mmol) was stirred at 28 °C for 30 min in a 5:2 mixture of formic acid and NEt₃ (0.19 mL) before adding ketone **232** (100 mg, 0.37 mmol). Further 5:2 formic acid:NEt₃ mixture (0.19 mL) was added to aid stirring and solubility. The reaction mixture was stirred at 28 °C for 24 h before filtering through a plug of silica washing with EtOAc (10 mL). The solvent was then removed *in vacuo* and the resulting residue was purified by column chromatography eluting with 10% EtOAc in petroleum ether to give the title compound as a colourless oil (77 mg, 76%, 93% ee). $[\alpha]_D^{24} -9.2$ (c 1 in CHCl₃). IR (film) 3353, 1585, 1490, 1257, 1151, 1036, 755 cm⁻¹; δ_H (400 MHz, CDCl₃) 7.60 (1H, brs, OH), 7.26 (1H, t, $J = 7.7$, ArH), 6.85-6.80 (3H, m, ArH), 6.76-6.74 (1H, m, ArH), 6.73 (1H, d, $J = 3.0$, ArH), 6.50 (1H, d, $J = 3.0$, ArH), 4.95 (1H, t, $J = 7.0$, CHOH), 3.79 (3H, s, OCH₃), 3.71 (3H, s, OCH₃), 3.08 (2H, d, $J = 7.0$, CH₂), 3.00 (1H, brs, OH); δ_C (100 MHz, CDCl₃) 159.9 (C, Ar), 153.0 (C, Ar), 149.2 (C, Ar), 139.0 (C, Ar), 129.8 (CH, Ar), 127.4 (C, Ar), 121.9 (CH, Ar), 119.7 (CH, Ar), 117.8 (CH, Ar), 115.2 (CH, Ar), 114.2 (CH, Ar), 112.9 (CH, Ar), 112.5 (CH, Ar),

76.5 (CHOH), 55.9 (OCH₃), 55.3 (OCH₃), 44.3 (CH₂); MS (ES⁻) *m/z* 273 [M-H⁺]; HRMS (ES⁺) calcd. for C₁₆H₁₈NaO₄ [MNa⁺]: 297.1097; found: 297.1093.

Using Noyori's catalyst: (*p*-cymene)ruthenium(II)chloride dimer (2.3 mg, 0.004 mmol) and (R,R)-TsDPEN (1 mg, 0.002 mmol) was stirred at 28 °C for 30 min in a 5:2 mixture of formic acid and NEt₃ (0.19 mL) before adding ketone **232** (100 mg, 0.37 mmol). Further 5:2 formic acid:NEt₃ mixture (0.19 mL) was added to aid stirring and solubility. The reaction was carried out, worked up and purified as above to provide a colourless oil (91 mg, 79%, 91% ee). Data as above.

2,5-Dibromo-3,6-dimethoxy-terephthalic acid dimethyl ester (255)

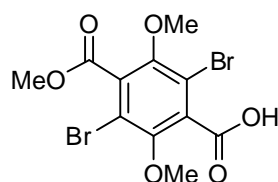


Dimethyl 2,5-dioxocyclohexane-1,4-dicarboxylate (1 g, 4.39 mmol) in AcOH (3 mL) was heated to 70 °C and NBS (869 mg, 4.88 mmol) was added carefully. The

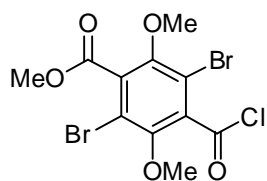
reaction mixture was heated to 90 °C for 40 min and then cooled to 60 °C for the addition of the remaining NBS (2.54 g, 14.27 mmol). The temperature was raised to 80 °C for 1 h and then cooled to 10 °C. The solids were filtered washing with AcOH (5 mL) and H₂O (5 mL). This material was then dissolved in a mixture of DCM (5.6 mL), MeOH (1.9 mL), AcOH (0.06 mL) and H₂O (0.9 mL) and was cooled to 0 °C. Na₂S₂O₄ (847 mg in 4 mL H₂O) was then added and the reaction mixture stirred at room temperature for 30 min. The organic solvents were removed *in vacuo* and the resulting suspension was filtered at 0 °C washing with ice-cold H₂O (10 mL). K₂CO₃ (2.08 g, 15.1 mmol) and MeI (0.56 mL, 9.03 mmol) were added to a suspension of this solid (578 mg, 1.51 mmol) in acetone (11 mL). The reaction mixture was stirred at room temperature for 48 h before filtering the insoluble material washing with acetone (3 x 20 mL). The filtrate was concentrated *in vacuo* and the resultant residue was purified by column chromatography eluting

with 10% EtOAc in petroleum ether to give the title compound as a white solid (275 mg, 17% over 3 steps). m.p. 152 °C; IR (film) 2946, 1726, 1438, 1375, 1256, 1007 cm^{-1} ; δ_{H} (400 MHz, CDCl_3) 3.98 (6H, s, CH_3), 3.88 (6H, s, CH_3); δ_{C} (100 MHz, CDCl_3) 164.9 (2C=O), 151.1 (C, 2Ar), 134.1 (C, 2Ar), 114.0 (C, 2Ar), 62.8 (2 CO_2CH_3), 53.2 (2 CH_3); MS (ES^+) m/z 433 [MNa^+ , ^{79}Br , ^{79}Br], 435 [MNa^+ , ^{79}Br , ^{81}Br], 437 [MNa^+ , ^{81}Br , ^{81}Br]; HRMS (ES^+) calcd. for $\text{C}_{12}\text{H}_{12}\text{Br}_2\text{NaO}_6$ [MNa^+ , ^{79}Br , ^{81}Br]: 434.8873; found 434.8875.

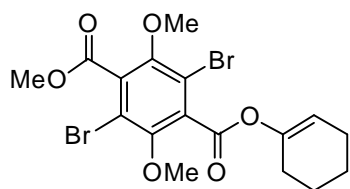
2,5-Dibromo-3,6-dimethoxy-terephthalic acid monomethyl ester (256)



Diester **255** (500 mg, 1.21 mmol) was dissolved in dioxane (5 mL) and 1M NaOH (1.21 mL) was added. The reaction mixture was heated to reflux overnight before allowing to cool to room temperature. H_2O (20 mL) was added and extracted with DCM (10 mL) to remove any remaining starting material. 2M HCl was added to acidify the aqueous phase and extracted with DCM (2 x 20 mL). Dried (MgSO_4), filtered and the solvent removed *in vacuo*. The resulting yellow solid was purified using column chromatography eluting with 100% EtOAc to give the title compound as a white solid (192 mg, 40%). IR (film) 3024, 2945, 1743, 1691, 1378, 1283, 1007 cm^{-1} ; δ_{H} (300 MHz, CDCl_3) 8.28 (1H, s, CO_2H), 3.99 (3H, s, OCH_3), 3.95 (3H, s, OCH_3), 3.90 (3H, s, OCH_3); δ_{C} (100 MHz, CDCl_3) 168.6 (C=O), 165.1 (C=O), 151.3 (C, Ar), 151.2 (C, Ar), 134.4 (C, Ar), 133.4 (C, Ar), 114.2 (C, Ar), 113.8 (C, Ar), 63.1 (CH_3), 53.4 (CH_3), 31.1 (CH_3); MS (ES^+) m/z 419 [MNa^+ , ^{79}Br , ^{79}Br], 421 [MNa^+ , ^{79}Br , ^{81}Br], 423 [MNa^+ , ^{81}Br , ^{81}Br]; HRMS (ES^+) calcd. for $\text{C}_{12}\text{H}_{12}\text{Br}_2\text{NaO}_6$ [MNa^+ , ^{79}Br , ^{81}Br]: 420.8717; found 420.8719.

2,5-Dibromo-4-chlorocarbonyl-3,6-dimethoxy-benzoic acid methyl ester (257)

256 (500 mg, 2.08 mmol) dissolved in SOCl_2 (3 mL, 41.7 mmol) and heated to reflux for 3 h. The reaction mixture was allowed to cool to room temperature and excess SOCl_2 removed *in vacuo*. The resulting solid was triturated with hexane and filtered off to give the title compound as a pale yellow solid (340 mg, 63%). IR (film) 2946, 1775, 1730, 1374, 1253, 1009 cm^{-1} ; δ_{H} (500 MHz, CDCl_3) 4.00 (3H, s, OCH_3), 3.95 (3H, s, OCH_3), 3.91 (3H, s, CH_3); δ_{C} (125 MHz, CDCl_3) 165.1 (C=O), 164.7 (C=O), 151.5 (C, Ar), 149.8 (C, Ar), 137.6 (C, Ar), 135.0 (C, Ar), 114.3 (C, Ar), 112.0 (C, Ar), 63.3 (CH_3), 63.1 (CH_3), 53.4 (CH_3).

2,5-Dibromo-3,6-dimethoxy-terephthalic acid 1-cyclohex-1-enyl ester 4-methyl ester (263)

TMS silyl enol ether (329 mg, 1.93 mmol) was dissolved in THF and cooled to $-78\text{ }^\circ\text{C}$. MeLi (1.6 M in Et_2O) (1.32 mL, 2.13 mmol) was added and the reaction mixture was stirred at $-78\text{ }^\circ\text{C}$ for 1 h and then at room temperature for 1 h. It was then recooled to $-78\text{ }^\circ\text{C}$ and acid chloride **257** (500 mg, 1.93 mmol) was added and the mixture stirred at $-78\text{ }^\circ\text{C}$ for 1 h before allowing to warm to room temperature overnight. 2M HCl (10 mL) was added and extracted with EtOAc (2 x 20 mL) washing with H_2O (20 mL). The organic phase was dried (MgSO_4), filtered and the solvent removed *in vacuo*. The resulting oil was purified by column chromatography eluting with 5% EtOAc in petroleum ether to give the title compound as a white solid (125 mg, 14%). m.p. 116-117 $^\circ\text{C}$; IR (film) 2936, 1737, 1378, 1227, 1010, 589 cm^{-1} ; δ_{H} (400 MHz, CDCl_3) 5.61 (1H, m, CH), 3.98 (3H, s, CO_2CH_3), 3.91 (3H, s, OCH_3), 3.89 (3H, s, OCH_3), 2.37-2.31 (2H, m, CH_2), 2.22-

2.15 (2H, m, CH₂), 1.86-1.78 (2H, m, CH₂), 1.70-1.62 (2H, m, CH₂); δ_C (100 MHz, CDCl₃) 165.0 (C=O), 162.9 (C=O), 151.3 (C, Ar), 151.2 (C, Ar), 148.6 (C, Ar), 134.2 (C, Ar), 134.0 (C, Ar), 115.2 (CH), 114.1 (C, Ar), 114.0 (C, Ar), 62.9 (OCH₃), 53.3 (CO₂CH₃), 26.7 (CH₂), 23.8 (CH₂), 23.8 (CH₂), 22.7 (CH₂), 21.7 (CH₂); MS (ES⁺) m/z 499 [MNa⁺, ⁷⁹Br, ⁷⁹Br], 501 [MNa⁺, ⁷⁹Br, ⁸¹Br], 503 [MNa⁺, ⁸¹Br, ⁸¹Br]; HRMS (ES⁺) calcd. for C₁₇H₁₈Br₂NaO₆ [MNa⁺, ⁷⁹Br, ⁸¹Br]: 500.9343; found 500.9344.

Biological experimental data

Fermentation of *Amycolatopsis regifaucium*

Amycolatopsis regifaucium bacteria grown on GYM agar was inoculated into a 500 mL Erlenmeyer flask containing 100 mL of liquid (pre-seed) culture medium [galactose 2% (w/v), dextrin 2% (w/v), Bactosoytone (Difco) 1% (w/v), corn steep liquor 0.5% (w/v), (NH₄)₂SO₄ 0.2%, CaCO₃ 0.2%, pH 7.4]. It was cultured on a rotary shaker (180 rpm) at 30°C for 3 days. 1 mL of this seed culture was inoculated into 100 mL of production medium (prepared by adding glycerol 1% (v/v) to the seed culture medium). The production medium was shaken on the rotary shaker at 37°C for 5 days. The culture was centrifuged and the supernatant separated and adjusted to pH 2 using 6M HCl before extracting with butyl acetate (5 x 100mL). Dried (MgSO₄), filtered and solvent removed *in vacuo* to give an orange residue.

Preparation of GYM medium

Glucose (1.6 g), yeast extract (1.6 g), malt extract (4 g) and CaCO₃ (0.8 g) was added to distilled water (400 mL) and adjusted to pH 7.2 using 2M NaOH. Agar (4.8 g) was added and the mixture autoclaved (120°C). The mixture was then

melted under microwave irradiation (low heat, 5 min). 25 mL of the resulting liquid was then added to each of 4 petri dishes and left at room temperature to set.

Preparation of GPHF medium

Glucose (1.0 g), peptone from casein (500 mg), yeast extract (500 mg), beef extract (500 mg) and $\text{CaCl}_2 \cdot 2\text{H}_2\text{O}$ (74 mg) were added to distilled H_2O (100 mL) and adjusted to pH 7.2 using 2M NaOH. Agar (4.8 g) was added and the mixture autoclaved (120 °C). The mixture was then melted under microwave irradiation (low heat, 5 min). 25 mL of the resulting liquid was then added to each of 4 petri dishes and left at room temperature to set.

Cell culture

PANC-1 cells established from a human Caucasian pancreatic carcinoma were obtained from the European Collection of Cell Cultures (Porton Down, UK) and maintained in Dulbecco's modified Eagle's medium (DMEM) supplemented with 20% (v/v) foetal bovine serum, 2 nM glutamine and 0.1% (v/v) gentamicin. The medium was routinely changed every 3 days and cells were passaged by trypsinisation (using 0.2 mg/mL trypsin solution) at approximately 80% confluence. Nutrient deprived medium (NDM) was prepared as follows: CaCl_2 (1M) (0.6 mL), $\text{Fe}(\text{NO}_3)_3 \cdot 9\text{H}_2\text{O}$ (0.5 mg), KCl (200 mg), $\text{MgSO}_4 \cdot 7\text{H}_2\text{O}$ (100 mg), NaCl (3.2 g), NaHCO_3 (350 mg), NaH_2PO_4 (62.5 mg), phenol red (7.5mg), 1M HEPES buffer (12.5 mL) and MEM vitamin solution (5 mL) (Lonza, UK) were dissolved in doubly distilled H_2O (final volume 500 mL). The pH was adjusted to 7.2 using an aqueous saturated solution of NaHCO_3 . The medium was sterile filtered and stored at - 4°C.

Trypan blue assay

PANC-1 cells were seeded in 6 x 6 well plates and incubated in fresh DMEM (2 mL per well) at 37 °C under a 5% CO₂ / 95% air atmosphere until confluent. Serial dilutions of kigamicin C in both DMEM and NDM were prepared at 0, 0.001, 0.01, 0.1, and 10µg/mL and a control set of serial dilutions also prepared containing DMSO in NDM at the quantities used above. DMSO was used to dissolve the kigamicin C and therefore this is the carrier control. DMEM was removed from the wells and the cells washed with PBS buffer before adding the serial dilutions to the wells. Everything was carried out in duplicate. After 24 h incubation at 37 °C under 5% CO₂, the supernatant from each well was removed and set aside. 2 mL trypsin (0.2 mg/mL) was added to each well and incubated at 37 °C under 5% CO₂ / 95% air atmosphere for 5 min. The trypsinised cells were added to the supernatant removed from the same well. The combined mixture was then centrifuged at 200g for 5 min and the cells resuspended in 50 µL DMEM. 10 µL of cell suspension was then added to 90µL trypan blue dye and left at room temperature for 3 min after which time live and dead cells were counted under the microscope using a haemocytometer.

WST-1 assay

Cell viability was assayed by determination of formazan levels resulting from the metabolism of NADH to NAD⁺ using assay kits from Roche Diagnostics Ltd (Burgess Hill, UK). Assays were performed according to the manufacturer's instructions.

Cells were seeded in 96 well plates (1 x 10⁴ per well) and incubated in fresh DMEM for 24 h at 37 °C under 5% CO₂ / 95% air atmosphere. In order to seed the

plates at the correct concentration, cells were trypsinised and centrifuged before resuspending them in fresh medium (10 mL). An aliquot of cell suspension was diluted (100 μ L of cell suspension added to 100 μ L of medium) before counting cells using a haemocytometer. Once the concentration of cells per mL was known, the dilution factor could be calculated based on total number of cells and total volume of medium required.

Serial dilutions of kigamicin C in both DMEM and NDM were prepared at 0, 0.001, 0.01, 0.1, and 10 μ g/mL. Blank controls (containing only media) and low controls (containing untreated cells) were included on each plate. DMEM was removed from the wells and the cells were washed with warm PBS buffer before adding the serial dilutions (100 μ L per well). Each concentration was assayed in quadruplicate. After 24 h incubation at 37 °C under a 5% CO₂ / 95% air atmosphere, WST-1 reagent (Roche Diagnostics) was added to each well (10 μ L per well) and the plate incubated at 37°C under a 5% CO₂ / 95% air atmosphere for 1 h. The absorbance was then measured at 490 nm.

Lactate Dehydrogenase assay (LDH)

Cell death was assayed by determination of cellular release of LDH using assay kits from Roche Diagnostics Ltd (Burgess Hill, UK). Assays were performed according to the manufacturer's instructions.

Briefly, cells were seeded in 96 well plates (3×10^4 per well) and incubated in fresh DMEM for 24 h at 37 °C under 5% CO₂ / 95% air atmosphere. Serial dilutions of the compound to be tested, in both DMEM and NDM were prepared at 0, 0.001, 0.01, 0.1, 1.0, 10 and 100 μ g/mL. Blank controls (containing only media), low

controls (containing untreated cells) and high controls (containing cells lysed with 2% (v/v) Triton X to determine maximum cellular LDH levels) were included on each plate. DMEM was removed from the wells and the cells washed with warm PBS before adding the serial dilutions (100 μ L per well) of the compound to be tested. Each concentration was assayed in triplicate. After 24 h incubation at 37 °C under a 5% CO₂ / 95% air atmosphere, the plate was centrifuged and 80 μ L of supernatant from each well was transferred to a new 96 well plate. The LDH assay catalyst (diaphorase and NAD⁺) and dye solution (iodotetrazolium chloride and sodium lactate) were combined and 80 μ L of this reagent mix was added to each well. After 30 min at room temperature in the dark, the absorbance was measured at 490 nm. All experiments were carried out on at least three separate occasions.

References:

- (1) D. H. Li, K. P. Xie, R. Wolff, J. L. Abbruzzese, *Lancet*, **2004**, 363, 1049.
- (2) S. Shore, M. G. T. Raraty, P. Ghaneh, J. P. Neoptolemos, *Aliment. Pharmacol. Ther.*, **2003**, 18, 1049.
- (3) D. Grasso, M. N. Garcia, J. L. Iovanna, *Int. J. Cell Biol.*, **2012**, 2012, 760498.
- (4) T. Seufferlein, *Gut*, **2012**.
- (5) T. Seufferlein, J. B. Bachet, E. Van Cutsem, P. Rougier, *Ann. Oncol.*, **2012**, 23, 33.
- (6) E. P. DiMagno, *Ann. Oncol.*, **1999**, 10, 140.
- (7) S. Shore, D. Vimalachandran, M. G. T. Raraty, P. Ghaneh, *Surg. Oncol*, **2004**, 13, 201.
- (8) M. A. Tempero, *J.O.P*, **2008**, 4, 46.
- (9) G. H. Sakorafas, A. G. Tsiotou, G. G. Tsiotos, *Cancer Treat. Rev.*, **2000**, 26, 29.
- (10) S. C. Larsson, A. Wolk, *Br. J. Cancer*, **2012**, 106, 603.
- (11) G. W. Olsen, J. S. Mandel, R. W. Gibson, L. W. Wattenberg, L. M. Schuman, *Am. J. Public Health*, **1989**, 79, 1016.
- (12) P. K. Mills, W. L. Beeson, D. E. Abbey, G. E. Fraser, R. L. Phillips, *Cancer*, **1988**, 61, 2578.
- (13) W. Ye, J. Lagergren, E. Weiderpass, O. Nyren, H. O. Adami, A. Ekbom, *Gut*, **2002**, 51, 236.
- (14) D. S. Michaud, E. Giovannucci, W. C. Willett, G. A. Colditz, C. S. Fuchs, *Cancer Epidemiol. Biomarkers Prev.*, **2001**, 10, 429.
- (15) F. Wang, M. Herrington, J. Larsson, J. Permert, *Mol. Cancer*, **2003**, 2, 4.
- (16) M. Journal of Oncology Practice Schenk, A. G. Schwartz, E. O'Neal, M. Kinnard, J. K. Greenon, J. P. Fryzek, G. S. Ying, D. H. Garabrant, *J. Natl. Cancer Inst.*, **2001**, 93, 640.

-
- (17) R. R. Love, H. Leventhal, D. V. Easterling, D. R. Nerenz, *Cancer*, **1989**, 63, 604.
- (18) J. P. Begue, D. Bonnet-Delpon, *J. Fluorine Chem.*, **2006**, 127, 992.
- (19) H. A. Burris, M. J. Moore, J. Andersen, M. R. Green, M. L. Rothenberg, M. R. Madiano, M. C. Cripps, R. K. Portenoy, A. M. Storniolo, P. Tarassoff, R. Nelson, F. A. Dorr, C. D. Stephens, D. D. VanHoff, *J. Clin. Oncol.*, **1997**, 15, 2403.
- (20) Z. Zhang, H. Hatta, T. Ito, S. Nishimoto, *Org. Biomol. Chem.*, **2005**, 3, 592.
- (21) P. Pourquier, C. Gioffre, G. Kohlhagen, Y. Urasaki, F. Goldwasser, L. W. Hertel, S. Y. Yu, R. T. Pon, W. H. Gmeiner, Y. Pommier, *Clin. Cancer Res.*, **2002**, 8, 2499.
- (22) S. Cullinan, C. G. Moertel, H. S. Wieand, A. J. Schutt, J. E. Krook, J. F. Foley, B. D. Norris, C. G. Kardinal, L. K. Tschetter, J. F. Barlow, *Cancer*, **1990**, 65, 2207.
- (23) S. R. Bramhall, J. Schulz, J. Nemunaitis, P. D. Brown, M. Baillet, J. A. C. Buckels, *Br. J. Cancer*, **2002**, 87, 161.
- (24) C. M. R. Lima, M. R. Green, R. Rotche, W. H. Miller, G. M. Jeffrey, L. A. Cisar, A. Morganti, N. Orlando, G. Gruia, L. L. Miller, *J. Clin. Oncol.*, **2004**, 22, 3776.
- (25) H. Oettle, D. Richards, R. K. Ramanathan, J. L. van Laethem, M. Peeters, M. Fuchs, A. Zimmermann, W. John, D. Von Hoff, M. Arning, H. L. Kindler, *Ann. Oncol.*, **2005**, 16, 1639.
- (26) E. Van Cutsem, H. V. de Velde, P. Karasek, H. Oettle, W. L. Vervenne, A. Szawlowski, P. Schoffski, S. Post, C. Verslype, H. Neumann, H. Safran, Y. Humblet, J. P. Ruixo, Y. Ma, D. Von Hoff, *J. Clin. Oncol.*, **2004**, 22, 1430.
- (27) J. D. Berlin, P. Catalano, J. P. Thomas, J. W. Kugler, D. G. Haller, A. B. Benson, *J. Clin. Oncol.*, **2002**, 20, 3270.

-
- (28) G. K. Abou-Alfa, R. Letourneau, G. Harker, M. Modiano, H. Hurwitz, N. S. Tchekmedyian, K. Feit, J. Ackerman, R. L. De Jager, S. G. Eckhardt, E. M. O'Reilly, *J. Clin. Oncol.*, **2006**, 24, 4441.
- (29) C. Louvet, R. Labianca, P. Hammel, G. Lledo, M. G. Zampino, T. Andre, A. Zaniboni, M. Ducreux, E. Aitini, J. Taieb, R. Faroux, C. Lepere, A. de Gramont, *J. Clin. Oncol.*, **2005**, 23, 3509.
- (30) M. J. Moore, D. Goldstein, J. Hamm, A. Figer, J. R. Hecht, S. Gallinger, H. J. Au, P. Murawa, D. Walde, R. A. Wolff, D. Campos, R. Lim, K. Ding, G. Clark, T. Voskoglou-Nomikos, M. Ptasynski, W. Parulekar, *J. Clin. Oncol.*, **2007**, 25, 1960.
- (31) T. Conroy, F. Desseigne, M. Ychou, O. Bouche, R. Guimbaud, Y. Becouarn, A. Adenis, J. L. Raoul, S. Gourgou-Bourgade, C. de la Fouchardiere, J. Bennouna, J. B. Bachet, F. Khemissa-Akouz, D. Pere-Verge, C. Delbaldo, E. Assenat, B. Chauffert, P. Michel, C. Montoto-Grillot, M. Ducreux, U. Grp Tumeurs Digestives, P. Intergrp, *New England Journal of Medicine*, **2011**, 364, 1817.
- (32) R. G. H. Cotton, I. G. Jennings, *Eur. J. Biochem.*, **1978**, 85, 357.
- (33) N. J. Wheate, S. Walker, G. E. Craig, R. Oun, *Dalton Trans.*, **2010**, 39, 8113.
- (34) S. Wang, Y. Y. Li, Y. H. Liu, A. J. Lu, Q. D. You, *Bioorg. Med. Chem. Lett.*, **2008**, 18, 4095.
- (35) O. Al-Bataineh, J. Jenne, P. Huber, *Cancer Treat. Rev.*, **2012**, 38, 346.
- (36) S. E. Jung, S. H. Cho, J. H. Jang, J. Y. Han, *Abdom. Imaging*, **2011**, 36, 185.
- (37) L. L. Xiong, J. H. Hwang, X. B. Huang, S. S. Yao, C. J. He, X. H. Ge, H. Y. Ge, X. F. Wang, *J.O.P.*, **2009**, 10, 123.
- (38) I. Momose, S. Kunimoto, M. Osono, D. Ikeda, *Biochem. Biophys. Res. Commun.*, **2009**, 380, 171.
- (39) S. Awale, F. Li, H. Onozuka, H. Esumi, Y. Tezuka, S. Kadota, *Bioorg. Med. Chem.*, **2008**, 16, 181.

-
- (40) R. S. Kerbel, *Carcinogenesis*, **2000**, 21, 505.
- (41) G. Bergers, K. Javaherian, K. M. Lo, J. Folkman, D. Hanahan, *Science*, **1999**, 284, 808.
- (42) N. J. Nelson, *J. Natl. Cancer Inst.*, **1999**, 91, 820.
- (43) T. A. Bhat, R. P. Singh, *Food Chem. Toxicol.*, **2008**, 46, 1334.
- (44) A. C. Koong, V. K. Mehta, Q. T. Le, G. A. Fisher, D. J. Terris, J. M. Brown, A. J. Bastidas, M. Vierra, *Int. J. Radiat. Oncol. Biol. Phys.*, **2000**, 48, 919.
- (45) K. Koito, T. Namieno, T. Nagakawa, K. Morita, *Am. J. Roentgenol.*, **1997**, 169, 1263.
- (46) K. Izuishi, K. Kato, T. Ogura, T. Kinoshita, H. Esumi, *Cancer Res.*, **2000**, 60, 6201.
- (47) J. Lu, S. Kunimoto, Y. Yamazaki, M. Kaminishi, H. Esumi, *Cancer Sci.*, **2004**, 95, 547.
- (48) M. R. Cha, M. Y. Yoon, E. S. Son, H. R. Park, *Biosci. Biotechnol. Biochem.*, **2009**, 73, 2167.
- (49) F. Li, Y. M. He, S. Awale, S. Kadota, Y. Tezuka, *Chem. Pharm. Bull.*, **2011**, 59, 1194.
- (50) N. N. Win, S. Awale, H. Esumi, Y. Tezuka, S. Kadota, *Bioorg. Med. Chem.*, **2008**, 16, 8653.
- (51) S. Kunimoto, J. Lu, H. Esumi, Y. Yamazaki, N. Kinoshita, Y. Honma, M. Hamada, M. Ohsono, M. Ishizuka, T. Takeuchi, *J. Antibiot.*, **2003**, 56, 1004.
- (52) N. N. Win, S. Awale, H. Esumi, Y. Tezuka, S. Kadota, *Chem. Pharm. Bull.*, **2008**, 56, 491.
- (53) S. Awale, J. Lu, S. K. Kalauni, Y. Kurashima, Y. Tezuka, S. Kadota, H. Esumi, *Cancer Res.*, **2006**, 66, 1751.

-
- (54) S. Kunimoto, T. Someno, Y. Yamazaki, J. Lu, H. Esumi, H. Naganawa, *J. Antibiot.*, **2003**, 56, 1012.
- (55) T. Someno, S. Kunimoto, H. Nakamura, H. Naganawa, D. Ikeda, *J. Antibiot.*, **2005**, 58, 56.
- (56) M. Nakamura, H. Esumi, L. Jin, H. Mitsuya, H. Hata, *Anticancer Res.*, **2008**, 28, 37.
- (57) T. Masuda, S. Ohba, M. Kawada, M. Osono, D. Ikeda, H. Esumi, S. Kunimoto, *J. Antibiot.*, **2006**, 59, 209.
- (58) M. Osaki, M. Oshimura, H. Ito, *Apoptosis*, **2004**, 9, 667.
- (59) S. S. W. Ng, M. S. Tsao, S. Chow, D. W. Hedley, *Cancer Res.*, **2000**, 60, 5451.
- (60) N. S. Pellegata, F. Sessa, B. Renault, M. Bonato, B. E. Leone, E. Solcia, G. N. Ranzani, *Cancer Res.*, **1994**, 54, 1556.
- (61) I. Vivanco, C. L. Sawyers, *Nat. Rev. Cancer*, **2002**, 2, 489.
- (62) J. S. Waldron, I. Yang, S. G. Han, T. Tihan, M. E. Sughrue, S. A. Mills, R. O. Pieper, A. T. Parsa, *J. Clin. Neurosci.*, **2010**, 17, 1543.
- (63) E. Forgacs, E. J. Biesterveld, Y. Sekido, K. Fong, S. Muneer, Wistuba, II, S. Milchgrub, R. Brezinschek, A. Virmani, A. F. Gazdar, J. D. Minna, *Oncogene*, **1998**, 17, 1557.
- (64) P. L. M. Dahia, D. J. Marsh, Z. M. Zheng, J. Zedenius, P. Komminoth, T. Frisk, G. Wallin, R. Parsons, M. Longy, C. Larsson, C. Eng, *Cancer Res.*, **1997**, 57, 4710.
- (65) N. Halachmi, S. Halachmi, E. Evron, P. Cairns, K. Okami, M. Saji, W. H. Westra, M. A. Zeiger, J. Jen, D. Sidransky, *Genes Chromosom. Cancer*, **1998**, 23, 239.
- (66) E. Rhei, L. Kang, F. Bogomolny, M. G. Federici, P. I. Borgen, J. Boyd, *Cancer Res.*, **1997**, 57, 3657.

-
- (67) P. Cairns, K. Okami, S. Halachmi, N. Halachmi, M. Esteller, J. G. Herman, W. B. Isaacs, G. S. Bova, D. Sidransky, *Cancer Res.*, **1997**, 57, 4997.
- (68) J. T. Celebi, I. Shendrik, D. N. Silvers, M. Peacocke, *J. Med. Genet.*, **2000**, 37, 653.
- (69) A. Sakai, C. Thieblemont, A. Wellmann, E. S. Jaffe, M. Raffeld, *Blood*, **1998**, 92, 3410.
- (70) K. S. Masters, S. Brase, *Chem. Rev.*, **2012**, 112, 3717.
- (71) U. M. Hanumegowda, B. M. Judy, W. V. Welshons, C. S. Reddy, *Toxicol. Sci.*, **2002**, 66, 159.
- (72) V. C. Dhulipala, K. K. Maddali, W. V. Welshons, C. S. Reddy, *Birth Defects Res. B. Dev. Reprod. Toxicol.*, **2005**, 74, 233.
- (73) B. Bolon, V. E. V. Stomer, *Neurosci. Biobehav. Rev.*, **1992**, 16, 171.
- (74) K. C. Ehrlich, L. S. Lee, A. Ciegler, M. S. Palmgren, *Applied and Environmental Microbiology*, **1982**, 44, 1007.
- (75) E. K. Tangni, L. Pussemier, *J. Sci. Food Agric.*, **2007**, 87, 1263.
- (76) A. F. Zhai, Y. Zhang, X. N. Zhu, J. T. Liang, X. L. Wang, Y. C. Lin, R. Z. Chen, *Neurochem. Int.*, **2011**, 58, 85.
- (77) M. Millot, S. Tomasi, E. Studzinska, I. Rouaud, J. Boustie, *J. Nat. Prod.*, **2009**, 72, 2177.
- (78) K. Kobayashi, C. Nishino, J. Ohya, S. Sato, T. Mikawa, Y. Shiobara, M. Kodama, *J. Antibiot.*, **1988**, 41, 502.
- (79) K. Kobayashi, C. Nishino, J. Ohya, S. Sato, T. Mikawa, Y. Shiobara, M. Kodama, *J. Antibiot.*, **1988**, 41, 741.
- (80) J. A. Dale, D. L. Dull, H. S. Mosher, *J. Org. Chem.*, **1969**, 34, 2543.
- (81) W. M. Maiese, J. Korshalla, J. Goodman, M. J. Torrey, S. Kantor, D. P. Labeda, M. Greenstein, *J. Antibiot.*, **1990**, 43, 1059.

-
- (82) T. W. M. Lee, G. T. Carter, D. B. Borders, *J. Chem. Soc. Chem. Commun.*, **1989**, 1771.
- (83) D. Ma, C. Ma, M. Gao, G. Li, Z. Niu, X. Huang, *J. Parasitol. Res.*, **2012**, 2012, 654279.
- (84) H. Ui, A. Ishiyama, H. Sekiguchi, M. Namatame, A. Nishihara, Y. Takahashi, K. Shiomi, K. Otaguro, S. Omura, *J. Antibiot.*, **2007**, 60, 220.
- (85) Y. Koizumi, H. Tomoda, A. Kumagai, X. P. Zhou, S. Koyota, T. Sugiyama, *Cancer Sci.*, **2009**, 100, 322.
- (86) H. Hara, A. Kobayashi, K. Yoshida, M. Ohashi, S. Ohnami, E. Uchida, E. Higashihara, T. Yoshida, K. Aoki, *Cancer Sci.*, **2007**, 98, 455.
- (87) M. Isaka, S. Palasarn, K. Kocharin, J. Saenboonrueng, *J. Nat. Prod.*, **2005**, 68, 945.
- (88) C. Chutrakul, T. Boonruangprapa, R. Suvannakad, M. Isaka, P. Sirithunya, T. Toojinda, K. Kirtikara, *J. Appl. Microbiol.*, **2009**, 107, 1624.
- (89) R. Ratnayake, E. Lacey, S. Tennant, J. H. Gill, R. J. Capon, *Org. Lett.*, **2006**, 8, 5267.
- (90) R. Ratnayake, E. Lacey, S. Tennant, J. H. Gill, R. J. Capon, *Chem. Eur. J.*, **2007**, 13, 1610.
- (91) D. L. Sloman, J. W. Bacon, J. A. Porco, Jr., *J. Am. Chem. Soc.*, **2011**, 133, 9952.
- (92) J. R. Butler, C. Wang, J. Bian, J. M. Ready, *J. Am. Chem. Soc.*, **2011**, 133, 9956.
- (93) D. L. Sloman, B. Mitasev, S. S. Scully, J. A. Beutler, J. A. Porco, *Angew. Chem. Int. Ed.*, **2011**, 50, 2511.
- (94) E. M. K. Wijeratne, T. J. Turbyville, A. Fritz, L. Whitesell, A. A. L. Gunatilaka, *Bioorg. Med. Chem.*, **2006**, 14, 7917.

-
- (95) W. Zhang, K. Krohn, Z. Ullah, U. Florke, G. Pescitelli, L. Di Bari, S. Antus, T. Kurtan, J. Rheinheimer, S. Draeger, B. Schulz, *Chem. Eur. J.*, **2008**, 14, 4913.
- (96) K. C. Nicolaou, A. Li, *Angew. Chem. Int. Ed.*, **2008**, 47, 6579.
- (97) E. M. C. Gerard, S. Brase, *Chem. Eur. J.*, **2008**, 14, 8086.
- (98) T. A. Qin, R. P. Johnson, J. A. Porco, *J. Am. Chem. Soc.*, **2011**, 133, 1714.
- (99) V. Rukachaisirikul, U. Sommart, S. Phongpaichit, J. Sakayaroj, K. Kirtikara, *Phytochemistry*, **2008**, 69, 783.
- (100) M. M. Wagenaar, J. Clardy, *J. Nat. Prod.*, **2001**, 64, 1006.
- (101) T. Masuda, S. Ohba, M. Kawada, M. Iijima, H. Inoue, M. Osono, D. Ikeda, S. Kunimoto, *J. Antibiot.*, **2006**, 59, 215.
- (102) T. S. Wahyuni, W. Ekasari, A. Widyawaruyanti, Y. Hirasawa, H. Morita, N. C. Zaini, *Heterocycles*, **2009**, 79, 1121.
- (103) O. V. Singh, R. S. Kapil, C. P. Garg, R. P. Kapoor, *Tetrahedron Lett.*, **1991**, 32, 5619.
- (104) O. V. Singh, C. P. Garg, R. P. Kapoor, *Tetrahedron Lett.*, **1990**, 31, 2747.
- (105) I. K. Kostakis, R. Tenta, N. Pouli, P. Marakos, A. Skaltsounis, H. Pratsinis, D. Kletsas, *Bioorg. Med. Chem. Lett.*, **2005**, 15, 5057.
- (106) T. Watanabe, S. Katayama, Y. Nakashita, M. Yamauchi, *J. Chem. Soc., Perkin Trans. 1*, **1978**, 726.
- (107) N. Miyaura, A. Suzuki, *Chem. Rev.*, **1995**, 95, 2457.
- (108) R. A. Wilson, L. Chan, R. Wood, R. C. D. Brown, *Org. Biomol. Chem.*, **2005**, 3, 3228.
- (109) T. Patonay, A. Levai, E. Riman, R. S. Varma, *Arkivoc*, **2004**, 183.
- (110) E. Valeur, M. Bradley, *Chem. Soc. Rev.*, **2009**, 38, 606.
- (111) <http://www.bioaustralis.com>

-
- (112) D. F. Veber, S. R. Johnson, H. Y. Cheng, B. R. Smith, K. W. Ward, K. D. Kopple, *J. Med. Chem.*, **2002**, 45, 2615.
- (113) C. A. S. Bergstrom, M. Strafford, L. Lazorova, A. Avdeef, K. Luthman, P. Artursson, *J. Med. Chem.*, **2003**, 46, 558.
- (114) P. S. Johnson, T. Ryckmans, J. Bryans, D. M. Beal, K. N. Dack, N. Feeder, A. Harrison, M. Lewis, H. J. Mason, J. Mills, J. Newman, C. Pasquinet, D. J. Rawson, L. R. Roberts, R. Russell, D. Spark, A. Stobie, T. J. Underwood, R. Ward, S. Wheeler, *Bioorg. Med. Chem. Lett.*, **2011**, 21, 5684.
- (115) A. Suzuki, *Angew. Chem. Int. Ed.*, **2011**, 50, 6722.
- (116) T. Watanabe, N. Miyaura, A. Suzuki, *Synlett*, **1992**, 207.
- (117) W. J. Thompson, J. Gaudino, *J. Org. Chem.*, **1984**, 49, 5237.
- (118) O. Baudoin, D. Guenard, F. Gueritte, *J. Org. Chem.*, **2000**, 65, 9268.
- (119) S. P. Stanforth, *Tetrahedron*, **1998**, 54, 263.
- (120) S. Nakamura, H. Sugimoto, T. Ohwada, *J. Org. Chem.*, **2008**, 73, 4219.
- (121) A. K. Sharma, S. Amin, S. Kumar, *Polycyclic Aromat. Compd.*, **2002**, 22, 277.
- (122) W. M. Seganish, P. DeShong, *Org. Lett.*, **2006**, 8, 3951.
- (123) K. S. Feldman, R. F. Campbell, J. C. Saunders, C. Ahn, K. M. Masters, *J. Org. Chem.*, **1997**, 62, 8814.
- (124) V. G. Zaitsev, A. L. Mikhal'chuk, *Chirality*, **2001**, 13, 488.
- (125) R. Yella, *Synlett*, **2010**, 835.
- (126) H. O. House, R. A. Auerbach, M. Gall, N. P. Peet, *J. Org. Chem.*, **1973**, 38, 514.
- (127) R. Gompper, *Angew. Chem. Int. Ed.*, **1964**, 3, 560.
- (128) I. F. Montes, U. Burger, *Tetrahedron Lett.*, **1996**, 37, 1007.
- (129) Y. W. Fang, C. Z. Li, *J. Org. Chem.*, **2006**, 71, 6427.

-
- (130) M. Carril, R. SanMartin, I. Tellitu, E. Dominguez, *Org. Lett.*, **2006**, 8, 1467.
- (131) M. C. Willis, D. Taylor, A. T. Gillmore, *Org. Lett.*, **2004**, 6, 4755.
- (132) M. C. Willis, D. Taylor, A. T. Gillmore, *Tetrahedron*, **2006**, 62, 11513.
- (133) L. Boiaryna, M. K. El Mkaddem, C. Taillier, V. Dalla, M. Othman, *Chemistry*, **2012**, 18, 14192.
- (134) D. Das, S. Pratihar, S. Roy, *Org. Lett.*, **2012**, 14, 4870.
- (135) G. Liu, H. L. Liu, G. Qiu, S. Z. Pu, J. Wu, *Chem. Commun.*, **2012**, 48, 7049.
- (136) P. Liu, C. Li, E. J. M. Hensen, *Chem. Eur. J.*, **2012**, 18, 12122.
- (137) H. S. Yoon, X. H. Ho, J. Jang, H. J. Lee, S. J. Kim, H. Y. Jang, *Org. Lett.*, **2012**, 14, 3272.
- (138) Q. Cai, J. J. Yan, K. Ding, *Org. Lett.*, **2012**, 14, 3332.
- (139) R. J. Phipps, L. McMurray, S. Ritter, H. A. Duong, M. J. Gaunt, *J. Am. Chem. Soc.*, **2012**, 134, 10773.
- (140) A. Grossmann, D. Enders, *Angew. Chem. Int. Ed.*, **2012**, 51, 314.
- (141) W. R. Bowman, H. Heaney, P. H. G. Smith, *Arkivoc*, **2003**, 434.
- (142) T. Mizuhara, S. Oishi, N. Fujii, H. Ohno, *J. Org. Chem.*, **2010**, 75, 265.
- (143) S. Seto, *Tetrahedron Lett.*, **2004**, 45, 8475.
- (144) S. Park, S. Lee, *Bull. Korean Chem. Soc.*, **2010**, 31, 2571.
- (145) C. J. Pedersen, *J. Am. Chem. Soc.*, **1967**, 89, 7017.
- (146) Y. Q. Ye, H. Koshino, J. Onose, K. Yoshikawa, N. Abe, S. Takahashi, *Org. Lett.*, **2009**, 11, 5074.
- (147) N. Iwasawa, M. Otsuka, S. Yamashita, M. Aoki, J. Takaya, *J. Am. Chem. Soc.*, **2008**, 130, 6328.
- (148) A. I. Gurevich, T. N. Deshko, G. A. Kogan, M. N. Kolosov, V. V. Kudryash, V. V. Onoprien, *Tetrahedron Lett.*, **1974**, 2801.
- (149) K. Sonogashira, Y. Tohda, N. Hagihara, *Tetrahedron Lett.*, **1975**, 4467.

-
- (150) R. F. Heck, J. P. Nolley, *J. Org. Chem.*, **1972**, 37, 2320.
- (151) K. Albert, P. Gisdakis, N. Rosch, *Organometallics*, **1998**, 17, 1608.
- (152) R. J. Deeth, A. Smith, K. K. Hii, J. M. Brown, *Tetrahedron Lett.*, **1998**, 39, 3229.
- (153) P. Fitton, J. E. Y. McKeon, *Chem. Commun.*, 4.
- (154) X. Mi, M. M. Huang, Y. J. Feng, Y. J. Wu, *Synlett*, **2012**, 1257.
- (155) G. Zou, J. R. Zhu, J. Tang, *Tetrahedron Lett.*, **2003**, 44, 8709.
- (156) I. P. Beletskaya, A. V. Cheprakov, *Coord. Chem. Rev.*, **2004**, 248, 2337.
- (157) E. J. Reinhard, J. L. Wang, R. C. Durley, Y. M. Fobian, M. L. Grapperhaus, B. S. Hickory, M. A. Massa, M. B. Norton, M. A. Promo, M. B. Tollefson, W. F. Vernier, D. T. Connolly, B. J. Witherbee, M. A. Melton, K. J. Regina, M. E. Smith, J. A. Sikorski, *J. Med. Chem.*, **2003**, 46, 2152.
- (158) P. A. Turner, E. M. Griffin, J. L. Whatmore, M. Shipman, *Org. Lett.*, **2011**, 13, 1056.
- (159) J. Hassan, M. Sevignon, C. Gozzi, E. Schulz, M. Lemaire, *Chem. Rev.*, **2002**, 102, 1359.
- (160) T. R. Kelly, C. T. Jagoe, Q. Li, *J. Am. Chem. Soc.*, **1989**, 111, 4522.
- (161) S. Hosokawa, H. Fumiyama, H. Fukuda, T. Fukuda, M. Seki, K. Tatsuta, *Tetrahedron Lett.*, **2007**, 48, 7305.
- (162) R. Masuo, K. Ohmori, L. Hintermann, S. Yoshida, K. Suzuki, *Angew. Chem. Int. Ed.*, **2009**, 48, 3462.
- (163) J. S. Debenham, C. B. Madsen-Duggan, T. F. Walsh, J. Y. Wang, X. C. Tong, G. A. Doss, J. Lao, T. M. Fong, M. T. Schaeffer, J. C. Xiao, C. Huang, C. P. Shen, Y. Feng, D. J. Marsh, D. S. Stribling, L. P. Shearman, A. M. Strack, D. E. MacIntyre, L. H. T. Van der Ploeg, M. T. Goulet, *Bioorg. Med. Chem. Lett.*, **2006**, 16, 681.

-
- (164) T. Aoyama, T. Eguchi, T. Oshima, K. Kakinuma, *J. Chem. Soc. Perkin Trans. I*, **1995**, 1905.
- (165) C. Bolchi, M. Pallavicini, C. Rusconi, L. Diomede, N. Ferri, A. Corsini, L. Fumagalli, A. Pedretti, G. Vistoli, E. Valoti, *Bioorg. Med. Chem. Lett.*, **2007**, 17, 6192.
- (166) L. V. Desai, D. T. Ren, T. Rosner, *Org. Lett.*, **2010**, 12, 1032.
- (167) J. M. Fox, X. H. Huang, A. Chieffi, S. L. Buchwald, *J. Am. Chem. Soc.*, **2000**, 122, 1360.
- (168) K. L. Wang, M. Lu, A. Yu, X. Q. Zhu, Q. M. Wang, *J. Org. Chem.*, **2009**, 74, 935.
- (169) G. Bringmann, R. Walter, R. Weirich, *Angew. Chem. Int. Ed.*, **1990**, 29, 977.
- (170) A. McKillop, A. G. Turrell, D. W. Young, E. C. Taylor, *J. Am. Chem. Soc.*, **1980**, 102, 6504.
- (171) K. S. Feldman, S. M. Ensel, *J. Am. Chem. Soc.*, **1994**, 116, 3357.
- (172) D. A. Evans, C. J. Dinsmore, D. A. Evrard, K. M. Devries, *J. Am. Chem. Soc.*, **1993**, 115, 6426.
- (173) K. L. Wang, Q. M. Wang, R. Q. Huang, *J. Org. Chem.*, **2007**, 72, 8416.
- (174) M. A. Ciufolini, F. Roschangar, *J. Am. Chem. Soc.*, **1996**, 118, 12082.
- (175) M. Noji, M. Nakajima, K. Koga, *Tetrahedron Lett.*, **1994**, 35, 7983.
- (176) W. Schafer, B. Franck, *Chem. Ber.*, **1966**, 99, 160.
- (177) A. Fujii, S. Hashiguchi, N. Uematsu, T. Ikariya, R. Noyori, *J. Am. Chem. Soc.*, **1996**, 118, 2521.
- (178) S. Hashiguchi, A. Fujii, J. Takehara, T. Ikariya, R. Noyori, *J. Am. Chem. Soc.*, **1995**, 117, 7562.
- (179) D. J. Morris, A. M. Hayes, M. Wills, *J. Org. Chem.*, **2006**, 71, 7035.

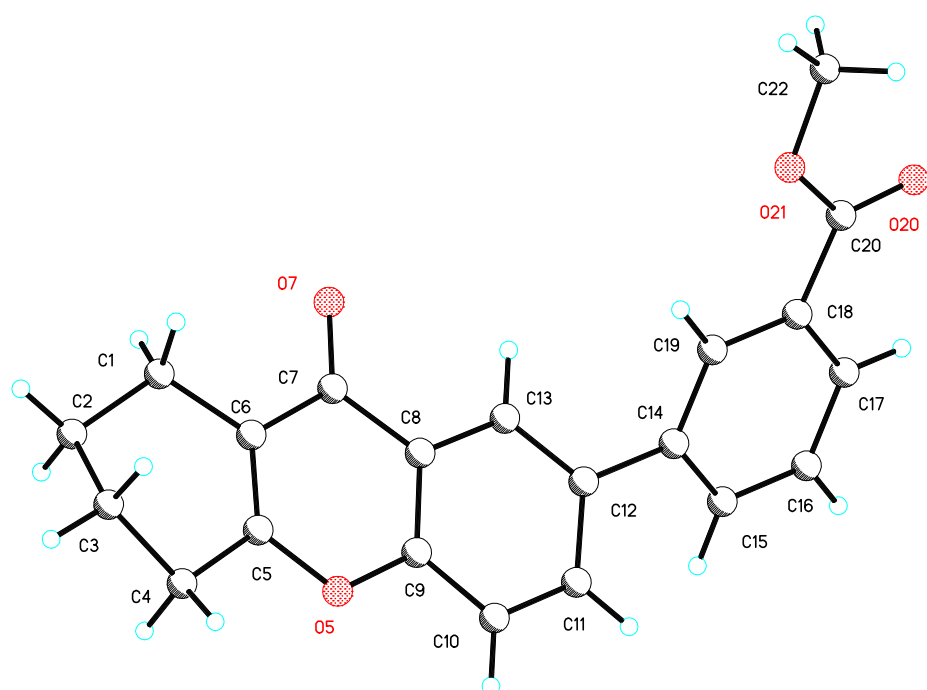
-
- (180) R. Soni, J. M. Collinson, G. C. Clarkson, M. Wills, *Org. Lett.*, **2011**, 13, 4304.
- (181) A. Hayes, G. Clarkson, M. Wills, *Tetrahedron-Asymmetry*, **2004**, 15, 2079.
- (182) Y. Jiang, X. Chen, Y. S. Zheng, Z. Y. Xue, C. Shu, W. C. Yuan, X. M. Zhang, *Angew. Chem. Int. Ed.*, **2011**, 50, 7304.
- (183) G. Zoidis, D. Benaki, V. Myrianthopoulos, L. Naesens, E. De Clercq, E. Mikros, N. Kolocouris, *Tetrahedron Lett.*, **2009**, 50, 2671.
- (184) H. W. Xu, G. F. Dai, G. Z. Liu, J. F. Wang, H. M. Liu, *Bioorg. Med. Chem.*, **2007**, 15, 4247.
- (185) J. L. Gras, R. Nougier, M. McHich, *Tetrahedron Lett.*, **1987**, 28, 6601.
- (186) H. M. Zhong, J. H. Sohn, V. H. Rawal, *J. Org. Chem.*, **2007**, 72, 386.
- (187) R. Clark, A. Takemura, N. Watanabe, O. Asano, T. Nagakura, K. Tabata; Eisai RandD Management Co Ltd: 2010.
- (188) E. Quesada, M. Stockley, J. P. Ragot, M. E. Prime, A. C. Whitwood, R. J. K. Taylor, *Org. Biomol. Chem.*, **2004**, 2, 2483.
- (189) A. Furstner, G. Seidel, *J. Org. Chem.*, **1997**, 62, 2332.
- (190) D. Oehlrich, S. M. E. Vidot, M. W. Davies, G. J. Clarkson, M. Shipman, *Tetrahedron*, **2007**, 63, 4703.
- (191) G. I. Feutrill, R. N. Mirrington, *Aust. J. Chem.*, **1972**, 25, 1719.
- (192) G. I. Feutrill, R. N. Mirrington, *Aust. J. Chem.*, **1972**, 25, 1731.
- (193) L. Hintermann, K. Suzuki, *Synthesis*, **2008**, 2303.
- (194) C. E. Wagner, P. W. Jurutka, P. A. Marshall, T. L. Groy, A. van der Vaart, J. W. Ziller, J. K. Furmick, M. E. Graeber, E. Matro, B. V. Miguel, I. T. Tran, J. Kwon, J. N. Tedeschi, S. Moosavi, A. Danishyar, J. S. Philp, R. O. Khamees, J. N. Jackson, D. K. Grupe, S. L. Badshah, J. W. Hart, *J. Med. Chem.*, **2009**, 52, 5950.

-
- (195) G. Y. A. Tan, S. Robinson, E. Lacey, R. Brown, W. Kim, M. Goodfellow, *Int. J. Syst. Evol. Microbiol.*, **2007**, 57, 2562.
- (196) C. P. Hartman, G. E. Fulk, A. W. Andrews, *Mutat. Res.*, **1978**, 58, 125.
- (197) M. Ishiyama, M. Shiga, K. Sasamoto, M. Mizoguchi, P. G. He, *Chem. Pharm. Bull.*, **1993**, 41, 1118.
- (198) T. Mosmann, *J. Immunol. Methods*, **1983**, 65, 55.
- (199) M. V. Berridge, A. S. Tan, K. D. McCoy, R. Wang *Biochemica*, 1996; Vol. 4, p 14.
- (200) G. Haslam, D. Wyatt, P. A. Kitos, *Cytotechnology*, **2000**, 32, 63.
- (201) O. Dym, E. A. Pratt, C. Ho, D. Eisenberg, *Proc. Natl. Acad. Sci. U. S. A.*, **2000**, 97, 9413.
- (202) G. Wang, J. P. Zhang, A. H. Dewilde, A. K. Pal, D. Bello, J. M. Therrien, S. J. Braunhut, K. A. Marx, *Toxicology*, **2012**, 299, 99.
- (203) R. H. Shoemaker, *Nat. Rev. Cancer*, **2006**, 6, 813.
- (204) T. Watanabe, S. Katayama, Y. Nakashita, M. Yamauchi, *Chem. Pharm. Bull.*, **1977**, 25, 2778.
- (205) M. E. Zwaagstra, H. Timmerman, R. S. Abdoelgafoer, M. Q. Zhang, *Eur. J. Med. Chem.*, **1996**, 31, 861.
- (206) C. Rochais, R. Yougnia, T. Cailly, J. S. D. Santos, S. Rault, P. Dallemagne, *Tetrahedron*, **2011**, 67, 5806.
- (207) T. Kukosha, N. Trufilkina, M. Katkevics, *Synlett*, **2011**, 2525.
- (208) H. Tsukamoto, Y. Kondo, *Org. Lett.*, **2007**, 9, 4227.
- (209) J. I. Matsuo, H. Kawai, H. Ishibashi, *Tetrahedron Lett.*, **2007**, 48, 3155.
- (210) O. P. J. van Linden, C. Farenc, W. H. Zoutman, L. Hameetman, M. Wijtmans, R. Leurs, C. P. Tensen, G. Siegal, I. J. P. de Esch, *Eur. J. Med. Chem.*, **2012**, 47, 493.

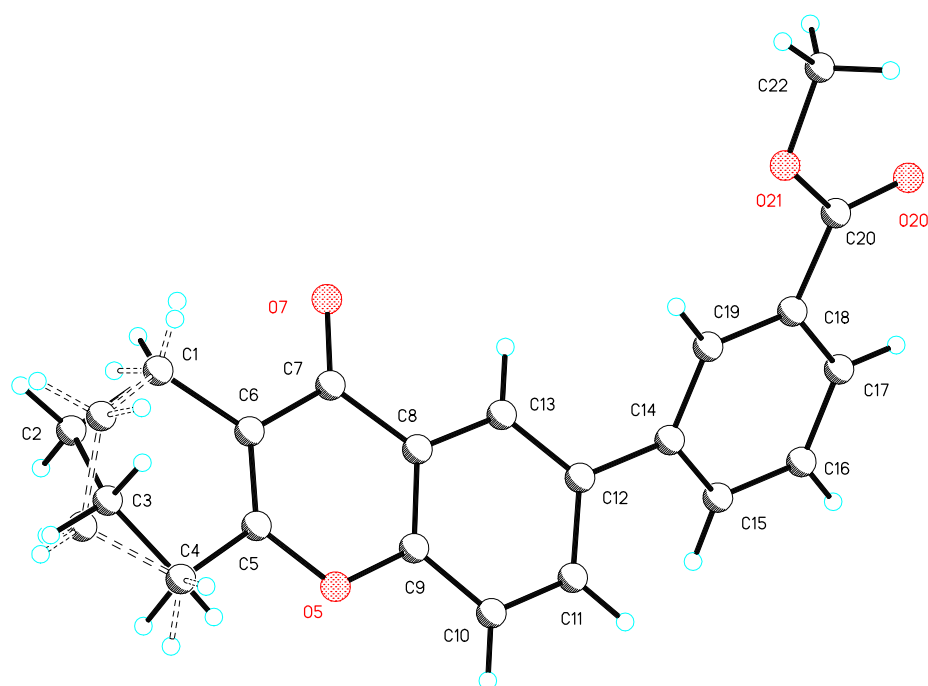
(211) J. Diment, E. Ritchie, W. Taylor, *Aust. J. Chem.*, **1969**, 22, 1721.

(212) M. Hatjimanoli, J. Favrebonvin, M. Kaouadji, A. M. Mariotte, *J. Nat. Prod.*, **1988**, 51, 977.

Appendix I

X-ray structure of 105:

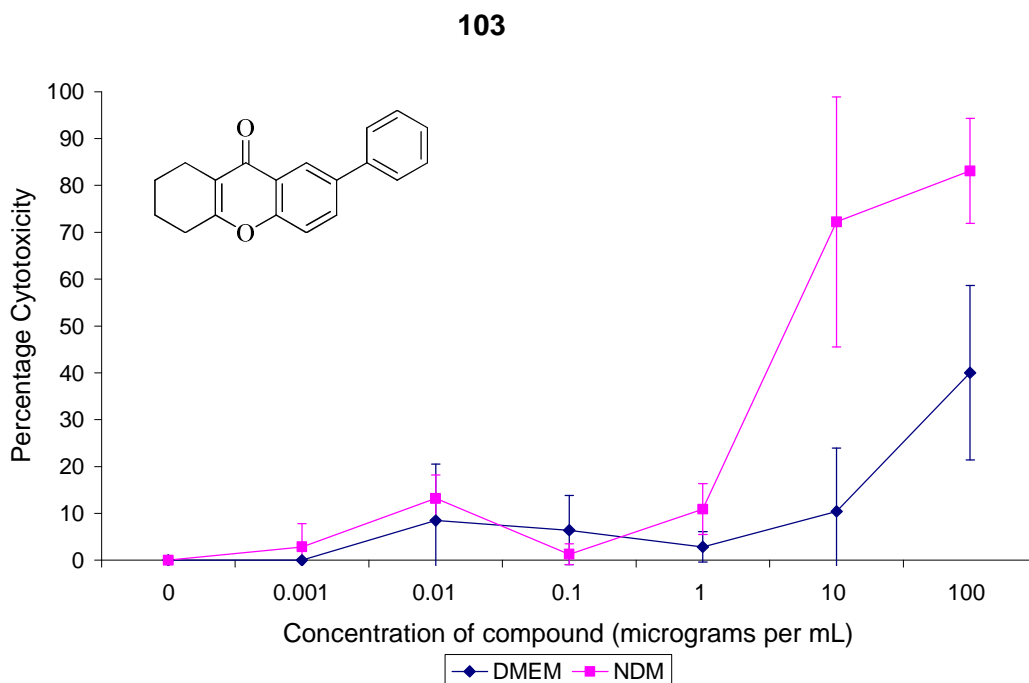
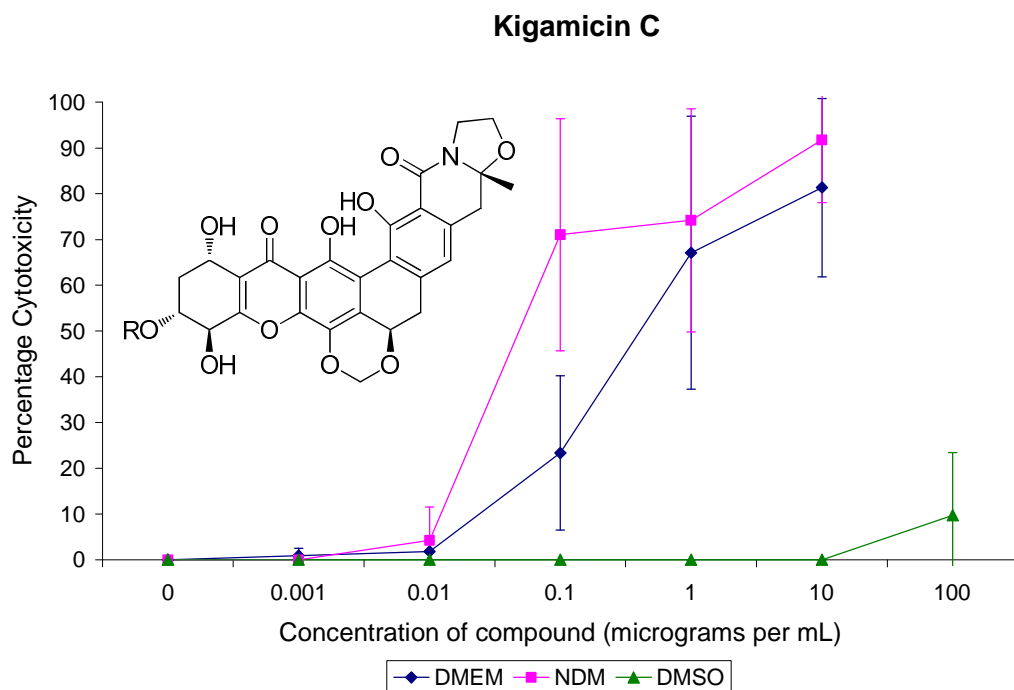
Solid state structure of **105** with atom labelling and disorder in the cyclohexyl ring removed for clarity



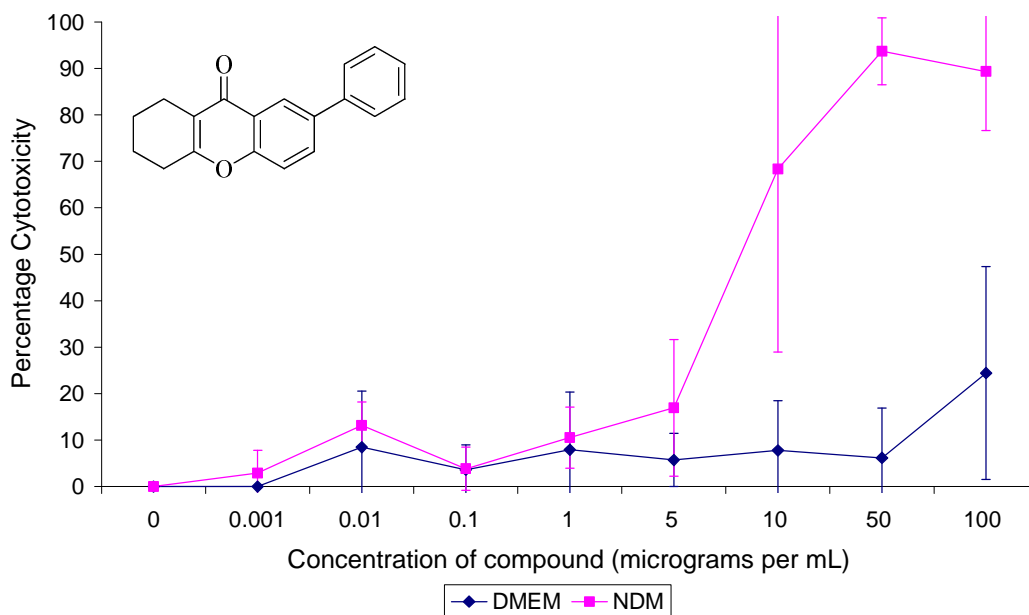
Depiction of solid state structure of **105** with atom labelling showing the disorder in the cyclohexyl ring.

Appendix II

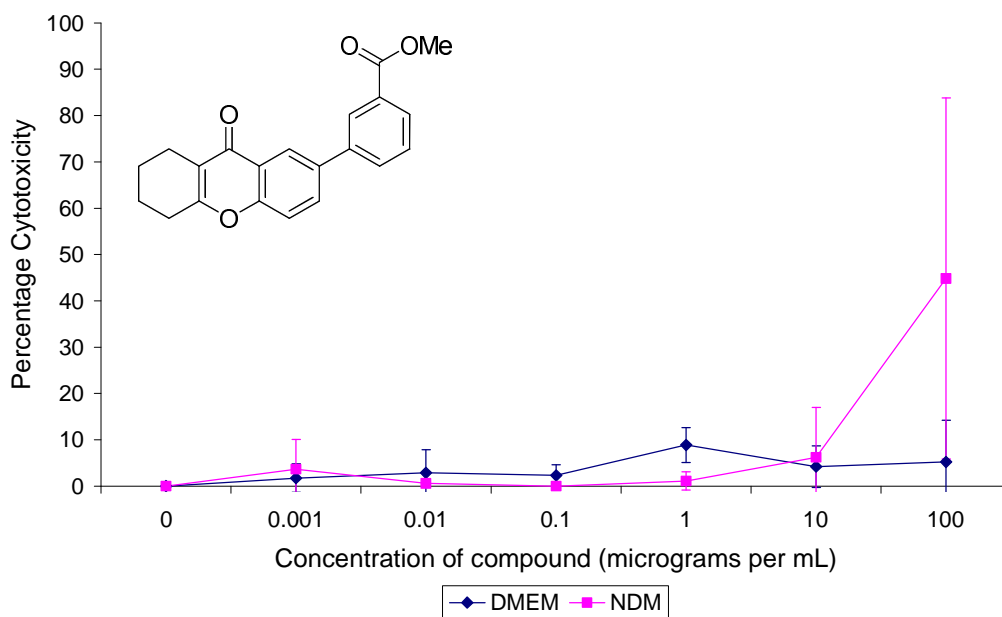
Graphs showing results of the LDH assay



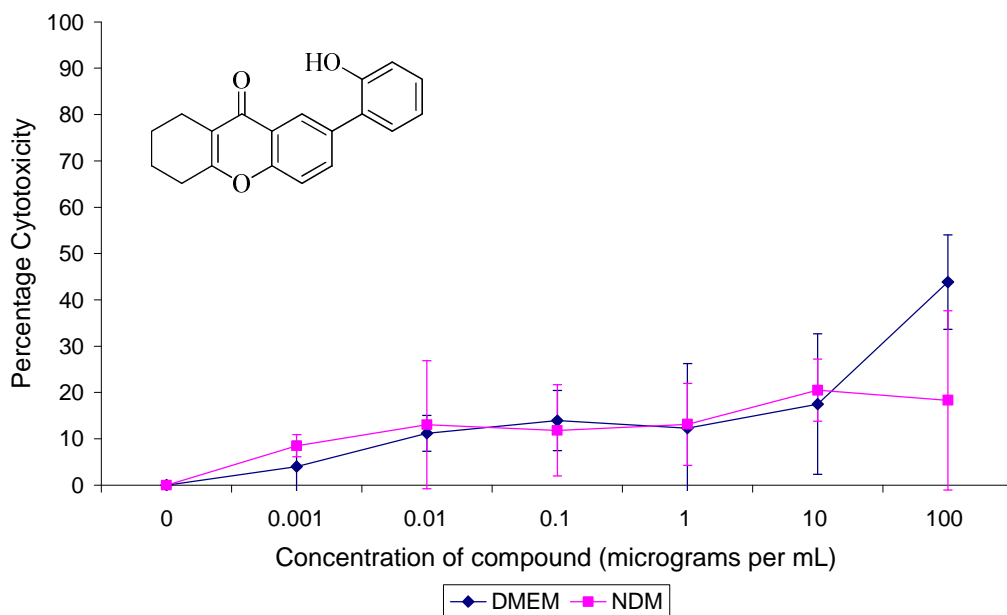
103 at Intermediate Concentrations



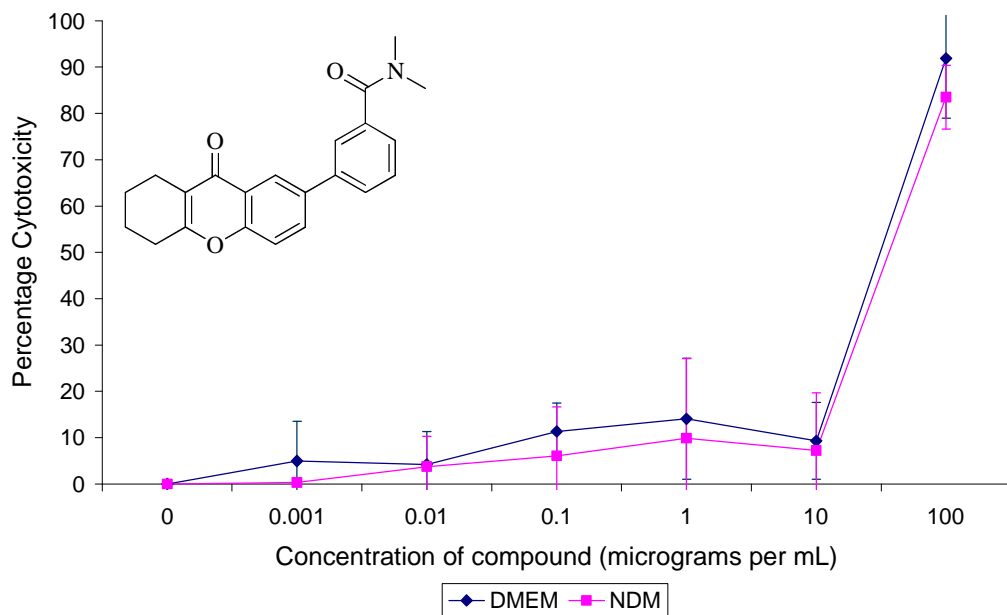
105



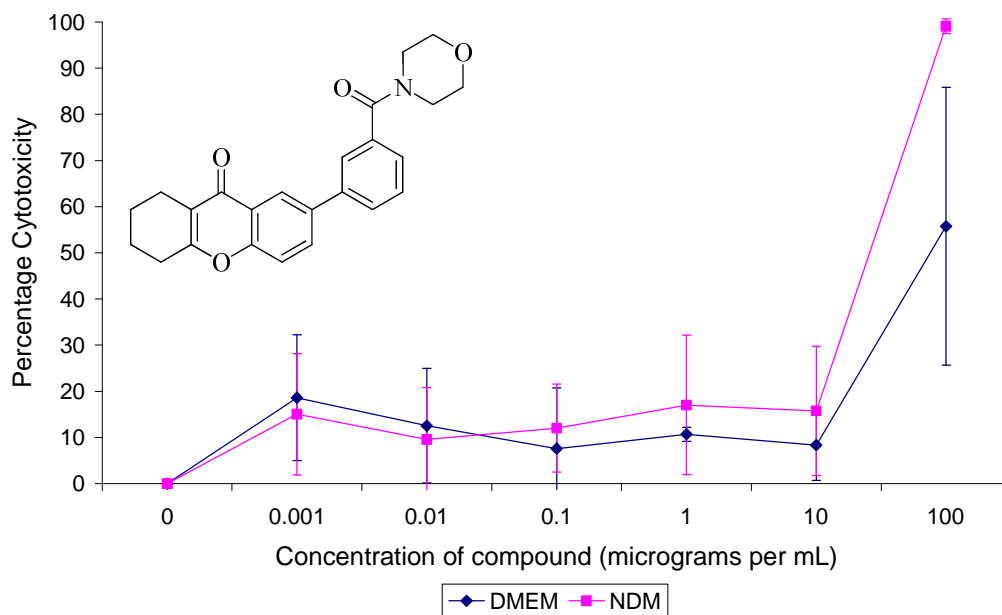
107



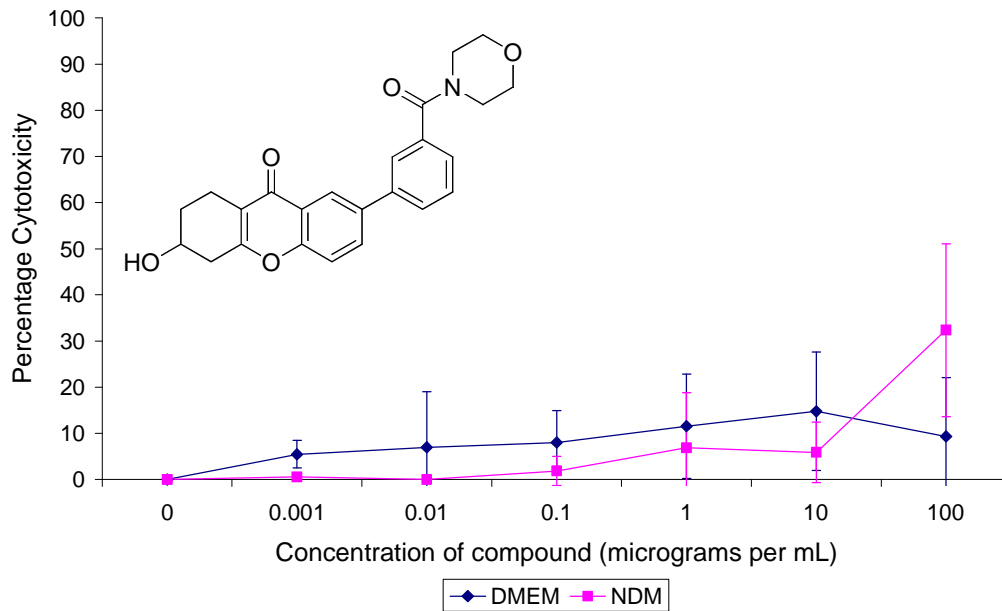
111



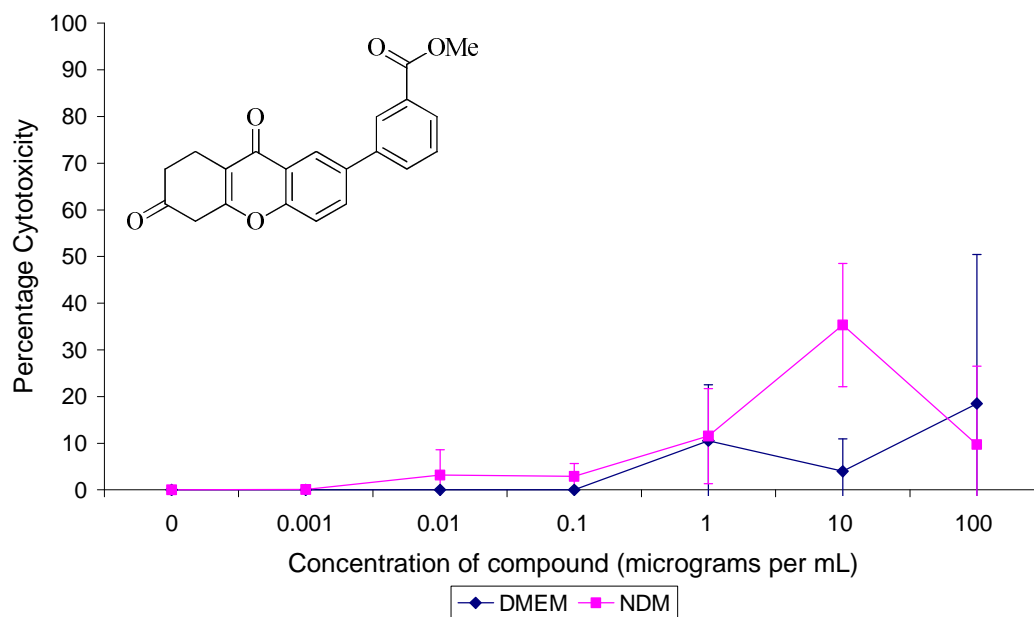
112



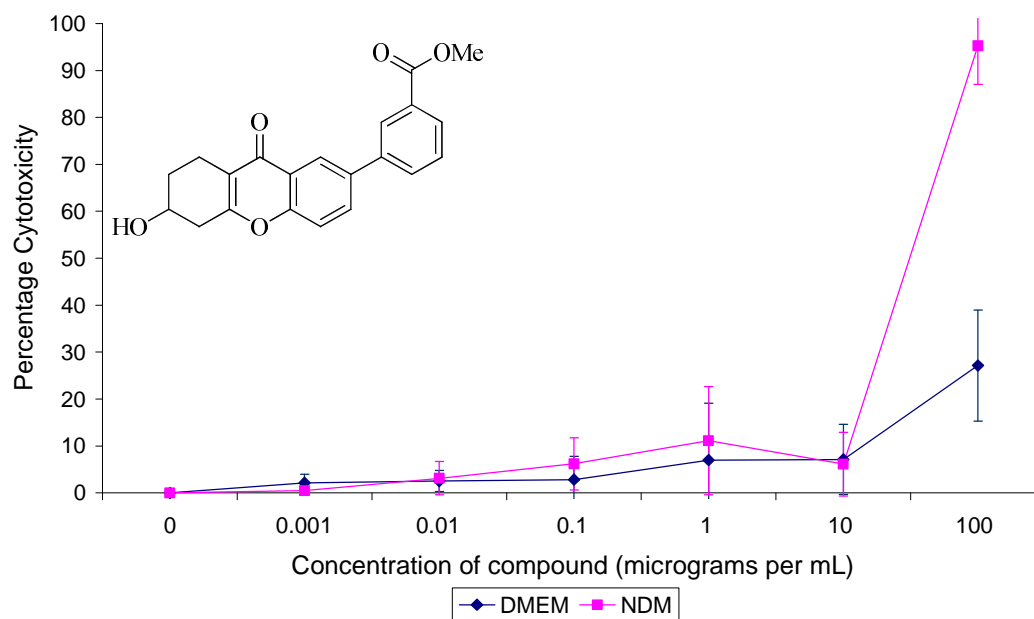
118



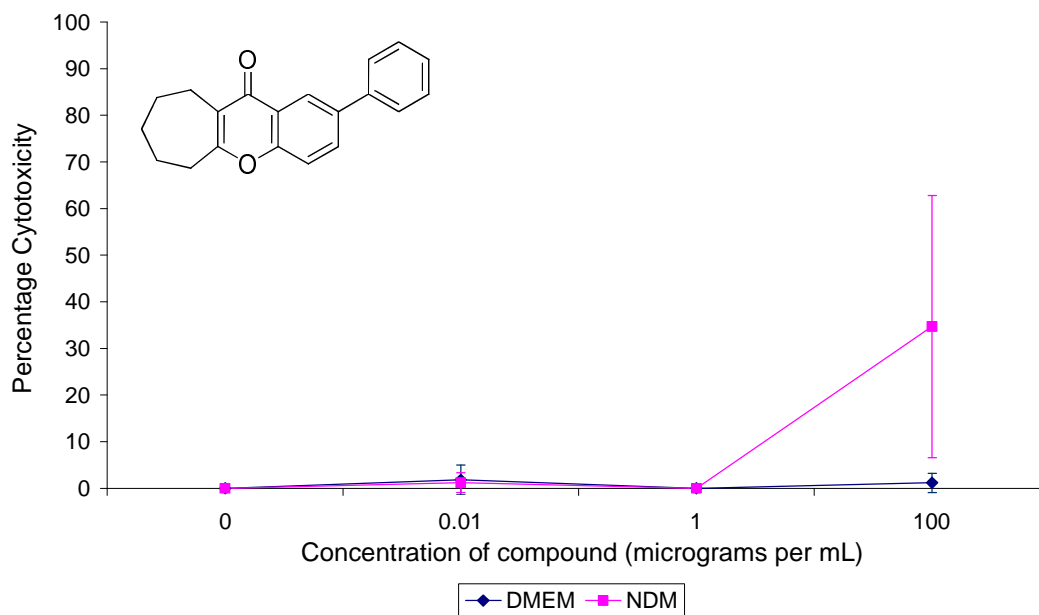
119



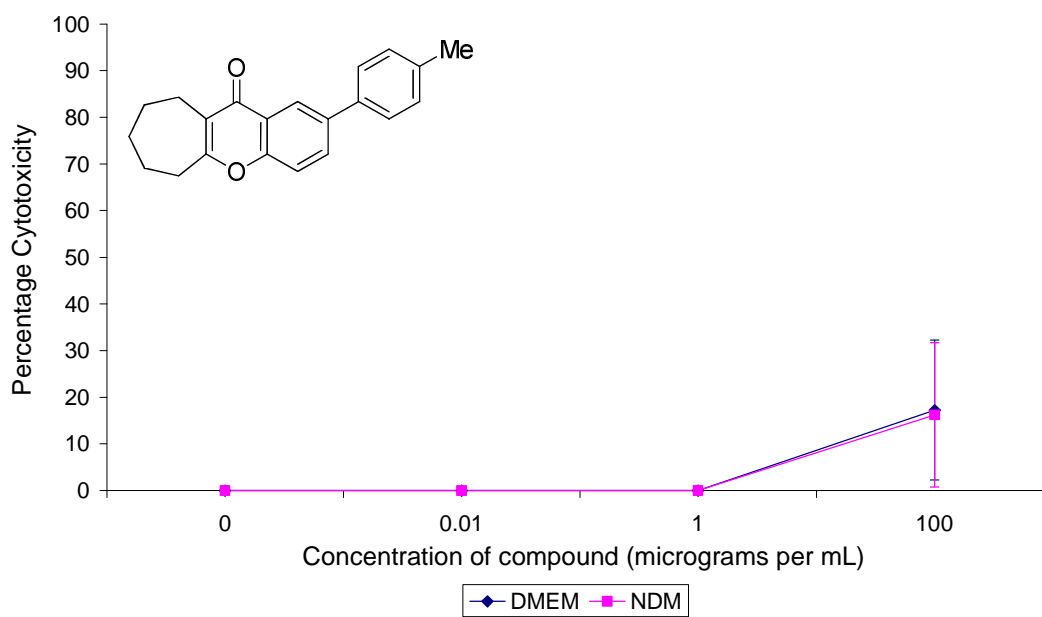
121



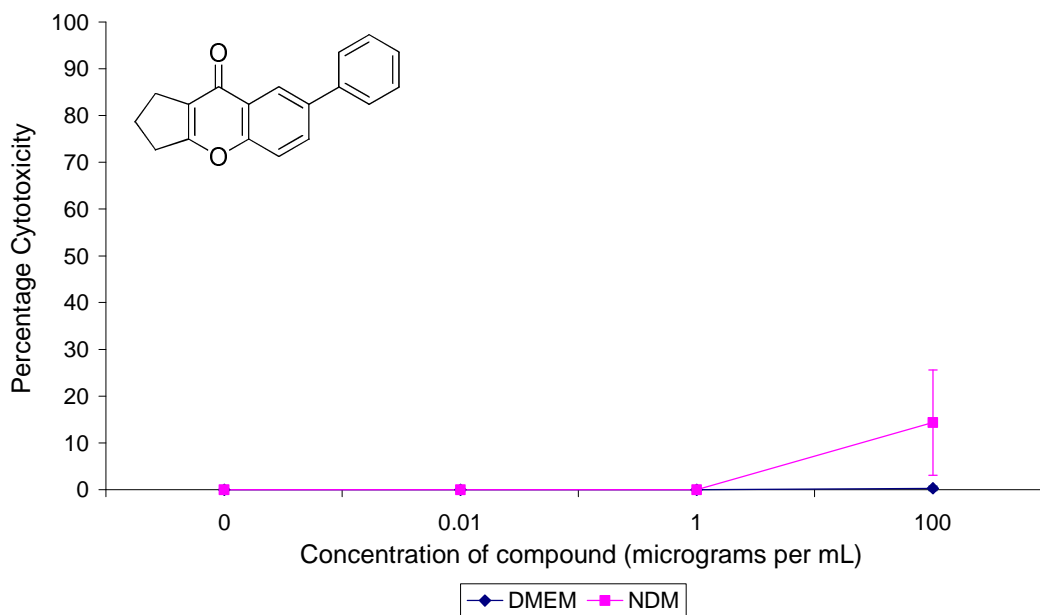
186



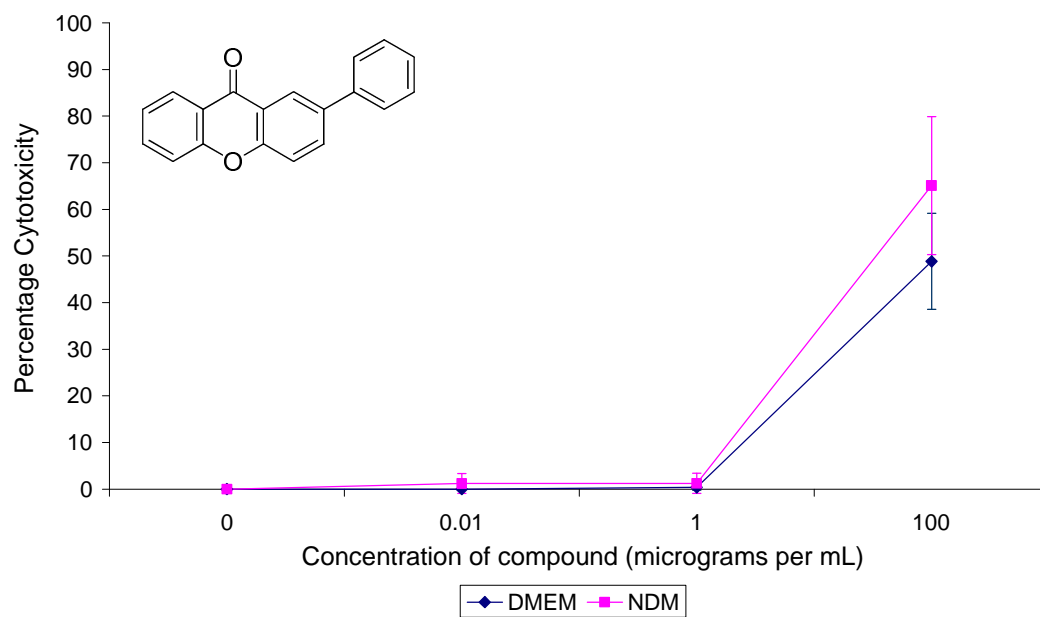
188



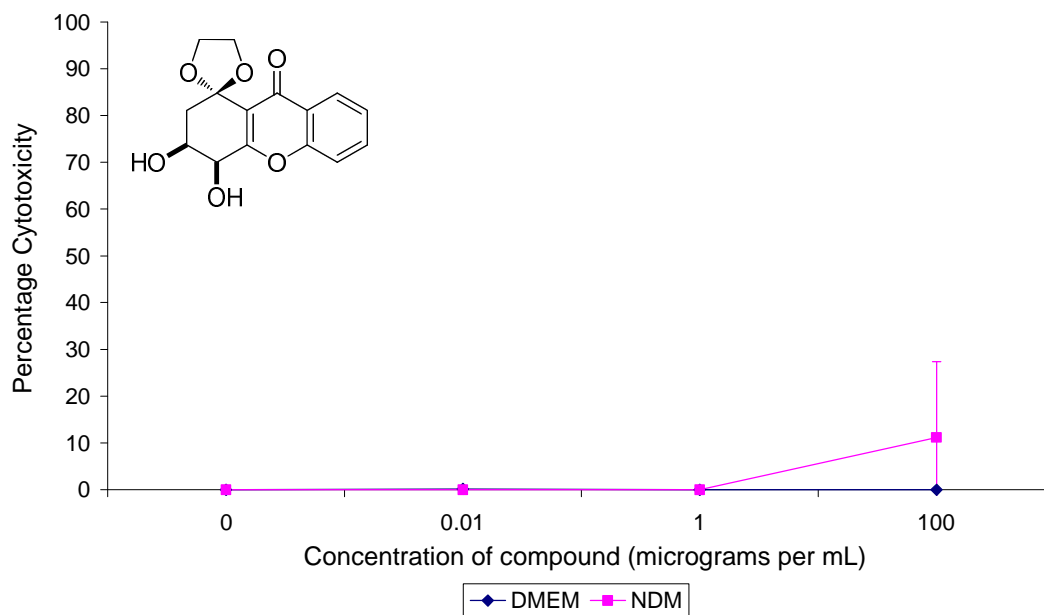
278



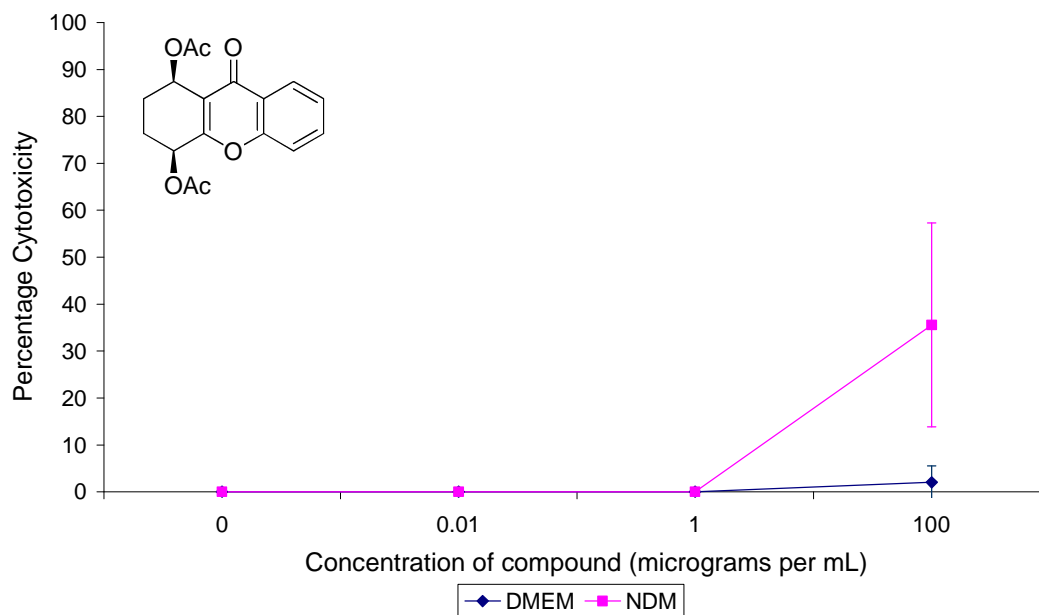
279



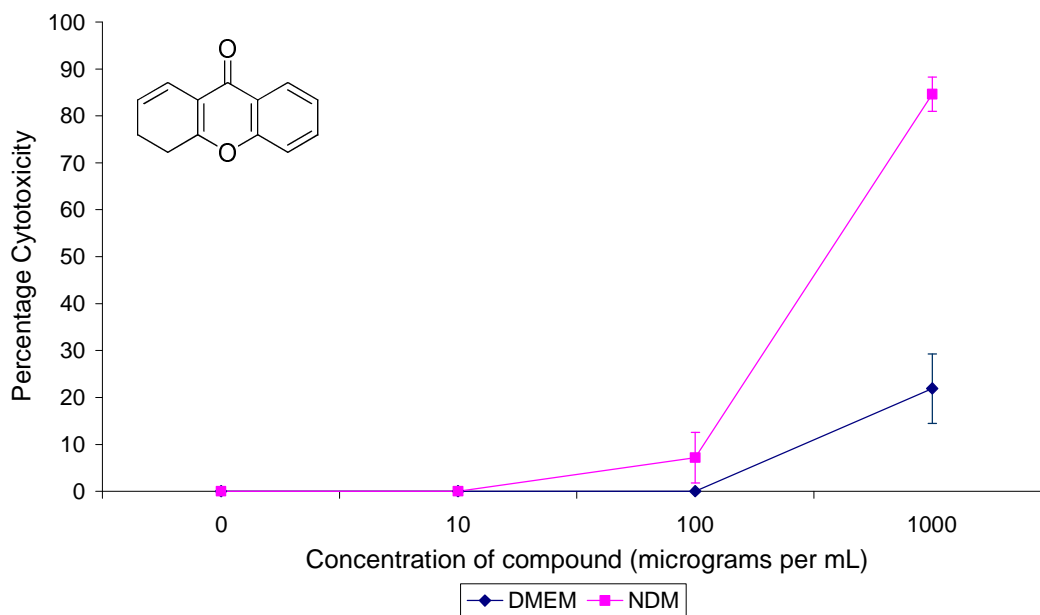
282



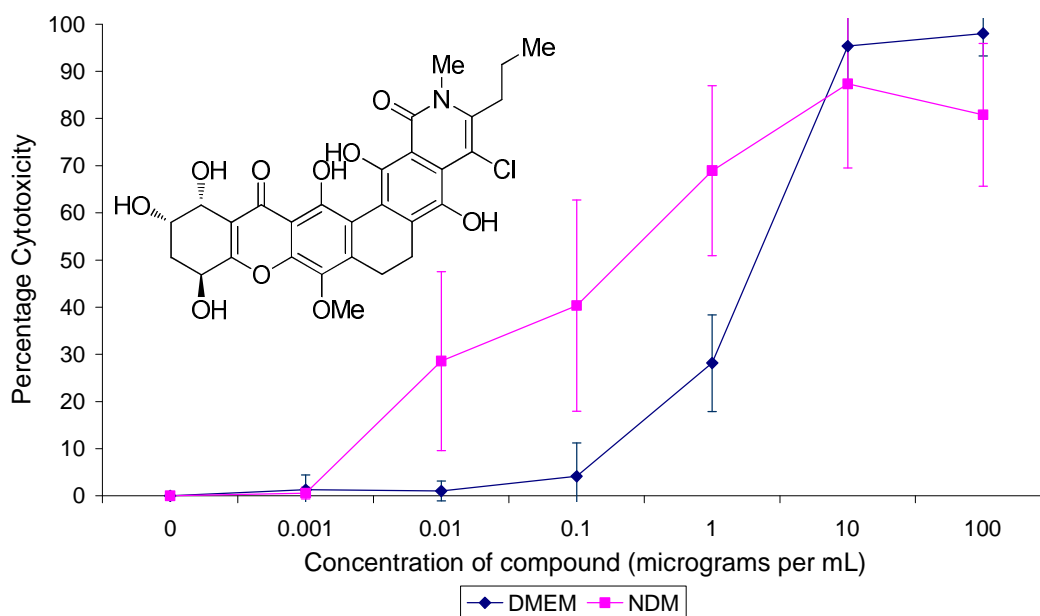
284



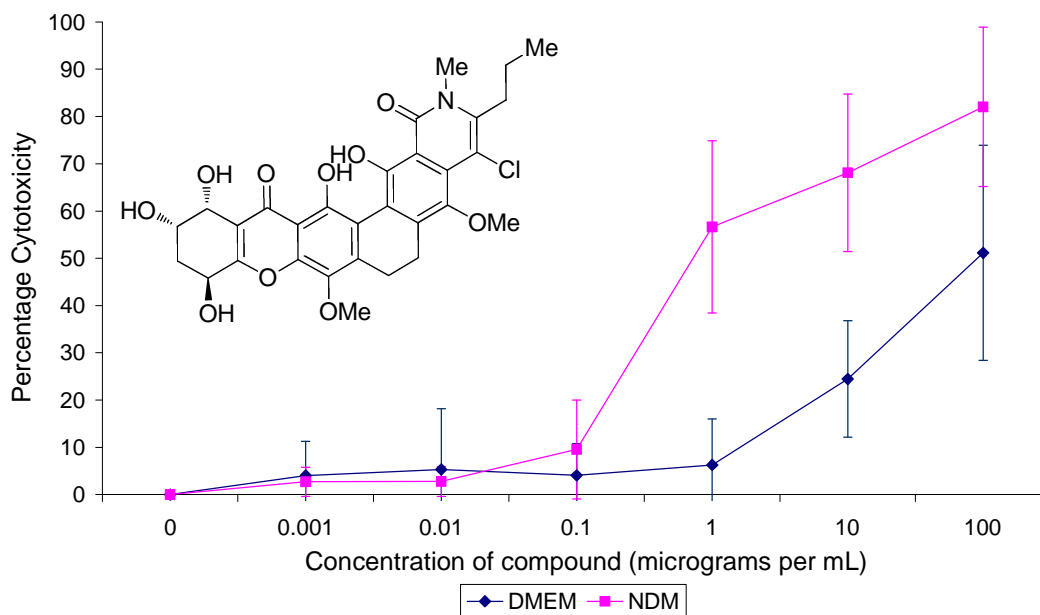
288



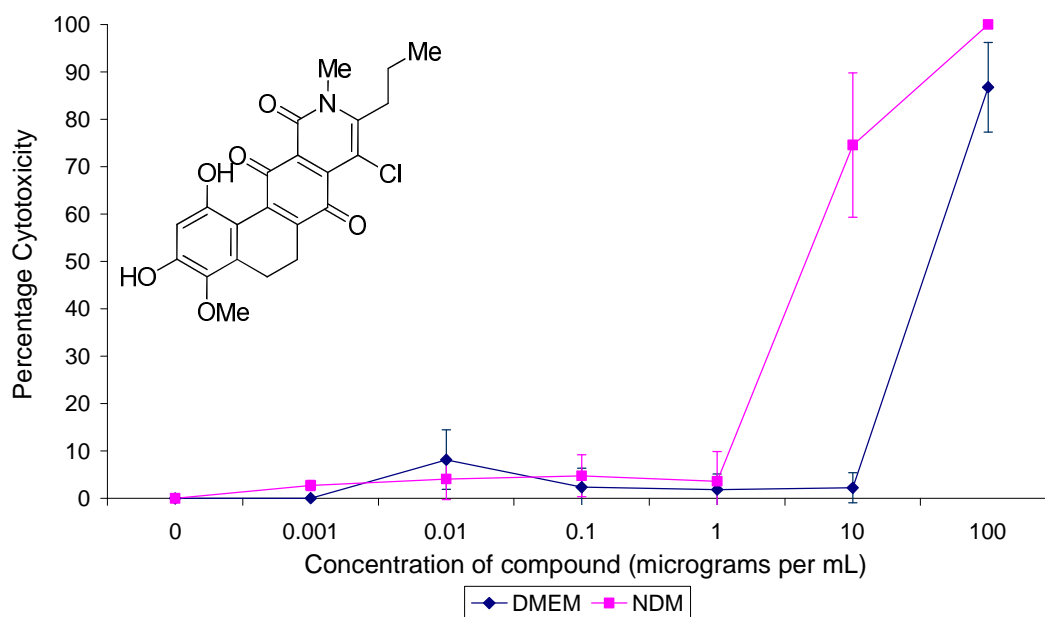
Kibdelone C



289



60



61

